

# **Investigating the role of the bone marrow microenvironment in multiple myeloma**

by

**Yu Sun MSc**

Thesis submitted in accordance with the requirements of the University of East  
Anglia for the degree of

Doctor in Philosophy

The University of East Anglia  
Norwich Medical School  
Department of Molecular Haematology  
Faculty of Medicine and Health Sciences

April 2019

This copy of thesis has been supplied on condition that anyone who consults it is understood to recognise that its copyright rests with the author and that use of any information derived therefrom must be in accordance with current UK Copyright Law. In addition, any quotation or extract must include full attribution.

## **DECLARATION**

This thesis represents the results of my own work (under the supervision of Dr Rushworth) and includes nothing that is the outcome of work done in collaboration, except where specifically indicated. The material contained within this thesis has not been presented, nor is currently being presented, either wholly or in part for any degree or other qualification.

-----

Yu Sun

This research was carried out in the  
Bob Champion Research & Education Building, Department of Molecular  
Haematology, Faculty of Medicine and Health Sciences,  
Norwich Medical School, University of East Anglia

## **ABSTRACT**

Multiple myeloma (MM) is the second most common hematologic malignancy in the UK, characterised by uncontrolled plasma cell proliferation in the bone marrow (BM). Though the survival rate is improving, the MM incidence rate is increasing. Currently, MM is still incurable as with time malignant plasma cells inevitably become resistant to the currently available drugs. The two primary mechanisms responsible for MM relapse are through the MM cell adaptation to the treatment induced stress and through the interaction with the BM microenvironment for protection. Thus, investigations of the mechanisms of MM cell drug resistance are needed to improve the MM patient outcomes.

The aims of this PhD project were to determine: 1) how MM cells escape the endoplasmic reticulum (ER) stress induced cell death; 2) how MM cell outsource autophagy to the BM microenvironment; 3) how bone marrow stromal cell (BMSC) derived NRF2 supports MM proliferation. The results show: 1) primary MM cells exhibit high NRF2 expression; 2) high NRF2 expression reduces the ER stress induced apoptosis in MM cells; 3) MM cells induce NRF2 upregulation in BMSC; 4) primary MM cells outsource autophagy to BMSC; 5) BMSC derived NRF2 supports autophagy.

To summarise, this PhD research project has identified mechanisms through which MM cells avoid endoplasmic reticulum (ER) stress induced apoptosis and how the BMSC-MM interaction support MM cells proliferation. In identifying these mechanisms, it is hoped that further work will result in new treatment strategies for patients with MM in the future.

## Contents

ABSTRACT.....	III
LIST OF FIGURES .....	I
LIST OF TABLES.....	VI
ACKNOWLEDGEMENTS.....	VII
PUBLICATIONS.....	IX
ABBREVIATIONS .....	XI
CHAPTER ONE.....	1
GENERAL INTRODUCTION.....	1
1.1 Multiple Myeloma (MM).....	2
1.1.1 Plasma Cell hierarchy.....	2
1.1.3 Plasma Cell Longevity Regulation.....	4
1.1.4 MM Diagnostic Criteria .....	6
1.1.5 MM Risk Factors.....	8
1.1.6 MM genetic abnormalities.....	9
1.2 Proteasome inhibition in MM treatment .....	11
1.2.1 Proteasome inhibitor bortezomib (Bz) .....	12
1.2.2 Proteasome inhibitor carfilzomib (Cfz).....	13
1.2.3 Proteasome inhibitor Ixazomib.....	13
1.3. Metabolic change in MM cells.....	14
1.4 Reactive oxygen species (ROS) role in MM malignancy .....	15
1.4.1 Sources of ROS .....	16
1.4.2 Cellular toxic effects of ROS .....	17
1.4.3 ROS stress and malignancy .....	18
1.4.4 Therapies targeting ROS .....	18
1.5 The role of NRF2 .....	19
1.5.1 NRF2 regulated glutathione system .....	20
1.5.2 NRF2/HO-1 system.....	21
1.5.3 NRF2/ NQO1 system .....	22
1.5.4 NRF2-P62-autophagy axis .....	22
1.5.5 Other NRF2 associated transcription Factors.....	22
1.6 The role of autophagy in MM progression.....	24
1.7 Sub Cellular Organelles Stress Associated Apoptosis .....	25
1.7.1 Endoplasmic reticulum (ER) stress associated apoptosis.....	26
1.8 The MM Bone Marrow (BM) Microenvironment .....	27

1.8.1 Components of MM BM Niche.....	28
1.8.2 Metabolic Changes in the MM BM Niche .....	29
1.8.3 BM niche role in oncogenesis .....	31
1.8.4 BMSC role in MM initiation .....	31
1.8.5 BM Role in MM Progression .....	32
1.8.6 MM cell remodel BM niche to favour malignancy .....	33
1.9 Research Rational, Aims and Objectives .....	34
1.9.1 Rationale.....	34
1.9.2 Aims .....	34
CHAPTER TWO .....	36
METHODS .....	36
2.1 Cell culture .....	37
2.1.1 Cell lines and culture conditions .....	37
2.1.2 Primary cell isolation.....	38
2.1.3 Calculating cell density .....	39
2.1.4 Cryopreservation of cells.....	40
2.1.5 Thawing cells.....	40
2.2 Viability and apoptosis assay .....	40
2.2.1 Morphology assay .....	40
2.2.2 Cell Titer-GLO assay .....	41
2.2.3 Annexin V-FITC, PI apoptosis assay .....	41
2.3 Flow cytometry .....	42
2.4 Microscopy.....	42
2.5 RNA expression analysis .....	43
2.5.1 Total RNA extraction .....	43
2.5.2 RNA quality control .....	44
2.5.3 cDNA synthesis .....	45
2.5.4 Relative quantitative RT-PCR.....	45
2.6 Protein expression analysis .....	46
2.6.1 Protein extraction.....	47
2.6.2 SDS polyacrylamide gel electrophoresis and Western Blot.....	47
2.7 Short hairpin RNA (shRNA) mediated gene silencing using lentivirus .....	49
2.7.1 RNA amplification .....	49
2.7.2 Plasmid purification.....	50

2.7.3 Plasmid precipitation .....	51
2.7.4 Lentivirus production .....	51
2.7.5 Lentivirus RNA isolation for titration .....	53
2.7.6 Lentivirus RNA titration.....	53
2.7.7 Lentivirus transduction.....	55
2.8 Promoter assay .....	56
2.9 ER-stress detection.....	56
2.10 GSH assay .....	57
2.11 <i>In vivo</i> mice experiments .....	57
2.11.1 NSG mice .....	57
2.11.2 MM cell xenograft.....	58
2.11.3 <i>In vivo</i> bioluminescent (BL) imaging.....	58
2.11.4 Mice scarification and BM cells isolation .....	58
2.12 Adenovirus GFP LC3B construct .....	59
2.13 Statistical analysis .....	60
CHAPTER THREE .....	61
HIGH NRF2 EXPRESSION CONTROLS ER STRESS INDUCED APOPTOSIS IN MM .....	61
3.1 Introduction .....	62
3.1.1 Understanding PI resistance in MM .....	62
3.1.2 The role of NRF2 in PI induced ER stress .....	62
3.1.3 The aim of the project.....	62
3.2 Results .....	63
3.2.1 Investigate NRF2 activity in MM cell lines and primary MM cells .....	63
3.2.2 shRNA targeted NRF2 silencing in MM cell .....	63
3.2.3. NRF2 function in MM cell survival .....	65
3.2.4 To investigate PI induced NRF2 activity in MM cells.....	67
3.2.5 To Determine if PI induced NFR2 activation by examining the activity of the ARE in the HO-1 promotor. ....	71
The above data confirm that the PI induced the NRF2 activation. ....	72
3.2.6 Evaluation of the NRF2-KD effect in MM cells .....	72
3.2.7 NRF2 inhibition up-regulated CHOP expression and induced ER stress .	75
3.2.8 Can PI induce CHOP expression and ER stress in NRF2-KD MM cells? 77	
3.2.9 NRF2 regulated CHOP protein expression in MM cells.....	79
3.2.10 NRF2 regulates GSH synthesis .....	79

3.2.11 GSH synthesis blocks ER stress in MM cells .....	81
3.2.12 NRF2-KD MM cells were sensitive to PI induced apoptosis.....	83
3.3 Summary and Discussion .....	83
CHAPTER FOUR.....	86
INVESTIGATING THE PROTECTIVE ROLE OF NRF2 IN BMSC ON MM.....	86
4.1 Introduction .....	87
4.1.1 BMSC plays a key role on MM progression .....	87
4.1.2 The NRF2 Function in BM Protection Effect on MM Cells.....	88
4.1.3 Aims and objectives .....	89
4.2 Results .....	90
4.2.1 BMSC protected MM cells from apoptosis.....	90
4.2.2 Determine MM cells induced ROS level on BMSC <i>in vitro</i> .....	91
4.2.3 Determine MM cells induced ROS level on BMSC <i>in vivo</i> .....	91
4.2.4 MM cells induced NRF2 expression in BMSC <i>in vitro</i> .....	95
4.2.5 <i>In vivo</i> experiment confirmed BMSC support MM cells engraftment in NSG model .....	95
4.2.6 NRF2-KD BMSC unable to protect MM cells in vitro. ....	97
4.2.7 NRF2-KD BMSC unable to support MM engraftment in NSG model <i>in</i> <i>vivo</i> .....	98
4.2.8 PI induced NRF2 expression in BMSC.....	100
4.2.9 Investigation of NRF2 expression in PI treated BMSC when were co- cultured with MM cells.....	101
4.2.10 BMSC reduced MM cell ROS response to PI treatment.....	102
4.2.11 Determining if NRF2 in BMSC confers resistance to MM in response to PI treatment.....	103
4.2.12 NRF2-KD BMSC unable to decrease the PI treated MM cell ROS levels .....	104
4.2.13 NRF2-KD in BMSC sensitised MM cells to PI treatment induced apoptosis .....	106
4.3 Discussion .....	107
CHAPTER FIVE .....	110
MM CELLS EXPORT AUTOPHAGY TO THE MM MICROENVIRONMENT	110
5.1 Introduction.....	111
5.1.1 Autophagy is the cellular way of protection.....	111

5.1.2 Cancer cells outsource autophagy for survival.....	111
5.1.3 Aims and objectives .....	111
5.2 Results .....	112
5.2.1 Investigation of autophagy levels in MM cell lines and primary MM cells .....	112
5.2.2 Autophagy levels in BMSC culture with primary MM and MM cell lines .....	112
5.2.3 Investigation of MM cells induced LC3 puncta formation in BMSC.....	113
5.2.5 MM cells outsourced autophagy burden to BMSC .....	115
5.2.6 Autophagy inhibitor blocked BMSC protection effect on MM cells .....	117
5.2.7 shRNA targeted ATG5 in BMSC.....	117
5.2.8 MM cells unable to induce LC3 puncta in ATG5-KD BMSC .....	118
5.2.9 Investigate ATG5 function in BMSC protection effect on MM cells <i>in vitro</i> .....	121
5.2.10 Investigate ATG5 function in BMSC protection effect on MM cells <i>in vivo</i> .....	121
5.2.11 NRF2 regulated P62 protein levels in BMSC .....	123
5.2.12 NRF2 regulated autophagy in BMSC.....	124
5.3 Discussion .....	125
CHAPTER SIX.....	128
OVERALL DISCUSSION .....	128
6.1 NRF2 regulation plays a key role for MM cell survival .....	129
6.1.1 MM cells upregulate NRF2 pathway for survival.....	130
6.1.2 NRF2 promotes the survival of MM cells through upregulating antioxidant defence systems and autophagy.....	131
6.1.3 BMSC upregulate NRF2 when in co-culture with MM cells.....	132
6.1.4 BMSC are less sensitive to PI induced apoptosis compared to MM cells .....	132
6.2 The role of the ER on survival of MM cells .....	133
6.2.1 MM cells endure ER stress.....	133
6.2.2 PI induces ER stress .....	133
6.2.3 ER stress responses.....	134
6.2.4 NRF2 regulate ER stress associated apoptosis.....	134
6.4 Autophagy role on survival of MM cells .....	135

6.4.1 MM cells upregulate autophagy for survival.....	135
6.4.2 BMSC upregulate autophagy to protect MM cells.....	135
6.4.3 Targeting NRF2 inhibition to overcome the drawback of autophagy inhibition treatment of MM .....	136
6.5 Concluding remarks and future investigations.....	136
BIBLIOGRAPHY .....	139

## List of Figures

FIGURE 1.1 HAEMATOPOIESIS IN THE BM .....	3
FIGURE 1.2 SIMPLIFIED MM ORIGINATE.....	4
FIGURE 1.3 SCHEMATIC REPRESENTATION OF PROTEASOME FUNCTION AND MECHANISM OF PI .....	12
FIGURE 1.4 SCHEMATIC REPRESENTATION OF MECHANISM OF PI .....	14
FIGURE 1.5 SCHEMATIC REPRESENTATION OF METABOLIC CHANGE ....	15
FIGURE 1.6 SCHEMATIC REPRESENTATION OF THE SOURCE OF ROS .....	17
FIGURE 1.7 SCHEMATIC REPRESENTATION OF THE KEAP1 MEDIATED NRF2 DEGRADATION.....	19
FIGURE 1.8 SCHEMATIC REPRESENTATION OF THE AUTOPHAGY REGULATION.....	25
FIGURE 1.9 SCHEMATIC REPRESENTATION OF THE UPR PATHWAY .....	27
FIGURE 1.10 SCHEMATIC REPRESENTATION OF THE BM MICROENVIRONMENT .....	28
FIGURE 2.1 STREAK PLATE.....	50
FIGURE 3.1 NRF2 LEVELS IN MM CELL LINES AND PRIMARY MM CELLS	63
FIGURE 3.2 SILENCING NRF2 IN MM CELLS USING SHRNA.....	64
FIGURE 3.3 NRF2-KD MM CELLS HAVE REDUCED HO-1 GENE EXPRESSION .....	64
FIGURE 3.4 NRF2-KD MM CELLS HAVE REDUCED GCLM GENE EXPRESSION .....	65
FIGURE 3.5 VIABILITY OF NRF2-KD MM CELLS ARE REDUCED .....	66
FIGURE 3.6 NRF2 INHIBITOR BRUSATOL INDUCES MM CELL APOPTOSIS .....	67
FIGURE 3.7 PI ACTIVATES NRF2 IN MM CELL LINES.....	67
FIGURE 3.8 PI ACTIVATES NRF2 IN MM CELL LINES.....	68
FIGURE 3.9 PI ACTIVATES NRF2 EXPRESSION IN PRIMARY MM CELLS ..	69
FIGURE 3.10 PI INDUCES HO-1 RNA EXPRESSION IN MM CELL LINES .....	69
FIGURE 3.11 PI INDUCES GCLM RNA EXPRESSION IN MM CELL LINES ...	70
FIGURE 3.12 PI INDUCES HO-1 RNA EXPRESSION IN PRIMARY MM CELLS .....	70

FIGURE 3.13 PI INDUCES GCLM RNA EXPRESSION IN PRIMARY MM CELLS .....	71
FIGURE 3.14 SCHEMATIC OF THE HUMAN PROMOTER CONSTRUCT .....	72
FIGURE 3.15 BZ AND CFZ ACTIVATE NRF2 IN MM CELLS .....	72
FIGURE 3.16 LESS NRF2 PROTEIN LEVELS WAS DETECTED IN NRF2-KD MM1S CELLS .....	73
FIGURE 3.17 LESS NRF2 PROTEIN LEVELS WAS DETECTED IN NRF2-KD U266 CELLS.....	73
FIGURE 3.18 BZ INDUCES LESS HO-1 RNA EXPRESSION IN NRF2-KD U266 CELLS .....	73
FIGURE 3.19 BZ INDUCED LESS GCLM RNA EXPRESSION IN NRF2-KD U266 CELLS .....	74
FIGURE 3.20 CFZ INDUCED LESS HO-1 RNA EXPRESSION IN NRF2-KD U266 CELLS .....	74
FIGURE 3.21 CFZ INDUCED LESS GCLM RNA EXPRESSION IN NRF2-KD U266 CELLS.....	75
FIGURE 3.22 NRF2-KD U266 CELLS HAVE UPREGULATED CHOP EXPRESSION BUT NOT ATF4 EXPRESSION .....	76
FIGURE 3.23 NRF2-KD MM1S CELLS HAVE UPREGULATED CHOP EXPRESSION BUT NOT ATF4 EXPRESSION .....	76
FIGURE 3.24 NRF2 REGULATED ER STRESS IN MM1S .....	77
FIGURE 3.25 NRF2 REGULATED ER-STRESS IN MM1S .....	77
FIGURE 3.26 PI INDUCED CHOP RNA EXPRESSION IN MM CELLS.....	78
FIGURE 3.27 PI INDUCED CHOP RNA EXPRESSION IN NRF-KD MM1S.....	78
FIGURE 3.28 NRF2 REGULATED CHOP PROTEIN EXPRESSION IN MM1S..	79
FIGURE 3.29 NRF2 REGULATED CHOP ROTEIN EXPRESSION IN U266 .....	79
FIGURE 3.30 PI INDUCED GSH SYNTHESIS .....	80
FIGURE 3.31 NRF2-KD MM1S HAVE LOWER PI INDUCED GSH LEVELS ....	80
FIGURE 3.32 NAC BLOCKED BZ INDUCED CHOP RNA EXPRESSION .....	81
FIGURE 3.33 NAC INHIBITED BZ INDUCED ER STRESS.....	81
FIGURE 3.34 BSO INCREASED BZ INDUCED CHOP RNA EXPRESSION .....	82
FIGURE 3.35 BSO INCREASED BZ INDUCED ER STRESS .....	82
FIGURE 3.36 NRF2-KD MM CELLS WERE SENSITIVE TO PI TREATMENT ..	83
FIGURE 3.37 SCHEMATIC REPRESENTATION OF NRF2- GCLM- GSH .....	84

FIGURE 3.38 SCHEMATIC REPRESENTATION OF NRF2 ACTIVITY IN PI TREATED MM CELLS .....	85
FIGURE 4.1 BMSC PROTECTED PRIMARY MM CELLS FROM APOPTOSIS .	90
FIGURE 4.2 MM CELLS INCREASED MITOSOX AND DCF LEVEL IN BMSC	91
FIGURE 4.3 BIOLUMINESCENCE IN VIVO IMAGES DETECTED THE DISEASE PROGRESSION IN MM XENOGRAFT NSG MODEL .....	92
FIGURE 4.4 FLOW CYTOMETRY ANALYSIS OF MM ENGRAFTMENT IN TO NSG MICE.....	92
FIGURE 4.5 ANTIBODY PANEL TO DETECT MITOCHONDRIAL ROS IN BMSC FROM BM OF MM XENOGRAFTED NSG MICE .....	93
FIGURE 4.6 CELLULAR AND MITOCHONDRIAL ROS DETECTION IN BMSC FROM BM OF MM XENOGRAFT NSG MICE.....	94
FIGURE 4.7 MM CELLS INDUCED BMSC NRF2 EXPRESSION .....	95
FIGURE 4.8 BIOLUMINESCENCE IN VIVO IMAGES DETECTED THE DISEASE PROGRESSION IN U266 AND BMSC XENOGRAFT MODEL .....	96
FIGURE 4.9 TUMOUR SIZE OF U266-LUCI/BMSC ENGRAFTMENT MICE ...	97
FIGURE 4.10 PRIMARY MM CELLS VIABILITY WAS DECREASED WHEN WERE CO-CULTURED WITH NRF2-KD BMSC COMPARED TO CONTROL KNOCKDOWN .....	98
FIGURE 4.11 BIOLUMINESCENCE IN VIVO IMAGES DETECTED THE DISEASE PROGRESSION IN U266 AND BMSC XENOGRAFT MODEL .....	99
FIGURE 4.12 IMAGES SHOW THE TUMOUR SIZE FROM U266/BMSC NRF2-KD ENGRAFTED MICE .....	99
FIGURE 4.13 DOSE DEPENDED ACCUMULATION OF NRF2 PROTEIN IN THE BMSC WHEN WERE TREATED WITH CFZ.....	100
FIGURE 4.14 PI INCREASED BMSC HO-1 AND GCLM MRNA EXPRESSION .....	101
FIGURE 4.15 PI TREATED MM CELLS INDUCED BMSC NRF2 UP-REGULATION.....	101

FIGURE 4.17 PRIMARY MM CELLS MITOCHONDRIA ROS LEVELS WERE INCREASED WHEN WERE CO-CULTURED WITH BMSC WITH PI TREATMENT .....	102
FIGURE 4.18 MM CELL DCF LEVELS WHEN WERE CO-CULTURED WITH BMSC WITH PI TREATMENT .....	103
FIGURE 4.19 NRF2 PROTEIN EXPRESSION IN NRF2-KD BMSC TREATED WITH CFZ.....	103
FIGURE 4.20 NRF2 MRNA EXPRESSION IN NRF2-KD BMSC .....	104
FIGURE 4.21 NRF2-KD BMSC HO-1 RNA EXPRESSION WHEN TREATED WITH CFZ.....	104
FIGURE 4.22 MITOCHONDRIAL ROS LEVELS IN NRF2-KD BMSC WERE HIGH WHEN CULTURED WITH PI TREATED MM1R .....	105
FIGURE 4.23 CELLULAR ROS WERE UNCHANGED IN NRF2-KD BMSC WHEN CULTURED WITH PI TREATED MM1R .....	105
FIGURE 4.24 NRF2-KD BMSC SENSITISED PRIMARY MM CELLS TO CFZ TREATMENT .....	106
FIGURE 4.25 NRF2-KD BMSC SENSITISED U266 TO PI TREATMENT .....	107
FIGURE 4.26 SCHEMATIC REPRESENTATION OF MM CELL INDUCED NRF2 REGULATION IN BMSC PROTECTS MM CELLS .....	109
FIGURE 5.1 BASAL LC3I AND LC3II EXPRESSION IN MM CELL LINE AND PRIMARY MM CELLS .....	112
FIGURE 5.2 BMSC LC3I AND LC3II EXPRESSION IN RESPONSE TO MM CO-CULTURE .....	113
FIGURE 5.3 LC3 EXPRESSION IN BMSC WHEN CO-CULTURED WITH MM CELL LINE OR PRIMARY MM CELLS .....	113
FIGURE 5.4 PRIMARY MM CELLS INDUCED LC3 PUNCTA FORMATION IN GFP-LC3 TAGGED BMSC.....	114
FIGURE 5.5 PRIMARY MM CELLS INDUCED LC3 PUNCTA NUMBER IN GFP-LC3 TAGGED BMSC .....	115
FIGURE 5.6 PRIMARY MM CELLS HAVE UNDEGRADED LC3 PUNCTA ....	116
FIGURE 5.7 MM CELLS ACTIVELY SECRETED EV WHICH WERE ACQUIRED BY BMSC.....	116

FIGURE 5.8 AUTOPHAGY INHIBITORS BLOCKED BMSC INDUCED PROTECTION OF MM CELLS.....	117
FIGURE 5.9 ATG5 RNA EXPRESSION IN ATG5-KD BMSC.....	118
FIGURE 5.10 PRIMARY MM CELLS INDUCED LC3 PUNCTA FORMATION IN BMSC BUT NOT IN BMSC WITH ATG5 KNOCKDOWN .....	120
FIGURE 5.11 PRIMARY MM CELLS VIABILITY WAS DECREASED WHEN CO-CULTURED WITH AUTOPHAGY IMPAIRED ATG5-KD BMSC COMPARED TO CONTROL KNOCKDOWN BMSC .....	121
FIGURE 5.12 BIOLUMINESCENCE <i>IN VIVO</i> IMAGES DETECTED THE DISEASE PROGRESSION IN U266 AND ATG5-KD BMSC XENOGRAFT MODEL .....	122
FIGURE 5.13 IMAGES SHOW THE TUMOUR FROM U266/BMSC ATG5-KD ENGRAFTMENT MICE.....	123
FIGURE 5.14 KD-NRF2 BMSC HAVE DECREASED P62 PROTEIN LEVEL ...	124
FIGURE 5.15 LC3 PUNCTA FORMATION IN THE NRF2-KD BMSC AFTER THE BMSC BEEN CO-CULTURED WITH PRIMARY MM CELLS	125
FIGURE 5.16 SCHEMATIC REPRESENTATION OF MM CELL INDUCED NRF2 MEDIATED AUTOPHAGY REGULATION IN BMSC PROTECTS MM CELLS .....	127
FIGURE 6.1 SCHEMATIC REPRESENTATION OF NRF2 REGULATION PROTECT MM CELLS.....	144

## List of Tables

TABLE 1.1 INTERNATIONAL MM WORKING GROUP DIAGNOSTIC CRITERIA OF MM .....	6
TABLE 1.2 INTERNATIONAL MM WORKING GROUP DIAGNOSTIC CRITERIA FOR RELATED PLASMA CELL DISORDERS.....	7
TABLE 1.3 POSSIBLE MM RISK FACTORS .....	8
TABLE 1.4 TYPES OF GENETIC ABNORMALITIES IN MM.....	9
TABLE 1.5 REPORTED MECHANISMS OF ACTION FOR BORTEZOMIB IN THE TREATMENT OF MM.....	13
TABLE 1.6 LIST OF NRF2 TARGETED ANTIOXIDANT RELATED GENES AND THEIR GENERAL FUNCTION.....	20
TABLE 2.1 OLIGONUCLEOTIDE SEQUENCES FOR REAL-TIME PCR (5' TO 3') .....	46
TABLE 2.2 ANTIBODIES FOR WESTERN BLOTTING .....	49
TABLE 2.3 MISSION SHRNA SEQUENCE .....	56
TABLE 2.4 ANTIBODY PENAL FOR CELL STAINING .....	59

## **ACKNOWLEDGEMENTS**

As I submit this dissertation, it is clear to me that many people have contributed to its creation. I would like to thank all those people who have helped and supported me during the past few years and made this dissertation possible.

My deepest gratitude is to my two advisors, Dr Stuart Rushworth and Prof Kristian Bowles. Joining their labs when starting my graduate studies at the University of East Anglia has been one of the best decisions that I ever made in my life. They supported me on every step of the way, teaching me how to address scientific problems, how to ask questions whose answers will move my projects along and how to write scientific literature. They also correct the grammars of my thesis and it would have been difficult to finish without their kindly support. Dr Rushworth and Prof Bowles gave me the freedom to explore the scientific questions that I found most interesting and to find solutions to problems that I encountered but were always there when I needed help or guidance. They supported me to attend numerous international meetings, allowing me to gain invaluable practice of presenting my work to my scientific peers. Both Dr Rushworth and Prof Bowles fostered lab camaraderie through many lab meeting and social events. Because of this I established lasting friendships with many of my colleagues Dr Lyubov Zaitseva, Manar Shafat, Chris Marlein, Rachel Piddock, Amina Abdul-Aziz, Jayna Mistry, Charlotte Hellmich, Jamie Moore, Eoghan Forde, Geneva Pillinger, Rebecca Horton, Adam Morfakis.

None of my projects could have been completed without the help of countless colleagues and friends in the Rushworth and Bowles lab. I want to particularly thank over 600 patients and their families for donating samples and thank Dr Matthew Lawes, Dr Angela Collins, MM clinic team, Dr Martin Auger, Dr Nimish Shah, Dr Katy Rice, Dr Hamish Lyall, junior doctors and nurses for all their help with collecting the sample.

Finally, and most importantly I want to express my deepest gratitude to my family, especially to my lovely daughter Tianyue who encourage me to keep trying. Without their constant love, support and care I could have never achieved what I have achieved. My parents, siblings and husband have supported me through every endeavour of mine. And though I know that the large spatial separation puts an incredible strain on my

family, they never stopped believing in me. I would like to thank them for everything that they have ever done for me.

## PUBLICATIONS

### Papers

1. (Co-first author) Amina M Abdul-Aziz, **Yu Sun**, Charlotte Hellmich, Christopher R Marlein, Eoghan Forde, Rachel E Piddock, Manar S Shafat, Adam Morfakis, Tarang Mehta, Federica Di Palma, Christopher J Ingham, Angela Collins, Judith Campisi, Kristian M. Bowles, Stuart A Rushworth. Acute myeloid leukemia induces pro-tumoral p16INK4a driven senescence in the bone marrow microenvironment, **Blood**, 2018 Nov, 6; doi: 10.1182/blood-2018-04-845420.
2. Abdul-Aziz AM, Shafat MS, **Sun Y**, Marlein CR, Piddock RE, Robinson SD, Edwards DR, Zhou Z, Collins A, Bowles KM, Rushworth SA, HIF1 $\alpha$  drives chemokine factor pro-tumoral signaling pathways in acute myeloid leukemia, **Oncogene**, 2018 Feb; 10.1038/s41388-018-0151-1.
3. **Sun Y**, Abdul Aziz A, Bowles K, Rushworth S, High NRF2 expression controls endoplasmic reticulum stress induced apoptosis in multiple myeloma, **Cancer letter**, 2018 Jan, 1;412:37-45.
4. Piddock RE, Loughran N, Marlein CR, Robinson SD, Edwards DR, **Yu S**, Pillinger GE, Zhou Z, Zaitseva L, Auger MJ, Rushworth SA, Bowles KM, **Blood Cancer J**, 2017 Mar, 10;7(3):e539.

### Posters

1. NCRI Cancer Conference, UK, 2018  
Presentation Title: Multiple myeloma increases autophagy in the bone marrow stromal cells which is regulated by NRF2 signalling
2. NCRI Cancer Conference, UK, 2018  
Poster Title: Dysfunctional mitochondria are exported from myeloma cells to the bone marrow microenvironment
3. 3rd EACR Conference on Cancer Genomics, UK, 2017  
Poster Title: NRF2 Prevents Bortezomib induced Endoplasmic Reticulum Stress Apoptosis via the Negative Regulation of CHOP
4. The 58th American Society of Hematology Annual Meeting and Exposition, USA, 2016  
Poster Title: Dual Activation of NRF2 in Multiple Myeloma and Bone Marrow Mesenchymal Stromal Cells Regulates Chemotherapy Resistance

5. 21st Congress of The European Hematology Association, Denmark, 2016

Poster Title: NRF2 Activity in Bone Marrow Mesenchymal Stromal Cell Protects Multiple Myeloma from Carfilzomib and Bortezomib induced Cell Death

## ABBREVIATIONS

AMPK	5' AMP-activated protein kinase
ARE	Antioxidant response element
IRE1	Inositol-requiring enzyme 1
ATF4	Activating transcription factor 4
ATF6	Activating transcription factor 6
ATP	Adenosine triphosphate
BM	Bone marrow
BMSC	Bone marrow mesenchymal stromal cell
BSO	Buthionine sulfoximine
BZ	Bortezomib
cDNA	Complementary deoxyribonucleic acid
CFZ	Carfilzomib
CHOP	CCAAT-enhancer-binding protein homologous protein also C/EBP Homologous Protein
DAPI	4',6-diamidino-2-phenylindole
DMEM	Dulbecco's Modified Eagle Medium
DMSO	Dimethyl sulfoxide
DNA	Deoxyribonucleic acid
DNase	Deoxyribonuclease
dNTPs	Deoxynucleotide
dsDNA	Double stranded DNA
E. coli	Escherichia coli
ECL	Electrochemical luminescence
EDTA	Ethylenediaminetetraacetic acid
ER	Endoplasmic reticulum
FBS	Fetal bovine serum
GAPDH	Glyceraldehyde-3-phosphate dehydrogenase
GCLM	Glutamate-cysteine ligase
GFP	Green fluorescent protein
GSH	Glutathione
HO-1	Heme oxygenase
IL-6	Interleukin-6
IRE1	Inositol-requiring enzyme 1

KD	Knock down
KEAP1	Kelch-like ECH-associated protein 1
LB	Lysogeny broth
MGUS	Monoclonal gammopathy of undetermined significance
MM	Multiple myeloma
MMSC	MM Stem Cell
MOI	Multiplicity of infection
MOMP	Mitochondrial outer membrane permeabilisation
mRNA	Messenger RNA
mut	Mutant
NAC	N Acetyl Cysteine
NADH	Nicotinamide adenine dinucleotide hydride
NADPH	Nicotinamide adenine dinucleotide phosphate
NQO1	Quinone oxidoreductase 1
NRF2	Nuclear factor (erythroid-derived 2)-like 2
NSG	Non-obese diabetic/severe combined immunodeficiency
PBS	Phosphate buffered saline
PCR	Polymerase chain reaction
PI	Proteasome inhibitor
PI3K	Phosphoinositide-3 kinase
PVDF	Polyvinylidene difluoride
RNA	Ribonucleic Acid
RNase	Ribonuclease
ROS	Reactive oxygen species
RPMI	Roswell Park Memorial Institute
RT-PCR	Reverse transcription polymerase chain reaction
Sam68	The Src-Associated substrate in Mitosis of 68 kDa
SDS	Sodium dodecyl sulfate
shRNA	Short hairpin RNA
SMM	Smoldering multiple myeloma
ssDNA	Single-stranded DNA
WT	Wildtype

**CHAPTER ONE**  
**GENERAL INTRODUCTION**

## **1.1 Multiple Myeloma (MM)**

It is currently estimated that 240,000 people are living with blood cancer in the UK [1]. Multiple myeloma is the second most common blood cancer and accounts for 2% of all new cancers diagnosed in the UK in 2015 (5540 new diagnosed MM patients). Nearly 1 in 10,000 people will be diagnosed with MM each year. MM incidence rates have increased by 32% in the UK since the early 1990s [2]. The median survival rate for MM is approximately 5 years and the disease presently remains incurable [2]. Thus, studies which lead to new drugs that target MM are necessary to improve outcomes in this disease.

MM is an age related disease with approximately two-thirds of patients diagnosed over the age of 65 years [3]. MM treatment includes initial therapy, stem cell transplantation, consolidation/maintenance therapy, and relapse treatment. However, patients aged over 75 cannot receive stem cell transplantation therapy [4]. Thus, the mortality rates for MM in the UK are highest in people aged over 85 years of age, which in part reflects the challenges of managing older patients with current therapies.

### **1.1.1 Plasma Cell hierarchy**

MM is a cancer of uncontrolled terminally differentiated plasma cell proliferation, which infiltrates and accumulates in the bone marrow (BM) with detectable monoclonal protein in the serum or urine [5]. The plasma cell belongs to lymphoid lineage cell, which is derived from long term and short-term BM blood stem cell (Figure 1.1). The blood stem cell differentiates into a lymphoid stem cell, then lymphoid blast. Next, the B cell is matured into plasma cells under stimuli. Various mutations in the plasma cells in the BM niche, allows for its transformation into MM [6].

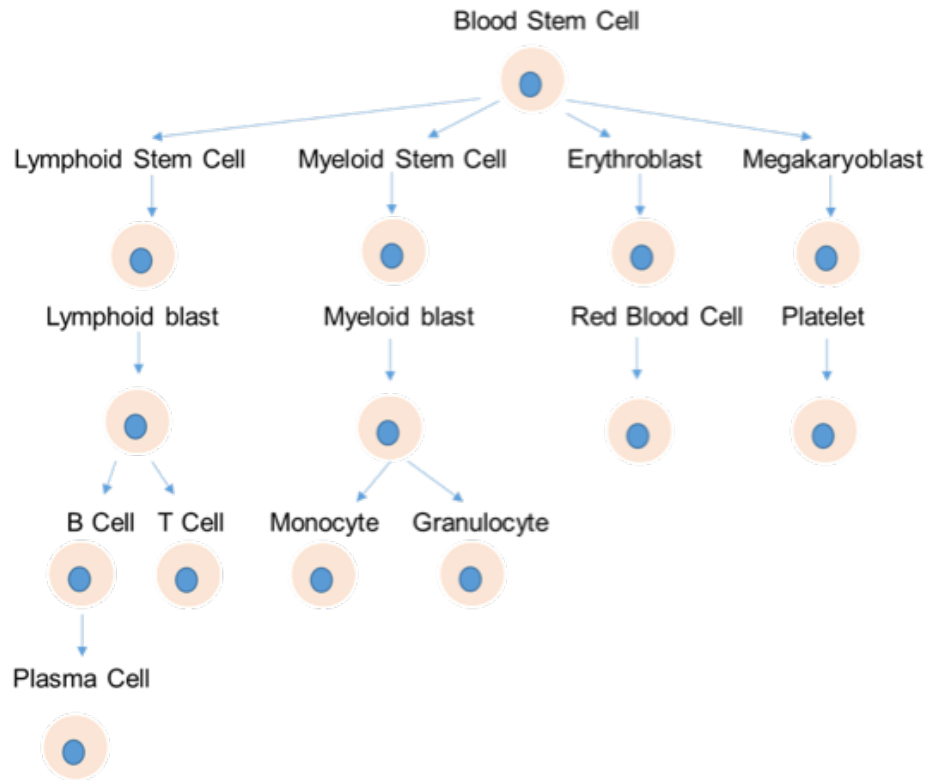


**Figure 1.1 Haematopoiesis in the BM**

*Plasma cells originate from BM blood stem cell. The blood stem cell differentiates first into a lymphoid stem cell, then into a lymphoid blast. Next, the B cell is matured into plasma cells under local stimuli.*

### 1.1.2 MM Stem Cells

The exact MM stem cell (MMSC) phenotype is still not fully determined. For example, clonotypic B cell have been reported to have more clonogenic potential than MM cells and to be able to differentiate into MM cells (Figure 1.2) [7]. Though whether clonotypic B cells are MMSC is still not clear. Moreover, the clonotypic B cell has been reported of responsible for the MM drug resistance [8].

Thus, the MMSC maybe an attractive model for MM disease relapse. In favour of this is the idea that the stem cells are quiescence in nature and thus more resistant to chemotherapy. In addition, the cell that causes relapse must be inherently chemotherapy resistant. Therefore, this argues that as the drugs designed to target MM cells and debunk most of the disease do not target the MMSC, leading to the argument that drugs which target MMSC may prevent relapse and allow this disease to be a curable one.

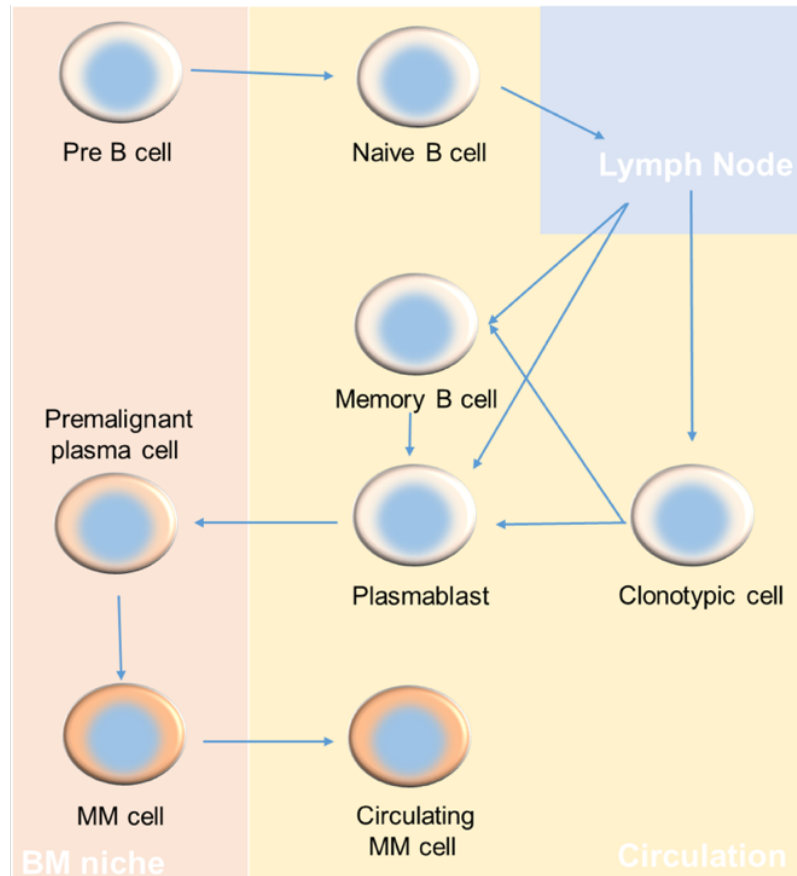


**Figure 1.2 Simplified MM originate.**

*B cell is originated from hematopoietic stem cells in the BM and then Pre-B cells enter the circulation and mature in lymph node. The plasma blast return to the BM, where the malignancy process initiated and proliferate in the BM niche. A small fraction of MM cells will enter the circulation and respond for the relapse. Some of the clonotypic cells arise from the lymph node also have the potential to differentiate to plasma blast.*

### **1.1.3 Plasma Cell Longevity Regulation**

A plasma cells is derived from terminal differentiated B cells. After, a B cell is activated by antigen stimuli and differentiated into short-lived, antibody-secreting plasma blasts, part of which migrate into BM niche and develop into long-lived plasma cells [9]. Contrary to the 1960's concept that plasma cells only survive for a few days in response for an immune stimuli [10-13], there is now accumulating evidence that the plasma cells survive for weeks, months [14-16] or even more than 10 years without memory B cells [17]. One reported mechanism for plasma cell longevity is B lymphocyte-induced maturation protein 1 (Blimp1) linked autophagy and endoplasmic reticulum (ER) function for the plasma cell survival.

Blimp1 is first identified as a transcriptional repressor targeting c-Myc [18], Pax5 [19], CIITA [20], SpiB and Id3 [21]. Blimp1 silences B cell transcription and leads B cell differentiating into plasma cells. Pax5, for example, maintains the identity of mature B cells and Blimp1 upregulation suppresses Pax5 and Pax5 targeted genes, which code for B cell surface receptors, signal transducer and transcriptional regulators in mature B cells. Thus, the Blimp1 upregulation leads to the B cells loss of identity and its transformation into plasma cells [22].

Blimp1 also been reported as a transcriptional activator and Blimp1 upregulation leads to antibody producing in B-lymphoid lineage [23], which lead to the expansion of ER. One of the mechanisms is Blimp1 activated mTOR signalling, which modulates the protein synthesis or the organelle biogenesis in response to stimuli and resulted in enhanced immunoglobulin production [24]. Moreover, Blimp-1 enhances the amino acid level to support the antibody production, through upregulating carriers, such as CD98, and blocking the inhibitory Sestrin–AMPK (5' AMP-activated protein kinase axis)[25]. Through these machineries, Blimp1 supports the antibody production. Upon antibody production, the endoplasmic reticulum (ER) is in stress, as the ER is overloaded with protein for folding, processing and exporting, which lead to the unfolded protein response (UPR). The process for UPR is to halt protein translation, to degrade misfolded proteins, and to activate the chaperones production involved in protein folding. If the UPR could not restore cell normal function, then UPR leads the cells toward apoptosis. UPR also results in the expansion of ER which covers most of the cell [26]. Together, this suggest that Blimp1 regulation affects ER swelling resulting in more antibody folding and export from the cell.

It is interesting to note that autophagy, a self-degradative process, blocks the Blimp1 role of promoting antibody production in plasma cells, as autophagy decreases ER volume and antibody secretion, as well as increase metabolism and survival of plasma cells [27]. The above evidence suggests that Blimp1 links autophagy and ER function for the plasma cell survival. In 1.7.1, I describe the autophagy role in MM survival in details. Overall, Blimp1 mediated plasma cell survival is interconnected with autophagy and ER function and ultimately essential processes for the maintenance and survival of MM cells.

### 1.1.4 MM Diagnostic Criteria

Symptomatic MM follows from a progression starting with monoclonal gammopathy of undetermined significance (MGUS) through asymptomatic MM and then finally symptomatic MM. The International MM Working Group diagnostic criteria for MM and the diagnostic criteria for distinguish different types of plasma cell disorder are shown below (Table 1.1, Table 1.2).

**Table 1.1 International MM Working Group Diagnostic Criteria of MM**

<b>Definition</b>	BM clonal plasma cells >10% or biopsy-proven bony or extramedullary plasmacytoma and any one of the CRAB features and MM-defining events described below
<b>End organ damage</b>	Hypercalcemia: serum calcium >0.25 mM or >2.75 mM Renal insufficiency; creatinine clearance <40 mL/ min or serum creatinine >177ML  Anaemia: haemoglobin value 20 to 100g/L  Bone lesions: one or more osteolytic lesion (skeletal radiography, CT, etc).  If BM <10% clonal plasma cells, more than one bone lesion is required to distinguish from solitary plasmacytoma with minimal marrow involvement
<b>Malignancy biomarkers</b>	>60% clonal plasma cells on BM examination  Serum involved / uninvolved free light chain ratio >100  Involved free light chain: kappa or lambda > normal range  Uninvolved free light chain < normal range  Absolute light chain >100mg/L  More than one focal lesion on MRI > 5mm.

The table was extracted from International MM Working Group [28].

**Table 1.2 International MM Working Group Diagnostic Criteria for Related Plasma Cell Disorders**

<b>Plasma Disorder</b>	<b>Definition</b>
Smoldering MM	Serum IgG or IgA >30g /L, urinary monoclonal protein >500mg /24h, clonal BM plasma cells 10-60% and no MM or amyloidosis.
Non-IgM MGUS	Serum monoclonal protein <30g/L, clonal BM plasma cells <10%, no end-organ damage (hypercalcemia renal insufficiency, etc.), no plasma cell proliferative disorder associated amyloidosis.
IgM MGUS	Serum IgM monoclonal protein <30g/L. No anemia, no constitutional symptoms, no hyperviscosity, no lymphadenopathy, no hepatosplenomegaly, no plasma cell proliferative disorder associated amyloidosis.
Light chain MGUS	Free light chain ratio >1.65 or <0.26 No immunoglobulin heavy chain, no end-organ damage, no plasma cell proliferative disorder associated amyloidosis, Clonal BM plasma cells <10%, urinary monoclonal protein <500mg/24h.
Solitary plasmacytoma	Solitary lesion or soft tissue of bone with clonal plasma cells, normal BM no clonal plasma cells, Spine and pelvis, no end-organ damage, no plasma cell proliferative disorder associated amyloidosis.
Solitary minimal BM involvement	Solitary lesion or soft tissue of bone have clonal plasma cells, clonal BM plasma cells <10%. Spine and pelvis (exception: primary solitary lesion), no end-organ damage, no plasma cell proliferative disorder associated amyloidosis.
POEMS syndrome	Polyneuropathy, monoclonal plasma cell proliferative disorder Major criteria: sclerotic bone lesions, Castleman’s disease, VEGFA levels increasing. Minor criteria: Organomegaly, overloaded extravascular volume, endocrinopathy, skin disorder, papilloedema, thrombocytosis/ polycythemia.
Systemic amyloidosis	AL Amyloid-related systemic syndrome, positive amyloid staining, light-chain-related amyloid, monoclonal plasma cell proliferative disorder.

The table was extracted from International MM Working Group [28].

### 1.1.5 MM Risk Factors

Currently, it is still unknown the causes of MM, but several risk factors have been identified which appear to increase an individual's risk of developing MM as shown in Table 1.3.

**Table 1.3 Possible MM risk factors**

<b>Risk factors</b>	<b>How it affects MM accident</b>
Family history	People have 2-3-fold chance to develop MM or MGUS [29-32] with immediate family members that diagnosed with MM or MGUS.
Lowered immunity	People who take immunity lowering drugs have increased MM accident: Less than 1% who have received an organ transplant develop MM [33-35].  People with human immunodeficiency virus have an increased risk of MM [36, 37] .
medical conditions	Autoimmune condition (Alkylosing spondylitis, autoimmune, haemolytic anaemia, systemic lupus erythematosus pernicious anaemia [38-44].  Genetic condition: [45]
Body weight and diet	Evidence that show diet affect MM risk are weak [46, 47]. Vegetarian diet may lower MM risk [48-51].
Radiation exposure	The risk of MM was increased for personal exposure to UV radiation during adulthood [52, 53].
Chemical exposure	Benzene, a wildly used carcinogen [54-56] has been proved to be a risk factor of MM.

Besides a slight increase in MM incident for the people with immediate family members with MM, the identified MM risk factors are not strongly associated with MM incident. Since, till now, there are no known causes of MM and no strong risk factors that are associated with MM, currently, there is a lack of strategies to prevent the disease.

### 1.1.6 MM genetic abnormalities

Four common methods are used to detect the genetic changes: 1) karyotyping (detect the number and structure of chromosomes); 2) Fluorescence in-situ hybridisation (chromosomes were stained with fluorescent marker to detect and localise the specific DNA sequences on a chromosome); 3) gene expression profiling (to evaluate the activity of genes in a snapshot); 4) next generation sequencing (to determine the precise DNA sequence). The types of genetic abnormalities in MM are listed in Table 1.4.

**Table 1.4 Types of genetic abnormalities in MM**

Genetic errors	Examples
Chromosome abnormalities	Alterations in chromosome number: hyperdiploidy, MM cells have more than two copies of a chromosome [57].  Alterations in chromosome structure:  Chromosome deletion, common chromosome deletions in MM are del(13q) and del(17q) [58, 59].  Chromosome duplication, 1q gain [60].  Chromosome translocation, common translocation abnormalities are between chromosome 4 and 14, known as t(4; 14) or t(11; 14) [60, 61].
Genes that control cell growth	Gene mutation (p53, RAS, et al.) control cell growth in MM patients [62-65].
Epigenetic changes	Histone modification [66, 67]

The development of MM also involves certain germline mutations according to several MM family studies [29-32], including: CDKN2A [68], lysine specific demethylase 1 [69], immunoglobulin VH genes [70], hyper phosphorylated paratarg-7 [71, 72], hyaluronic synthase 1 [73] and a meta-analysis of two genome-wide association (GWA) studies has identified single-nucleotide polymorphisms localising to a number of genomic regions that are robustly associated with MM risk [74]. The above finding confirm that MM is a genetically heterogeneous disease.

Gene mutation is thought to be the critical event for the plasma cells transforming to MM cells and it is becoming apparent that different genetic subtypes of MM maybe more likely to respond to particular chemotherapy drugs [63, 75]. Thus, identifying MM genetic subtype and treating it accordingly, is a possible way to improve the treatment of the disease. In addition, genetic subtype also affects prognosis in patients with MM. Genetic subtype affects how quickly MM may progress and furthermore how likely MM patients will respond to certain treatments. Accordingly, MM subtype is associated with differences in survival rates for patients treated with the disease. The most common MM genetic subtypes are: t(4;14), del(13q), del(17p), 1q21gain, t(11;14), hyperdiploidy [76]. The International MM Working Group defines t(4;14), del(17p), t(14;16), t(14;20), hypodiploidy, and gain(1q)/del(1p) as being high-molecular-risk markers, and defines t(4;14), del(17/17p), t(14;16), t(14;20), nonhyperdiploidy, and gain(1q) as poor prognosis markers [77]. Favourable prognosis markers have also been reported, such as trisomies 3, trisomies 5 [78] and gain of 5(q31) [79] improved outcome with hyperdiploid MM. Other meta-analysis study also confirm that t(4;14), t(14;16), t(14;20), del(17p) and gain(1q21) are poor prognosis markers [80]. These findings confirm that treating MM patients according to their genetic subtype will enhance outcomes.

Genome-wide association studies identified MM risk loci that is related with autophagy [81]. Firstly, dysregulation of autophagy has been identified as contributing with dysregulated B cell differentiation, which increases the MM susceptibility [81]. MM oncogenesis study identified five loci that support IRF4-MYC-mediated autophagy, including eQTL effects WAC (at 10p12.1) and Hi-C looping interactions (at 8q24.21 and 16q23.1). The 7p15.3 association ascribable to rs4487645 has been confirmed to regulate differential IRF4 binding mediated by c-MYC-interacting CDCA7L [82]. These reports confirm that the autophagy may influence B cell differentiation. Secondly, dysregulation of autophagy has been identified as contributing to MM development. Mammalian target of rapamycin (mTOR) is a central regulator of cellular metabolism and contribute to cancer development, which is highly activated in many MM patients [83]. mTOR related genes ATG5 mediated the IRF4-MYC related autophagy, which contribute to the MM development [81]. The above reports point to a relationship between autophagy regulation and MM initiation

and development. Therefore, chemotherapy targeting autophagy may improve the treatment outcome.

## **1.2 Proteasome inhibition in MM treatment**

The main treatment for MM is chemotherapy, including steroids and biological therapy. BM transplant or radiation therapy are also used for the treatment of MM [84]. Besides these treatments, more targeted drugs are being developed and evaluated to treat the MM. For example, one of the mainstays of the MM drugs are proteasome inhibitors (Bortezomib, Carfilzomib or Ixazomib), which prevent proteasomes from breaking down proteins in the cells to inhibit the proliferation of MM cells. However, despite the availability of several different drugs to treat MM at this point in time relapse for patients remains inevitable and MM is still regarded as an incurable disease. We envisage that novel therapeutic approaches will be necessary to cure MM and targeting the environment in which MM proliferates may be one possible target.

The ubiquitin proteasome degradation system is a main cellular pathway to degrade unwanted, misfolded or damaged proteins. The proteasome degradation system is capable of degrading the majority of regulatory proteins in eukaryotic cells, thus regulating many cellular processes, including the regulation of cell cycle, the regulation of DNA repair, apoptosis and responses to oxidative stress [85]. Inhibition of proteasome activity can disrupt normal cellular functions and can induce cell death caused by the accumulation of unwanted proteins [86].

The proteasome is a cylindrical like protein complex that functions through the breaking of peptide bonds. The central pore of the proteasome is formed by four rings and each ring binds with 7 proteins. The inner two rings of the core include 7  $\beta$  subunits with protease active sites on the interior surface of the two rings, and this is the degradation site for targeted proteins. The outer two rings contain  $\alpha$  subunits, which form the entering site for the targeted proteins. To initiate the ubiquitin proteasome degradation process, poly-ubiquitin tags are first attached to targeted proteins, then the  $\alpha$  subunits in the outer two rings of the proteasome bind to "cap" structures or regulatory particles that recognize the poly-ubiquitin tags. After the

binding of ubiquitin and proteasome, the protein is lead to the two inner rings of the proteasome and the protein degradation process is initiated.

Cancer cells are more sensitive to proteasome inhibitor induced apoptosis than non-malignant cells because cancer upregulates proteasome activity in order to cope with oncogene activation and up-regulated metabolism [87]. MM is particularly dependent on the ubiquitin-proteasome system as a mechanism to avoid over produced misfolded protein accumulation in the endoplasmic reticulum and prevent ER stress induced cell death. Thus, MM cells are particularly sensitive to treatments that target the proteasome.

20S subunit is the core of proteasome activation, which exhibits three enzymatic activities: chymotrypsin-like, trypsin-like and post-glutamyl peptide hydrolase-like [88]. The 20S subunit has been the main targeting site of many of the therapeutic proteasome inhibitors. Proteasome inhibitor treatment is widely used in the MM therapy [89], and these induce accumulation of proteins which in turn activates the apoptotic cascade, growth arrest and cell death. The main proteasome inhibitors are described below.

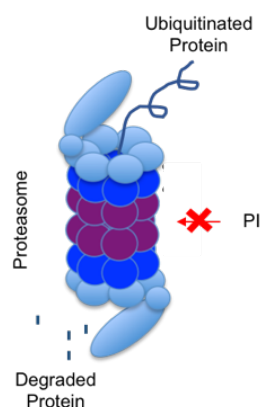


**Figure 1.3 Schematic representation of proteasome function and mechanism of PI**

*Proteasome recognise ubiquitin tagged protein and degraded the protein. PI binding to proteasome and inhibit the process.*

### **1.2.1 Proteasome inhibitor bortezomib (Bz)**

Bz (PS-341, Velcade) was the first proteasome inhibitor clinically used for MM, which is administered via subcutaneous injection. Bz belongs to the peptide boronic acid

analogues and reversibly binds to the chymotrypsin-like site in the 20S core of proteasome [90, 91]. Bz is an established therapeutic drug used in the treatment of MM patients for first line and relapsed or refractory MM [92-94]. It may also be used for maintenance treatment once remission of the MM has been achieved [95]. Many reported mechanisms of Bz effect on MM cells (Table 1.5).

**Table 1.5 Reported mechanisms of action for bortezomib in the treatment of MM**

<b>Mechanism of Action of Bortezomib</b>	<b>Reference</b>
Induce apoptosis.	[96]
Induce NF-kB activity.	[97]
Reduce adherence of MM cells to BMSC.	[98]
Block VEGF, IL-6, Ang-1, Ang-2, and IGF-1 secretion in BMSC.	[99].
Alter expression of proangiogenic mediators and tumour suppressor p53.	[100, 101].
Trigger the differentiation of MSCs into osteoblasts and induce apoptosis of osteoclast.	[102]
Bz disrupts the unfolded protein response by increasing the endoplasmic reticulum (ER) stress in MM cells caused by high production of immunoglobulins.	[103, 104].

### **1.2.2 Proteasome inhibitor carfilzomib (Cfz)**

Carfilzomib (PR-171) is a proteasome inhibitor which belongs to epoxy ketone class of drugs and irreversibly binds to the chymotrypsin-like site in the 20S core of proteasome [105]. Cfz is administered via intravenous infusion, in the clinic. Unlike Bz, Cfz has minimal activity against off-target enzymes and has demonstrated clinical activity against Bz-resistant MM cells [92, 94, 106].

### **1.2.3 Proteasome inhibitor ixazomib**

Ixazomib is the first clinical oral PI and can be used as a single reagent [107]. Similar to Bz, Ixazomib is a peptide boronic acid analogue [108], which is designed to be administered via oral to improve treatment compliance. For example, the Bz administration is associated with the risk of peripheral neuropathy and the Cfz administration requires twice-weekly IV infusion [107, 109]. Oral PI Ixazomib is not

only convenience for the drug administration, but also is more tolerable for prolonged therapy.

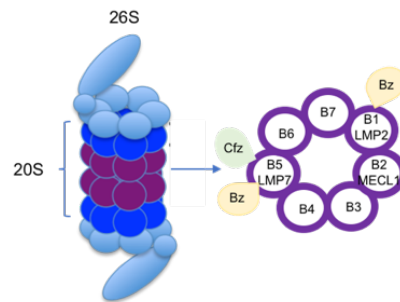


**Figure 1.4 Schematic representation of mechanism of PI**

*Present the binding position of Bz and Cfz on the PI.*

### 1.3 Metabolic change in MM cells

Cancer cells undergo metabolic rearrangements to meet the bioenergetic and biosynthetic demands for proliferation and drug resistance [110]. Increased aerobic glycolysis and decreased oxidative phosphorylation are common metabolic shifts in cancer cells and are thought to support the bioenergetics demands of the tumour. In addition, cancer cells shift other metabolism enzymes including, succinate dehydrogenase, fumarate hydratase, and pyruvate kinase and isocitrate dehydrogenase to produce more biosynthetic intermediates to support tumoural biosynthetic demands. Taken together these findings demonstrate cancer to be a ‘metabolic disease’.

MM cell expansion and paraprotein production places huge energy demands on the malignant plasma cell. Glucose and glutamine metabolism shift have been described in MM cells as supporting the tumoural energy requirements, with both playing roles in drug resistance, proliferation and apoptosis [111]. MM upregulate glucose metabolism to favour progression [112], which lead to the therapy strategy of inhibit the glucose metabolism to prevent MM progress and inhibitors that targeting Hexokinase II (HKII) activation show promising outcomes. The first step of glycolysis relies on the enzymes of hexokinase family to convert glucose into glucose-6-phosphate. HKII activation needs the binding of the voltage-dependent anion channel (VDAC), which is located on the outer membrane of mitochondria. HKII is stabilised

by phosphoinositide-3 kinase (PI3K)/Akt signalling, which lead the design of inhibitors that targeting PI3K to inhibit the HKII and autophagy as well to treat MM.

MM cells also upregulate glutamine metabolism. Ammonia (converted from glutamine) levels have been identified to be constantly high in MM cells, which reflects the shift of glutamine metabolism [113]. Glutamine is a precursor of GSH and is regulated by the NRF2 pathway (the detailed mechanism is described in the 1.7 the role of NRF2 part) [114]. GSH is an important cellular antioxidant and is also consumed in the protein folding correction event. As the MM cells produce large amount paraprotein, which need to be folded in the ER causing ER stress, the NRF2 regulated glutamine metabolism is essential to release the ER stress and prevent ER stress induced apoptosis.

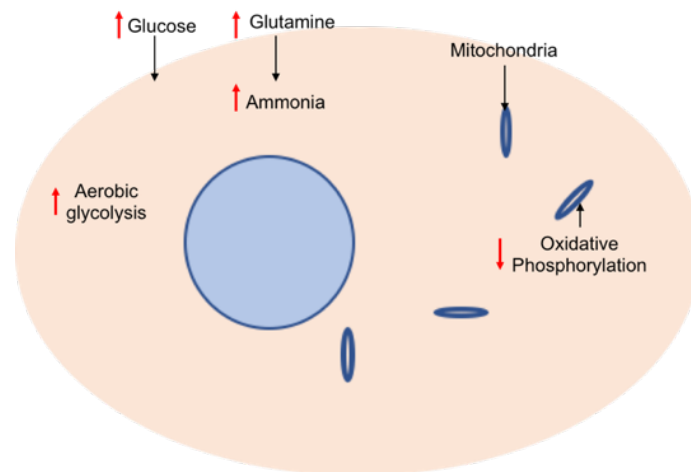


**Figure 1.5 Schematic representation of metabolic change**

MM cells upregulate aerobic glycolysis and glutamine metabolism, while down regulate oxidative phosphorylation.

#### **1.4 Reactive oxygen species (ROS) role in MM malignancy**

MM cells function to produce large amount of monoclonal immunoglobulin and/or light chain protein, one cellular consequence of this is to lead to cellular stress through induction of ROS [115]. Conversely ROS is believed to be a key player in disturbing intracellular protein synthesis in the MM cells. Topf and colleagues have shown that ROS production from external stimuli or from mitochondrial pathologies negatively affects protein synthesis [116] and in turn this reduces the MM cells capacity to maintain proteins synthesis for cell growth, proliferation and paraprotein production. Mechanistically cellular stress regulates translation, such as misfolded protein induced

stress in the ER, UV irradiation, amino acid starvation, hypoxia, viral infections and oxidative stress [117]. Besides that, ROS is involved in regulation of cell survival. While in redox homeostasis cellular, ROS maintains the proper function of redox-sensitive signalling proteins, which enables the cellular response to endogenous and exogenous stimuli; in redox unbalanced cells, oxidative stress may lead to aberrant cell death and tumour growth [118]. In summary tumour cells are characterised by enhanced oxidative stress and metabolism due to oncogene activation, they possess higher level of ROS and lower levels of antioxidant molecules than non-malignant cells, leading cancer cells more vulnerable to ROS induced cell death. Thus, suggesting that targeting ROS in the treatment of MM is a potentially viable strategy.

#### **1.4.1 Sources of ROS**

To lead us to therapeutic interventions targeting the ROS pathways we must first understand the processes which regulate ROS in MM. Reactive oxygen species (ROS) and reactive nitrogen species (RNS) are free radicals that are derived from both endogenous sources and exogenous sources. The endogenous sources of free radicals include mitochondria, peroxisomes, endoplasmic reticulum and phagocytic cells. The exogenous sources of free radicals include pollution, alcohol, tobacco smoke, heavy metals, transition metals, industrial solvents, pesticides and certain drugs like halothane, paracetamol and radiation.

Mitochondria is the main source of reactive oxygen species (ROS), which contribute to mitochondrial damage in a range of pathologies and retrograde redox signalling in cells [119, 120]. Complex I (NADH dehydrogenase) and complex III (ubiquinone cytochrome c reductase) are the two major sites in the electron transport chain that produce superoxide radicals. Mitochondrial superoxide dismutase converts superoxide anions to hydrogen peroxide. Monoamine oxidase,  $\alpha$ -ketoglutarate dehydrogenase and glycerol phosphate dehydrogenase in the mitochondria also contribute to the ROS production. Furthermore peroxisomal enzymes (acyl CoA oxidases, D-amino acid oxidase, L- $\alpha$ -hydroxy oxidase, urate oxidase, xanthine oxidase and D-aspartate oxidase), which degrade long chain fatty acids, produce ROS [121]. In the mitochondria, the peroxisomes generate  $H_2O_2$  in the reactions that transfer electrons to oxygen.

The endoplasmic reticulum is another source of ROS [122]. For example, when the proteins are folded in ER to form the disulfide bonds from cysteine,  $H_2O_2$  is generated.  $H_2O_2$  is a source of ROS. Moreover, to correct an improperly paired disulfide bonds, the antioxidant GSH is consumed, which further increases the ROS stress in MM [123].

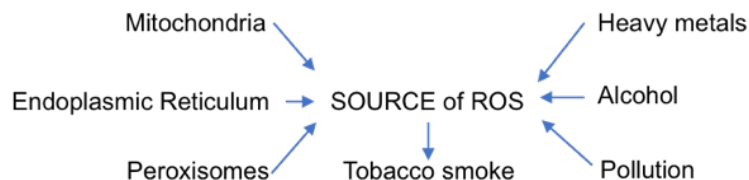


**Figure 1.6 Schematic representation of the source of ROS**

*Endogenous sources of ROS include heavy metals, alcohol, pollution and tobacco smoke et al. Exogenous sources of ROS include mitochondria, ER and peroxisomes.*

### 1.4.2 Cellular toxic effects of ROS

As ROS is highly reactive, elevated ROS levels disturb the cell fate through damaging essential biomolecules such as, nucleic acids, proteins, and lipids [124].

#### Nucleic Acids

All components of DNA such as purine and pyrimidine bases, deoxyribose sugar backbone are sensitive to ROS, especially the  $OH^\bullet$  radical [125]. ROS induces nucleic acid mutations including single and double stranded breaks in DNA. When under ROS stress, the mitochondrial DNA show more mutations than nucleic DNA. This is postulated to be because the mitochondrial DNA are co-located to the main ROS source in the cells [126].

The RNA molecule is more sensitive to ROS than DNA. RNA is single stranded and there are no repair mechanisms to manage damage. Furthermore the RNA are also located closer to the ROS source than DNA [127].

#### Protein

The oxidation of proteins can be induced by both radical species including  $O_2^{\bullet-}$ ,  $OH^\bullet$ , peroxy, alkoxy, hydroperoxy as well as non-radical species such as  $H_2O_2$ ,  $O^3$ , and singlet oxygen [128]. Oxidized amino acids form protein–protein cross linkages, which results in protein, receptors/ transport protein and enzyme protein malfunction

[129]. The amino acid residues lysine, proline, threonine and arginine are the most sensitive to ROS stress.

### **1.4.3 ROS stress and malignancy**

ROS induced DNA damage is considered to be the major event of cell oncogenesis [130]. Patients with cancer associated risk disorders have been observed to have elevated ROS induced DNA damage level or deficient in DNA damage repair system. For example, patients with Li-Fraumeni syndrome, which is an inherited cancer predisposition disorder, carries TP53 mutation. Impaired p53 activation associate with increased oxidative stress, which leads to oxidative DNA damage, and may lead to genomic instability and initiate the cancer [131].

One of the major mutations induced by ROS is through the ROS triggered guanine modification, causing G→T transversions [132]. If the mutation site is in oncogenes or tumour suppressor genes, the cells may subsequently initiate malignancy and cancer progression. For that reason, ROS are both involved in the initiation and progression of cancer.

### **1.4.4 Therapies targeting ROS**

Proteasome inhibitors induce MM apoptosis partly through increased intracellular oxidative stress by elevating endoplasmic reticulum stress [133]. Reports show that proteasome inhibitors repress transcription of the mitochondrial thioredoxin reductase, which directly induces oxidative and endoplasmic reticulum stresses in MM cells [133-135]. ROS generation plays a critical role in the apoptosis induced by the proteasome inhibitor Bz, as evidence by the observation that the disruption of mitochondrial function and the induction of apoptosis can be almost totally rescued by ROS scavengers [136]. Modalities (i.e., radiation, photodynamic therapy, and specific chemotherapeutic drugs) generating ROS have been shown the therapeutic effect on malignant B-cells [137]. As MM cells undergo ER stress induced by the accumulation of misfolded protein, the role of ROS in ER stress induced cell death is another focus in this project. In addition, I will study mitochondrial function in the MM cells to elucidate the mechanisms by which MM cells interact with BMSC to reduce intracellular and mitochondrial ROS levels in malignant plasma cells to escape cell death.

If manipulation of the cellular response to oxidative stress is to be therapeutically exploited in MM therapy, then strategies need to be developed from a scientific understanding of these interactions.

### 1.5 The role of NRF2

NRF2 is tightly regulated while bound to KEAP1 in the cytoplasm. As KEAP1 is the sensor of cellular oxidative stress, NRF2 nuclear translocation is considered to be an indicator of ROS stress. As my project is targeted to the ROS induced cell stress response and apoptosis, I will investigate NRF2 function in MM cells under normal conditions and in response to MM chemotherapy.

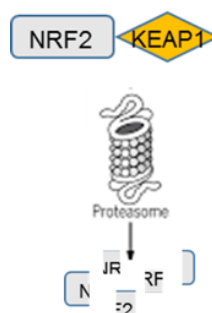


**Figure 1.7 Schematic representation of the KEAP1 mediated NRF2 degradation**  
*KEAP1 binding to NRF2 protein then initiate the proteasome degradation process.*

Nuclear factor (erythroid-derived 2)-like 2 (NRF2) is the key regulator for cellular antioxidant defence and ROS is the key activator of NRF2 [138]. Under normal condition, Kelch-like ECH-associated protein 1 (KEAP1) binds to NRF2 and facilitates the ubiquitination and degradation of NRF2 through proteasome [139]. When cells is in oxidative stress, ROS levels is increasing and the cysteines in KEAP1 been modified to form disulfide bond, which changes the conformation of the hinge region by thiol oxidation and releases the NRF2 [140]. NRF2 is then modified by PKC $\delta$  and Akt and translocated to the nucleus [140]. In the nuclus, NRF2 binding with small Maf proteins, and then active many gene promoters that contain the antioxidant response element (ARE) sequence [141]. NRF2 binding to ARE requires cAMP responsive element-binding protein-dependent acetylation [142]. NRF2 activates cytoprotective genes through binding to a cis-acting enhancer sequence upstream of the antioxidant response element, [143], which are present in the promoter regions of its target genes [144]. These genes include Nicotinamide adenine dinucleotide phosphate (NADPH) or nicotinamide adenine dinucleotide hydride (NADH): quinone

oxidoreductase 1 (NQO1), Glutamate-cysteine ligase (GCLM), Heme oxygenase (HO-1), as well as proteins involved in scavenging ROS and glutathione (GSH) biosynthesis and regeneration. Mitochondria is the main cellular ROS producer and NRF2 regulates substrate availability for mitochondrial respiration, which may affect mitochondrial ROS production [145].

**Table 1.6 List of NRF2 targeted antioxidant related genes and their general function**

NRF2 target genes	Functions
Superoxide dismutase 3	ROS catabolism [146]
Glutathione peroxidase	ROS catabolism [147]
Peroxiredoxin	ROS catabolism [148]
Glutathione reductase	Regeneration of oxidized factor [149]
Thioredoxin reductase	Regeneration of oxidized factor [150]
Glutamate-cysteine ligase	Synthesis of reducing factor [151]
Glucose-6-phosphate dehydrogenase	Synthesis of reducing factor [152]
Phosphogluconate dehydrogenase	Synthesis of reducing factor [153]
Heme oxygenase	Stress response protein [154]
p62	Autophagy [155]

### 1.5.1 NRF2 regulated glutathione system

Gene promoters that contain the ARE sequence include many of those involved in xenobiotic response and Phase II metabolism, as well as glutathione (GSH) biosynthesis and recycling (Diagram shown in chapter3 discussion 3.37).

GSH is one of the most abundant endogenous antioxidants in cells. GSH can be detected in nearly all types of cells in the body. When GSH is activated, the concentration of GSH can achieve millimolar level. GSH works together with glutathione reductase, glutathione peroxidases and glutathione S-transferases to form the glutathione system for ROS detoxification. First, glutathione S-transferases triggers the joining of GSH to a variety of electrophilic compounds and then GSH is oxidized to glutathione disulfide. The glutathione peroxidases breakdown the by-

products of these reactions, hydrogen peroxide and organic hydroperoxides [156] Glutathione reductase reduces glutathione disulfide back to GSH. Through this cycle, GSH reduce disulfide bonds to cysteines.

GSH has been reported to be involved in many cellular defence events, such as antioxidant defence, detoxification of electrophilic xenobiotic, redox regulated signal transduce regulation, cysteine pool, cell proliferation regulation, deoxyribonucleotide synthesis regulation, immune responses regulation, leukotriene regulation and prostaglandin metabolism regulation [157].

As an acetylated cysteine residue, N-acetyl-cysteine (NAC), is a rate-limiting substrate for GSH synthesis [158]. NAC is an effective scavenger of ROS and a major pool of cellular cysteine. NAC is widely used in clinic and research to manage the effects of ROS stress. Combining NAC with stimuli to replenish GSH levels is an established way to investigate GSH function.

Under ROS stimuli, most of the GSH is in the reduced form because of upregulated glutathione reductase activation in cells. Thus, detection of GSH is a reliable way to determine the state of cellular oxidant levels. Glutathione S-transferases are also observed to be overexpressed in many tumours, where they appear to functionally regulate MAPK pathways and are reported to be involved in chemotherapy resistance [159].

### **1.5.2 NRF2/HO-1 system**

Heme oxygenase-1 (HO-1) and HO-2 are two HO isoforms found in mammals. While HO-2 is expressed constitutively in cells, HO-1 is an inducible 32-kDa protein. Inducers of HO-1 include: heme, ROS, heavy metals, growth factor, cytokines, modified lipids [160].

HO-1 catalyzes heme degradation and produces iron ions, biliverdin and CO. As an antioxidant, biliverdin regulates inflammation, apoptosis, cell proliferation, fibrosis, and angiogenesis. Through the Fenton reaction, iron facilitates ROS generation and is involved in many enzyme activities as a core element. CO is also reported to be anti-apoptotic, anti-proliferative and anti-inflammatory.

As HO-1 expression is inducible and the HO-1 gene is activated by the NRF2, HO-1 levels can be used to determine the activation of NRF2.

### **1.5.3 NRF2/ NQO1 system**

As a metabolizing enzyme, NQO1 protects normal cells from ROS induced stress. NQO1 catalyzes two-electron reduction of quinones to hydroquinone, which is then conjugated and excreted. NADH or NADPH are the electron donor for NQO1 reaction. NQO1 supports the cancer cell in coping with high ROS levels. Upregulated NQO1 expression is linked with many human malignancies and linked with cancer progression and chemo-resistance.

### **1.5.4 NRF2-P62-autophagy axis**

P62 is a autophagy receptor with multiple signaling moieties, including ZZ-type zinc finger domain, nuclear localization signals, nuclear export signal and KEAP1 interacting region [161]. Thus, P62 linked autophagy regulates many signaling pathways, such as, NRF2, NF-kB and mTOR [162]. Besides that, P62 links autophagy and redox homeostasis. That is because KEAP1 has two roles which are 1] modify P62 to form autophagosome and 2] regulating the NRF2 ubiquitination for proteasome degradation. When cells are under stress conditions, P62 recruits KEAP1 to active autophagy, which leads to the accumulation of NRF2 as a result of lack of KEAP1 regulated NRF2 degradation [163, 164]. The activated NRF2 then enters the nucleus and promotes the expression of P62, which forms a positive feedback loop in response to cellular stress. In my project, I silence the NRF2 in cells, to test if it can break the feedback loop and sensitise the MM to apoptosis. Because KD NRF2 impairs the cellular antioxidant responds, which leads ROS stress and ROS induced apoptosis, and impairs P62 mediated autophagy, which block the cells to clear away unwanted cellular components and leading to cell death.

### **1.5.5 Other NRF2 associated transcription Factors**

NRF1 regulates mitochondrial respiration, mitochondrial DNA transcription and replication through activation of the expression of a number of metabolic genes. NRF1 works together with NRF2 (see below) to active the expression of nuclear-encoded ETC proteins, mitochondrial transcription factor A and mitochondrial transcription factor B1 and B2. Together these proteins regulate nuclear and mitochondrial genomes

and regulate the three mitochondrial-encoded COX subunits. Through the above regulation NRF1 links together nuclear DNA synthesis and mitochondrial function.

NRF1 is indispensable for mice normal development and healthy growth of cells, as Jefferson reported that homozygous NRF-1 mutant mice are embryonic lethal [165] but NRF2 is indispensable for mice development, as Chan reported that the homozygous NRF-2 mutant mice reached adulthood, and reproduced [166]. These studies suggest that NRF1 plays a distinctive role from NRF2 for the regulation of cellular homeostasis and organ integrity [167].

The exact mechanisms of NRF1 regulation are not fully understood, since NRF1 mutant mice die in utero. Some studies show that NRF1 regulate ATPase protein p97/VCP which is associated with various cellular activities. NRF1 also appears to regulate the proteasome 26S subunit transcriptional expression. When the cells have been treated with PI, NRF1 support the recovery of proteasome pathway through upregulation of proteasome 26S subunit transcriptional expression [168, 169].

Since NRF1 is localized in the cytoplasm and is bound to the ER membrane, NRF1 nuclear translocation is considered to be an indicator of ER stress. NRF1 is phosphorylated by Cyclin D1-dependent kinase and the regulation of NRF1 is independent of Keap1, which suggests that either NRF1 does not respond directly to ROS stimuli or NRF1 utilizes other factors to sense ROS levels in the cells.

NRF3 and NRF1 proteins were identified many years ago, however compared with NRF1, the NRF3 transcriptional response to oxidative stress and the NRF3 function are less well understood.

NRF3 is a glycoprotein that binds to the ER and the nuclear membrane. Three NRF3 isoforms have been identified with the A form being glycosylated and the B and C forms being un-glycosylated. This observation suggests that the membrane binding and releasing of NRF3 is mediated by the glycosylated A form. However the detailed function of the three isoforms appear to be poorly understood at present.

NRF3 has a similar structure to NRF1. NRF3 function in some respects is thought to be similar to NRF1. Like NRF1, NRF3 is not activated by ROS, however, unlike

NRF1, NRF3 has been reported to repress transcription of ARE-regulated genes in human cells [170]. In this paper the authors report that NRF3 disturbs the binding of small Maf proteins to the ARE and thus negatively regulates ARE-mediated NQO1 expression.

NRF3 has been detected with high levels in mammalian placenta and the B cell lineage, which suggest NRF3 may play a role in the B cell maturation, However in an experimental knockout of NRF3 in mice, the animals show no difference compared to wild type in phenotype, fertility, gross anatomy and behaviour which suggests redundancy in its mechanism or the presence of compensatory pathways [171].

### **1.6 The role of autophagy in MM progression**

As MM cells produce large amounts of paraprotein, the cells are under constant stress conditions due to the misfolding of protein. There are 3 main mechanisms for the cells to manage this, including the ubiquitin-proteasome pathway, unfolded protein response pathway and autophagy.

Autophagy is a cellular way to degrade or recycle unnecessary or dysfunctional components, such as defective organelles, protein aggregates, and intracellular microbes [172]. There are three types of autophagy has been investigated in detail that are include macroautophagy, microautophagy, and chaperone-mediated autophagy. macroautophagy, microautophagy, and chaperone-mediated autophagy. In my project, the macroautophagy is investigated. Macroautophagy involve double-membraned vesicle (autophagosome), which later infuse with lysosome and be degraded and recycled.

The concept that views autophagy as a bulk degradation process has changed, instead, more reports show that the autophagy is selective [161]. Selective autophagy targeting different cellular components for degradation, for example, organelles (mitophagy and pexophagy), ribosomes, macromolecular, specific proteins or protein aggregates. P62 is a key selective receptor, which is binding both with LC3B and ubiquitin to form autophagosome for degradation [173].

Once formed the autophagosome, it is then fused with lysosomes to initiate phagosome degradation. As described before, NRF2-P62- autophagy forms a positive loop to upregulate autophagy as a mechanism to reduce cellular oxidative stress.

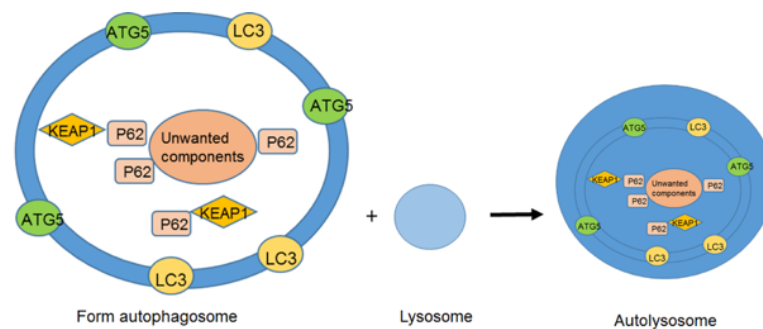


**Figure 1.8 Schematic representation of the autophagy regulation**

*P62 is modified by KEAP1 and then binding to the unwanted components. ATG5 and LC3 are building blocks to form the autophagosome.*

Autophagy is a cellular event of adaptation to stress and promote cell survival, but autophagy also promotes cell death. In addition, autophagy plays a key role in memory B cell and long-lived plasma cell survival [174]. As primary MM cells shows upregulated autophagy [175], it is reasonable to hypothesise a pro-tumoural role for autophagy in MM cell proliferation and drug resistance in the BM microenvironment.

Autophagy has both positive and negative effects on cell function and survival. On the one hand, highly activated autophagy has been reported to suppress tumours or MM [176], through the initiation of cell death and senescence [177]. On the other hand, autophagy is beneficial for tumour or MM [178] maintenance and progression [179]. Autophagy is also increasing the sensitivity of MM cells to PI treatment [155]. As PI is the corner stone of MM treatment, the combination of autophagy inhibition and PI treatment may provide new therapy strategy. Thus, reveal the mechanism of autophagy regulation in MM and its microenvironment is in need.

### **1.7 Sub Cellular Organelles Stress Associated Apoptosis**

Organelles in the plasma cell include lysosomes, mitochondria and the endoplasmic reticulum, which have been investigated for their roles in MM disease progression and chemotherapy resistance in this project.

During apoptosis, intra-nuclear chromatin change is widely accepted as the crucial event, but changes in the cytoplasmic compartment and altered organelle structure and function [180] also play essential roles in the initiation of programmed cell death [181, 182]. For example, 1) cytoskeleton reorganization, with fragmentation of the microfilament bundles [183] and the formation of actin and tubulin thick bundles [184], facilitate the shrinkage of the cells during apoptosis; 2) enlarged and swollen ER in cancer cells [185]; 3) Golgi apparatus, as an oxidative stress sensor [186], undergoes fragmentation, swelling and distension [184, 186, 187]; 4) the lysosomes, key role for cellular degradation, cause increased membrane permeabilization and stimulate the release of apoptosis promoting factors such as BCL-2 family members, which in turn regulate mitochondria function [188-191]; 5) permeabilization of mitochondrial membranes plays a key role in cell apoptosis as well as the regulation of mitochondria mass, mitochondria translocation and mitochondria membrane potential [192-195]. Accordingly, in this project, ER stress, mitochondria stress and lysosome associated autophagy are investigated to decode the mechanisms of how MM cells utilise the BMSC to avoid apoptosis induced by chemotherapy, through mitochondrial and endoplasmic reticulum interaction, which exchange calcium or lipid. [196-199].

### **1.7.1 Endoplasmic reticulum (ER) stress associated apoptosis**

ER is an organelle in eukaryotic cells that form a membrane enclosed network. As a vesicular system, ER is connected with the outer nuclear membrane and mitochondria, forming a tube or sac like membrane enclosed network in eukaryotic cells. This system is intimately involved in  $\text{Ca}^{2+}$  homeostasis and xenobiotics detoxification [200]. There are two types of ER, the rough ER located in the outer side of the cell and embedded with ribosomes for the protein synthesis, and the smooth ER not embedded with ribosome which functions as a site for lipid manufacture and metabolism.

When the ER is under stress (for example when the MM cells produce large amount of paraprotein) the ER initiates the unfolded protein response (UPR). There are 3 pathways that regulate UPR responds. The UPR function to: 1) preventing the translation of protein to restore normal cell function; degrading misfolded protein to clear away unwanted protein aggregation; 3) initiating the production of molecular chaperones used for the correct folding of protein.

Activating transcription factor 6 (ATF6) is a transmembrane transcription factor. Misfolded protein in the ER will cleave the ATF6 and activate the transcription of ER chaperones. Inositol-requiring enzyme 1 (IRE1) is a transmembrane protein, which sense the ER stress and active RNase activity, leading the upregulation of ER chaperones. ER stress also induce protein kinase RNA-like endoplasmic reticulum kinase activation, which inhibit the protein synthesis and active activating transcription factor (ATF4). If the UPR cannot resort the normal cell function, then CHOP mediated apoptosis is initiated.

In MM cells, the large amount of paraprotein production induces the UPR, and eventually if the UPR cannot restore the normal function of the cell, the ER will initiate ER associated apoptosis that is mediated by CHOP expression. Through ER stress in myeloma has been investigated, the drugs to targeting ER stress and sensitise MM cells to chemotherapy is still in need for investigate.

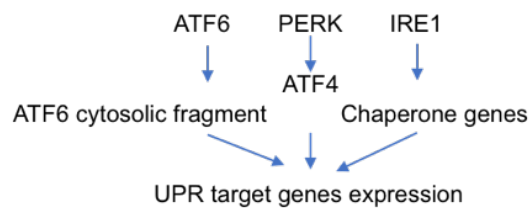


**Figure 1.9 Schematic representation of the UPR pathway**

*While ER is in stress, three pathways are involved in the UPR activation.*

## 1.8 The MM Bone Marrow (BM) Microenvironment

It is clear that the non-malignant cells of the BM interact with MM cells and support their survival, proliferation and drug resistance [201-203] via an interplay of cytokines, chemokines, adhesion molecules and proteolytic enzymes [204]. These supporting cells are known as the BM microenvironment. As the BM niche is the location for the malignant plasma cells and in other contexts the BM microenvironment has been shown to be protective to BM resident cells, then I hypothesise that drug targeting of the MM BM niche may improve the treatment of MM.

Targeting the cells of the BM microenvironment, which provides the protective niche for malignant plasma cells, may provide opportunities to eradicate residual disease

and prevent relapse. Accordingly, to realise this opportunity it will be important to decode the mechanisms of the interaction between MM cell and BM niche, to decode how BM niche supports the proliferation and drug resistance of MM cells and to find new strategy to induce apoptosis in MM cells or sensitise the MM cells to chemotherapy.

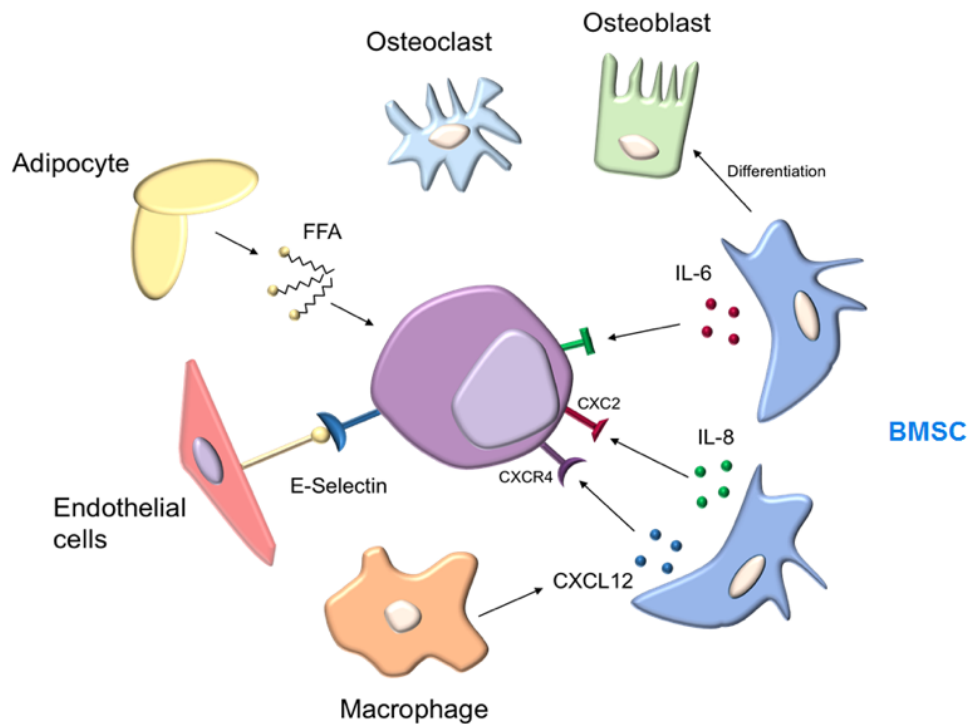


**Figure 1.10 Schematic representation of the BM microenvironment**

*MM cells are connected with different cell types in the BM microenvironment. For example, adipocyte provides nutrition, BMSC secrete IL-8 or IL-6 to support the proliferation of MM cells.*

### 1.8.1 Components of MM BM Niche

Bone is composed of two organ systems, the skeleton and the haematopoietic BM. Endocrine, paracrine and autocrine factors regulate the marrow cells to remodel bone and regulate haematopoiesis [205]. The BM contains several cell types, such as haematopoietic stem cells (HSC), bone marrow stromal cells (BMSC), BM adipocytes, resident tissue macrophages, neurons, osteoblasts, endothelial cell and immune cells [206]. All the cell types are tightly regulated to maintain a healthy BM niche. For example, the regulation of osteoblast and osteoclast activity is fundamental for normal bone health. Increased osteoclast activity initiates bone resorption and it is triggered and regulated by many factors including IL-6, IL-1b, tumour necrosis factor (TNF)- $\alpha$ ,

parathyroid hormone-related protein, macrophage inflammatory protein-1a, RANK, RANKL, osteoprotegerin and annexin II [207, 208]. Decreased osteoblast activity is associated with reduced new bone formation. It is evident that the different cell types in the BM need to be tightly regulated to maintain the normal bone function.

### **1.8.2 Metabolic Changes in the MM BM Niche**

Cancer is associated with local and systemic metabolic changes [209-211]. Otto Warburg first proposed that dysfunctional cellular respiration initiates all cancers [212]. He found out that impaired respiration initiates cancers and glycolysis compensate the cellular energy need. This phenomenon is described as the ‘Warburg effect’ [213]. Accumulating studies confirm that in cancer cells electron transport may not be coupled to ATP synthesis [214] and any mitochondrial defect that would impair respiration contribute to Warburg effect thus leading to carcinogenesis [214, 215]. These findings point out the metabolic change is a key player in cancer initiation.

Metabolic change is also reported as important in the early events of MM genesis [216]. For example, patients with Gaucher disease exhibit over 30-fold risk of developing MM [217]. Gaucher disease is an inherited metabolic disorder characterized with high level lyso-glucosylceramide, which support B cells and promote plasma cell differentiation [217]. These findings suggest that the metabolic rearrangement is an important MM initiation factor.

Moreover, metabolic change in BM niche is also thought to be a contributing factor in the progression of MGUS to MM [218]. Ludwig et al discovered that most of the metabolic rearrangement is detected in the development of MGUS patient not in the progress of MM patient [219]. Other reports show that the metabolic change of BM microenvironment is independent of MM cells [104, 107,108]. These findings provide further evidence that metabolic change in BM is an important MM initiator.

According to above research, drugs targeting metabolic in MM may provide new therapy strategy for the treatment of MM [112]. As the two most studied metabolic rearrangement are in glucose and glutamine metabolism [220], drugs targeting these two metabolic processes are promising, for example, drugs that targeting HKII, which is the first enzyme to catalyse the glucose metabolism, is currently in clinical trial for MM treatment.

The metabolic changes between healthy and MM cells are as described below.

1) Anabolism is a process to synthesis complex molecules, which requires energy. Anabolism is the building-up aspect of metabolism. Anabolism is a cellular metabolic process to synthesize molecules, which is essential for cell proliferation and tumour growth. Thus, to detect the anabolism in the MM cell BM microenvironment is an effective way to determine the MM cell effect on their niche metabolism. Decreased anabolism was detected in the MM patients' BM that include essential amino acids, isoleucine and threonine, as well as the hypoxanthine and xanthine, which are fragments of nucleotide. Since the MM cells proliferate in the BM niche, it is reasonable to suggest that the decreased anabolism in BM is to facilitate the anabolism of MM cells [219].

2) Compared to healthy patients, majority of MM patients are detected with high level of uric acid [221]. Uric acid is the end product of nucleic acid metabolism [222]. During the proliferation of cancer cells, the serum uric acid level is increasing. And others show that high level serum uric acid is associated with cancer progression [223].

3) Reports show that the metabolism of hypoxanthine to xanthine is increased in the MM patients' BM [219]. Hydrogen peroxide (a by-product of hypoxanthine metabolism to xanthine) is detected in MM patient's BM [219].

4) Finally, hypoxia induced glycolysis upregulation is believed to promote cancer growth and development. Glycolytic metabolism is high in BM niche, due to its hypoxic nature [224]. High level glycolytic metabolism facilitates and maintains quiescent haematopoietic stem cells [205, 225, 226], thus contributing to MM relapse and drug resistance [227]. MM relapses from residual disease sequestered in the hypoxic BM microenvironment and therefore hypoxic conditions and changes in glucose metabolism may be important in MM [228]. Furthermore, patients with advanced stages of MM show increased glucose uptake in the tumour and this is correlated with decreased survival rate [229, 230]. In vitro experiments show that targeting insulin-responsive glucose transporter GLUT4 to downregulate the glucose uptake in MM cells is effective to induce apoptosis in MM cells [228]. Thus, suggesting that glucose uptake is important for the MM cell survival.

### **1.8.3 BM niche role in oncogenesis**

The BM niche is the home for many types of cell, thus dysregulated BM niche may affect the attached cells and provide a favourable microenvironment for tumour growth. The BM niche may be dysregulated by several different mechanisms and the bone formation and bone resorption, also called bone metabolism, dysregulation is a key trigger of BM niche dysregulation. Because, the over activated bone resorption reshapes the BM no cellular composite and resulting with the blood cells lost its 'physical home'. A report confirms this concept, which shows dysregulated bone metabolism resulting in disrupted haematopoiesis [231]. In another study researchers showed that genetic alteration in the osteo-progenitors (knockdown Dicer1 gene in the osteo-progenitors), disturbed the HSC niche and induced malignant change in haematopoiesis resulting in myelodysplasia and secondary leukaemia in the experimental mice [232]. The above evidence suggests that the dysregulated bone metabolism impairs the BM niche which favours oncogenesis.

### **1.8.4 BMSC role in MM initiation**

There are many different types of cells in the BM niche, and BMSC is important to form and maintain the niche [118]. BMSC give rise to cells which form the skeleton [233]. The plasticity of BMSC is instrumental in the formation the niche and it is this cell that most research has been focused on in the context of the MM protection and proliferation.

Many researchers have identified that the BMSC is involved in many steps of MM initiation. First, BMSC mediated the maturing of B cells to plasma cells. For the B cell to mature to a plasma cell it needs attachment of lymphoid cell to BMSC and the process also requires the expression of stromal-derived-factor-1 (SDF1) also known as C-X-C motif chemokine 12 (CXCL12) on the surface of BMSC as well as expression of the chemokine receptor, chemokine (C-X-C motif) ligand 4 (CXCL4) or CXCL7 on the surface of MM cells [205]. Inhibition of SDF1 prevents BMSC meditated protection of MM cells [234]. Second BMSC also mediate MM specific change in tumour metabolism as previously discussed in section '1.2.2. MM BM niche metabolic change'. Third, BMSC is essential for the homing of MM cells and support the MM cell proliferation. Thus, targeting BMSC maybe provide a new therapy strategy to prevent the MM initiation. For example, Bz pre-treated BM is less

protective for MM cells. An in vivo experiment further confirms this concept. In this experiment, drugs which target BMSC are administered in mice prior to MM cell engraftment. Results show that the BMSC targeting drug prevents the homing of MM cells to the BM and decreases the efficiency of tumour engraftment [235]. Together, this data suggests that BMSC is a main cell type in the BM niche that supports MM.

### **1.8.5 BM Role in MM Progression**

Interactions between MM cells and BMSC increase MM growth and drug resistance [98]. Several factors have been identified as mediators of MM-BMSC interaction including: 1) the vascular cell adhesion molecule 1/integrin  $\beta$ 1; 2) intercellular adhesion molecule 1/integrin  $\beta$ 2; 3) mucin 1 cell surface-associated axes (triggering a bidirectional signalling cascade, which activates NF- $\kappa$ B and MAPK1 pathways in BMSC and induce the secretion of IL-6, CXCL12, IGF-1, and VEGFA that further support MM progression [62]; 4) Notch1 receptor on MM cells binds to BMSC and prevents apoptosis from alkylating and intercalating agents by a p21-dependent and NF- $\kappa$ B independent mechanism [99]. From these studies it is clear that new therapeutic strategies are needed to disrupt the interaction between MM cells and BMSC and thus prevent the progression of MM and sensitise MM cells to chemotherapy.

Primary MM cells lose their proliferation potential after being separated from their BM niche and cultured without BM mesenchymal stromal cell (BMSC) [236]. Many mechanisms describing the pro-tumoural effects of BMSC for the benefit of MM cells have been reported. Besides SDF-CXCR4 mediated MM cells and BMSC attraction, MM cells adhere to BMSC through expressing VLA-4, which binds to VACM expressed on BMSC. After the adherence is established, the MM cells induce signal pathways in the BMSC. For example, NF- $\kappa$ B role of promoting MM cell progression will be described in the '1.2.9 MM remodel BMSC to favour malignancy'. MM also upregulates secretion by the BMSC of pro-tumoural cytokines including IL-6 which triggers the MM cells to express VEGF, which forms a positive loop to feedback to promote progression of MM [237].

BMSC regulation of osteoclasts has also been identified as promoting MM growth. To absorb the bone, osteoclasts seal the targeted bone matrix surface and degrade the bone,

through secreting hydrochloric acid and acidophilic. The transforming growth factor beta (TGF- $\beta$ ) and insulin growth factor I (IGF-I) that are secreted by dissolved bone matrix and the platelets that are recruited promote MM cell growth [238, 239]. The above studies suggest that BMSC plays a key role for MM progression via the regulation of osteoclast.

### **1.8.6 MM cell remodel BM niche to favour malignancy**

The concept that cancer cells remodel their niche to favour tumour progression has been demonstrated in several different types of cancer [240, 241]. For example, serum from breast cancer patients is also proved to be able to remodel the microenvironment to favour the cancer cell. Sera with higher levels of PDGF-AB, intercellular adhesion molecule 1 and vascular cell adhesion protein 1 have all been found to be pro-tumoural in this setting [242]. Furthermore, microvesicles produced by cancer cells and circulating free DNA released from cancer cells have been shown to remodel the malignant niche [243, 244]. All this evidence suggests that cancer cells utilise several different mechanisms to remodel their niche to promote tumour progression.

The concept of MM cells promoting bone destruction came initially from the clinical observation that many patients with MM develop lytic bone lesions. Osteolytic bone lesions in patients with MM may lead to compression fractures. Furthermore, patients with MM have abnormal hematopoiesis as evidenced by the frequent clinical observation of anaemia. The anaemia observed in patients with MM is often multifactorial but in part is due to the hematopoietic cells being replaced by plasma cells in the BM. Understanding the mechanisms through which MM remodels the BM niche is envisaged to provide further insights as to how MM cells promote bone resorption, compromise the normal haematopoietic BM function, it is expected this will eventually result in novel approaches to prevent the MM progression within the BM. Research studying mechanisms of MM cells induced bone absorption reveals that MM cells promote osteoclast formation through upregulation of the production of RANKL and TNF- $\alpha$ , and downregulation of the production of RANKL decoy receptor and OPG [245]. Together these changes promote the absorption of bone. MM cells also modulate osteoclast function through cell – cell fusion. This concept is examined by the detection of transcriptionally active chromosomes of MM origin in around 30% of osteoclasts isolated from MM patients' BM niche [246].

MM cells also contribute to bone loss through inhibition of osteoblast activity. The increased TGF- $\beta$  and IL-3 levels are detected in MM patients that function to inhibit the osteoblast activity. The osteoblast differentiation factor, osteogenic protein-2 expression is also inhibited by MM cells [247]. As osteoblasts function to form new bone, Plasma cell induced inhibition of osteoblast activity contributes to bone disease in patients with MM.

## **1.9 Research Rational, Aims and Objectives**

### **1.9.1 Rationale**

MM evolves to become resistant to chemotherapy in part through the protective effects of the BM microenvironment interaction. Accordingly, new treatment strategies are needed to realise improved outcomes for patients.

MM is an age-related disease with the majority of the new cases diagnosed in patients over the age of 65 years old. Furthermore, with the aging population the MM incidence rate is increasing. Despite many new drugs developed for the treatment of MM, the disease presently remains incurable. Relapse following treatment is inevitable and median survival following diagnosis is about 5 years. The sub organelles of the MM cells such as mitochondria and ER are associated with stress induced apoptosis. The mechanism of how the sub organelles of MM cells adapt to the malignant cell burden, paraprotein producing burden and chemotherapy requires further investigation. Such experiments will help determine the mechanisms regulating the stress response and thus I postulate to lead to new ways to sensitise the malignant MM cells to chemotherapy.

### **1.9.2 Aims**

The primary aims of the project are:

- 1) to evaluate the signalling pathways regulation on MM cells chemotherapy resistance and survival
- 2) to evaluate how MM cells, regulate BMSC to provide supportive microenvironment
- 3) to identify new therapy strategies to disrupt the interaction of MM and BMSC to sensitise the MM cells to chemotherapy.

### **1.9.3 Objectives**

To achieve the aims of the project the following approaches are applied.

- 1) To establish an in vitro co-culture system to culture the MM patient BM aspirate derived MM cells and BMSC. Then characterise the basal state of MM cells and BMSC and investigate the interaction of MM cells and BMSC.
- 2) To investigate the role of ER stress and mitochondria function in MM cells and determine the upstream regulation factors involved in the stress response which may sensitise the MM cells to chemotherapy.
- 3) To establish the mechanism of the tumour protective effect of the MM cells and BMSC interaction and by doing so determine the key factors which may be targeted to break the protection chain and leave the MM cells more sensitive to apoptosis or chemotherapy.

**CHAPTER TWO**  
**METHODS**

## **2.1 Cell culture**

### **2.1.1 Cell lines and culture conditions**

To protect both the samples and the environment, all the cell culture procedures were carried out in sterile biological safety class II cabinets (SCANLAF, MARS Safety Class 2, Labogene) with standard aseptic procedures. To protect the operator, the airflow of the cabinet is directed around the handler and into the air grille. Then the air flow under the work top, up to the top of the cabinet from the back and is filtered through the High-Efficiency Particulate Air (HEPA) filters. To prevent contamination, HEPA filtered air is blown down from the top to cover materials on the work surface. HEPA filtered outward air, then is either recirculated back into the laboratory (for handling cell line) or expelled from the building by an exhaust fan (for handling MM patients' BM aspirates), through ductwork.

MM derived cell lines (MM1S, MM1R, U266, RPMI8226, H929) were obtained from the European Collection of Cell Cultures and DNA-fingerprinting authenticated. 5TMG1 were obtained from Dr Oyajobi, The University of Texas Health Science Center, San Antonio, USA. All the MM cell lines were suspended cells and maintained in Roswell Park Memorial Institute (RPMI) 1640 Medium (Gibco) supplemented with 10% (v/v) fetal bovine serum (Gibco), 1% penicillin-streptomycin (HyClone™ Penicillin-Streptomycin 100X solution, GE Healthcare). MM cell lines were grown in T25 or T75 flasks (Nunclon Delta surface, Thermo) and passaged to maintain the cell density in around  $3 \times 10^5$  -  $6 \times 10^5$  cells/mL.

BM stroma cells (BMSC) are adherent cells and maintained in a Dulbecco's Modified Eagle Medium (DMEM, Gibco) supplemented with 15% (v/v) (for MEFs) or 20% (v/v) (for human BMSC) fetal bovine serum (FBS, Gibco), 1% penicillin-streptomycin (HyClone™ Penicillin-Streptomycin 100X solution, GE Healthcare). BMSC were grown in T25 or T75 flasks (Nunclon Delta surface, Thermo) and passaged when they reached 80% confluence. The hydrophilic cell culture surface of the flask facilitates cell attachment. Briefly, when cells reached above 80 % confluence, medium was aspirated and cells were washed with phosphate buffered saline (PBS, without calcium and magnesium) to rinse out the FBS (FBS inactivates Trypsin). The cells were then dissociated by trypsin (Trypsin-EDTA 0.25%, phenol res.) at 37 °C for a few minutes

(for human BMSC). Completed media was added to the detached cells to inactivate the trypsin and then cells were resuspended at ratio between 1:3 to 1:5. Cells were then seeded with culture medium.

HEK293T are human embryonic kidney derived adherent cells, which were obtained from Dr. Ariberto Fassati (University College London, London, UK). HEK293T cells are maintained in DMEM supplemented with 10% (v/v) fetal bovine serum and 6 mM L-glutamine at 60%-90% confluence in 10 mm plate. HEK293T cells have a weak attachment to the tissue culture plate, therefore during subculture the cells only require 1 mL 0.125% Trypsin. Trypsin was washed off by PBS for 1-3 min, the plate was swirled until the cells were detached from the plate, and then the cells were pipetted to obtain single cell suspension. Medium replaced every other day.

All the cells were cultured in HERAcell 150i CO<sub>2</sub> incubator (Thermo Scientific), which provides 95% relative humidity, 37 °C and 5 % CO<sub>2</sub> environment. All the culture medium was pre-warmed to 37 °C in Grant Instruments SUB Unstirred Water Baths to prevent temperature induced stress to the cells.

The co-culture methods include direct contact and indirect contact through transwell. Briefly, for direct co-culture, the BMSC is seeded on the plate overnight, and then co-culture MM cells on it; for transwell co-culture, the BMSC is seeded on the plate overnight, and then the MM cells that cultured in the insert well is fitted on top of the plate. The ratio of BMSC and MM cells is between 1:3 to 1:4.

### **2.1.2 Primary cell isolation**

Primary MM cells and BMSC were obtained from MM patients' heparinized BM aspirates with informed consent in accordance with the Declaration of Helsinki and following approval by the Health Research Authority of the National Health Service, United Kingdom. BM aspirates from MM patients were diluted 1:1 in Hanks' buffer with ethylenediaminetetraacetic acid (EDTA) and then isolated using Histopaque1077 density-gradient centrifugation method. Density gradient separation procedure removed both red blood cells and died cells. Briefly, 10 mL Histopaque 1077 (sterile-

filtered, density 1.077 g/mL, Sigma) was added at the bottom of a sterile 50 mL conical centrifuge tube, then 10 mL of diluted BM sample was gently added on top of the Histopaque. The mixture was centrifuged at  $400\times g$  (Eppendorf, centrifuge 5804), room temperature, for 20 min with no brake. The mononuclear cells (the layer between the plasma and Histopaque) was carefully removed with sterile pasteur pipet and placed into a 15 mL conical tube. PBS was added to the tube, which was centrifuged at  $400\times g$ , room temperature, for 7 min. The supernatant was discarded and 1mL red cell lysis buffer was added into the mixture for a minute to lyse red blood cells and then PBS was added to neutralise the red cell lysis solution. Cells were then centrifuge at  $400\times g$ , room temperature, for 7 min and supernatant discarded and cell pellet resuspended in complete media.

The cells isolated from the BM were then cultured in complete medium for 24 h to obtain the BMSC. BMSC attach to the surface of the flask and primary MM cells were then purified from the supernatant using magnetic-activated positive selection cell sorting with CD138<sup>+</sup> MicroBeads (Miltenyi Biotec, Auburn, CA). The cells were magnetically labelled with CD138 microbeads and then loaded on to a magnetic column (MACS). The CD138 negative cells passed through the MACS column with 3 washes with cold MACS buffer (PBS with 0.5% bovine serum albumin and 2 mM EDTA). The MM cells were eluted by removing the magnetic field and forcing the cells out of the column with a plunger. The purified CD138<sup>+</sup> cells were then used in experiments described below.

### **2.1.3 Calculating cell density**

Cells were counted using haemocytometer (Fisher Scientific) with a gridded chamber of 0.1  $\mu\text{L}$  capacity. The cell numbers were counted and converted to cell density. Briefly, 10  $\mu\text{L}$  cells were mixed with 10  $\mu\text{L}$  0.4% trypan blue (Sigma-Aldrich) for 1 min to stain the dead cells. Then 10  $\mu\text{L}$  cells were loaded onto the haemocytometer and counted under a light microscope. Cells stained blue were dead cells. If the cells located on the border of the grid, only count top and left side. Sum up four grids cell numbers and convert it to cell density using the following equation.

$$\text{Cell Density (cells/mL)} = \frac{\text{Total cell number (4 grid)}}{2} \times 10^4$$

10, 000 is to convert grids capacity (0.1  $\mu\text{L}$ ) to 1 mL, 2 is the dilution factor as the cells were diluted with trypan blue in a ratio of 1:1.

#### **2.1.4 Cryopreservation of cells**

Cryopreservation is a method to maintain the cell stock. At low temperature ( $< -80$   $^{\circ}\text{C}$ ), cells protein and gene are stable. Dimethyl sulfoxide (DMSO) minimize the formation of ice crystal to prevent it from damaging the cell membrane. Briefly, for suspension cells,  $5 \times 10^6$  cells were collected. For adherent cells, 1/3 cells were collected from one T75 flask when reached 80% confluence. Cells were centrifuged at  $300 \times g$  for 5 min. The supernatant was discarded and the cells were resuspended in 1 mL freezing medium (5%-10% DMSO according to the cell type). The cells were then put in a cell freezing box in the  $-80$   $^{\circ}\text{C}$  freezer for 24 h. The freezing box facilitated the temperature drop at a ratio of 1  $^{\circ}\text{C}/\text{min}$ .

#### **2.1.5 Thawing cells**

The thawing procedure was to minimize the stress of the frozen cells when thawing. That is work quickly and seed cells with high density. Briefly, the cells were immediately thawed in a  $37$   $^{\circ}\text{C}$  water bath for no more than 1 min (gently swirling the vial). Then the cells were slowly added to 9 mL pre-warmed medium (dropwise). The cells were then centrifuged at  $200 \times g$  for 5 min. The medium was discarded, and the cell was gently re-suspended in complete medium in T25 flask.

### **2.2 Viability and apoptosis assay**

#### **2.2.1 Morphology assay**

Dead cells cannot maintain membrane integrity. As trypan blue only penetrates in the cells without membrane integrity, 0.4% trypan blue staining method was used to detect dead cells. It is to count the viable (no staining) and dead cell (stained with blue colour) numbers to get the percentage of the dead cells.

During apoptosis, nucleus of the cells becomes condensed and then dissembled, while nucleus of healthy cell is generally spherical and even distributed. Accordingly, morphology assay of cell nucleus is used to determine apoptosis and health cell numbers. Two staining reagents are used, Hoechst 33342 (Thermo Fisher Scientific, 5  $\mu$ M in PBS) to stain the nucleus of live cells and 4', 6-diamidino-2-phenylindole (DAPI, 300 nM in PBS) to stain the nucleus of fixed cells. Then it is to image the cells with fluorescent microscopes (emit light: 350 nm, filter: 460 nm) or with confocal microscopy (excitation 352 nm, emission 520nm) and count the viable cells and apoptosis cells according to the nuclear morphology.

### **2.2.2 Cell Titer-GLO assay**

Cell Titer-GLO Luminescent Cell Viability Assay (Promega, Southampton, UK) was used to determine viable cells by measure intracellular adenosine triphosphate (ATP) level. ATP level represents cell metabolic level and viable cells. Briefly, cells were seeded into 96 well plates in quadruplicates at  $1 \times 10^5$  cells per well in 100  $\mu$ L culture medium. 100  $\mu$ L CellTiter-Glo<sup>®</sup> Reagent was added in each well and mixed on an orbital shaker (700 rpm, 2 min). This was used to equilibrate the reaction for 10 minutes in dark to stabilize the luminescent signal. 150  $\mu$ L sample from each well was transferred to an opaque-walled white 96-well plate. Luminescence was then recorded on FLUOstar Optima Microplate Reader (BMG LABTECH, Germany) at 570 nm wavelength.

### **2.2.3 Annexin V-FITC, PI apoptosis assay**

During apoptosis, cells translocate membrane phosphatidylserine to the cell surface, which can be detected by Annexin V staining – conjugated to a fluorochrome (FITC excited by 488 laser and detected using FL1 channel on a flow cytometer). Propidium iodide (PI) can only penetrate dead cells and stain the nucleus (excited by 488 laser and detected using FL3 channel on a flow cytometer). Here I used both Annexin V and PI to detect apoptotic cell and dead cells, as well as the live cell population (Annexin V/PI negative). Cells were washed with PBS and centrifuged to discard the supernatant, then the cells were resuspended in annexin-binding buffer to  $\sim 1 \times 10^6$  cells/mL. Cells were stained with Annexin-V and Propidium Iodide (PI)

(eBioscience™ Annexin V-FITC Apoptosis Detection Kit, ThermoFisher) for 15 min at room temperature followed by analysis by flow cytometry (CyFlow Cube 6 flow cytometer, Sysmex, Milton Keynes, UK).

### **2.3 Flow cytometry**

Different flow cytometers were used according to the purpose of the detection. CyFlow Cube 6 is used for up to 2 colour detection, for example, apoptosis assay. BD FACSAria II for cell sorting to enrich the cells that were either infected with Luci or mCherry. Beckman coulter for up to 4 colour detection and for up to 7 colour detection.

Multiple colour detection is needed for the hematologic study, as multiple cell surface marker proteins are needed to be detected to distinguish cells types among primary MM BM cells.

Briefly, histopaque1077 density-gradient method isolated primary samples were first filtered with 0.4 mesh. Then the cells were washed with PBS. The cells were centrifuged and were suspended in 100 µL PBS (filtered with 0.22 µm, 1%FBS, 2mM EDTA and sterilised). Next the cells were stained with different cell surface antibodies according to the staining panel of the cell type for 15-30 min in dark. Finally, the cells were wash with PBS and analysed by flow cytometer.

For the design of the co-staining panel, the chromophores were selected according to their emission wave length to avoid overlapping or bleaching of the signal. Before analysing the cells, perform the compensation experiment to optimise the accuracy of the co-staining data. The calculation of the compensation is performed by the software automatically.

### **2.4 Microscopy**

According to the purpose of the experiment, different types of microscopy were used including confocal microscopy, high resolution fluorescent microscopy, normal fluorescent microscopy and normal microscopy.

For the confocal microscopy method, the cells were cultured on plate with the bottom layer is made of glass. As the laser detection system can only detect signals from the refractive index of glass.

The live cell nuclei staining is using Hoechst (30 min staining in dark, then wash the cells). The fixed cell nuclei staining is using DAPI (30 min staining in dark, then wash the cells).

The methanol fixation method was used to fix the cells. Briefly, the cells were seeded on coverslips in a 24 well plate and then treat the cell according to the purpose of the experiment. At the end point of the experiment, take off the media and add 200  $\mu$ L ice cold methanol for 7 min in  $-20^{\circ}\text{C}$  freezer. Then took off the methanol and wash with PBS. Next, add 200  $\mu$ L DAPI that is diluted with 1:5000 ratio and put the plate on a shaker for 5 min. Finally, wash the cells three times with PBS and briefly wash it in water, followed put the coverslip on the glass slide with 10  $\mu$ L mounting solution. Store the slide in  $4^{\circ}\text{C}$  dark room until imaging.

## **2.5 RNA expression analysis**

Generally, it is difficult to detect low abundance RNA (ribonucleic acid) expression from a sample directly. To generate the profile of RNA expression in a sample, quantitative reverse transcription and PCR (polymerase chain reaction) are combined to amplify the number of specified RNA. First, the total RNA is isolated from cells. Second, the isolated RNA is reverse transcribed into complementary deoxyribonucleic acid (cDNA) by reverse transcriptase. Finally, the synthesised cDNA was used as the template for the qPCR reaction.

### **2.5.1 Total RNA extraction**

ReliaPrep RNA cell miniprep Kit (Promega) was used to extract total RNA. Guanidine thiocyanate was used to disrupt nucleoprotein complexes and release the RNA, 1-Thioglycerol to inactivate the ribonucleases, chaotropic salts to facilitate the bonding of nucleic acids to the column, and RNase-free DNase I to digest contaminating genomic DNA. Lysates were then passed through a column to isolate the RNA. Briefly,

suspended cells was washed with phosphate buffered saline (PBS), then cell pellet was digested with ice cold BL lysis buffer supplemented with TG and transferred to RNase-free Eppendorf tube. Adherent cells were washed with PBS and applied ice cold BL lysis buffer supplemented with TG. The lysis buffer was pipetted over the cells and lysate transferred to Ribonuclease (RNase)-free Eppendorf tube, then the lysate was vortexed for 30 seconds. Absolute isopropanol was added in the lysate, which was further vortexed for 5 seconds. The lysate was transferred to column and centrifuged (1 min, 12000 g, at room temperature). The nucleic acids were bound to the column. Column was washed with RNA wash solution, then was added deoxyribonuclease (DNase) I and incubated for 15 minutes at room temperature. Column was then washed with column wash solution once and RNA wash solution twice. The RNA was air dried for 1 minute and eluted with DNase/RNase free water.

### **2.5.2 RNA quality control**

DNA, RNA and protein solution absorb ultraviolet light passing through it. The quality of the RNA can be determined according to the 'Beer's Law' equation by detecting the absorbance. The concentration of the RNA was calculated by the 260 nm absorbance ( $A_{260}$  reading 1.0 = 50  $\mu\text{g/mL}$  double-stranded DNA, = 40  $\mu\text{g/mL}$  RNA and = 33  $\mu\text{g/mL}$  single-stranded DNA).

The purity of the nucleic acid without protein was indicated by the 260/280 nm absorbance ratio. Because aromatic amino acids have maximized absorption at 280 nm wave length, the absorbance measurements at 280 nm are used to estimate the amount of protein in the sample. The ratio between 1.8- 2.2 is accepted as pure nucleic acid, while the ratio beyond this range is regarded as sample contaminated with protein. The purity of the RNA without solvent was indicated by the 260/230 nm absorbance ratio. The sample with ratio above 1.8 is accepted as pure RNA and ratio below 1.8 is regarded as RNA contaminated with solvent (typical contamination is ethanol or nucleic acid).

NanoDrop ND-1000 spectrophotometer (Thermo Scientific) was used to analyse the concentration and quality of the RNA. For RNA measurement, the spectrophotometer requires to be loaded 0.5- 2  $\mu\text{L}$  of sample (detection range 2 – 12,000  $\text{ng}/\mu\text{L}$ ). The

advantage of using NanoDrop ND-1000 spectrophotometer is the simplified procedure. The sample does not need to be added in any reagent or to be diluted. The disadvantage of the absorbance method is indistinguishable of all nucleic acids (double stranded DNA (dsDNA), RNA and single-stranded DNA (ssDNA)). Because all nucleic acids (dsDNA, RNA and ssDNA) have similar absorbance at 260 nm, the method can not specify which form of nucleic acid is presented in the sample. Briefly, the spectrophotometer was first blanked by 2  $\mu$ L of DNase/RNase free water. Then, 2  $\mu$ L of each RNA sample was added to the sensor and then the concentration was measured. Sample concentrations were recorded along with the 260/280 ratio and 260/230 ratio.

### **2.5.3 cDNA synthesis**

To synthesize double stranded complementary DNA (cDNA) from a single stranded RNA, qPCRBIO cDNA synthesis kit (PCR Biosystems, London, UK) was used. This includes modified MMLV reverse transcriptase, which is not inhibited by ribosomes, the kit also contains short primer sequences which binds to the 3' end of the isolated RNA template, RNase inhibitor which prevents degradation of RNA, anchored oligo, random hexamers, enhancers, deoxynucleotide (dNTPs) and  $MgCl_2$ . Reverse transcription was performed on a BIO-RAD T100 Thermal Cycler. Briefly, 7.5  $\mu$ L RNA (from 4.0 pg up to 0.4  $\mu$ g of total RNA) was mixed with 2  $\mu$ L 5x cDNA Synthesis Mix and 0.5  $\mu$ L 20x RTase (with RNase inhibitor). This was incubated at 42°C for 30 minutes (for most of applications that GC content <65%), 85°C for 10 minutes and cooled down to 4°C immediately (lid temperature 105 °C). cDNA was stored at 4°C until used.

### **2.5.4 Relative quantitative RT-PCR**

Relative quantitative real-time PCR allows us to compare changes in gene expression between a set of samples. For this I used the SYBR green based method of detection (qPCRBIO SyGreen Mix, PCR Biosystems). Predesigned KiCqStart SYBR Green primers were purchased from Sigma. SYBR green is a fluorescent dye that binds to dsDNA and releases fluorescent signal, which can be detected at the end of each PCR cycle. Briefly, the cDNA was mixed with SyGreen Mix and primer, and this was placed in a 96 or 384 well plate. The cycling conditions were 95 °C for 2 min as pre-

amplification to activate the polymerase and denature the cDNA. Second, the cDNA was amplified through 45 cycles (95 °C for denaturation of the dsDNA, for 15 seconds and 60°C for annealing and extending the ssDNA, for 10 seconds and 72°C for 10 seconds) on a 96 or 384-well LightCycler 480 (Roche, Burgess Hill, UK). The specified mRNA expression was normalized against glyceraldehyde 3-phosphate dehydrogenase (GAPDH) or  $\beta$ -actin. Sequences of real-time PCR primers used in this study are listed in Table 2.1.

**Table 2.1 Oligonucleotide sequences for real-time PCR (5' to 3')**

Gene	Forward (5' to 3')	Reverse (3' to 5')
GAPDH	GCACCACCAACTGCTTAGC	GGCATGGACTGTGGTCATA
NRF2	CGTTTGTAGATGACAATGAG	AGAAGTTTCAGGTGACTGAG
HO-1	ATGACACCAAGGACCAGAGC	GGGCAGAATCTTGCACTTTG
GCLM	TGCAGTTGACATGGCCTGTT	TCACAGAATCCAGCTGTGCAA
ATF4	CCTAGGTCTCTTAGATGATTACC	CAAGTCGAACTCCTTCAAATC
CHOP	CTTTTCCAGACTGATCCAAC	GATTCTTCCTCTTCATTTCCAG
B-ACTIN	GATCAAGATCATTGCTCCTC	TTGTCAAGAAAGGGTGTAAC
ATG5	AAGACCTTTCATTCAGAAGC	CATCTTCAGGATCAATAGCAG
CYPD	ACGAGAACTTTACTACTGAAG	CAACCAGTCTGTGTCTTTATGG

## 2.6 Protein expression analysis

Western blot or protein immunoblot method was used to analyse the specified protein expression. First, the protein was extracted, denatured and separated through gel electrophoresis. Second, the protein was transferred to a polyvinylidene difluoride (PVDF) membrane and bound with antibodies that specifically target it. Finally, the

protein can be visualised through the secondary antibody, which binds to the first antibody.

### **2.6.1 Protein extraction**

For the whole protein extraction, radioimmunoprecipitation assay buffer (50 mM Tris, pH 8.0, 150 mM NaCl, 1% NP-40, 0.1% SDS, 0.5% sodium deoxycholate, supplemented with phosphatase inhibitor cocktail tablet and protease inhibitor cocktail tablet from Roche) was used. This buffer quickly lyses the cells and solubilizes the proteins which include membrane-bound proteins. For the protein located in the nucleus, NE-PER nuclear and cytoplasmic extraction reagents (Thermo scientific) were used. This buffer effectively separates cytoplasmic and nuclear protein. Briefly, for the whole protein extraction, the cells were washed with PBS and the ice cold lysis buffer was added to the cells. For the nuclear protein extraction, the cells were first washed with PBS and then added with ice cold CER buffer I. After vortex for 15 s, the lysate was put in ice for 10 min. Second the lysate was added with CER II buffer, and incubated on ice for 1 min, then the mixture was centrifuged and the supernatant (cytoplasmic extraction) was discarded. Finally, the pellet was added with NER buffer and incubated on ice and then centrifuged. Supernatant (nuclear protein) was placed in a fresh tube and stored at -80°C until use.

### **2.6.2 SDS polyacrylamide gel electrophoresis and Western Blot**

Sodium dodecyl sulfate (SDS)-polyacrylamide gel electrophoresis was used to separate proteins by their molecular mass. Briefly, the lysate was first centrifuged at 4 °C, 10000 g, for 10 min and the supernatant was collected and then the loading buffer was added to the samples, and mixed, heated to 100 °C for less than 5 min. Thereafter, the protein sample was loaded to the acrylamide gels. The gels were run at 200 V for 1 h in the running buffer (Tris-Base 3.03 g, glycine 14.4 g, SDS 1 g in 1 L dH<sub>2</sub>O). After the electrophoresis, the proteins were transferred from the gel onto a polyvinylidene fluoride (PVDF) membrane for analysis, The PVDF membrane was pretreated with methanol. The wet transfer apparatus was filled with the transfer Buffer (3.03 g of Tris-Base, 14.4 g of glycine and 200 mL of methanol in 1 L dH<sub>2</sub>O), and the transfer was run at 100 V for 1 h. All subsequent incubation steps were

performed with constant agitation on a shaker. Following the transfer, the membranes were blocked in a solution of 5% BSA or 5% milk in PBS with 0.1% Tween (PBST) for 1 h at room temperature.

The membranes were incubated with the primary antibody diluted in 5% BSA or 5% milk PBST, at 4°C overnight. The membranes were washed 5 times with PBST for 5 min per wash. The horseradish peroxidase (HRP) conjugated secondary antibody was diluted in 5% BSA or 5% milk PBST. The membranes were incubated with the respective secondary antibodies for 1 h at room temperature. The membranes were washed with PBST 5 times for 5 minutes each. Next, the membranes were developed using the enhanced chemiluminescence (ECL) reagent (GE healthcare, Little Chalfont, UK). The solution A and solution B were mixed in a 1:1 ratio. Then, the resulting solution covered the membranes for 1 minute, and further drained off. The membranes were imaged using the Chemdoc-It2 Imager (UVP). Images were stored and then processed using Image J. Table 2.2 show the list of antibodies used for Western Blotting.

**Table 2.2 Antibodies for Western Blotting**

Primary antibodies			
Name	Isotype	Dilution	Supplier
Anti- $\beta$ -actin	mouse monoclonal	1:1000	R&D Systems, MAB1536
anti-NRF2	rabbit monoclonal	1:1000	Abcam, 62352
anti-GAPDH	rabbit monoclonal	1:1000	Cell Signaling Technology, D16H11
anti-Sam68	rabbit monoclonal	1:1000	Santa Cruz Biotechnology, sc-1238
anti-CHOP	rabbit monoclonal	1:1000	Cell Signaling Technology, 1649
anti-P62	rabbit monoclonal	1:1000	Abcam, ab109012
Anti-LC3	rabbit monoclonal	1:1000	Cell Signaling Technology, 4108S
Secondary antibodies			
Name		Dilution	Supplier
Goat anti-mouse IgG HRP		1:1000	Dako, Agilent, P0447
Goat anti-Rabbit IgG HRP		1:1000	Dako, Agilent, P0448

## 2.7 Short hairpin RNA (shRNA) mediated gene silencing using lentivirus

### 2.7.1 RNA amplification

MISSION® TRC shRNA plasmid need to be recovered, purified and amplified. To reviving the *E. coli*, a sterile loop was jabbed into the glycerol stock, then was streaked gently across the agar plate as show below. The sterile loop was changed for each streak. The streaked plate was put at 37 °C hot room for 14 h to allow the revival of the stored bacteria. The single clones normally is shown along the third streak.

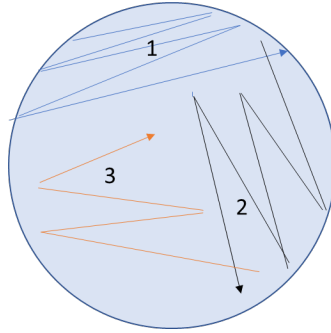


**Figure 2.1 Streak plate**

Three steps to streak the plate.

To purify and amplify the *E. coli*, 4-5 single clones were picked (avoid satellite colonies in antibiotic depleted area) and was transferred into culture tube with 5 mL sterile LB, individually. It was swirled at 250 rpm, at 37 °C overnight. This procedure was carried out to ensure the homogeneity of the *E. coli*.

### **2.7.2 Plasmid purification**

NucleoSpin® Plasmid kit (Macherey-Nagel, Germany) was used to purify the plasmid from *E.coli*. The bacteria were lysed by SDS/alkaline buffer. After neutralisation, precipitated protein, genomic DNA, and cell debris were pelleted, then the plasmid bound with the column, and contaminations like salts, metabolites and soluble macromolecular cellular components were washed out by centrifuge force. Purified plasmid DNA was eluted by sterile dH<sub>2</sub>O.

Briefly cells were centrifuged for 30 s at 11,000 x g and the supernatant was discarded as much as possible. Second, 250 µL Buffer A1 was added to resuspend the pellet completely. Third, 250 µL Buffer A2 was added. The tube was gently inverted for 6–8 times to avoid shearing of genomic DNA and was incubated at room temperature for up to 5 min until lysate appeared to be clear. Fourth, 300 µL Buffer A3 was added. The tube was gently inverted for 6–8 times until blue samples turned colourless completely without any traces of blue. Fifth, after the tube was centrifuged for 5 min at 11,000 x g at room temperature, 750 µL of the supernatant was transferred onto the column and centrifuged for 1 min at 11,000 x g. The remaining lysate was loaded and centrifuged. Sixth, the column was washed with preheated 500 µL Buffer AW (50 °C)

for 1 min at 11,000 x g, then was washed with 600  $\mu$ L Buffer A4 for 1 min at 11,000 x g. Finally, the column was dried through centrifuging for 2 min at 11,000 x g and was incubated with 50  $\mu$ L sterile ddH<sub>2</sub>O at room temperature for 1 min, then was centrifuged for 1 min at 11,000 x g to elute the plasmid. Plasmids were stored at -20 °C before use.

### **2.7.3 Plasmid precipitation**

For effective transfection, the optimal plasmid DNA concentration should be above 180 ng/ $\mu$ L. Ethanol precipitation is a widely-used method to concentrate plasmid DNA, as ethanol efficiently precipitates nucleic acid when salt is present and the plasmid DNA can be achieved at desired concentration. Briefly the plasmid was mixed thoroughly with 3 M sodium acetate (pH 5.2, 10%) and ice cold 100% ethanol (2.5- 3 fold v/v), the DNA was precipitated at -20 °C overnight. Then the mixture was centrifuged at 13000 rpm, 4°C, for 30 min. Second, the pellet was washed twice with 500  $\mu$ L ice cold 75% ethanol (centrifuged at 4 °C for 10 min). Third, the trace ethanol was removed through spin at 13,000 rpm for 10 s). Finally, the pellet was dried by air and resuspended in ddH<sub>2</sub>O (nuclease free, 0.22  $\mu$ m filtered).

### **2.7.4 Lentivirus production**

Gene silencing or gene knockdown is a method to reduce the expression of a target gene in cells. Unlike gene knock-out (for example, CRISPR-CAS9), which is to eliminate target gene expression by removing essential DNA sequences from the cells, RNA interference that selectively inactivate targeting mRNA by double-stranded RNA, can reduce gene expression from 50 – 95% of total target RNA expressed. The method enables the essential gene required for survival of the cells to be investigated and the disease-related gene to be investigated by their link between gene expression level and disease progression. RNA interference includes siRNA and shRNA methods. shRNA could integrate in DNA for stable shRNA expression thus is widely used for RNAi. Compared to cell lines, primary cells are relatively difficult for shRNA delivery, thus lentivirus-delivered short hairpin RNA (shRNA) -mediated knock down method was used. The used shRNA is MISSION® shRNA, a lentiviral clone, which is a sequence- verified plasmid from Sigma. Low in degradation and turnover rate, shRNA

has a tight hairpin turn, a loop structure, to decrease gene expression via RNA interference with target RNA sequence. MISSION® shRNA NRF2 plasmid was purchased from Sigma-Aldrich and transferred into HEK 293T cells. MISSION® pLKO.1-puro Control Vector was used as the control lentivirus (SHC001, Sigma-Aldrich).

The MISSION® TRC shRNA plasmid or control vector was transformed into *Escherichia coli* (*E. coli*) strain DH5 $\alpha$  T1R, colonies were picked and the plasmid isolated and stored at -20 °C. After amplification of the shRNA plasmid/control plasmid, it was co-transfected into the HEK 293T cells with pCMV $\Delta$ R8.91 (the packing plasmid expressing gag-pol) and pMD.G (the envelope plasmid expressing VSV-G) to produce lentivirus. Both of the two plasmids were kindly provided by Dr. Ariberto Fassati (University College London, London, UK).

Gag (a polyprotein), Pol (a reverse transcriptase), and Env (the envelope protein) are three major proteins encoded in the lentivirus genome. Gag produces the viral core structure and core proteins. Pol is encoded to produce a reverse transcriptase, affecting integrase activity and RNase H activity, which is essential during genome reverse transcription. Three plasmids were co-transfected to the packaging cells to produce lentivirus. The plasmids are pCMV $\Delta$ R8.91 (packing plasmid expressing gag-pol), pMD.G (envelope plasmid encoding VSV-G), and shRNA plasmid.

FuGENE (Promega, Fitchburg, WI, USA) was used to transfect plasmids to the packaging cells, HEK293T. Nonliposomal FuGENE® Transfection Reagent is widely used for transfection due to its high efficiency and low toxicity. The reagent does not require removal of serum or culture medium and does not require washing or changing of medium after introducing the reagent/DNA complex.

Briefly, a 10 cm plate was seeded with HEK293T cells to 60% confluency and was changed with 7.5 mL complete medium without antibiotics. 1  $\mu$ g of each packaging plasmids were mixed with 1.5  $\mu$ g shRNA plasmid and were topped up to 15  $\mu$ L with TE buffer, then it was mixed with 18  $\mu$ L FuGENE (room temperature) in 200  $\mu$ L Opti-MEM (Life Technologies, Gaithersburg, MD, USA) reduced serum medium. The

mixture was added to the plate drop wise. The plate was swirled gently and put in culture incubator for 24 h. The medium was discarded and replaced with 7.5 mL fresh complete medium without antibiotics. The medium was collected and replaced at 48, 72 and 96 h. The collected medium was frozen immediately at -80 °C. 150 µL medium was collected and frozen separately each time for titration.

### **2.7.5 Lentivirus RNA isolation for titration**

NucleoSpin RNA Virus Isolation Kit (Macherey-Nagel, Germany) was used to isolate lentivirus RNA. After the cells were lysed by RAV1, the RNA was bound to the column. For low-concentrated viral RNA, carrier RNA (inert RNA >200 nt) was used to improve binding and recovery of the RNA. Contaminations (salts, metabolites and soluble macromolecular cellular components) were washed out by centrifuge force using washing buffer. The nucleic acids were then eluted by water. Briefly, first, 70 µL of each time point collected medium was combined and 150 µL of which was mixed with 600 µL Buffer RAV1 with Carrier RNA, then it was incubated for 5 min at 70 °C. Second, after 600 µL 100 % ethanol was mixed by vortex for 10–15 s, 700 µL of the mixture was transferred to the column and was centrifuged for 1 min at 8,000 x g. Repeat the step to reload all the mixture to the column. The flow-through fraction was discarded and collection tube (2 mL) was changed for each step. Third, the column was washed by 500 µL RAW buffer for 1 min at 8,000 x g to remove the contaminants and PCR inhibitors. Then the column was washed with 600 µL Buffer RAV3 for 1 min at 8,000 x g again. Fourth, the column was washed with 200 µL Buffer RAV3 for 2–5 min at 11,000 x g, then it was centrifuged again to remove all the ethanol in the Buffer. Finally, the column was incubated with 50 µL RNase-free H<sub>2</sub>O (preheated to 70 °C) for 1–2 min, then the RNA was eluted by centrifugation for 1 min at 11,000 x g.

### **2.7.6 Lentivirus RNA titration**

The purified RNA was first treated with DNase I to degrade the DNA contamination, then quantitative RT-PCR was performed for the lentivirus RNA titration. Quant-X™ One-Step qRT-PCR SYBR® Kit (Clontech) and Lenti-X reverse transcription

polymerase chain reaction (qRT-PCR) titration kit (Clontech Laboratories, California, USA) were used.

Briefly, First, for the DNase I reaction, after 12.5  $\mu\text{L}$  RNA sample was mixed with 2.5  $\mu\text{L}$  DNase I Buffer (10x), 4  $\mu\text{L}$  DNase I (5 units/ $\mu\text{L}$ ) and 6  $\mu\text{L}$  RNase-free Water, the mixture was incubated at 37°C for 30 min, followed by 70°C for 5 min in a BIO-RAD T100 Thermal Cycler. The mixture was stored on ice, while preparing the next procedure.

Second, master reaction mixture for qRT-PCR was prepared on ice, which was a mixture of 8  $\mu\text{L}$  RNase-free water, 12.5  $\mu\text{L}$  Quant-X Buffer (2X), 0.5  $\mu\text{L}$  Lenti-X Forward Primer (10  $\mu\text{M}$ ), 0.5  $\mu\text{L}$  Lenti-X Reverse Primer (10  $\mu\text{M}$ ), 0.5  $\mu\text{L}$  ROX Reference Dye LSR or LMP (50X), 0.5  $\mu\text{L}$  Quant-X Enzyme and 0.5  $\mu\text{L}$  RT Enzyme Mix. The actual volume of each reagent was 10% more than was described before to ensure enough master reaction mixture for the reaction.

Third, PCR grade 8-well strips were used to make 10-fold serial dilutions of Lenti-X RNA Control Template and the viral RNA with EASY Dilution Buffer. The first well of Lenti-X RNA Control Template contents  $5 \times 10^7$  copies/ $\mu\text{L}$  and the fifth well contents  $5 \times 10^2$  copies/ $\mu\text{L}$ . The standard curve of Lenti-X RNA Control Template was calculated according to the concentration. 3 wells for control of serial dilutions of Lenti-X RNA Control Template were loaded with EASY Dilution Buffer only. Each purified RNA sample was diluted to four 10-fold serial dilutions. To remove bubbles from the mixture, the strips was tapped gently and was centrifuged at 2000 rpm, 4°C for 1 min.

Fourth, for the PCR reaction, a 96-well PCR plate was placed on ice, and 23  $\mu\text{L}$ /well of master reaction mixture was loaded into the wells (in duplicate). 2  $\mu\text{L}$ /well of Lenti-X RNA Control Template dilutions, control EASY Dilution Buffer and RNA sample dilutions were loaded into the wells. To remove bubbles from the mixture, the plate was centrifuged at 2000 rpm, 4°C for 2 min. The LightCycler 480 (Roche, Burgess Hill, UK) was programmed as below, 42°C 5 min and 95°C 10 s for RT reaction, repeat 95°C 5 s and 60°C 30 s for qPCR x 40 Cycles, 95°C 15 s – 60°C 30 s for melt curve analysis then all 60°C–95°C. The standard curve was plotted through average

Ct values from the control dilution duplicates (y axis) and copy number (log scale, x axis).

To determine the RNA sample copy numbers, each RNA dilution copy numbers were calculated through the standard curve according to the cycle threshold (Ct values). The mean copy number was generated through back-calculated starting copy number value of each RNA dilution. The formula is shown below.

$$\text{Copies/ml} = \frac{(1 \times 10^7 \text{ copies concentration})(1000 \text{ convert } \mu\text{l to ml})(2 \text{ DNase dilution})(50 \text{ elution volume})}{(150 \text{ total sample volume})(2 \text{ sample volume added to well})}$$

Next, the copy number was converted to transducing units (TU/mL). The formula is shown below. 100000 is the division factor, which was the viral copy number and viral infectivity ratio. It was determined by counting GFP positive cells that were infected with the lentiviral vectors expressing GFP through a conventional fluorescent microscope (performed by Dr. Lyuba Z, UEA, UK).

$$\text{TU/ml} = \frac{\text{Copies/ml}}{100000}$$

Sixth, the 100 kDa Concentration Amicon Ultra centrifugal filter (EMD Millipore, Massachusetts, USA) was used to concentrate the virus. The virus medium was thawed on ice overnight then it was loaded to the upper reservoir of the Amicon and was centrifuged at 1000 x g, 4°C in a swinging-bucket rotor. The concentrated virus was frozen and stored at – 80 °C until needed. The final volume was recorded. Finally, the formula for calculate the volumes of virus that is needed for desired Multiplicity of infection (MOI) is shown below. MOI is the number of virus particles per cell.

$$\text{volume} = \frac{(\text{cell number}) (\text{MOI})}{\text{TU/ml}}$$

### 2.7.7 Lentivirus transduction

1 µg/mL polybrene was used to enhance the efficiency of transduction. As a cationic polymer, it can improve transduction efficiency 100- 1000 fold through neutralizing the charge repulsion between virions and sialic acid on the cell

surface. The virus was thawed on ice to prevent the degradation. The desired volume of virus was added on the polybrene-treated cells that were cultured in antibiotic free medium and was gently mixed, then the cells were in culture incubator overnight and topped up with fresh antibiotic free medium. Generally, MOI 30 is used for lentivirus transduction to BMSC and lower than MOI 10 is used for lentivirus transduction to MM cells. The gene silencing can be detected from the transduction after 72 h. Table 2.3 show the shRNA sequencing.

**Table 2.3 Mission shRNA sequence**

Name	Clone ID	TRCN	SEQUENCE
Nrf2	NM_006164. 2-1144s1c1	000000 7558	CCGGCCGGCATTTCCTAAACACAA CTCGAGTTGTGTTTAGTGAAATGCC GGTTTTT
ATG5	NM_004849. 1-1170s1c1	000015 1963	CCGGCCTGAACAGAATCATCCTTAA CTCGAGTTAAGGATGATTCTGTTCA GGTTTTTTG

## 2.8 Promoter assay

The HO-1 promoter construct (pHO-1Luc4.0 and pHO-1mut ARE) was a kind gift from X. Chen, Baylor institute of Medicine, Houston. For the reporter assays, a total of 0.5 µg of reporter plasmids and pRL-CMV control constructs were co-transfected into U226. The transfected cells were incubated for 48h before the indicated treatments. For reporter assay, the cells were treated with Dual-Luciferase Reporter Assay System (Promega) and were evaluated by (FLUOstar optima Microplate Reader BMG LABTECH, Germany) with luminometer.

## 2.9 ER-stress detection

ER-Tracker™ Red (BODIPY® TR Glibenclamide, Thermo Scientific) was purchased from Invitrogen. The live cellular ER-stress levels were determined according the manufacturer's guidelines by flow cytometry. Briefly, HBSS-washed cells was stained

with ER-Tracker™ Red for 30 minutes at 37 °C, then analysed by CyFlow Cube 6 flow cytometer (Sysmex, Milton Keynes, UK).

## **2.10 GSH assay**

GSH-Glo™ Assay was purchased from Promega. The cellular GSH levels were determined according to the manufacturer's guidelines by (FLUOstar optima Microplate Reader BMG LABTECH, Germany) with luminometer. Briefly, GSH-Glo reagent was added to cells in 96 well white plate and the mixture was incubated for 30 minutes. Then cells were added with reconstituted luciferin detection reagent, incubated for 15 minutes. Then, the luminous signal was detected.

## **2.11 *In vivo* mice experiments**

Project license and personal license were obtained for the regulated procedures on the living animals. I carried out this work under the direct supervision of my supervisor in the Disease Modelling Unit (DMU) facility at the University of East Anglia, where the mouse was housed in individually ventilated cages and were maintained under specific pathogen-free conditions in accordance with regulations of UK Home Office and the Animal Scientific Procedures Act. 8-10 week old mouse were used for all the experiments. NSG mice were purchased from Jackson Laboratories (Bar Harbor, ME, USA).

### **2.11.1 NSG mice**

NSG, also called NOD scid gamma, NOD-scid IL2R $\gamma$ null or NOD-scid IL2R $\gamma$ manull. NSG mice are a widely used immune deficient strain to avoid host immune system responses and improve the immune cell engraftment efficiency, which is developed by Dr. Leonard Shultz from The Jackson Laboratory. Specifically, there are two mutations in the mice. Severe combined immune mutant is the DNA repair complex protein Prkdc deficiency and resulted with impaired B and T cell; the complete null allele of the IL2 receptor common gamma chain mutant inhibit cytokine signalling and impaired the NK cells.

### **2.11.2 MM cell xenograft**

For the *in vivo* detection of the MM cell engraftment, pCDHluciferase-T2A-mCherry lentiviral construct (Luc) were used to infect the MM cells (a kind gift from Prof. Dr. Med. Irmela Jeremias, Helmholtz Zentrum München, Munich, Germany). MM-Luci cells will shift luciferin to red light *in vivo* at 37 °C and the signal can be detected by the Bruker In-Vivo Xtreme Imaging Systems. The MM-Luci cells were sorted by BD FACSAria III cell sorter (BD Biosciences) on FL3 channel. 6-8 week old NSG mice were either subcutaneous (SC) or intravenous (IV) injected with MM-Luci cells. For the SC administration, the MM-Luci and BMSC cells (3:1 ratio, in 200 µL PBS) were injected under the loose skin over the flank of each mice. For the IV administration, the mice were first warmed at 37 °C in individual warming boxes for no more than 10 minutes, the cells (in 200 µL PBS) were injected with 27-gauge needle with 1 ml syringe. Pressure was applied to the injection site to avoid bleeding.

### **2.11.3 *In vivo* bioluminescent (BL) imaging**

Bruker In-Vivo Xtreme Imaging Systems (Bruker Corp., Massachusetts, USA) imager for *in vivo* bioluminescent (BL) imaging was used to evaluate the engraftment of MM cells in anaesthetised NSG mice. 200 µl of D-luciferin (Thermo Fisher Scientific, 15 mg/mL in PBS) was intraperitoneal (IP) injected into each mice 10 minutes before anaesthesia (2-3% isoflurane with oxygen). The mice were transferred to the Bruker specimen chamber, which is fitted with nose cone isoflurane/oxygen delivery device to maintain anaesthesia during imaging. The light, X-ray and luminescent images were acquired within 5 minutes to avoid faded signal. The mice were monitored closely until they were recovered from anaesthesia. Bruker MI SE software and Image J were used to process the images.

### **2.11.4 Mice scarification and BM cells isolation**

At the ending point of experiment, for example, weight loss more than 20%, reduced motility, bilateral hind leg paraplegia, over grooming or rough and patchy fur, tumour at 10mm (SC MM injected animals), a schedule 1 method was used to sacrifice the mice (Usually mice were exposed to CO<sub>2</sub>, followed by neck dislocation). To harvest the BM cells, the tibia and femurs were isolated and were cut in the middle, then the

bones were placed in a 0.5 mL Eppendorf tube with a hole at the bottom to allow the BM cells passing through. The BM cells were collected by centrifugation of no more than 10 seconds at 400g with 1.5 ml Eppendorf tube. Hybri-Max buffer were used to lysis the red cells. BM cells were then stained with different antibody panels to evaluate the desired cell population. For example, anti hCD33 and anti hCD45 staining panel determines MM cell population, mCD45<sup>-</sup>/CD105<sup>+</sup>/CD31<sup>-</sup>/Ter119<sup>-</sup> staining panel determines mBMSC population. The antibody panel used to determine desired cell population is listed in Table 2.4.

**Table 2.4 Antibody panel for cell staining**

Cell	Antigen	Fluorochrome	Species	Supplier
BMSC	CD45 <sup>-</sup>	BV420	Human	BioLegend
	CD45 <sup>-</sup>	BV510	Mouse	BioLegend
	CD105 <sup>+</sup>	FITC	Mouse	Miltenyi Biotec
	CD31 <sup>-</sup>	Percp	Mouse	Miltenyi Biotec
	Ter119 <sup>-</sup>	APC	Mouse	Miltenyi Biotec
	CD140a <sup>-</sup>	APCcy7	Mouse	Miltenyi Biotec
	CD33 <sup>-</sup>	PE	Human	Miltenyi Biotec

## 2.12 Adenovirus GFP LC3B construct

Adenovirus GFP LC3B was a kind gift from Thomas Wileman. Briefly, LC3BF 5'-ATCGCTCGAGCTACCATGCCCTCGGAGAAGAGCTTC-3' and LC3BR 5'-ATCGGGATCCCTAGACGGAAGATTGCACTCC-3', were cloned into pEGFP-C1 (Clontech, 6084-1) between the XboI and BamHI sites. Then the construct was combined with replication-defective recombinant human adenovirus [248].

### **2.13 Statistical analysis**

The Mann Whitney test was used to compare results in control to treated groups. Results with  $p < 0.05$  were considered statistically significant (\*). Two-way ANOVA with Sidak's post-test was used to compare changes in individual primary sample under treatment. Results with  $p < 0.05$  were considered statistically significant (\*). Results represent the mean  $\pm$  SD of 4 independent experiments. For Western blotting, data are representative images of 3 independent experiments. I generated statistics with Graphpad Prism 5 software (Graphpad, San Diego, CA, USA).

**CHAPTER THREE**  
**HIGH NRF2 EXPRESSION CONTROLS ER STRESS INDUCED**  
**APOPTOSIS IN MM**

## **3.1 Introduction**

### **3.1.1 Understanding PI resistance in MM**

Genetic studies show that MM is a complex heterogeneous disease and adapted to multi-drug treatments [249-252]. As a result, the newly designed drugs, for example PI, are increasingly used in clinic for the treatment of MM but MM patients quickly develop resistance to the drugs and relapse. Until now, MM is still an incurable blood cancer [253-256]. Thus, there is a need to decode the mechanisms of PI resistance to improve the outcomes of MM treatment.

### **3.1.2 The role of NRF2 in PI induced ER stress**

MM cells are high in ER stress. ER is a sub cellular organelle, which is a protein folding compartment. In MM cells, the ER has to cope with substantial incorrect folded paraprotein production. PI prevents the degradation of proteins, which further elevates ER-stress and increases intracellular oxidative stress in MM cells and induces ER stress associated apoptosis [86, 257-259]. These evidences suggest that PI resistant MM cells may activate survival mechanism to avoid ER stress associated apoptosis.

NRF2 regulation may support the MM cells to elevate ER stress. NRF2 regulates ER-stress through the negative regulation of CHOP [260]. During ER stress, CHOP is induced by ATF4, and then mediates ER stress associated apoptosis. This concept is supported by a report, which confirms high NRF2 activity prevents ER-stress induced apoptosis by preventing the induction of CHOP [261]. PI induces NRF2 activity in many cell types including MM cells [262, 263], which provide the MM cells a survival mechanism to avoid ER stress induced apoptosis.

### **3.1.3 The aim of the project**

Reports suggest that deregulating redox homeostasis in MM increases sensitivity of MM to Bz [263] and elevated glutathione levels block Bz induced stress responses [264]. Since NRF2 activation positively regulates glutathione levels and negatively regulates CHOP, therefore, I wanted to determine: 1) Is NRF2 highly expressed in

MM? 2) Does silencing NRF2 reduce cell viability? 3) Does the NRF2 regulate glutathione and CHOP in response to PI treatment?

## 3.2 Results

### 3.2.1 Investigate NRF2 activity in MM cell lines and primary MM cells

NRF2 upregulation has been reported in various cancers [265-267], which suggests the NRF2 activation as pro tumour. To test whether this was the case in multiple MM, I first characterised the basal expression of NRF2 in MM cell lines and primary MM cells. High NRF2 expression was detected in all MM cell lines and 4/8 primary MM samples (Figure 3.1).

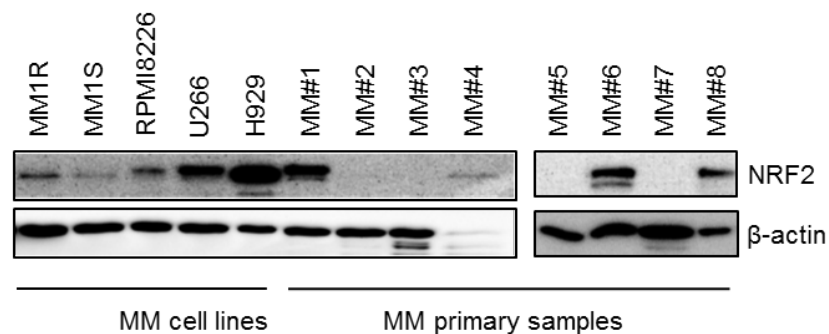


**Figure 3.1 NRF2 levels in MM cell lines and primary MM cells**

*Whole cell protein from MM cell lines and primary MM cells was extracted and was compared for the NRF2 protein expression by Western blotting. Blots were reprobbed for β-actin for loading control.*

### 3.2.2 shRNA targeted NRF2 silencing in MM cell

Next, I used NRF2 targeted shRNA to silence NRF2 in MM cells. The shRNA KD method is commonly used to determine the functional consequence of silencing gene activity. According to Figure 3.1, I chose the MM cells line, MM1S (low NRF2 expression) and U226 (high NRF2 expression) as in vitro models. Figure 3.2 shows that NRF2 targeted lentivirus reduced NRF2 mRNA expression in both cell lines.

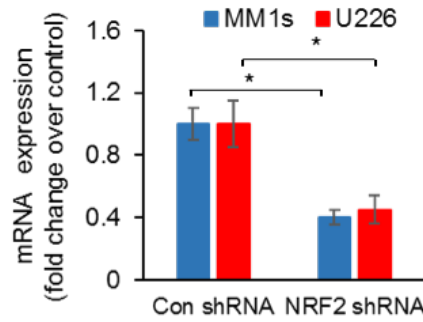


**Figure 3.2 Silencing NRF2 in MM cells using shRNA**

*MM1S and U266 were infected with lentiviral mediated NRF2 targeted shRNA. Then RNA was extracted and analysed for NRF2 expression and GAPDH was used for normalisation. Then the NRF2 mRNA expression fold change was normalised with their control group to compare the NRF2-KD efficiency between two cells. The Mann Whitney test was used to compare results in control to treated groups. Results with  $p < 0.05$  were considered statistically significant (\*). Results represent the mean  $\pm$  SD of 3 independent experiments.*

To determine if NRF2 activation was inhibited by NRF2 targeted shRNA, I used qPCR to detect the expression of NRF2 regulated gene HO-1 and GCLM. Both these genes carry an antioxidant response element (ARE) in their promoters [268, 269]. Moreover, HO-1 has been shown to play an essential role in drug resistance in MM cells and GCLM is a modifier subunit of the rate limiting enzyme, glutamate cysteine ligase in GSH synthesis [270]. Figure 3.3 and 3.4 show that NRF2-KD MM cells decreased HO-1 and GCLM messenger RNA (mRNA) expression.

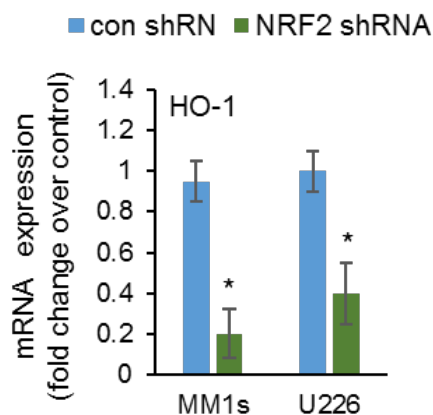


**Figure 3.3 NRF2-KD MM cells have reduced HO-1 gene expression**

*Lentiviral mediated shRNA KD of NRF2 in MM1S and U266. RNA was extracted and analysed for HO-1 expression and GAPDH was used for normalisation. Empty vector was transduced in the cells as control group. The Mann Whitney test was used to compare results in control to treated groups. Results with  $p < 0.05$  were considered statistically significant (\*). Results represent the mean  $\pm$  SD of 3 independent experiments.*

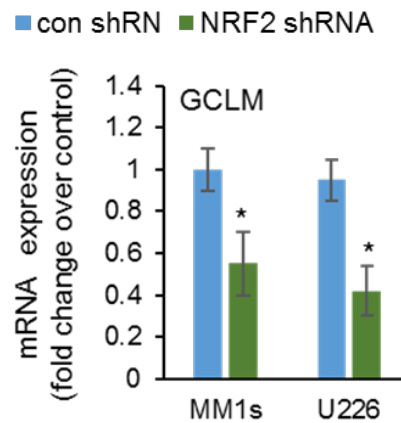


**Figure 3.4 NRF2-KD MM cells have reduced GCLM gene expression**

*Lentiviral mediated shRNA KD of NRF2 in MM1S and U266. RNA was extracted and analysed for GCLM expression and GAPDH was used for normalisation. The Mann Whitney test was used to compare results in control to treated groups. Results with  $p < 0.05$  were considered statistically significant (\*). Results represent the mean  $\pm$  SD of 3 independent experiments.*

### 3.2.3. NRF2 function in MM cell survival

To prove that the NRF2 activity is essential for the MM cell survival, I evaluated NRF2-KD MM cell viability using flow cytometer with PI/Annexin V staining to measure apoptosis. Results show that the viability of NRF2-KD U226 and MM1S were significantly reduced (Figure 3.5).

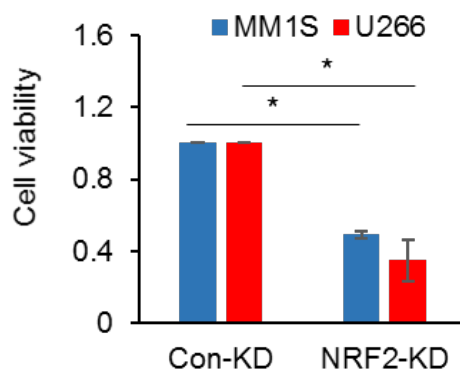


**Figure 3.5 Viability of NRF2-KD MM cells are reduced**

*Lentiviral mediated shRNA KD of NRF2 in MM1S and U266, and then analysed for cell viability using flow cytometer with PI/Annexin V staining. The Mann Whitney test was used to compare results in control to treated groups. Results with  $p < 0.05$  were considered statistically significant (\*). Results represent the mean  $\pm$  SD of 3 independent experiments.*

Finally, I wanted to determine if blockade of NRF2 using a chemical inhibitor could mimic the effect using shRNA. As inhibitor that could specially target NRF2 is in need of develop, I selected brusatol to treat the MM1S and primary MM sample. Brusatol is a quassinoid compound extracted from *Brucea javanica*. As a general translation inhibitor, brusatol causes a decline in the protein levels of short-lived proteins, including NRF2 [271]. Data show brusatol decreased cell viability of primary MM cells and MM cell lines (Figure 3.6). Since a subset of MM cells were resistance to brusatol, the data suggest that NRF2 activation is critical for the survival of a subset of MM cells.

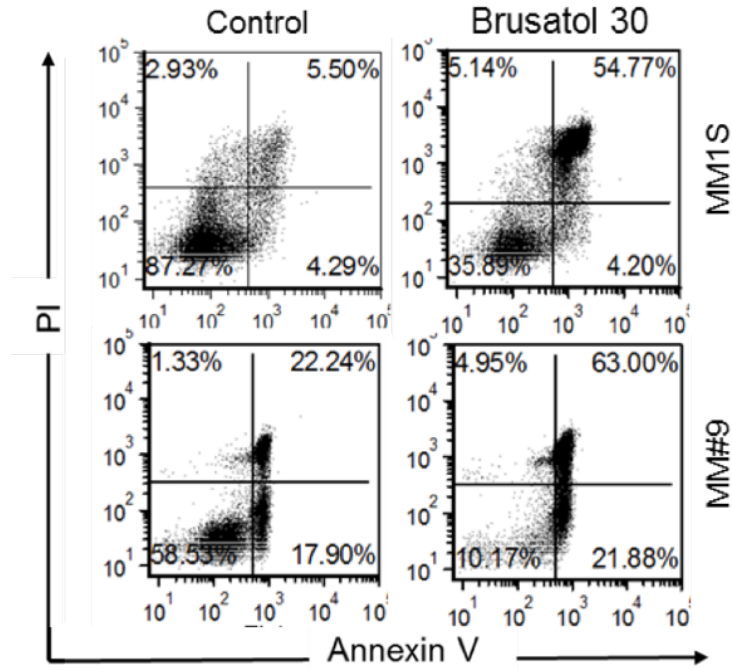


**Figure 3.6 NRF2 inhibitor brusatol induces MM cell apoptosis**

*MM1S cells and primary MM cells were treated with brusatol (30 nM) for 24h and then analysed for apoptosis using flow cytometer with PI/Annexin V staining.*

### 3.2.4 To investigate PI induced NRF2 activity in MM cells

PI is increasingly used in the treatment of MM. I therefore evaluated NRF2 expression in PI treated MM cell lines to evaluate if NRF2 may function as a mechanism of resistance to PI. I evaluated nuclear NRF2 expression, as it better reflects NRF2 activation. Results show PI induced NRF2 protein level in nuclear extracts (Figure 3.7-8) of all MM cell lines.

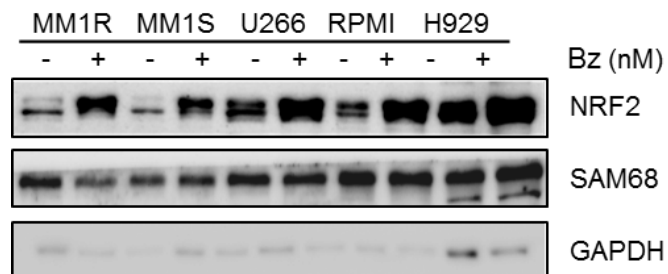


**Figure 3.7 PI activates NRF2 in MM cell lines**

*MM cell lines were treated with Bz (10 nM) for 4h. Nuclear protein was then extracted, and Western blotting was performed for NRF2 protein expression. Sam68 is for positive loading control (Sam68: the Src-Associated substrate in Mitosis of 68 kDa is specifically expressed in nucleic) and GAPDH is for negative loading control (GAPDH is not expressed in nucleic). Blots were reprobed for SAM68 and GAPDH for loading control.*

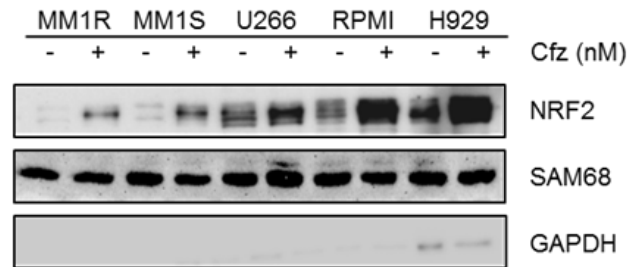


**Figure 3.8 PI activates NRF2 in MM cell lines**

*MM cell lines were treated with Cfz (10 nM) for 4h. Nuclear protein was then extracted, and Western blotting was performed for NRF2 protein expression. Blots were reprobed for SAM68 and GAPDH for loading control.*

As it is difficult to acquire enough primary MM samples to analyse the nuclear NRF2 expression by Western Blot method. For detecting the PI effects in primary MM cells, confocal imaging method was used. Figure 3.9 shows that NRF2 accumulated and presented in the nucleus of primary MM cells treated with PI.

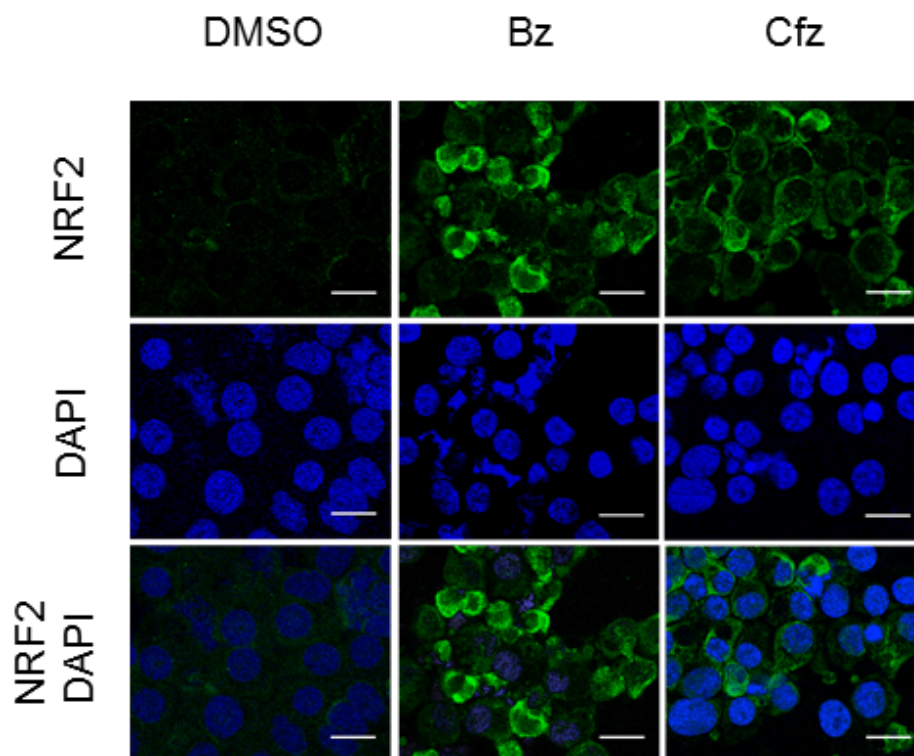


**Figure 3.9 PI activates NRF2 expression in primary MM cells**

*Primary MM cells were treated with Bz or Cfz (10 nM) for 4h. Cells were fixed and stained with NRF2 and DAPI and then analysed using confocal microscope method. Scale bar = 10  $\mu$ m.*

To evaluate if accumulated nucleic NRF2 protein initiates NRF2 regulated gene expression, I examined the HO-1 and GCLM mRNA expression in PI treated MM cell lines and primary MM cells, using qPCR (Figure 3.10-3.13).

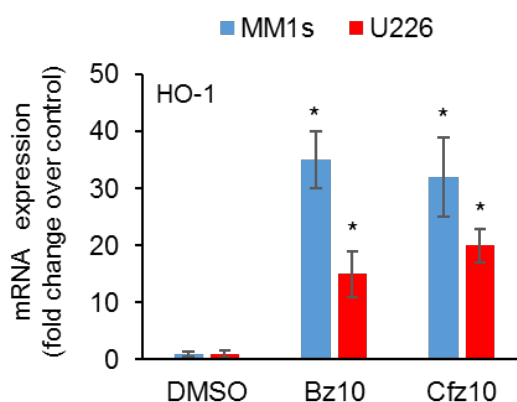


**Figure 3.10 PI induces HO-1 RNA expression in MM cell lines**

MM cell lines were treated with Bz or Cfz for 4h at 10 nM. RNA was extracted and analysed using qRT-PCR for HO-1 expression. Gene expression was normalised to GAPDH. The Mann Whitney test was used to compare results in control to treated groups. Results with  $p < 0.05$  were considered statistically significant (\*). Results represent the mean  $\pm$  SD of 3 independent experiments.

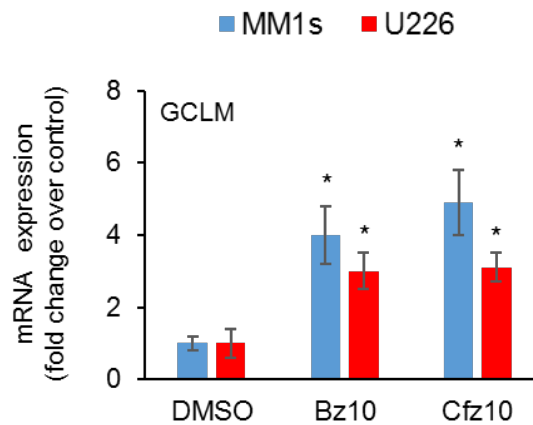


**Figure 3.11 PI induces GCLM RNA expression in MM cell lines**

MM cell lines were treated with Bz or Cfz for 4h at 10 nM. RNA was extracted and analysed using qRT-PCR for GCLM expression. Gene expression was normalised to GAPDH. The Mann Whitney test was used to compare results in control to treated groups. Results with  $p < 0.05$  were considered statistically significant (\*). Results represent the mean  $\pm$  SD of 3 independent experiments.

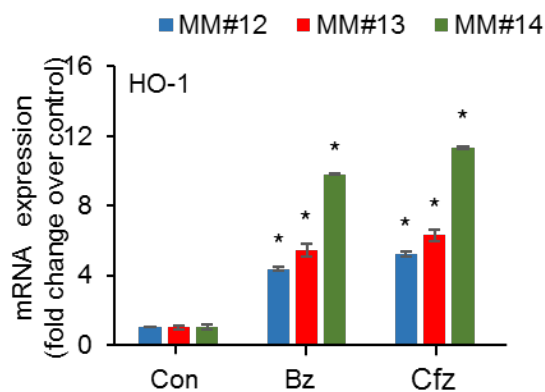


**Figure 3.12 PI induces HO-1 RNA expression in primary MM cells**

Primary MM cells were treated with Bz or Cfz for 4h at 10 nM. RNA was extracted and analysed using qRT-PCR for HO-1 expression. Gene expression was normalised to GAPDH. Two-way ANOVA with Sidak's post-test was used to compare changes in individual primary sample under treatment. Results with  $p < 0.05$  were considered

statistically significant (\*). Results represent the mean  $\pm$  SD of 3 independent experiments.

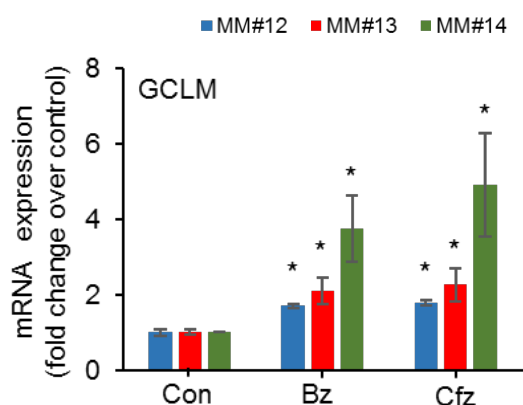


**Figure 3.13 PI induces GCLM RNA expression in primary MM cells**

Primary MM cells were treated with Bz or Cfz for 4h at 10 nM. RNA was extracted and analysed using qRT-PCR for GCLM expression. Gene expression was normalised to GAPDH. Two-way ANOVA with Sidak's post-test was used to compare changes in individual primary sample under treatment. Results with  $p < 0.05$  were considered statistically significant (\*). Results represent the mean  $\pm$  SD of 3 independent experiments.

### 3.2.5 To Determine if PI induced NRF2 activation by examining the activity of the ARE in the HO-1 promoter.

To confirm that PI activates NRF2 in MM, HO-1 promoter assay method was used. A wild type HO-1 promoter or a mutant (mut) HO-1 promoter (NRF2 antioxidant response element mutated, ARE; Figure 3.14) were transfected into MM1S. To generate a mutated ARE in the HO-1 promoter, pHO-1Luc4.0mARE, the conserved GC nucleotides in the inverted ARE element were mutated to TA using the GeneTailor mutagenesis kit according to the manufacturer's instructions (Invitrogen). The PCR primers used in the mutagenesis were 5'-GGCGGATTTTGC TAGATT-TTATTGAGTCACCA-3' (forward primer, the underlined AT represents GC to TA mutation) and 5'-TGTTTCCCTTCCGCCTAAAACGATCTA-AAA-3' (reverse primer).

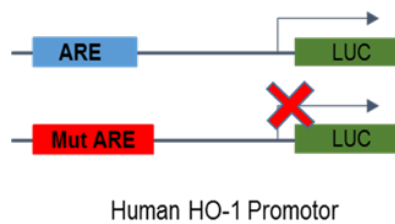


**Figure 3.14 Schematic of the human promoter construct**

*Human HO-1 promoter construct (pHO-1Luc4.0) or human HO-1 promoter with ARE mutation construct (pHO-1mutARE).*

Cells were then treated with PI and promoter activity was determined. Figure 3.15 shows that mutant HO-1 promoter (mutARE) had a significant reduction in activity compared to wildtype (ARE).

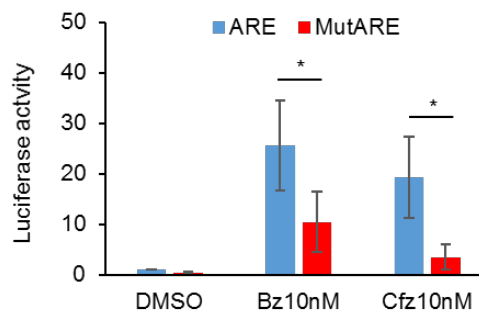


**Figure 3.15 Bz and Cfz activate NRF2 in MM cells**

*MM1S cells were transfected with pHO-1Luc4.0 or pHO-1mutARE for 48h and then no treatment (as control) or treated with Bz or Cfz (10 nM) for 24h. Luciferase activity assay was used to detect HO-1 promoter activation. The Mann Whitney test was used to compare results in control to treated groups. Results with  $p < 0.05$  were considered statistically significant (\*). Results represent the mean  $\pm$  SD of 3 independent experiments.*

The above data confirm that the PI induced the NRF2 activation.

### 3.2.6 shRNA mediated NRF2 depletion in MM cells

To investigate the NRF2 function in PI resistant MM cells, I first silenced NRF2 in MM cells and evaluated the PI induced NRF2 protein expression. Figure 3.16-17 show that PI induced NRF2 up-regulation was inhibited in NRF2-KD MM cells.

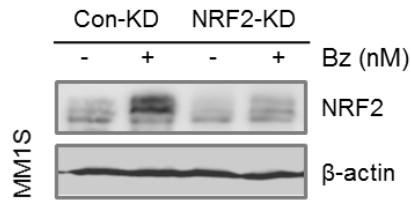


**Figure 3.16 Less NRF2 protein levels was detected in NRF2-KD MM1S cells**

*Lentiviral mediated shRNA KD of NRF2 in MM1S. Cells were then treated with Bz or Cfz (10 nM) for 4h and whole cell protein was extracted, and Western blotting was performed for NRF2 protein expression. Blots were reprobred for beta-actin as loading control.*

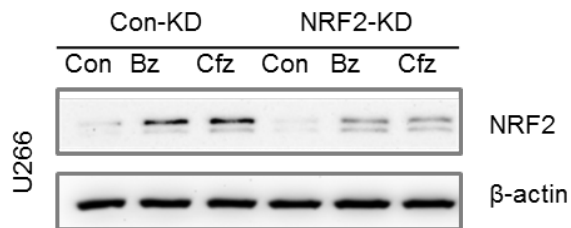


**Figure 3.17 Less NRF2 protein levels was detected in NRF2-KD U266 cells**

*Lentiviral mediated shRNA KD of NRF2 in U266. Cells were then treated with Bz or Cfz (10 nM) for 4h and whole cell protein was extracted, and Western blotting was performed for NRF2 protein expression. Blots were reprobred for beta-actin loading control.*

Next, experiments were designed to determine if NRF2-KD in MM cells have lower NRF2 regulated gene expression. Figure 3.18-21 show that PI induced NRF2 regulated genes were inhibited in NRF2-KD U266. Taken together these data confirm that PI activates NRF2 induced transcription of target genes in MM cells.

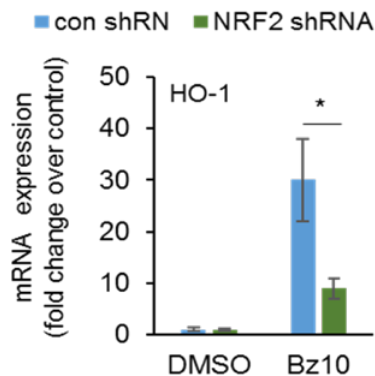


**Figure 3.18 Bz induces less HO-1 RNA expression in NRF2-KD U266 cells**

Lentiviral mediated shRNA KD of NRF2 in U266 cells. Cells were then treated with Bz for 4h. RNA was extracted and analysed for HO-1. Gene expression was normalised to GAPDH. The Mann Whitney test was used to compare results in control to treated groups. Results with  $p < 0.05$  were considered statistically significant (\*). Results represent the mean  $\pm$  SD of 3 independent experiments.

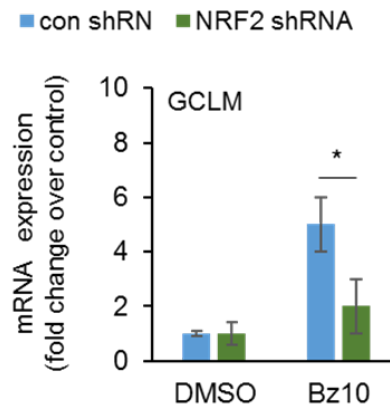


**Figure 3.19 Bz induced less GCLM RNA expression in NRF2-KD U266 cells**

Lentiviral mediated shRNA KD of NRF2 in U266 cells. Cells were then treated with Bz for 4h. RNA was extracted and analysed for GCLM. Gene expression was normalised to GAPDH. The Mann Whitney test was used to compare results in control to treated groups. Results with  $p < 0.05$  were considered statistically significant (\*). Results represent the mean  $\pm$  SD of 3 independent experiments.

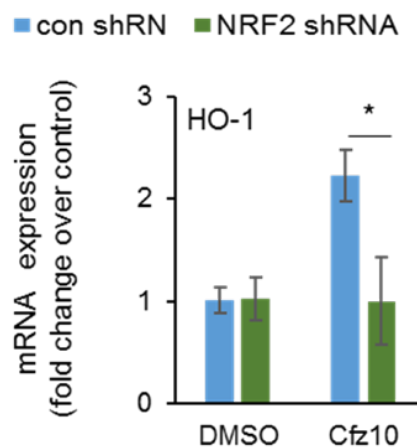


**Figure 3.20 Cfz induced less HO-1 RNA expression in NRF2-KD U266 cells**

Lentiviral mediated shRNA KD of NRF2 in U266 cells. Cells were then treated with Cfz for 4h. RNA was extracted and analysed for HO-1. Gene expression was normalised to GAPDH. The Mann Whitney test was used to compare results in control to treated groups. Results with  $p < 0.05$  were considered statistically significant (\*). Results represent the mean  $\pm$  SD of 3 independent experiments.

to treated groups. Results with  $p < 0.05$  were considered statistically significant (\*). Results represent the mean  $\pm$  SD of 3 independent experiments.

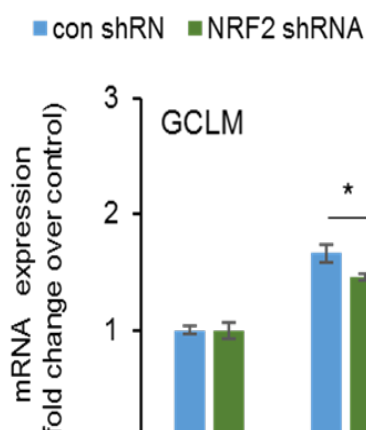


**Figure 3.21 Cfz induced less GCLM RNA expression in NRF2-KD U266 cells**

*Lentiviral mediated shRNA KD of NRF2 in U266 cells. Cells were then treated with Cfz for 4h. RNA was extracted and analysed for GCLM. Gene expression was normalised to GAPDH. The Mann Whitney test was used to compare results in control to treated groups. Results with  $p < 0.05$  were considered statistically significant (\*). Results represent the mean  $\pm$  SD of 3 independent experiments.*

### 3.2.7 NRF2 inhibition up-regulated CHOP expression and induced ER stress

MM cells present higher levels of ER stress as a consequence of the large amount of paraprotein (incorrect folded protein) production [257, 259, 272]. Moreover, PI further increases ER stress as more proteins accumulate in the MM cells when the proteasome degradation system is inhibited [86]. I therefore wanted to explore if upregulated NRF2 expression decreases ER stress associated apoptosis in response to PI. First, I showed that NRF2-KD in U226 and MM1S cells upregulated CHOP expression, but not ATF4 expression (Figure 3.22-23).

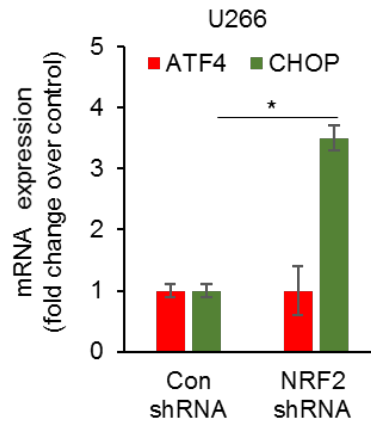


**Figure 3.22 NRF2-KD U266 cells have upregulated CHOP expression but not ATF4 expression**

*Lentiviral mediated shRNA KD of NRF2 in U266. RNA was extracted and analysed for ATF4 and CHOP. Gene expression was normalised to GAPDH. The Mann Whitney test was used to compare results in control to treated groups. Results with  $p < 0.05$  were considered statistically significant (\*). Results represent the mean  $\pm$  SD of 3 independent experiments.*

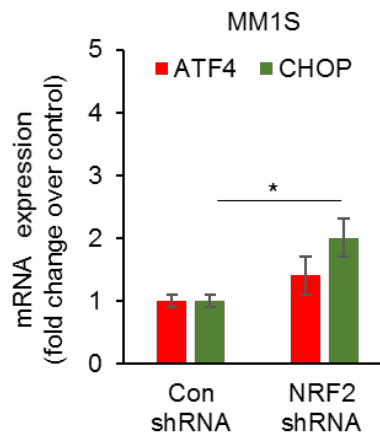


**Figure 3.23 NRF2-KD MM1S cells have upregulated CHOP expression but not ATF4 expression**

*Lentiviral mediated shRNA KD of NRF2 in MM1S. RNA was extracted and analysed for ATF4 and CHOP. Gene expression was normalised to GAPDH. The Mann Whitney test was used to compare results in control to treated groups. Results with  $p < 0.05$  were considered statistically significant (\*). Results represent the mean  $\pm$  SD of 3 independent experiments.*

Next, I wanted to determine if NRF2-KD MM cells have higher ER stress. Figure 3.24 shows that using the ER tracker assay, NRF2-KD cells had a higher ER stress compared to control-KD cells.

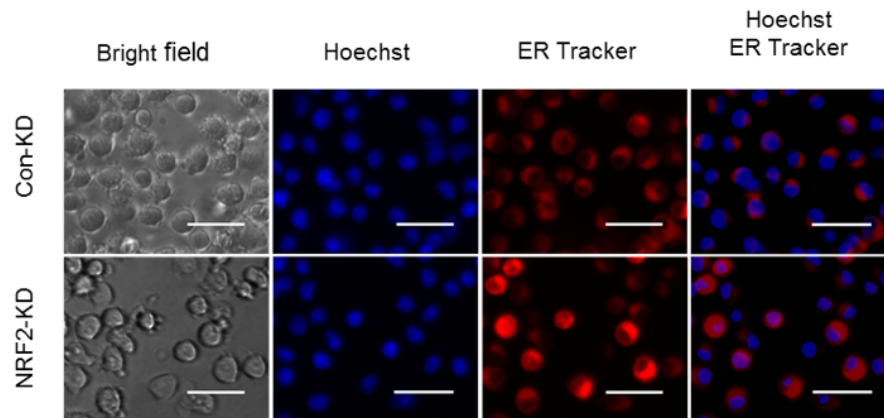


**Figure 3.24 NRF2 regulated ER stress in MM1S**

*Control-KD and NRF2-KD MM1S cells were incubated with the Hoechst 33342 and ER Tracker then visualized by fluorescence microscopy. Scale bar = 20  $\mu$ M.*

### 3.2.8 Can PI induce CHOP expression and ER stress in NRF2-KD MM cells?

I demonstrated that PI treated NRF2-KD cells have further increased ER-stress by flow cytometry (Figure 3.25). Next, I used qPCR method to examine if CHOP and ATF4 gene expression increased in response to PI treatment. Figure 3.26 shows that CHOP was increased in MM1S cells in response to PI.

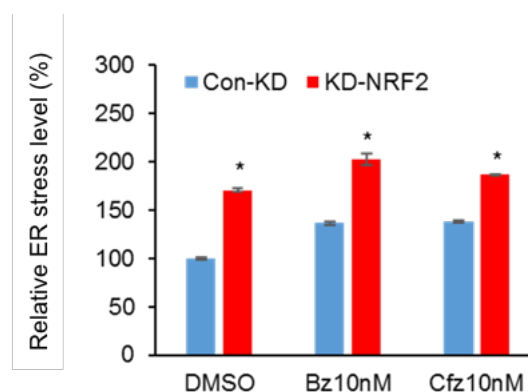


**Figure 3.25 NRF2 regulated ER-stress in MM1S**

*Control-KD and NRF2-KD MM1S cells were incubated with the Hoechst 33342 and ER Tracker then analysed by flow cytometry. The Mann Whitney test was used to compare results in control to treated groups. Results with  $p < 0.05$  were considered*

statistically significant (\*). Results represent the mean  $\pm$  SD of 3 independent experiments.

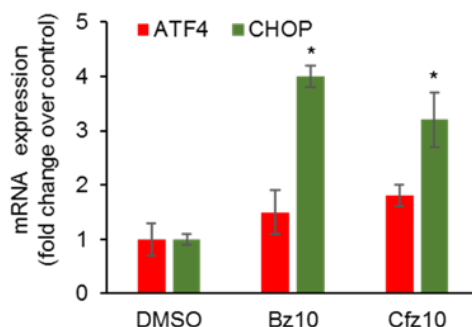


**Figure 3.26 PI induced CHOP RNA expression in MM cells**

MM1S cells were treated with PI for 4h and RNA was extracted and analysed for ATF4 and CHOP. Gene expression was normalised to GAPDH. The Mann Whitney test was used to compare results in control to treated groups. Results with  $p < 0.05$  were considered statistically significant (\*). Results represent the mean  $\pm$  SD of 3 independent experiments.

Next, I analysed CHOP mRNA expression in PI treated NRF2-KD cells to determine if ER stress induced CHOP expression. Figure 3.27 shows that NRF2-KD cells have a significant increased CHOP expression when they were treated with PI compared to control-KD cells.

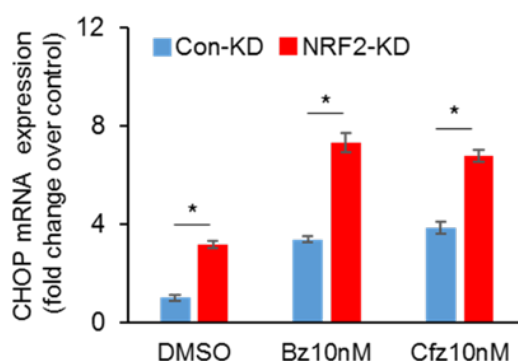


**Figure 3.27 PI induced CHOP RNA expression in NRF-KD MM1S**

NRF2-KD MM1S cells were treated with PI for 4h and RNA was extracted and analysed for CHOP. Gene expression was normalised to GAPDH. The Mann Whitney test was used to compare results in control to treated groups. Results with  $p < 0.05$  were considered statistically significant (\*). Results represent the mean  $\pm$  SD of 3 independent experiments.

### 3.2.9 NRF2 regulated CHOP protein expression in MM cells

Next, I examined if NRF2 regulates CHOP protein expression in MM cells. To do this I knocked down NRF2 in MM cells and performed a Western blot for CHOP expression. Figure 3.28 and 3.29 show that in NRF2-KD cells treated with PI have increased CHOP expression.

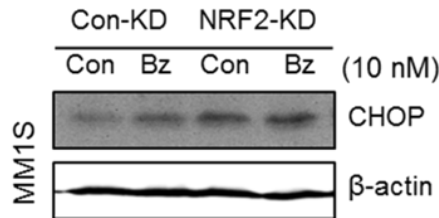


**Figure 3.28 NRF2 regulated CHOP protein expression in MM1S**

*Lentiviral mediated shRNA KD of NRF2 in MM1S. Cells were treated with PI for 4 h. Protein was extracted, and Western blotting was performed for CHOP protein expression. Blots from Figure 3.14 were reprobred for CHOP protein expression.*

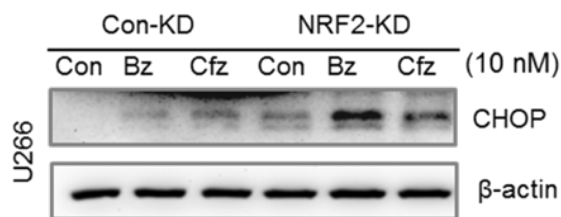


**Figure 3.29 NRF2 regulated CHOP rotein expression in U266**

*Lentiviral mediated shRNA KD of NRF2 in U266. Cells were treated with PI for 4 h. Protein was extracted, and Western blotting was performed for CHOP protein expression. Blots from Figure 3.17 were reprobred for CHOP protein expression.*

### 3.2.10 NRF2 regulates GSH synthesis

There are two ways for NRF2 to regulate CHOP gene expression. One is by direct binding to the CHOP promoter, another is from an indirect pathway, which is mediated through the NRF2 regulated GSH synthesis pathway [260] [273]. To confirm if GSH plays a role in regulating CHOP expression in MM cells, I first analysed the GSH levels in PI treated MM cell lines. Figure 3.30 shows that Bz increased GSH levels in MM1S.

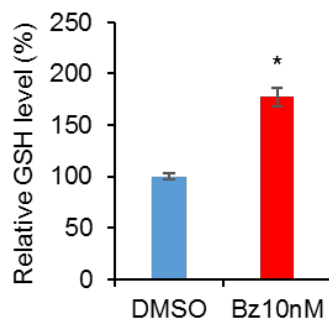


**Figure 3.30 PI induced GSH synthesis**

*MM1S cells were treated with Bz (10 nM) for 4h. A GSH assay was performed to detect GSH level. The Mann Whitney test was used to compare results in control to treated groups. Results with  $p < 0.05$  were considered statistically significant (\*). Results represent the mean  $\pm$  SD of 3 independent experiments.*

In 1.5.1 I described that NRF2 regulated GSH synthesis. Then, NRF2-KD was used to determine if NRF2 regulates GSH levels in MM cells. Figure 3.31 shows that GSH levels were not significantly increased in NRF2-KD MM cells compared to Con-KD cells, which confirms reduced NRF2 decreasing GSH production.

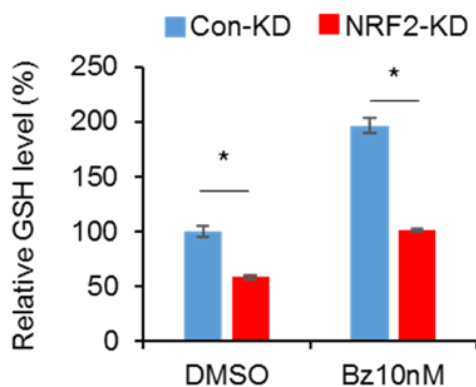


**Figure 3.31 NRF2-KD MM1S have lower PI induced GSH levels**

*Con-KD and NRF2-KD MM1S cells were treated with Bz (10 nM) for 4h. GSH assay was performed to detect GSH level. The Mann Whitney test was used to compare results in control to treated groups. Results with  $p < 0.05$  were considered statistically significant (\*). Results represent the mean  $\pm$  SD of 3 independent experiments.*

### 3.2.11 GSH synthesis blocks ER stress in MM cells

To confirm that the GSH regulates CHOP expression and ER stress in MM cells, I supplemented the MM cells with N-Acetyl Cysteine (NAC), a precursor of GSH. Figure 3.32-33 show that NAC blocked Bz induced CHOP and ER stress responses. These data confirm that GSH level is essential in MM cells for the CHOP regulation and ER stress.

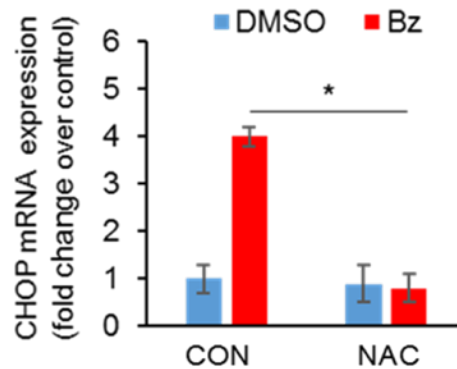


**Figure 3.32 NAC blocked Bz induced CHOP RNA expression**

*MM1S cells were treated with Bz (10 nM) in combination with NAC (100  $\mu$ M). Then RNA was extracted and analysed using qRT-PCR for CHOP expression. Gene expression was normalised to GAPDH. The Mann Whitney test was used to compare results in control to treated groups. Results with  $p < 0.05$  were considered statistically significant (\*). Results represent the mean  $\pm$  SD of 3 independent experiments.*

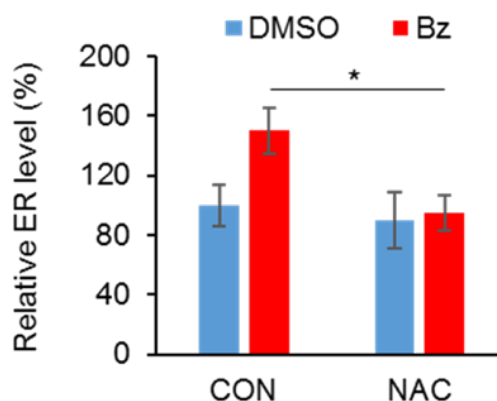


**Figure 3.33 NAC inhibited Bz induced ER stress**

*MM1S cells were treated with Bz (10 nM) in combination with NAC (100  $\mu$ M). Cells were incubated with the ER Tracker and analysed by flow cytometry. Results expressed as relative median fluorescence intensity. The Mann Whitney test was used to compare results in control to treated groups. Results with  $p < 0.05$  were considered*

statistically significant (\*). Results represent the mean  $\pm$  SD of 3 independent experiments.

Next, I wanted to determine if the GSH synthesis inhibitor, buthionine sulfoximine (BSO) increases Bz induced CHOP mRNA expression and ER stress responses. Figure 3.34-35 show that BSO increased Bz induced CHOP and ER stress responses.

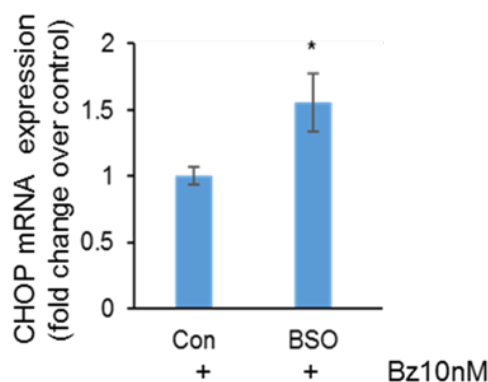


**Figure 3.34 BSO increased Bz induced CHOP RNA expression**

*MM1S cells were treated with Bz (10  $\mu$ M) in combination with buthionine sulphoximine (BSO) 5  $\mu$ M for 4h and then RNA was extracted and analysed using qRT-PCR for CHOP expression. Gene expression was normalised to GAPDH. The Mann Whitney test was used to compare results in control to treated groups. Results with  $p < 0.05$  were considered statistically significant (\*). Results represent the mean  $\pm$  SD of 3 independent experiments.*

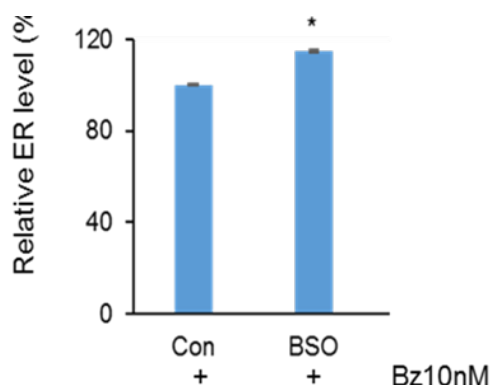


**Figure 3.35 BSO increased Bz induced ER stress**

*MM1S cells were treated with Bz (10 nM) in combination with (BSO) 5  $\mu$ M for 4h. Cells were incubated with the ER Tracker and analysed by flow cytometry. Results expressed as relative median fluorescence intensity. The Mann Whitney test was used to compare results in control to treated groups. Results with  $p < 0.05$  were considered*

statistically significant (\*). Results represent the mean  $\pm$  SD of 3 independent experiments.

### 3.2.12 NRF2-KD MM cells were sensitive to PI induced apoptosis

Finally, I wanted to determine if NRF2-KD sensitises MM cells to PI induced apoptosis. Figure 3.36 shows that NRF2-KD MM cells were sensitive to PI induced cell death.

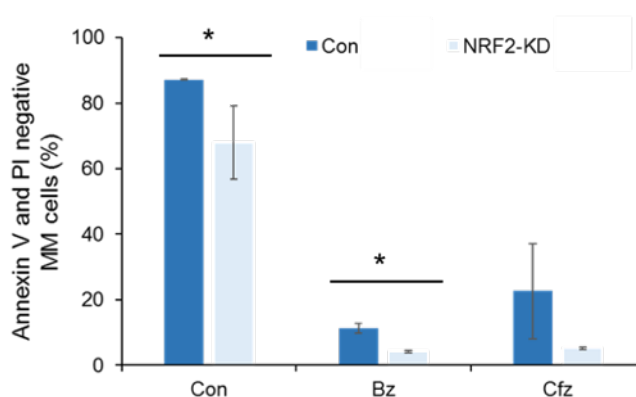


**Figure 3.36 NRF2-KD MM cells were sensitive to PI treatment**

*Con-KD or NRF2-KD MMIS or U266 were incubated with Bz or Cfz (10 nM) for 36h and then cell apoptosis was analysed using flow cytometer with PI/Annexin V staining. The Mann Whitney test was used to compare results in control to treated groups. Results with  $p < 0.05$  were considered statistically significant (\*). Results represent the mean  $\pm$  SD of 3 independent experiments.*

## 3.3 Summary and Discussion

PI is a first line drug for MM, however patients inevitably relapse through the development of drug resistant clones [249-252, 274]. Thus, a new MM therapy strategy is in needed to treat patients that become resistant to PI. In this chapter, I show that NRF2 inhibition could be that new target and this could allow resistant clones to become resensitised to PI inhibitors.

Here I show that high levels of NRF2 in 50% of primary MM cells tested and in all MM cell lines tested, which suggest the NRF2 protect MM cells. I think multiple reasons resulted with only 50% of primary MM cells were detected with high NRF2.

For example: 1) the primary MM samples were derived from different stage of disease progression from 10% to 100% MM cells infiltrated in the BM, which will give variety of NRF2 levels (table 1.1); 2) there are multiple gene mutation events in MM patients, which may lead to different NRF2 expression; 3) the primary samples include untreated newly diagnosed patients, patients going through chemotherapy or relapse patients that will have different NRF2 expression accordingly.

I performed NRF2 inhibition experiment to exam if NRF2 regulation protect MM cells, and data show NRF2 inhibition sensitised MM cells to apoptosis. My data are consistent with another report, which shows that regulating ROS in MM cells enhances its sensitivity to Bz and is NRF2 dependent [263].

I confirm that NRF2 promotes MM cell survival at least partly by mediating the CHOP, a NRF2 regulated ER stress response protein. Moreover, I confirm that PI prompts NRF2 upregulation in MM cells, which decreases CHOP expression and increases GSH production. Silencing NRF2 decreases PI induced GSH level and induces CHOP expression. Apoptosis assay shows that NRF2 inhibition sensitises MM cells to PI treatment.

As described in 1.5.1, NRF2 regulates GCLM expression and thus active GSH synthesis and recycling [275]. In MM cells, I discovered that PI upregulates NRF2 regulated CHOP expression, which is mediated by GSH. I confirmed that PI induces GSH, and NRF2 silencing decreases GSH in MM cells. My data are consistent with reported works that confirm GSH regulates MM survival from PI treatment and I extended that observation to place CHOP downstream of GSH.



**Figure 3.37 Schematic representation of NRF2- GCLM- GSH**

*NRF activates the GCLM gene expression. GCLM was then involved in the GSH synthesis.*

In summary, though NRF2 protects non-malignant cells from oxidative stress, it also has a pro-tumoural role especially in MM cells. Here I have shown that NRF2 enhances the chemotherapy resistance via the up-regulation of the GSH synthesis. The data show that PI activates the NRF2 pathway, which negatively regulates ER stress via inhibition of CHOP expression. NRF2 upregulation increases the GSH synthesis, which blocks the CHOP induced apoptosis (summarised in figure 3.37). Accordingly, the project may lead to a new MM treatment strategy that is to identify a clinically relevant NRF2 inhibitor to sensitise MM cells to PI.

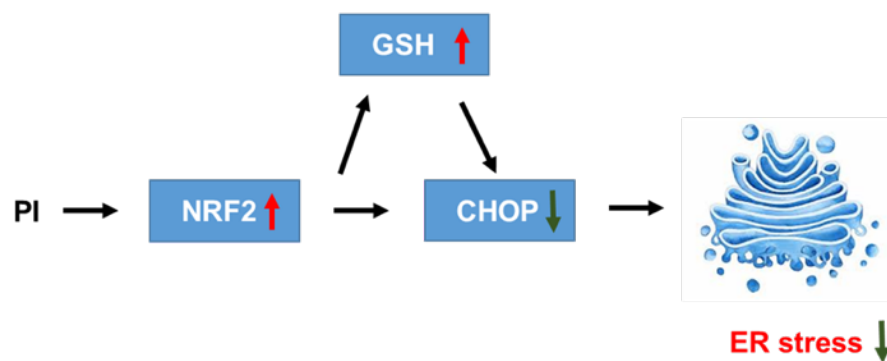


**Figure 3.38 Schematic representation of NRF2 activity in PI treated MM cells**

*Pi induces the NRF2 activation and resulted with elevated GSH level which decrease the CHOP expression and decreased the ER stress.*

**CHAPTER FOUR**  
**INVESTIGATING THE PROTECTIVE ROLE OF NRF2 IN**  
**BMSC ON MM**

## **4.1 Introduction**

### **4.1.1 BMSC plays a key role on MM progression**

The pathogenic role of the BM niche in the progression of MGUS and SMM to MM is crucial [203]. The BM niche is not only the location for the MM cell proliferation, but also protects MM cells against chemotherapy. The MM-BM niche interaction is bidirectional and MM BM niche is different in its cellular and non-cellular composition compared to the healthy BM niche [276]. Thus, this section of my thesis aims to study the interaction between MM and the BM niche and identify new targets that could improve MM treatment.

The BM niche is a spatial microenvironment, which consist of different cell types and BMSC is one of the cells that has been heavily investigated for its protective role on MM cells. It is widely established that BMSC support the growth of MM cells [277]. For example, the MM cells attach to the BMSC and trigger the secretion of interleukin-6 (IL-6) from BMSC, which in turn promotes the proliferation of the MM cells [278]. Others have shown that binding of MM cells to the BMSC are essential for the chemotherapy resistance [278-282]. Moreover, BMSC function is essential for the progression of MM. For example, DKK1 is highly expressed in the MM derived BMSC, which promote the permissive interaction of MM-BMSC which leads to MM progression [283]. Besides these examples, several mechanisms of how BMSC promote MM progression have been identified, for example: BMSC secreted exosomes activate immune suppressor cells in the BM mediated by STAT3/STAT1 and the immune suppressor cells suppress immune response which favours MM progression [284]; the vascular cell adhesion molecule 1/integrin  $\beta$ 1 mediated MM and BMSC interaction promote the activity of osteoclast, which favours MM progression [285]; mucin 1 cell surface-associated axes 1 active MYC promotor in the MM cells and is involved in the progression of MGUS to MM [151]. BMSC also secrete chemotactic cytokines such as IL-6, CXCL12, IGF-1 and VEGFA that favour MM cells. Taken together, these studies suggest a special role for the BMSC in regulating the survival, proliferation and chemotherapy resistance of MM.

Furthermore, the MM-BMSC interaction are bidirectional in that MM cells also stimulate BMSC to create a favourable microenvironment for their survival, for example: MM cells over express  $\beta 1$  integrin, which mediated the adhesion of MM and BMSC, which then causes BMSC to increase the secretion of IL-6 and activate STAT3 signalling in MM cells [286];  $\beta 1$  integrin together with gp130 (IL-6 $\beta$  receptor) also mediate focal adhesion formation and active proline-rich tyrosine kinase activity, which is linked with MM progression [287]; MM cells express IL-17A, which both increase the MM cell proliferation and induce IL-6 production from BMSC [288]; ubiquitin-binding protein, p62 regulates the modification of NF- $\kappa$ B, p38 MAPK and JNK in BMSC that increase osteoclast genesis and MM cell proliferation [289]. The above research suggests that interrupting the interaction of MM-BMSC is necessary to prevent the progression of MM and sensitise the MM cells to chemotherapy.

#### **4.1.2 The NRF2 Function in BM Protection Effect on MM Cells**

In Chapter 3 I described how MM needs to regulate ROS as they produce superoxide as a byproduct of paraprotein folding/production in the ER. Moreover, within the group I work, published data shows that AML induces ROS in BMSC [290]. Therefore, in this research I first wanted to determine if BMSC have increased ROS when in close proximity to MM cells. The MM cells produce and secrete paraproteins to the surrounding BM microenvironment, which could lead to increased stress in the local environment. Furthermore, when the MM patient is in treatment, the BMSC is also exposed to chemotherapy. Therefore, I hypothesise that the BMSC have increased ROS levels when located close to MM cells as well as in response to MM chemotherapy.

Universally expressed in nearly all types of cells, NRF2 is the main cellular way to sense the ROS change and upregulate the antioxidant defence systems needed to regulate the elevated ROS. In chapter three, I have reported that NRF2 regulation in MM cells plays a key role for the survival of MM cells. In this chapter, I will further decode the mechanism of NRF2 function in MM by examining the role of NRF2 in BMSC and its effect on MM cell survival.

NRF2 function in the BMSC protection effect on MM cells has not been investigated, but the NRF2 function in bone metabolism, BM and BMSC has attracted some attention. For example, a report shows that NRF2 is a key player for the normal postnatal bone acquisition [291]. Another report shown that activating the NRF2 pathway is essential in the treatment of spinal cord injury [292]. When BMSC is in stress (such as oxidation stress or chemotherapy), the BMSC upregulate NRF2 for protection [293]. These studies highlight the protective role of NRF2 in the bone and the BMSC under normal stressed conditions.

#### **4.1.3 Aims and objectives**

The last chapter showed that NRF2 regulates ER stress associated apoptosis which protects MM cells from PI induced cell death. This highlights a role for NRF2 protection in MM. Next, I wanted to determine if NRF2 regulates BMSC protection of MM. To investigate this idea, I asked the following questions; 1) Do MM cells induce ROS stress and NRF2 upregulation in BMSC? 2) Do PI induce ROS stress and NRF2 upregulation in BMSC? 3) Does silencing NRF2 expression in BMSC reverse BMSC protection of MM cells and sensitise MM cells to chemotherapy?

## 4.2 Results

### 4.2.1 BMSC protected MM cells from apoptosis

It is widely accepted that MM cells cannot survive without the support of the BM/BMSC both *in vitro* and *in vivo*. To confirm this observation, I isolated primary MM cells and then cultured these cells with or without BMSC isolated from patients with MM. Moreover, I treated these co-cultured cells with Cfz for 24 hr. The MM cells are suspended cells and the BMSC is adherent cell. Primary MM cells are generally not form tight connection within 24h co-culture. I washed the MM cells off the BMSC and gating out detached BMSC in the FSC/SSC chart (The size of primary MM cells is smaller than BMSC). Figure 4.1 shows that primary MM cells have increased apoptosis when cultured alone compared to MM cells cultured on BMSC. Moreover, MM cells were protected from chemotherapy induced apoptosis by co-culture with BMSC.

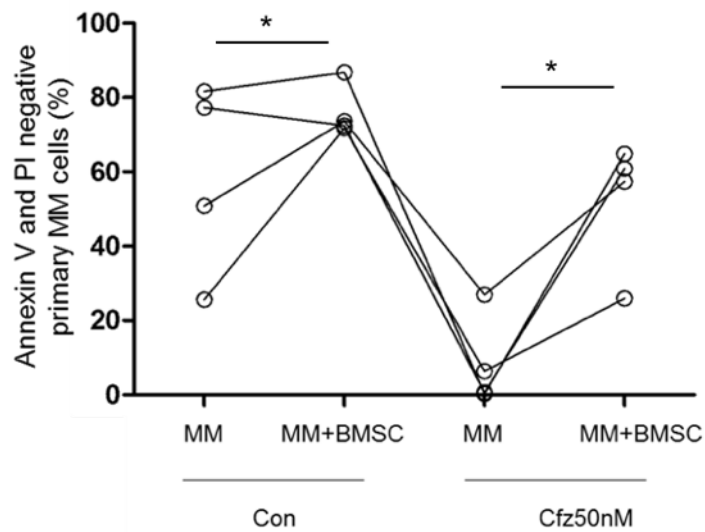


**Figure 4.1 BMSC protected primary MM cells from apoptosis**

Freshly purified primary MM cells isolated from MM patients were co-cultured with or without BMSC and were treated with Cfz (50 nM) for 24h. Joined bar show the changes of single primary MM cells cultured with or without BMSC. Viable primary MM cells were analysed using a flow cytometer with PI/Annexin V staining. Two-way ANOVA with Sidak's post-test was used to compare changes in individual primary sample under treatment. Results with  $p < 0.05$  were considered statistically significant (\*). Results represent the mean  $\pm$  SD of 4 independent experiments.

#### 4.2.2 Determine MM cells induced ROS level on BMSC *in vitro*

As NRF2 senses ROS [138], next I wanted to determine if MM cells induce ROS stress in BMSC. To do this I examined both mitochondrial and cellular ROS, using the dyes MitoSOX and DCF, in BMSC that were co-cultured with MM cells. Figure 4.2A and Figure 4.2B show that primary MM cells increased both MitoSOX and DCF MFI levels in BMSC.

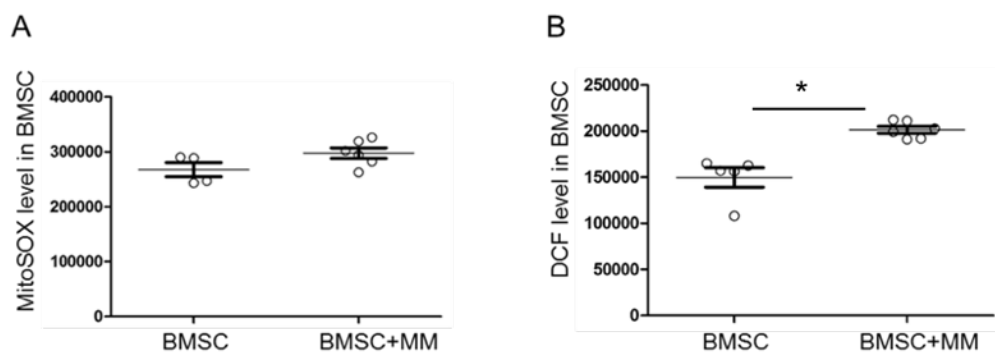


**Figure 4.2 MM cells increased MitoSOX and DCF level in BMSC**

Primary MM cells isolated from MM patients were co-cultured with or without BMSC. (A) MitoSOX levels in BMSC were analysed using flow cytometer with human CD105 APC and MitoSOX (PE-Cy5 channel) staining and expressed as MFI. (B) DCF levels in BMSC were analysed using flow cytometer with human CD105 APC and DCF (FITC channel) staining and expressed as MFI. Two-way ANOVA with Sidak's post-test was used to compare changes in individual primary sample under treatment. Results with  $p < 0.05$  were considered statistically significant (\*). Results represent the mean  $\pm$  SD of 5 independent experiments.

#### 4.2.3 Determine MM cells induced ROS level on BMSC *in vivo*

It is important to understand if the ROS increase, I observed in BMSC in *in vitro* co-cultures, also observed in the BMSC of *in vivo* MM models. To do this I injected primary MM cells, which were infected with a lentivirus encoding luciferase (luci) into the tail of NSG mice. If MM cells could engraftment in the mice, then it will localise in the BM of mice. I did this so I could visualise primary MM engraftment in NSG mice in live animal imaging. Figure 4.3 shows the engraftment of MM cells in the BM of mice on day 20 as measured by *in vivo* live imaging using the *in vivo* Bruker

Xtreme. Figure 4.4 shows that when I isolated the BM cells of NSG engrafted mice it contains human CD45<sup>+</sup> and human CD38<sup>+</sup> cells. The results confirm that primary MM cells engraft into the BM of NSG mice after 20 days.

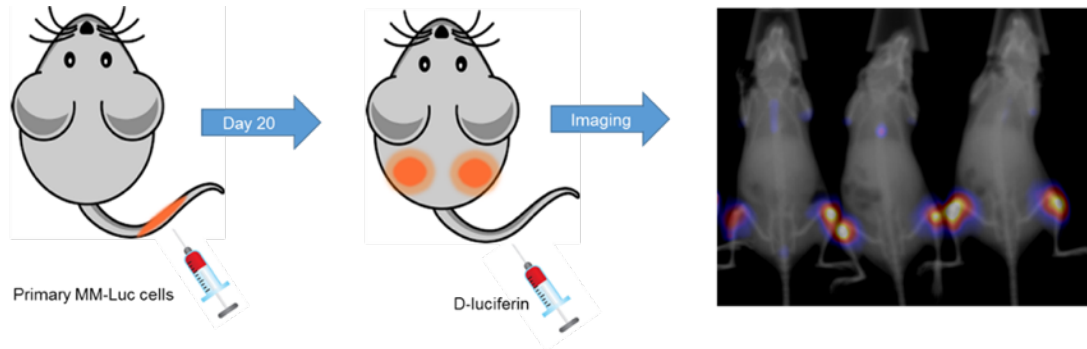


**Figure 4.3 Bioluminescence *in vivo* images detected the disease progression in MM xenograft NSG model**

*Three primary cells were infected with Luci.  $1 \times 10^6$  MM-Luci cells were injected in the tail of NSG mice (IV). Bioluminescence method was used to monitor the engraftment of cells at day 20.*

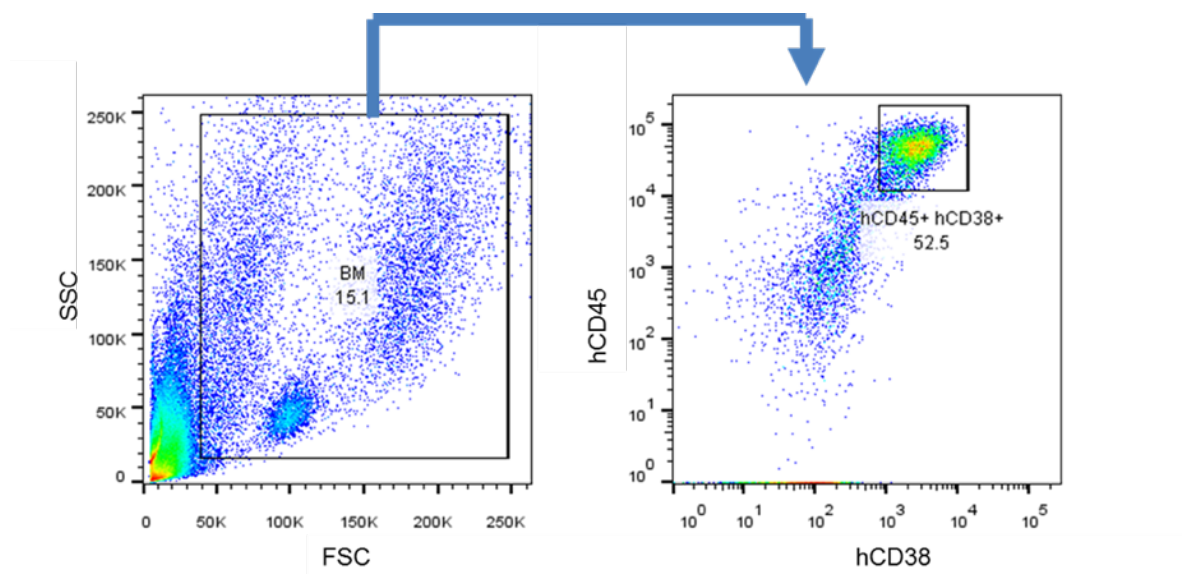


**Figure 4.4 Flow cytometry analysis of MM engraftment in to NSG mice**

*$1 \times 10^6$  primary MM cells were injected in the tail of NSG mice (IV). Mice were sacrificed at day 25 and then the BM of NSG was isolated. Using human CD45<sup>+</sup> BV421 and human CD38<sup>+</sup> APC marker to evaluate the engraftment.*

Next, I injected primary MM cells without the luci tag into the NSG mice to determine if MM caused a change in ROS level in NSG BMSC. I didn't want the luci tag on the MM cells as it may interfere with the flow cytometry analysis for the ROS levels in the BMSC. Figure 4.5 shows the antibody panel for flow cytometric analysis of the BMSC from NSG isolated BM. Figure 4.6A and 4.6B show the MitoSOX and DCF level in BMSC from MM engrafted NSG and human CD34+ cord blood engrafted NSG as a control. FSC/SSC is to gate out unwanted cell fragment, then gating out the human and mice hematopoietic cells by human CD45/ mice CD45. Platelet endothelial and erythroid cells are gating out by mice CD31 and mice Ter119. Finally, using mice CD105 to gate the BMSC cells and MitoSOX level is quantified.

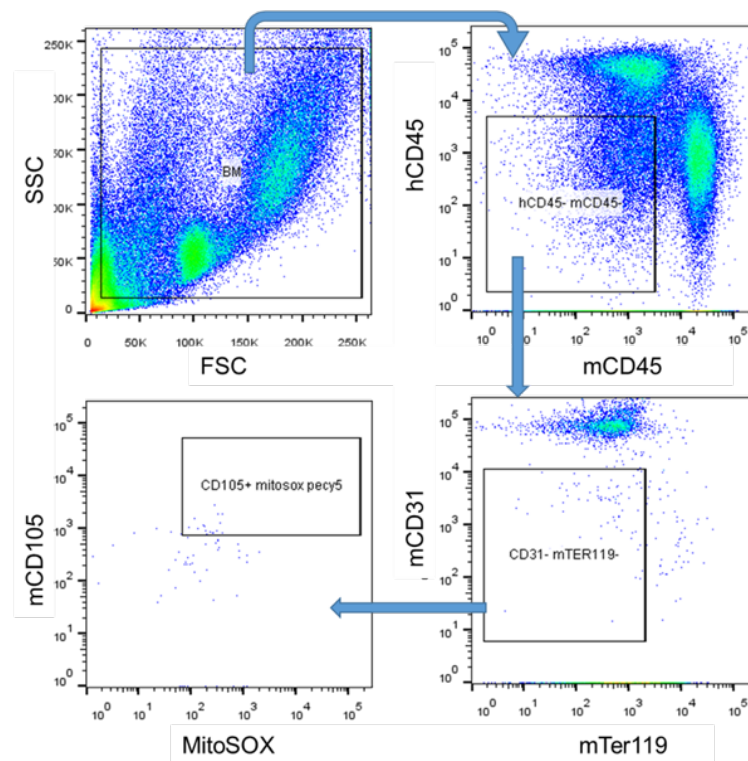


**Figure 4.5 Antibody panel to detect mitochondrial ROS in BMSC from BM of MM xenografted NSG mice**

*1x10<sup>6</sup> primary MM cells were injected into the tail of NSG mice (n=4). Human CD34<sup>+</sup> engrafted NSG mice were used as control group. Mice were sacrificed at day 25 and then the BM of NSG from MM engrafted and CD34<sup>+</sup> engrafted mice were isolated. Flow cytometry was used to detect MitoSOX level in BMSC. The antibodies used were human anti-CD45-BV421, mouse anti-CD45-BV510, mouse anti-CD31-APC, mouse*

*anti-TER119-APC-Cy7, mouse anti-CD105-FITC. PE channel is used to evaluate MitoSOX level in BMSC.*

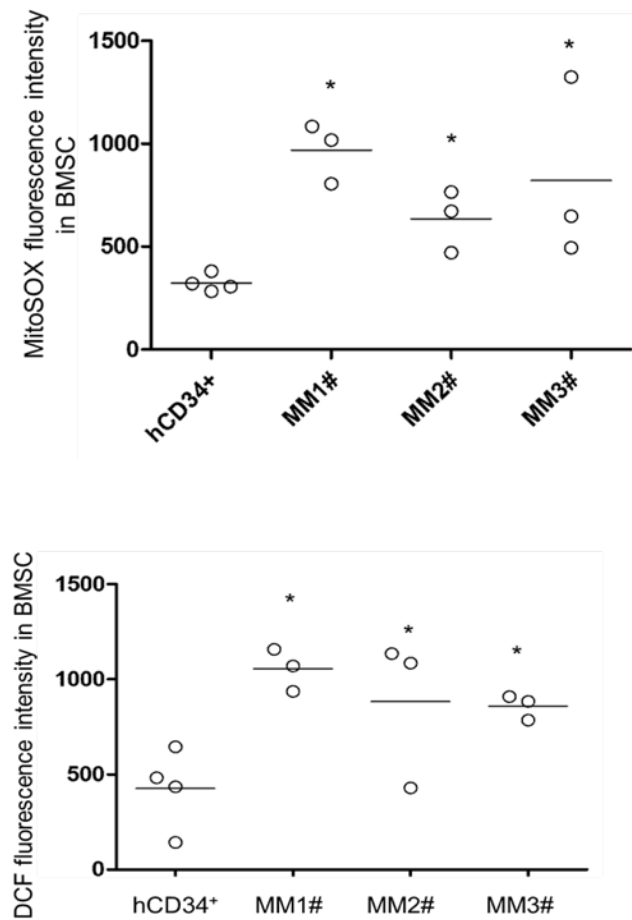


**Figure 4.6 Cellular and mitochondrial ROS detection in BMSC from BM of MM xenograft NSG mice**

*1x10<sup>6</sup> primary MM cells were injected into the tail of NSG mice (n=4). 2x10<sup>5</sup> human cord blood derived CD34<sup>+</sup> cells were engrafted into NSG mice and used as control group. Mice were sacrificed at day 25 and then the BM of NSG from MM engrafted and CD34<sup>+</sup> engrafted mice were isolated. Flow cytometry was used to detect MitoSOX and DCF level in BMSC. The antibodies used were human anti-CD45-BV421, mouse anti-CD45-BV510, mouse anti-CD31-PE-Cy5, mouse anti-TER119-APC, mouse anti-CD105-APC-Cy7, mouse anti-CD140a-PE. FITC channel was used to evaluate DCF level in BMSC. Two-way ANOVA with Sidak's post-test was used to compare changes in individual primary sample under treatment. Results with  $p < 0.05$*

were considered statistically significant (\*). Results represent the mean  $\pm$  SD of 4 independent experiments.

These data show that MM engrafted into NSG mice induced both cellular and mitochondrial ROS in BMSC when compared to normal CD34+ cells. However, what causes this increase in ROS is not known. Moreover, what effected the ROS has on BMSC is also unknown. These are two questions I aim to answer in the following results section.

#### 4.2.4 MM cells induced NRF2 expression in BMSC *in vitro*

Since NRF2 is the key regulator of cellular ROS, I hypothesised that BMSC upregulate NRF2 activity in response to the elevated ROS levels derived from the co-culture with MM.

An *in vitro* time course experiment was performed to detect the NRF2 protein expression in the BMSC that was co-cultured with MM cells. Figure 4.7 shows NRF2 protein level was increased after co-culture with MM cells. These data suggest the BMSC upregulates NRF2 pathways in responds to a stimulus from MM cells.

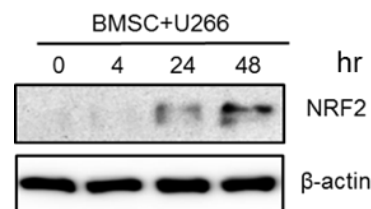


**Figure 4.7 MM cells induced BMSC NRF2 expression**

BMSC were co-cultured with MM cells for indicated hours and then BMSC protein was extracted and Western blotting was performed for NRF2 protein expression. Blots were reprobbed for  $\beta$ -actin loading control.

#### 4.2.5 *In vivo* experiment confirmed BMSC support MM cells engraftment in NSG model

BMSC are adherent cells, thus it is difficult to localise BMSC into the BM of the mice through tail injection. To confirm that BMSC protects MM cells *in vivo*. I used a different MM model to show this. In this model I subcutaneously injected the MM cell

line U266-Luci, with or without human BMSC in the NSG mice. If BMSC support the proliferation of MM cells, then the MM cells will expand under the skin of the mice, at the injection site. Figure 4.8 shows the engraftment of U266 cells was significantly increased when they were injected together with BMSC. The *in vivo* experiment confirms that BMSC supported the progression of MM cells. Figure 4.9 shows the size of the tumour.

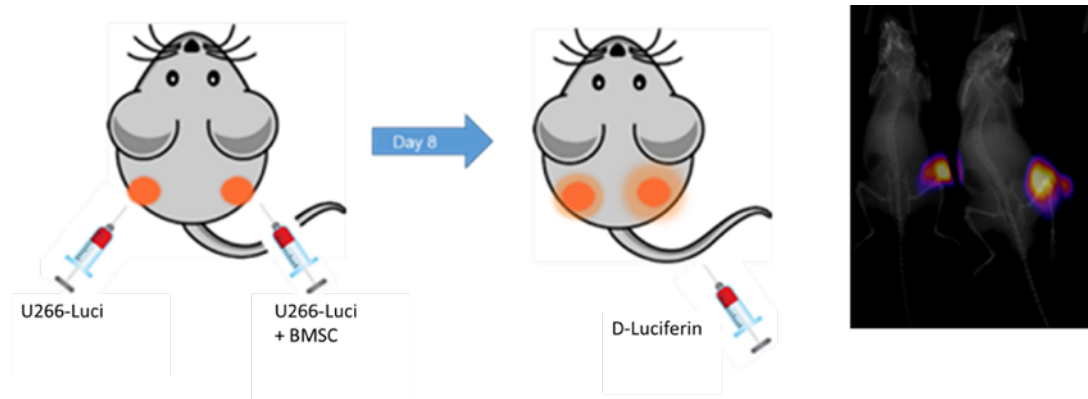


**Figure 4.8 Bioluminescence *in vivo* images detected the disease progression in U266 and BMSC xenograft model**

*Control group  $1 \times 10^6$  U266-Luc cells or co-culture group  $1 \times 10^6$  U266-Luc cells with  $0.5 \times 10^6$  BMSC cells were injected in the NSG mice subcutaneously. The control cells were injected in the left side and the co-culture cells were injected in the right side. Bioluminescence method was used to monitor the engraftment of cells.*

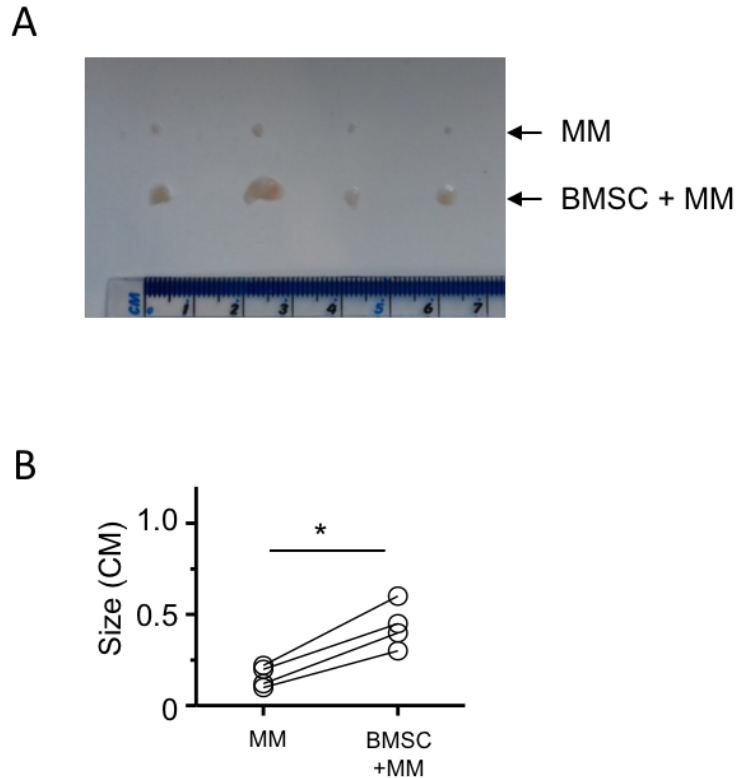


**Figure 4.9 Tumour size of U266-luci/BMSC engraftment mice**

*Control group  $1 \times 10^6$  U266-Luci cells or co-culture group  $1 \times 10^6$  U266-Luci cells with  $0.5 \times 10^6$  BMSC cells were injected in the NSG mice subcutaneously. The control cells were injected in the left side and the co-culture cells were injected in the right side. The mice were sacrificed upon tumour formation at day 8 and then the tumour was dissected out and measured (A and B). Joined bars show the tumour sizes in separate mice inoculated with a single primary MM subjected to BMSC co-culture or monoculture. Two-way ANOVA with Sidak's post-test was used to compare changes in individual mice under treatment. Results with  $p < 0.05$  were considered statistically significant (\*). Results represent the mean  $\pm$  SD of 4 individual mice.*

#### **4.2.6 NRF2-KD BMSC unable to protect MM cells in vitro.**

To determine the role of NRF2 in BMSC, MM cells primary MM cells were co-cultured with NRF2-KD BMSC or control BMSC for 6 days and then the viable MM cell numbers were determined. The NRF2-KD-BMSC method and confirmation of NRF2-KD is show in Figure 4.19-20. Figure 4.10 confirms the NRF2-KD BMSC is less supportive of MM cell survival.

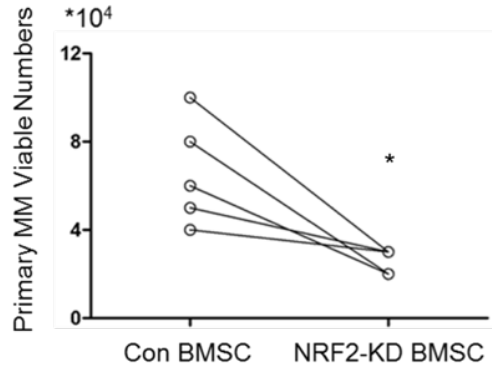


**Figure 4.10 Primary MM cells viability was decreased when were co-cultured with NRF2-KD BMSC compared to control knockdown**

Primary MM cells were co-cultured with Con-KD or NRF2-KD BMSC for 6 days, then the MM cells viability was determined by trypan blue method. Joined bar show changes of individual primary sample. Two-way ANOVA with Sidak's post-test was used to compare changes in individual mice under treatment. Results with  $p < 0.05$  were considered statistically significant (\*). Results represent the mean  $\pm$  SD of 5 independent experiments.

#### 4.2.7 NRF2-KD BMSC unable to support MM engraftment in NSG model *in vivo*

To confirm the supportive role of NRF2 in BMSC on MM cells, I KD NRF2 in BMSC and then I subcutaneously injected MM cell line U266, which were infected with Luci, with control BMSC or NRF2-KD BMSC in the NSG mice. Figure 4.11 shows the engraftment of U266 cells was significantly decreased when they were injected together with NRF2-KD BMSC. This *in vivo* experiment confirms NRF2 plays a key role for the BMSC to support the progression of MM cells. Figure 4.12 shows the size of the tumours.

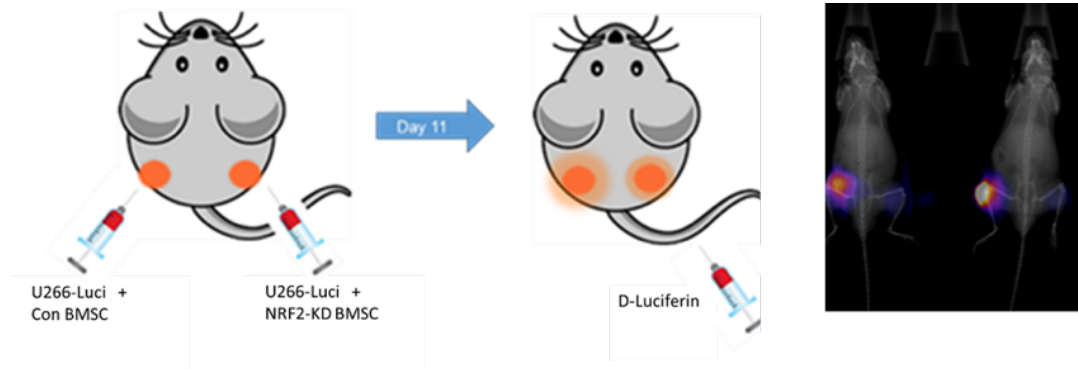


**Figure 4.11 Bioluminescence *in vivo* images detected the disease progression in U266 and BMSC xenograft model**

*Control group  $1 \times 10^6$  U266-Luci cells with  $0.5 \times 10^6$  control BMSC or NRF2-KD group  $1 \times 10^6$  U266-Luci cells with  $0.5 \times 10^6$  NRF2-KD BMSC cells were injected in the NSG mice subcutaneously. The control cells were injected in the left side and the co-culture cells were injected in the left side. Bioluminescence method was used to monitor the engraftment of cells.*

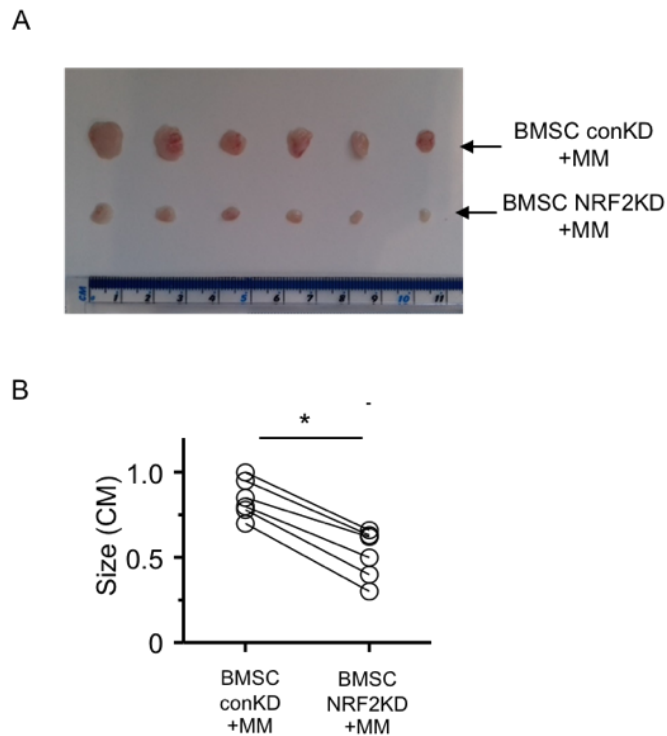


**Figure 4.12 Images show the tumour size from U266/BMSC NRF2-KD engrafted mice**

*Control group  $1 \times 10^6$  U266-Luci cells with  $0.5 \times 10^6$  control-KD BMSC or NRF2-KD group  $1 \times 10^6$  U266-Luci cells with  $0.5 \times 10^6$  NRF2-KD BMSC cells were injected in the NSG mice subcutaneously. The control cells were injected in the left side and the KD cells were injected in the right side. Bioluminescence method was used to monitor the engraftment of MM cells. The mice were sacrificed upon tumour formation at day 11 and then the tumour was measured. Joined bars show the tumour sizes in separate mice inoculated with U266 subjected to control or NRF2-KD BMSC. Two-way ANOVA with Sidak's post-test was used to compare changes in individual mice under*

treatment. Results with  $p < 0.05$  were considered statistically significant (\*). Results represent the mean  $\pm$  SD of 6 independent experiments.

#### 4.2.8 PI induced NRF2 expression in BMSC

As chapter 3 shows that NRF2 regulation in MM cells plays a key role in the MM cell chemotherapy resistance, in this section I want to identify if NRF2 regulation in BMSC plays a key role in the MM cell chemotherapy resistance. To determine if BMSC upregulates NRF2 pathway in response to PI treatment, I first, characterised if NRF2 protein expression is increased in BMSC when treated with PI for 4 or 24 hrs. Figure 4.13 shows the dose depended NRF2 protein expression in response to PI treatment after 4 and 24h.

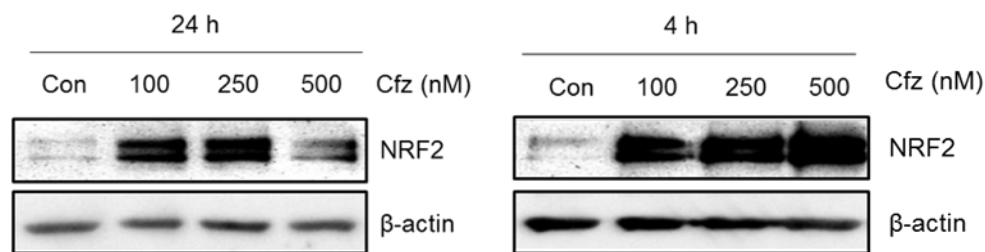


**Figure 4.13 Dose depended accumulation of NRF2 protein in the BMSC when were treated with Cfz**

*BMSC were treated with different doses of Cfz for 4h and 24h and BMSC protein was extracted and Western blotting was performed for NRF2 protein expression. Blots were reprobred for β-actin loading control.*

Figure 4.13 shows that NRF2 protein levels in BMSC were increased in response to PI treatment. Next, I wanted to evaluate if the increased NRF2 protein translated to increase downstream NRF2 regulated genes. Figure 4.14 shows that Bz and Cfz treatment induced the NRF2 regulated genes HO-1 and GCLM in BMSC that were co-cultured with MM1S.

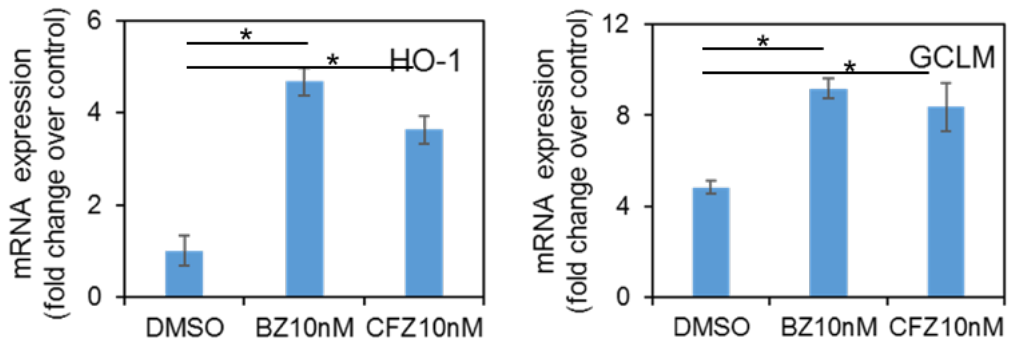


**Figure 4.14 PI increased BMSC HO-1 and GCLM mRNA expression**

BMSC were co-cultured with MM1S in the transwell for 24h and then treated with Bz or Cfz (100 nM) for 4h. RNA was extracted and analysed using qRT-PCR for HO-1 and GCLM expression. Gene expression was normalised to GAPDH. The Mann Whitney test was used to compare results in control to treated groups. Results with  $p < 0.05$  were considered statistically significant (\*). Results represent the mean  $\pm$  SD of 3 independent experiments.

#### 4.2.9 Investigation of NRF2 expression in PI treated BMSC when were co-cultured with MM cells.

Since PI increases NRF2 expression by inhibiting its continuous degradation by the proteasome, next I wanted to determine if NRF2 expression was increased in PI treated BMSC when co-cultured with MM cells. I co-cultured the MM cells with BMSC, then the cells were treated with PI for 4h and the BMSC NRF2 protein levels were determined. Figure 4.15 shows that the PI treated BMSC NRF2 protein were elevated when co-cultured with MM cells.

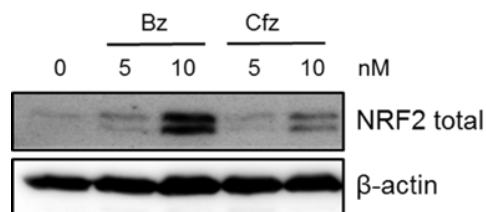


**Figure 4.15 PI treated MM cells induced BMSC NRF2 up-regulation**

MM1S were co-cultured with BMSC followed by treatment with Bz or Cfz (10 nM) for 4h and BMSC whole cell protein was extracted and Western blotting was performed for NRF2 protein expression. Blots were reprobbed for  $\beta$ -actin loading control.

#### 4.2.10 BMSC reduced MM cell ROS response to PI treatment

Since PI is reported to increase the ROS production in MM cells [133], I wanted to determine how BMSC protect MM from PI induced cell death and whether ROS levels were important. To do this I used the ROS level indicators, DCF and MitoSox to determine if BMSC reduce MM cellular stress induced by PI treatment.

The MM cells were cultured alone or in combination with BMSC and then the cells were treated with PI. Results show that mitochondrial ROS levels were high in PI treated primary MM cells compared to PI treated MM cells when co-cultured with BMSC (Figure 4.17). However, total ROS levels as measured by DCF were not significantly changed (Figure 4.18). One reason for the difference of cellular and mitochondrial ROS levels is the nature of the ROS production, as the majority of cellular ROS is produced in the mitochondria [294]. For example, the ROS in MM cells could have been changed by the media or been transferred to the BMSC and induce ROS in BMSC, which shown in Figure 4.6.

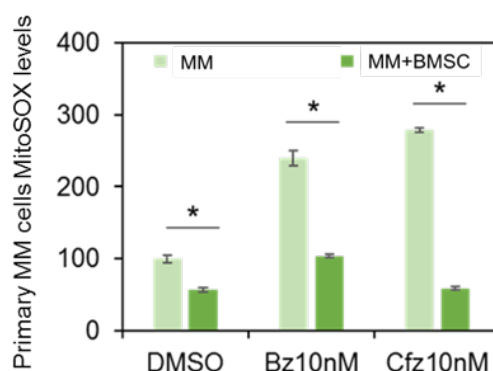


**Figure 4.16 Primary MM cells mitochondria ROS levels were increased when were co-cultured with BMSC with PI treatment**

*Primary MM cells were co-cultured with BMSC and treated with Bz or Cfz for 24h then MM cell apoptosis was analysed using flow cytometer with MitoSox staining. The Mann Whitney test was used to compare results in control to treated groups. Results with  $p < 0.05$  were considered statistically significant (\*). Results represent the mean  $\pm$  SD of 3 independent experiments.*

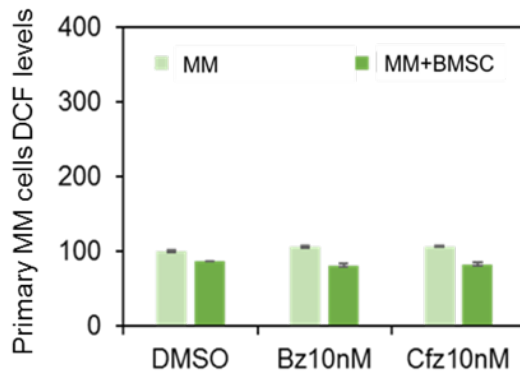


**Figure 4.17 MM cell DCF levels when were co-cultured with BMSC with PI treatment**

*Primary MM cells were co-cultured with BMSC and were treated with Bz or Cfz for 24h then MM cell apoptosis was analysed using flow cytometer with DCF staining.*

#### 4.2.11 Determining if NRF2 in BMSC confers resistance to MM in response to PI treatment

Next, I wanted to determine if NRF2 plays a role in the BMSC protection effect on MM cells. This is because NRF2 activity was activated in BMSC in response to PI treated MM cells. To do this I silenced the NRF2 gene in the BMSC to determine if this impairs BMSC protection of MM cells when co-cultured together. Figure 4.19 shows that lentivirus shRNA targeted NRF2 reduced NRF2 protein expression when treated with Cfz. Figure 4.20 shows that lentivirus shRNA targeted NRF2 BMSC have decreased NRF2 mRNA expression. Figure 4.21 shows that shRNA targeted NRF2 BMSC have reduced HO-1 expression in response to Cfz.

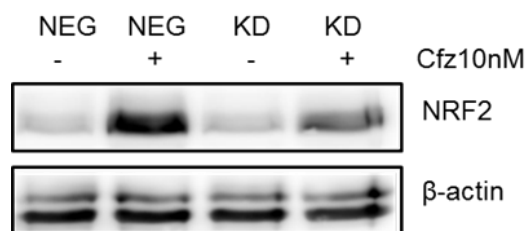


**Figure 4.18 NRF2 protein expression in NRF2-KD BMSC treated with Cfz**

*NRF2-KD and control-KD BMSC were treated with Cfz for 4h and BMSC whole cell protein was extracted and Western blotting was performed for NRF2 protein expression. Blots were reprobed for β-actin loading control.*

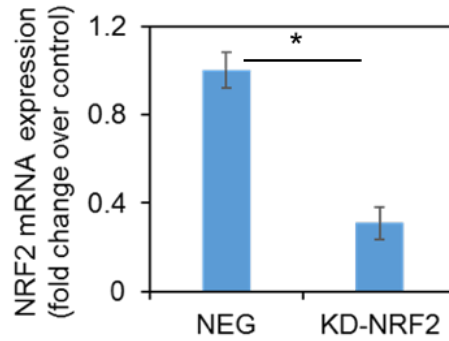


**Figure 4.19 NRF2 mRNA expression in NRF2-KD BMSC**

*Lentiviral mediated shRNA KD of NRF2 in BMSC. RNA was extracted and analysed using qRT-PCR for NRF2 expression. Gene expression was normalised to GAPDH. The Mann Whitney test was used to compare results in control to treated groups. Results with  $p < 0.05$  were considered statistically significant (\*). Results represent the mean  $\pm$  SD of 3 independent experiments.*

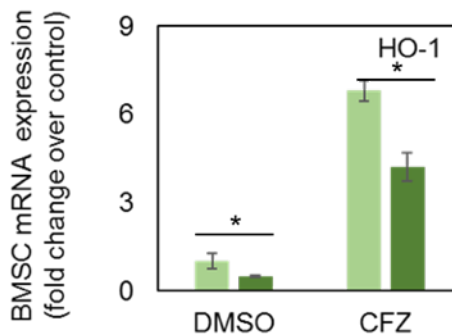


**Figure 4.20 NRF2-KD BMSC HO-1 RNA expression when treated with Cfz**

*Lentiviral mediated shRNA KD of NRF2 in BMSC. NRF2-KD BMSC were then treated with Cfz (10nM) for 4h and RNA was extracted and analysed using qRT-PCR for HO-1 expression. Gene expression was normalised to GAPDH. The Mann Whitney test was used to compare results in control to treated groups. Results with  $p < 0.05$  were considered statistically significant (\*). Results represent the mean  $\pm$  SD of 3 independent experiments.*

*Those data confirm the successful NRF2 knockdown in BMSC.*

#### **4.2.12 NRF2-KD BMSC unable to decrease the PI treated MM cell ROS levels**

To determine the role of NRF2 in the BMSC on MM cells I first examined if lentivirus shRNA targeted NRF2 in BMSC affect ROS levels in PI treated MM. Figure 4.22

shows that the MM cells cultured with NRF2-KD BMSC have higher mitochondria produced ROS levels and the total cellular ROS level were not significantly changed (figure 4.23).

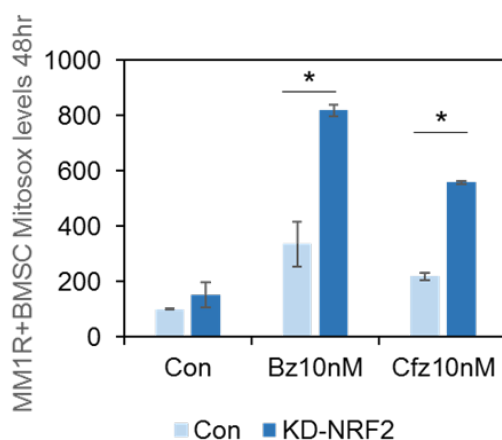


**Figure 4.21 Mitochondrial ROS levels in NRF2-KD BMSC were high when cultured with PI treated MM1R**

*MM1R cells were cocultured with NRF2-KD BMSC and treated with Bz or Cfz for 24h then MM mitochondrial ROS analysed using flow cytometer with Mitosox staining. The Mann Whitney test was used to compare results in control to treated groups. Results with  $p < 0.05$  were considered statistically significant (\*). Results represent the mean  $\pm$  SD of 3 independent experiments.*

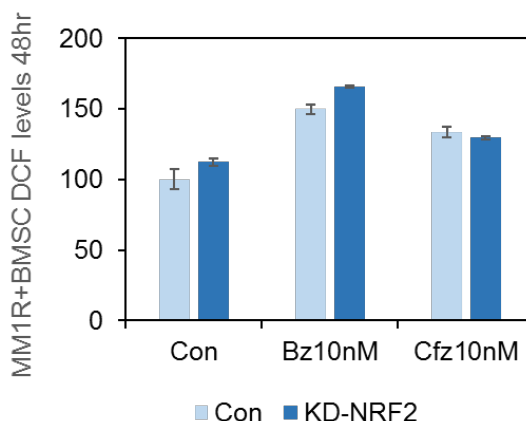


**Figure 4.22 Cellular ROS were unchanged in NRF2-KD BMSC when cultured with PI treated MM1R**

*MM1R cells were cocultured with NRF2-KD BMSC and treated with Bz or Cfz for 24h then MM cellular ROS was analysed using flow cytometer with DCF staining.*

The above data suggest the NRF2 played a key role in regulating mitochondrial ROS levels in both BMSC and MM cells when treated with PI.

#### 4.2.13 NRF2-KD in BMSC sensitised MM cells to PI treatment induced apoptosis

Knockdown NRF2 in BMSC may block the BMSC protection effect on MM cells. Because: 1) the BMSC decreased the ROS levels in the co-cultured MM cells; 2) the NRF2-KD BMSC unable to decrease the ROS levels in the co-cultured MM cells (Figure4.22).

To confirm the hypothesis that BMSC-NRF2 protected MM cell from PI induced apoptosis, I silenced NRF2 in BMSC and co-cultured them and then subjected them to PI treatment. Figure 4.24-25 show that the primary MM cells and MM cell lines were sensitised to PI treatment when co-cultured with NRF2 silenced BMSC.

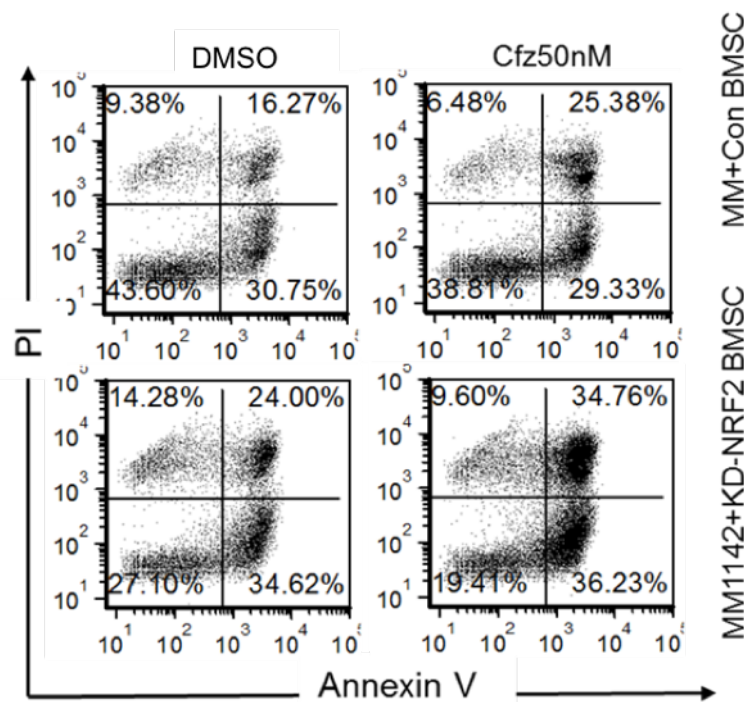


**Figure 4.23 NRF2-KD BMSC sensitised primary MM cells to Cfz treatment**

*Primary MM cells were co-cultured with NRF2-KD BMSC and treated with Cfz for 24h then MM cell apoptosis was analysed using flow cytometer with PI/Annexin V staining.*

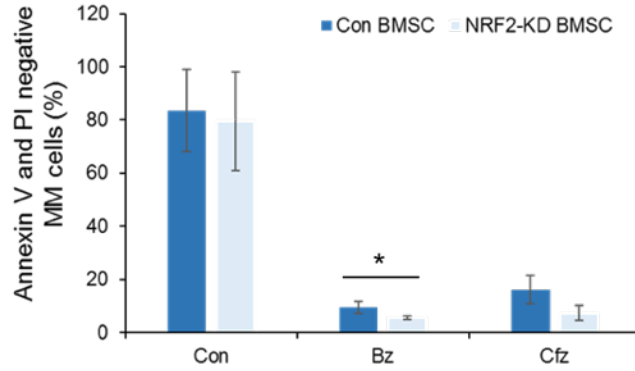


**Figure 4.24 NRF2-KD BMSC sensitised U266 to PI treatment**

*U266 or MM1S cells were cocultured with NRF2-KD BMSC and treated with Bz or Cfz for 24h then viable MM cells were analysed using flow cytometer with PI/Annexin V staining. The Mann Whitney test was used to compare results in control to treated groups. Results with  $p < 0.05$  were considered statistically significant (\*). Results represent the mean  $\pm$  SD of 3 independent experiments.*

### 4.3 Discussion

The mechanism of how BMSC protect MM cells from chemotherapy is in need of investigation. As currently, the chemical that have been tested in *in vitro* experiments that could effectively induce the MM cell death are eventually develop relapse in clinical application. This suggests the MM cells acquire protection from BM microenvironment. We need investigate the interaction of MM cells and BM microenvironment to find out how to interrupt microenvironment interaction with MM cells. In this chapter, I describe that NRF2 regulation in BMSC is a new mechanism of how MM-BMSC interaction could be targeted to disrupt the BMSC protection role on MM cells.

First, I confirmed that BMSC protect primary MM cells from apoptosis. My data are consistent with reported works that MM cells interact with BMSC for protection and I extended that observation to place ROS as a mediator of cell to cell interaction.

To prove ROS is a mediator of cell to cell interaction, First, I used *in vitro* and *in vivo* experiments to confirm that MM cells induce ROS in BMSC when in co-culture.

Second, I confirmed that BMSC decrease ROS level in MM cells as well. xThe above data confirm that ROS is a mediator of MM and BMSC interaction.

Next, as NRF2 is the key regulator of ROS, I explore the NRF2 role in the BMSC and MM interaction. First, I knocked down NRF2 in BMSC, which blocked its ROS decreasing role on MM cells. As upregulation of NRF2 in MM cells protect the cells from chemotherapy induced apoptosis this leads me to think that NRF2 activity in BMSC may affect the MM cells sensitivity to chemotherapy, The data confirm that PI induce more ROS and more apoptosis in MM cells when it was co-cultured with NRF2 silenced BMSC compared to control BMSC.

The BMSC protect MM cells at least partly through regulating ROS. This is because ROS regulation is essential for the MM cell survival, as ROS overproduction induces MM apoptosis and PI further increase ROS, which trigger more apoptosis of MM cells [133]. My data confirm this idea, as I detected BMSC decreasing ROS level in co-cultured MM cells.

Since NRF2 is the key cellular way to promote ROS detoxification, I hypothesised that MM cells induce ROS in BMSC and BMSC upregulate NRF2 to reduce the ROS stress. The data presented here confirm that the MM cells induce ROS in BMSC both *in vivo* and *in vitro*. Furthermore, KD-NRF2 in BMSC block its ROS decreasing role in MM cells. These data confirm that NRF2 regulation in BMSC is essential for its protection effect on MM cells. One question still remains and that is how ROS is transferred from MM cells to BMSC. This is an interesting question and I can suggest how this might be the case. One possibility is that MM cells transport some cellular components to the BMSC for recycling. Or maybe ROS in the form of superoxide is exported from the MM cell and absorbed or dealt with by the neighbouring BMSC.

BMSC is supporting the proliferation and chemotherapy resistance of MM cells. Studies show that interrupting the attachment of MM cells to BMSC sensitises the MM cells to treatment. For example, BMSC produces SDF-1 and its receptor, CXCR4 is presented on the surface of MM cells, which plays a key role for MM cells trafficking and homing [295, 296]. Interrupting the SDF-1-CXCR4 axis decreases the BMSC protection effect on MM cells [296-298]. But as the cell to cell attachment is important for normal cells, tissue and whole body to coordinate and function normally,

it is difficult to design drugs that inhibit the cancer and BMSC cell attachment and at the same time not cause damage to normal cells.

Here I have identified other ways to disturb the interaction of MM-BMSC. NRF2 inhibition may provide a powerful way to disrupt the BMSC protection effect on the MM cells. Though the interruption of MM to BMSC attachment have shown a good effect on sensitising of MM cells to the treatment, the compact BM niche where the MM and BMSC are crowded together is difficult to target. New strategies to interrupt not only the attachment of MM-BMSC but also the MM-BMSC attachment independent interaction are needed and NRF2 inhibition could be a feasible choice.

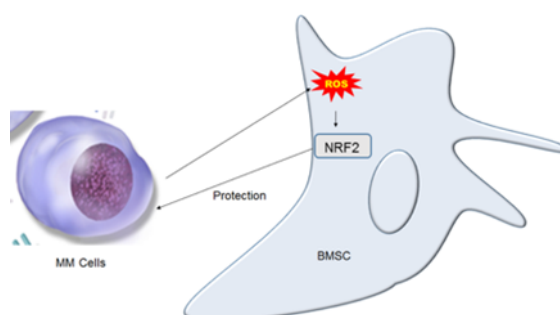


**Figure 4.25 Schematic representation of MM cell induced NRF2 regulation in BMSC protects MM cells**

*When co-culture MM cells with BMSC, MM cells induce the ROS stress in BMSC. As a respond, the BMSC then upregulate NRF2 expression. NRF2-KD in BMSC will block the BMSC protection effect on MM cells, which confirm NRF2 regulation in BMSC is important for the BMSC protect the MM cells against chemotherapy.*

**CHAPTER FIVE**  
**MM CELLS EXPORT AUTOPHAGY TO THE MM**  
**MICROENVIRONMENT**

## **5.1 Introduction**

### **5.1.1 Autophagy is the cellular way of protection**

To further understand how BMSC protect MM cells I next explored if autophagy in the BMSC is activated in response to MM coculture. MM have been shown to upregulate their own autophagy machinery to cope with cellular stress induced by paraprotein over production and injured sub cellular organelles and over activated autophagy induces cell death [299]. When the MM cells' own autophagy is unable to recycle the unwanted cellular components, MM cells may secrete its unwanted cellular components to the microenvironment. BMSC may support the MM cells by digesting their cellular components through autophagy. Therefore, I hypothesise that BMSC autophagy plays a key role in protecting MM cells. Furthermore, since NRF2 has been shown to regulate p62, which senses toxic cellular waste products, I further hypothesise that MM derived ROS activates BMSC NRF2 which upregulates p62 autophagy in BMSC of the MM microenvironment. In this chapter, I will decode the autophagy role in the BMSC protection effect on MM cells.

### **5.1.2 Cancer cells outsource autophagy for survival**

Reports have shown that some cancer cells outsource autophagy for survival [300]. The NRF2-P62-Autophagy axis link two essential cellular stress defence pathways together, as KEAP1, a sensor of ROS, regulates NRF2 degradation also regulates p62 mediated autophagosome forming [301]. First, it is important to determine the role of autophagy in MM and its tumour environment. Then I will aim to determine if NRF2 is involved in regulating this response. Thus, I hypothesis that MM autophagy is exported to the microenvironment by MM and that BMSC derived NRF2 regulates the formation of autophagy and ultimately the degradation of MM derived products.

### **5.1.3 Aims and objectives**

Since MM cells have high autophagy I want to determine if autophagy regulation is involved in the BMSC protection effect on MM cells and decode the autophagy regulation mechanism. This can be split into two main questions 1) Does MM cells activate BMSC autophagy? 2) Does NRF2 regulate MM induced autophagy in BMSC?

## 5.2 Results

### 5.2.1 Investigation of autophagy levels in MM cell lines and primary MM cells

As autophagy plays a key role for MM cell survival, I hypothesised that BMSC support MM cells proliferation by performing autophagy for the tumour cell. In the first experiment, I characterised the basal microtubule-associated protein 1A/1B-light chain 3 (LC3I, LC3II) protein turnover to evaluate the autophagy level in the MM cells. During formation of autophagosome, LC3 I is modified to form LC3 II, which is then degraded once it fused with lysosome. Thus, the turnover of LC3 I to LC3 II reflects the autophagy flux in the cells. Figure 5.1 shows that freshly isolated primary MM cells had higher turnover of LC3 I to LC3 II. It was hard to detect both the LC3 II band in MM cell lines, suggesting that MM cell lines are not a good model for these experiments. I think compares to the MM cell lines, freshly isolated BM primary MM cells should maintain more functions and markers seen in vivo, thus for the LC3 level, MM cell lines failed to present it.

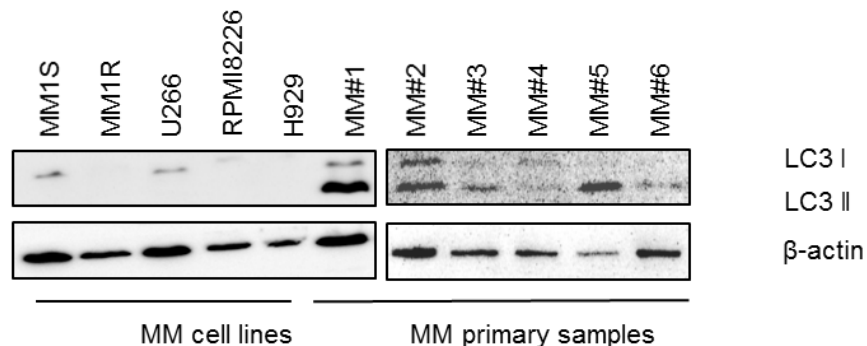


**Figure 5.1 Basal LC3I and LC3II expression in MM cell line and primary MM cells**

*Whole cell protein in MM cell lines or primary cells were extracted and Western blotting was performed for LC3 protein expression. Blots were reprobred for  $\beta$ -actin loading control.*

### 5.2.2 Autophagy levels in BMSC culture with primary MM and MM cell lines

Next, I wanted to determine if the MM-BMSC interaction affects the autophagy levels in MM cells. MM cells and BMSC were co-cultured, then MM cells were removed and protein isolated and whole cell lysate were analysed for LC3 protein expression. Figure 5.2 shows that the BMSC decreased the LC3 turn over in MM cells. To

determine if MM cells can induce autophagy in BMSC, I cultured both primary MM cells and MM cell lines on BMSC. MM cells were removed and BMSC were analysed for LC3I and LC3II expression. Figure 5.3 shows the primary MM cells, but not MM cell lines, increased the LC3II protein expression in BMSC.

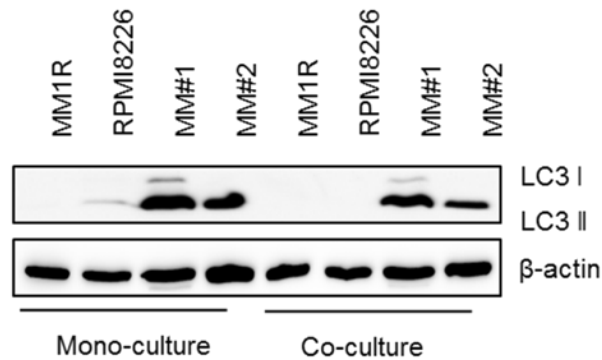


**Figure 5.2 BMSC LC3I and LC3II expression in response to MM co-culture**

*MM cell line or primary cells were cocultured with BMSC in transwell then whole cell protein in MM cell lines or primary cells were extracted and Western blotting was performed for LC3 protein expression. Blots were reprobbed for  $\beta$ -actin loading control.*

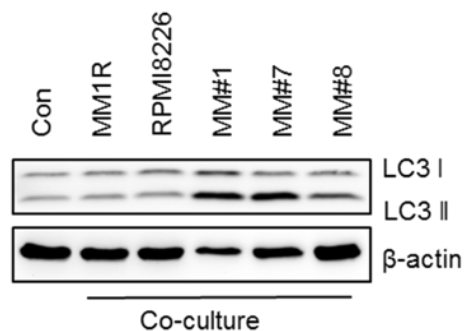


**Figure 5.3 LC3 expression in BMSC when co-cultured with MM cell line or primary MM cells**

*MM cell line or primary cells were cocultured with BMSC in transwell then whole cell protein from BMSC were extracted and Western blotting was performed for LC3 protein expression. Blots were reprobbed for  $\beta$ -actin loading control.*

### 5.2.3 Investigation of MM cells induced LC3 puncta formation in BMSC

To confirm that the MM cells increasing BMSC derived autophagy I used a second method to examine autophagy. This involved overexpressing LC3-tagged to GFP adenovirus in BMSC. Figure 5.4 confirms that BMSC been transduced with LC3-GFP

and then the BMSC been starved, I observed the formation of LC3 puncta. Moreover, when I cultured MM cells with BMSC and then washed off MM cells, this induced the formation of LC3-GFP puncta in BMSC. Next, I counted the puncta per field, and this is represented in Figure 5.5. The results show that MM induced LC3 puncta formation in BMSC. Together, these results suggest that MM induces LC3 puncta in BMSC.

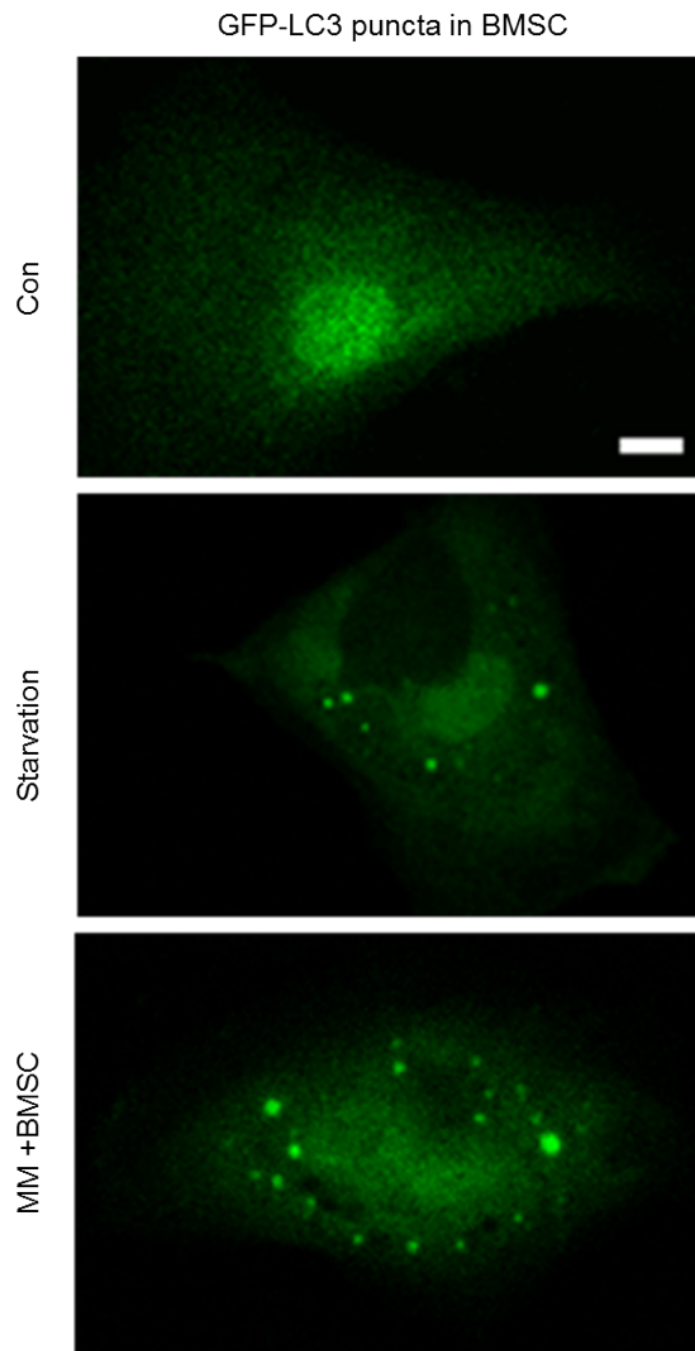


**Figure 5.4 Primary MM cells induced LC3 puncta formation in GFP-LC3 tagged BMSC**



BMSC (Figure 5.7). These data indicated the transfer of EV from MM cells which were acquired by BSMC.

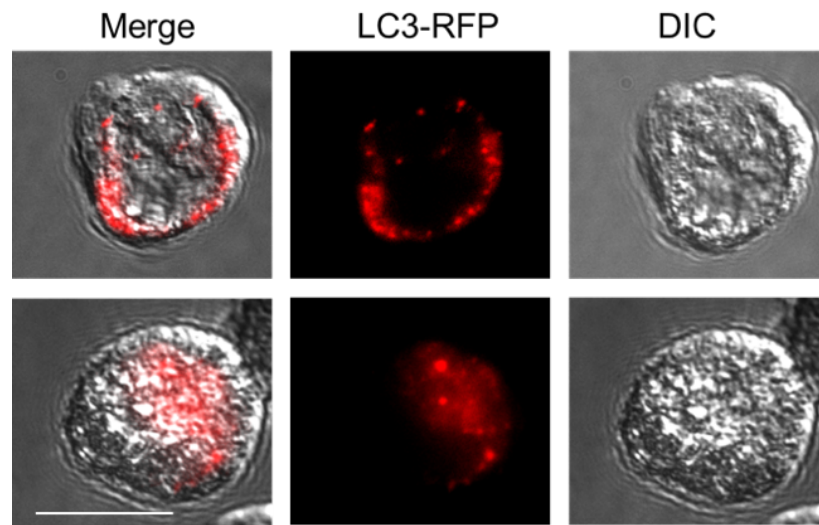


**Figure 5.6 Primary MM cells have undegraded LC3 puncta**

*RFP-LC3 tagged primary MM cells were visualised by confocal microscope, scale bar=10  $\mu$ m.*

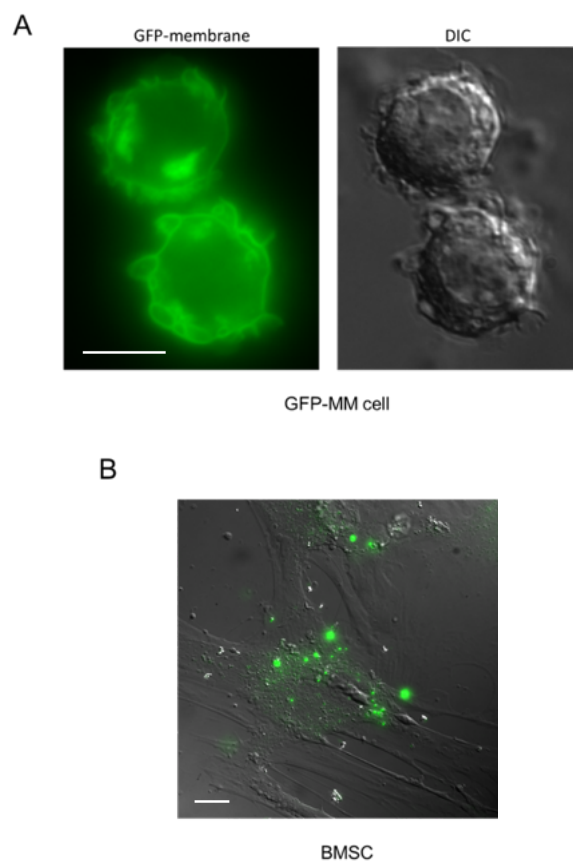


**Figure 5.7 MM cells actively secreted EV which were acquired by BMSC**

A. GFP-membrane virus tagged primary MM cells were visualised by confocal microscope, scale bar=10  $\mu$ m. B. GFP-membrane virus tagged primary MM cells co-cultured with BMSC for 24h and MM cells be washed away. BMSC was visualised by confocal microscope, scale bar=10  $\mu$ m.

### 5.2.6 Autophagy inhibitor blocked BMSC protection effect on MM cells

To confirm that the autophagy plays a key role for the BMSC supporting MM cells proliferation, I used two autophagy inhibitors to block autophagy in BMSC and then detected co-cultured viable MM cells. Figure 5.8 shows that HCQ (blocking the infusion of autophagosome and lysosome) and wortmannin (blocking ATG mediated formation of autophagosome) blocked the BMSC supportive role for the MM cell survival.

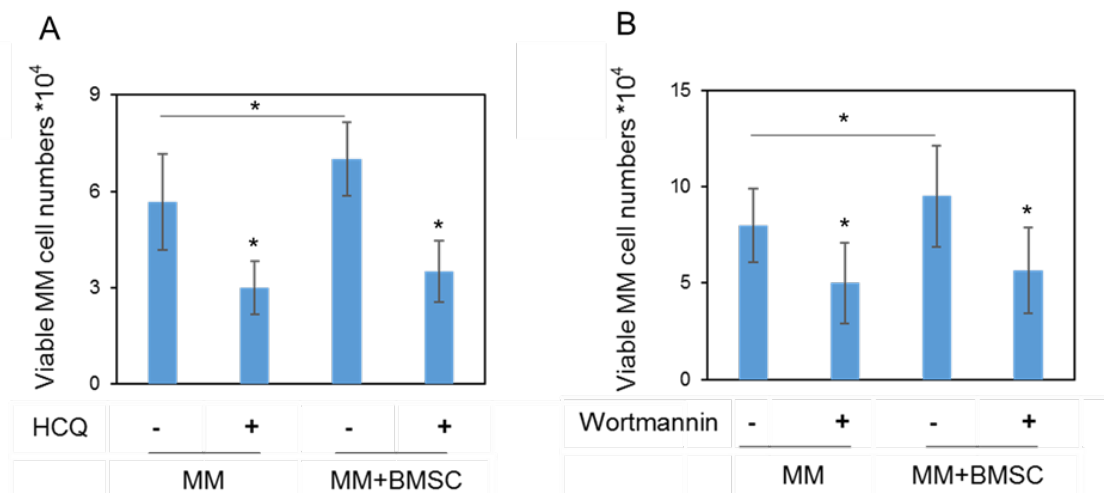


**Figure 5.8 Autophagy inhibitors blocked BMSC induced protection of MM cells** BMSC were treated with HCQ (20  $\mu$ M) or Wortmannin (5  $\mu$ M) for 24h then cultured with  $1 \times 10^5$  primary MM cells. MM viable cell numbers were assessed by trypan blue staining. The Mann Whitney test was used to compare results in control to treated groups. Results with  $p < 0.05$  were considered statistically significant (\*). Results represent the mean  $\pm$  SD of 4 independent experiments.

### 5.2.7 shRNA targeted ATG5 in BMSC

To understand if upregulated autophagy in BMSC is important for the BMSC protection effect on MM cells, I KD ATG5 in BMSC to impair its autophagy.

Figure 5.9 shows the ATG5 mRNA levels in BMSC after transduction with ATG5 shRNA expressing lentivirus.

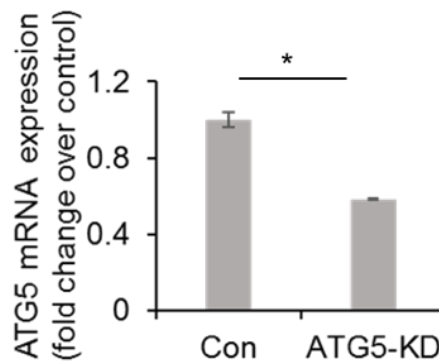


**Figure 5.9 ATG5 RNA expression in ATG5-KD BMSC**

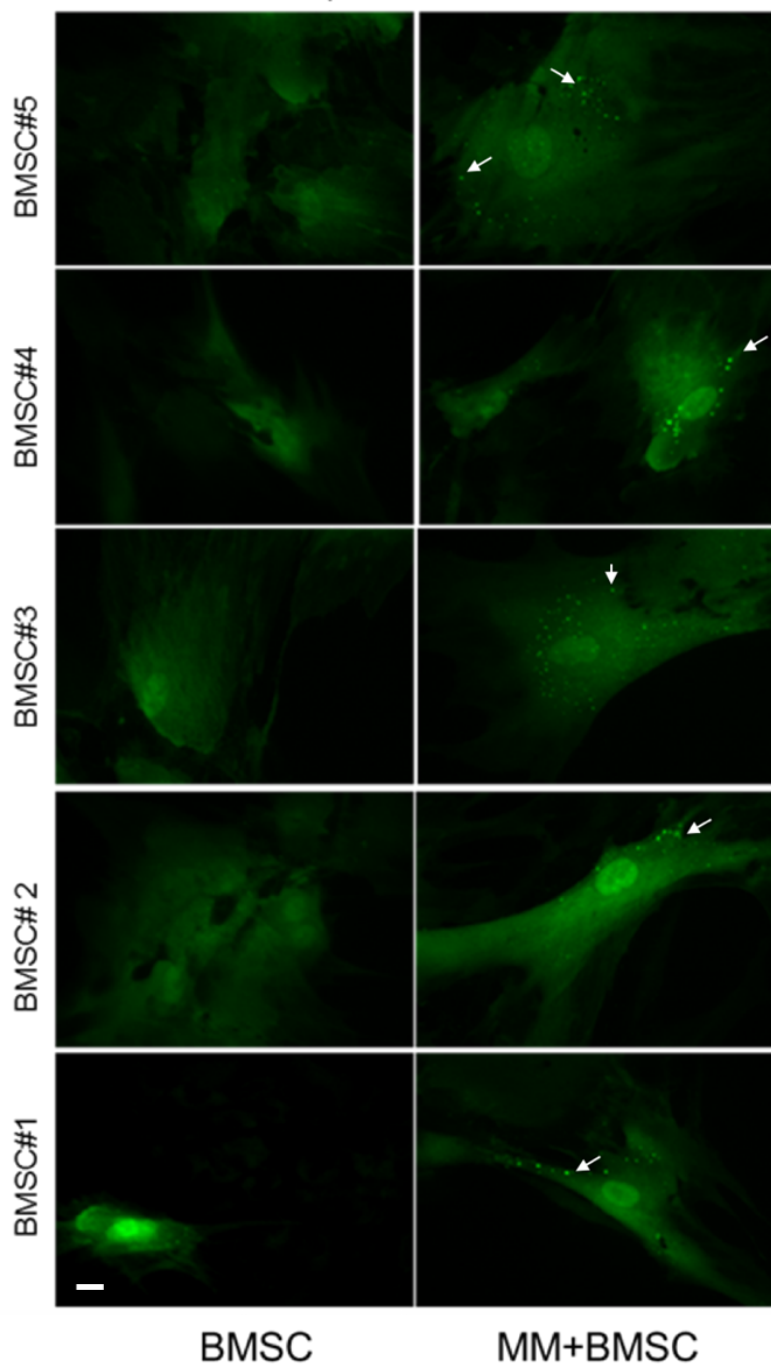
*BMSC were transduced with lentivirus containing shRNA targeted to ATG5 for 72h. BMSC RNA was then extracted and analysed using qRT-PCR for ATG5 expression. Gene expression was normalised to GAPDH. The Mann Whitney test was used to compare results in control to treated groups. Results with  $p < 0.05$  were considered statistically significant (\*). Results represent the mean  $\pm$  SD of 3 independent experiments.*

**5.2.8 MM cells unable to induce LC3 puncta in ATG5-KD BMSC**

Next, I infected five BMSC from five MM patients with LC3-GFP and ATG5 virus. Then co-cultured the BMSC with primary MM cells for 24h. (Figure 5.10) The images indicate if the autophagy in the ATG5-KD BMSC is compromised.

The ATG5-KD impaired autophagy in BMSC was confirmed, as Figure 5.10 shows that MM cells induced the puncta formation in BMSC and unable to induce the puncta formation in ATG5-KD BMSC. This suggests that the BMSC autophagy machinery is needed to process the waste from MM cells.

LC3-GFP puncta formation in BMSC



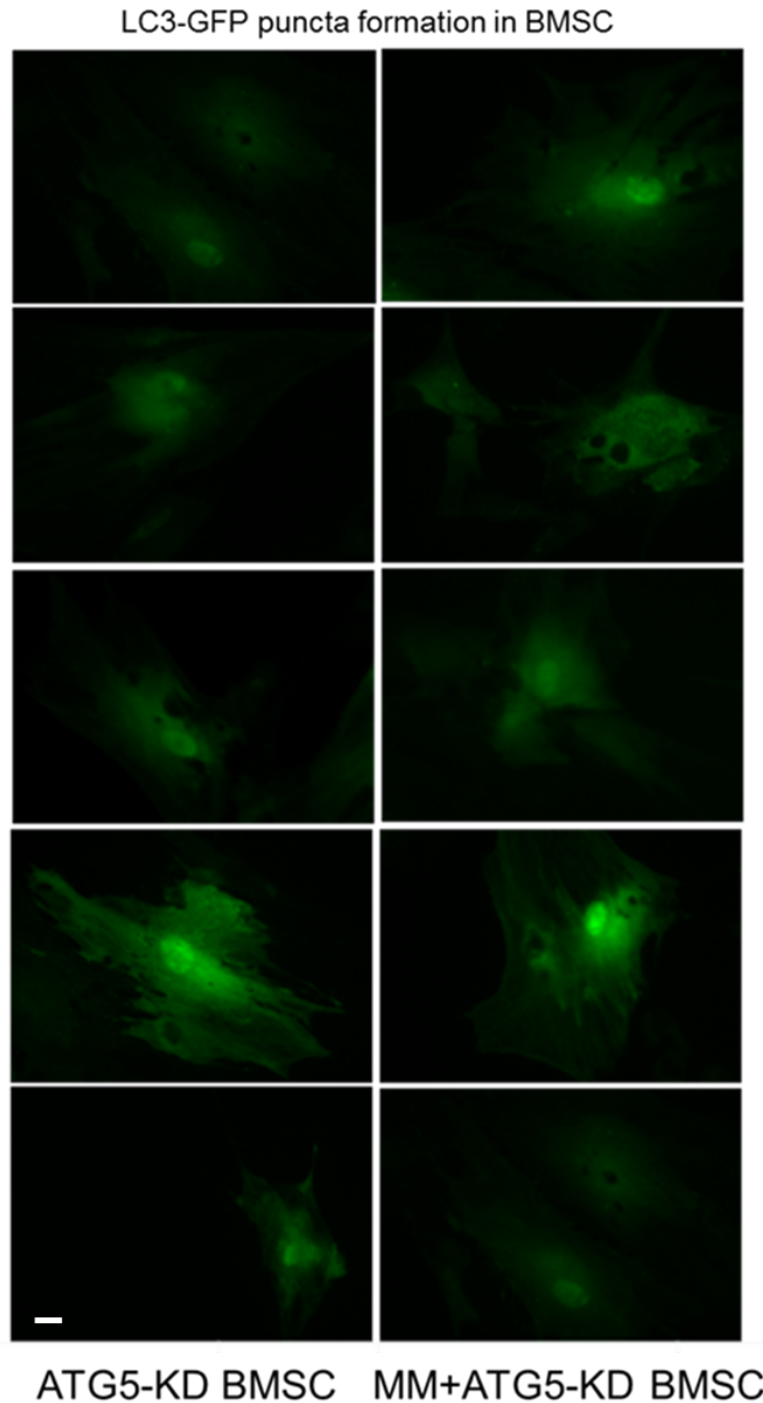


**Figure 5.10 Primary MM cells induced LC3 puncta formation in BMSC but not in BMSC with ATG5 knockdown**

*GFP-LC3 tagged control-KD BMSC or ATG5-KD BMSC were cultured alone or co-cultured with primary MM cells for 24 hrs. LC3 puncta were visualised by fluorescent microscope, scale bar=10  $\mu$ m.*

### 5.2.9 Investigate ATG5 function in BMSC protection effect on MM cells *in vitro*

To determine if autophagy in BMSC is protective to MM cells. I co-cultured four primary MM cells with ATG5-KD BMSC for 6 days and then determined the viability of MM cells. Figure 5.11 shows that ATG5-KD in BMSC impaired the BMSC support of MM cells.

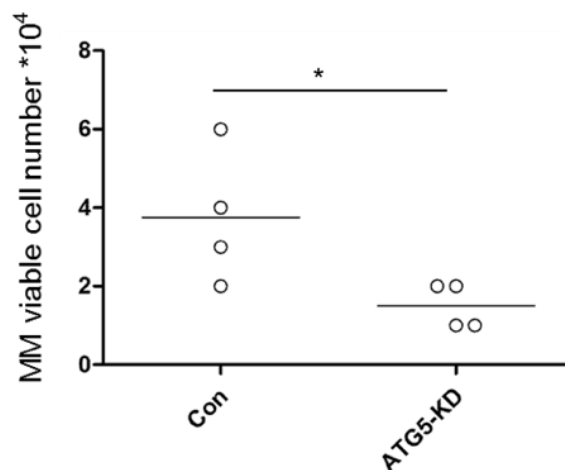


**Figure 5.11 Primary MM cells viability was decreased when co-cultured with autophagy impaired ATG5-KD BMSC compared to control knockdown BMSC**

*Four primary MM cells were co-cultured with Con-KD or ATG5-KD BMSC for 6 days, then the MM cells viability was determined by trypan blue method. The Mann Whitney test was used to compare results in control to treated groups. Results with  $p < 0.05$  were considered statistically significant (\*). Results represent the mean  $\pm$  SD of 4 independent experiments.*

The above data show that autophagy function is important for the BMSC support the MM cells proliferation.

### 5.2.10 Investigate ATG5 function in BMSC protection effect on MM cells *in vivo*

To determine the role of BMSC derived autophagy on MM cells, I knocked down ATG5 in BMSC and then I cultured the MM cell line U266 on control-KD cells or ATG5-KD cells and then these were subcutaneously injected into NSG mice. Figure 5.12 shows the engraftment of U266 cells was significantly decreased when they were injected together with ATG5-KD BMSC compared to control-KD BMSC. Figure 5.13

shows the size of tumours. This *in vivo* experiment confirms that BMSC derived autophagy plays a key role in supporting the progression of MM cells.

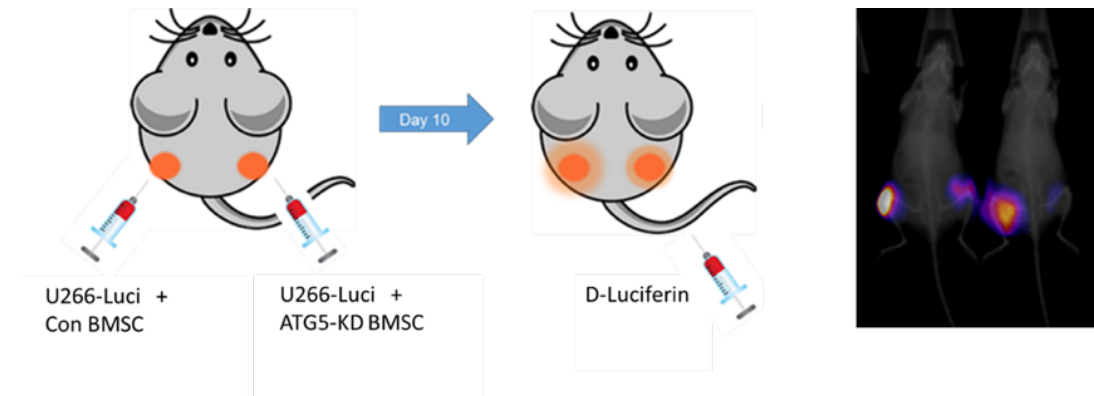
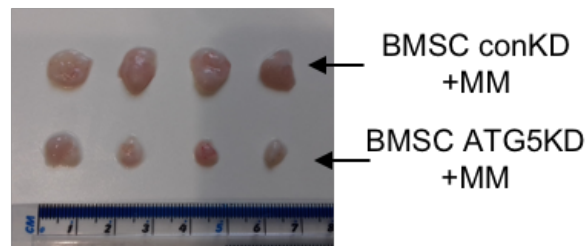


**Figure 5.12 Bioluminescence *in vivo* images detected the disease progression in U266 and ATG5-KD BMSC xenograft model**

*Control group  $1 \times 10^6$  U266-Luci cells with  $0.5 \times 10^6$  control-KD BMSC or ATG5-KD group  $1 \times 10^6$  U266-Luci cells with  $0.5 \times 10^6$  ATG5-KD BMSC cells were injected in NSG mice subcutaneously. The control cells were injected in the left side and the co-cultured cells were injected in the right side. Bioluminescence method was used to monitor the engraftment of cells at day 10.*

A



B

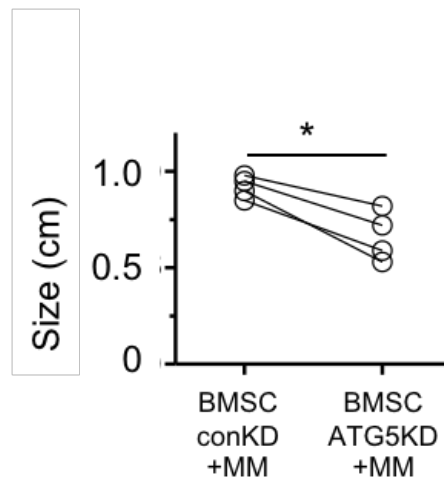


**Figure 5.13 Images show the tumour from U266/BMSC ATG5-KD engraftment mice**

Control group  $1 \times 10^6$  U266-Luci cells with  $0.5 \times 10^6$  control BMSC or ATG5-KD group  $1 \times 10^6$  U266-Luci cells with  $0.5 \times 10^6$  ATG5-KD BMSC cells were injected in the NSG mice subcutaneously. The control cells were injected in the left side and the co-culture cells were injected in the right side. The mice were sacrificed at day 14 and then the tumour was dissected and quantified. Joined bars show the tumour sizes in separate mice inoculated with U266 subjected to control or ATG5-KD BMSC. Two-way ANOVA with Sidak's post-test was used to compare changes in individual primary sample under treatment. Results with  $p < 0.05$  were considered statistically significant (\*). Results represent the mean  $\pm$  SD of 4 independent experiments.

### 5.2.11 NRF2 regulated P62 protein levels in BMSC

P62 is regulated by the NRF pathway, therefore I next wanted to determine if NRF2 regulates autophagy through the mediator of P62. I first KD NRF2 in BMSC and then

detected the P62 protein levels. Figure 5.14 shows the P62 protein levels is decreased in the NRF2-KD BMSC.

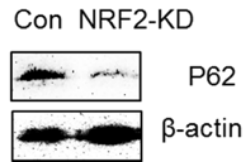
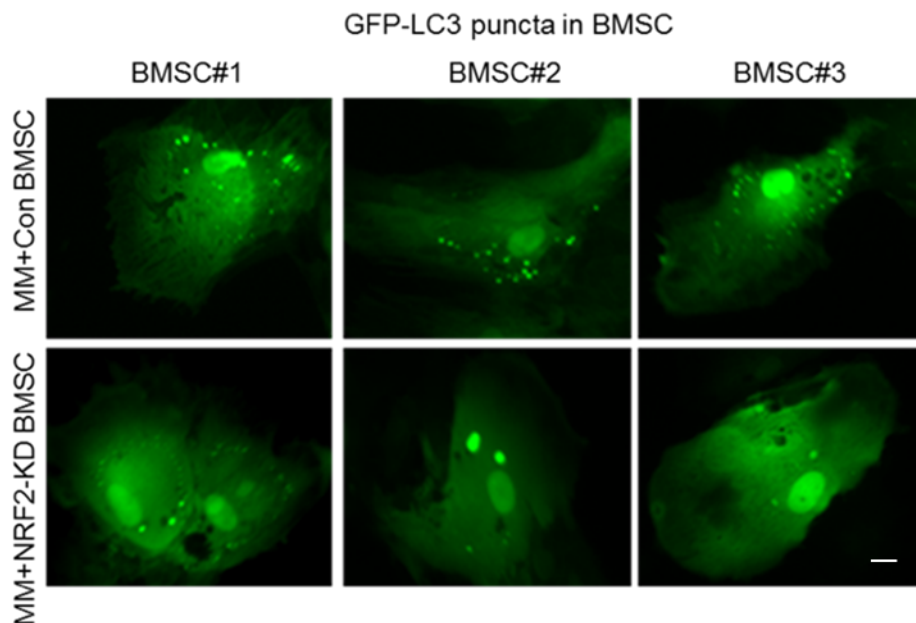


**Figure 5.14 KD-NRF2 BMSC have decreased P62 protein level**

*BMSC were transduced with virus to knockdown NRF2 or control-KD for 96h and BMSC whole cell protein was extracted and Western blotting was performed for P62 protein expression. Blots were reprobred for  $\beta$ -actin loading control.*

### 5.2.12 NRF2 regulated autophagy in BMSC

To confirm that NRF2 regulates autophagy in BMSC, I knocked down NRF2 in LC3-GFP labelled BMSC cells and then co-cultured them with primary MM cells. Figure 5.15 shows the MM cells induced less LC3 puncta in NRF2-KD BMSC.



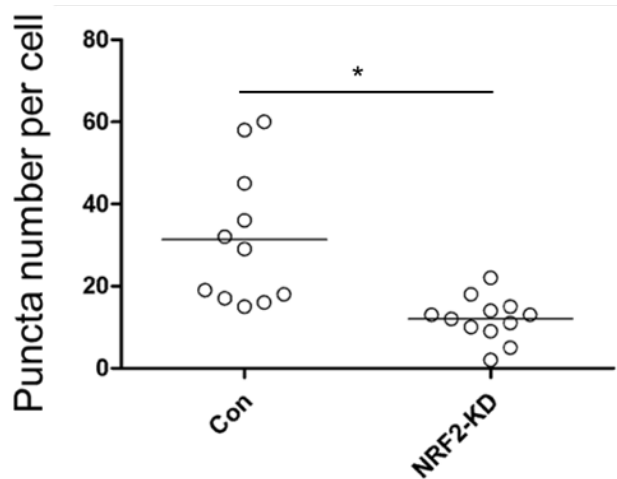


**Figure 5.15 LC3 puncta formation in the NRF2-KD BMSC after the BMSC been co-cultured with primary MM cells**

*GFP-LC3* tagged NRF2-KD BMSC were co-cultured with primary MM cells for 24h, then the LC3 puncta were visualised by fluorescent microscope and quantified, scale bar=10  $\mu$ m. Two-way ANOVA with Sidak's post-test was used to compare changes in individual primary sample under treatment. Results with  $p < 0.05$  were considered statistically significant (\*).

These results confirm that NRF2 supports P62 mediated autophagy in BMSC and plays a key role for the BMSC supported MM proliferation.

### 5.3 Discussion

In chapter 4, I described that the NRF2 regulation in BMSC is important for BMSC protection of MM cells that are co-cultured with. In this chapter, I aim to investigate autophagy role in the BMSC protection effect on MM cells, as NRF2 also regulate autophagy. As described in 5.1.1, MM have been shown to upregulate their own autophagy machinery for survival, which lead me to think does autophagy also play a role in BMSC protection effect on MM cells.

First, I confirmed that primary MM cells have constant high level of autophagy activation, and then I confirmed that primary MM cells induce autophagy upregulation in BMSC cells both from *in vivo* and *in vitro* experiments. I also extend my investigate

into decode how NRF2 regulate autophagy in BMSC to support the proliferation of MM cells. Finally, I confirm that NRF2 regulated autophagy upregulation is important for the BMSC support the MM cell proliferation.

Autophagy is the cellular way to remove malfunctioning sub cellular organelles or misfolded proteins. If the autophagy level is high, the cells are more prone to apoptosis. In this chapter, I show that the primary MM cells have higher basal autophagy levels than MM cell lines. That may explain why primary MM cells are more prone to apoptosis when were cultured alone and it may also suggest that MM cell lines are not the best model to study MM. As MM cell lines cannot present the high basal autophagy level as was shown in primary MM cells. Therefore, I focused on MM primary cells.

It is interesting to note that culture of MM and BMSC together affects their autophagy levels. Data show that the BMSC autophagy levels are upregulated when co-cultured with primary cells but not changed when co-cultured with MM cell lines. BMSC decreased autophagy level MM cells. This suggests that something is regulating this response and autophagy upregulation in BMSC may play a role in protecting MM cells from apoptosis. Further experiments show that if I impair BMSC autophagy by using knockdown of ATG5 this inhibits BMSC support of MM cells. Moreover, NRF2-KD BMSC impaired P62 mediated autophagy, resulting in reduced support and growth of MM cells both in vitro and in vivo.

Here I provide new mechanistic insight in the ways of how BMSC protect MM cells. It is possible that during PI treatment these responses are elevated, thus allowing MM cells to evade chemotherapy induced apoptosis. This suggests a potential therapeutic strategy by impairing autophagy and treating with PI for the treatment of MM.

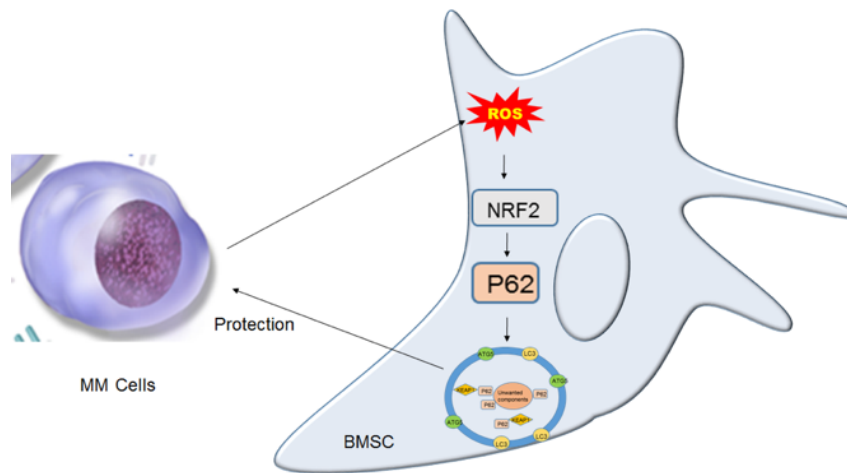


**Figure 5.16 Schematic representation of MM cell induced NRF2 mediated autophagy regulation in BMSC protects MM cells**

*When co-culture MM cells with BMSC, MM cells induce the ROS stress in BMSC. As a respond, the BMSC then upregulate NRF2 expression (described in chapter 4). NRF2-KD in BMSC will decrease P62 expression and the autophagy function in BMSC is comprised and block the BMSC protection effect on MM cells, which confirm NRF2 mediated autophagy upregulation in BMSC is important for the BMSC surport the MM cells proliferation.*

**CHAPTER SIX**  
**OVERALL DISCUSSION**

Currently, MM is incurable, as MM cells quickly resistant to all the clinical available drugs. To find a new therapy strategy is in need to investigate. From my team's previous research and published reports, I select the NRF2 pathway for the treatment of MM. Because (described in 1.4, 1.6 and 1.7.1) MM patients have been reported to present high level ROS, autophagy and ER stress. NRF2 pathway could regulate the above stress, which maybe a targetable pathway for the treatment.

I investigate the NRF2 regulation both in MM cells and BMSC. Because, one of the difficulties to find a new pathway for targeting is the BM microenvironment may respond to the treatment and protect MM cells. I need to confirm that the possible NRF2 inhibition treatment could not be comprised by the co-cultured BMSC. So, I use *in vitro* cell co-culture system and *in vivo* experiment to investigate the NRF2 function.

### **6.1 NRF2 regulation plays a key role for MM cell survival**

NRF2 regulation has been reported as having a role in both the prevention of tumorigenesis and the promotion of cancer progression. As the main cellular defence system, NRF2 regulates the response to ROS, drug excretion and maintenance of intracellular homeostasis. Thus, NRF2 is considered as a cancer suppressor, which protect normal cells and prevent carcinogenesis [302]. However, it is the same mechanism that also leads to NRF2 being considered as an oncogene, as NRF2 activation protects cancer cells and promotes cancer cell proliferation [303].

In my project, I focused on the pro-tumoral role of NRF2 in MM. I then explored whether and how inhibition of pro-tumoral NRF2 could be exploited in the treatment of patients with MM. Furthermore I considered the role of NRF2 in drug resistance to existing therapies as it has previously been reported that NRF2 activation contributes to MM cell resistance to PI, which is mediated by proteasome maturation protein [304]. My research explored additional mechanisms of NRF2 protection in MM cells. Consistent with other reports [264, 304-306], my data show that NRF2 inhibition sensitises MM cells to PI treatment.

### **6.1.1 MM cells upregulate NRF2 pathway for survival**

In addition to ROS, NRF2 upregulation has been reported to occur in response to two more mechanisms. The first mechanism is P62-autophagy-NRF2 axis, as several groups have reported that P62 or dysregulated autophagy activates NRF2 expression in liver disease [163], HEK293 cells [164], HeLa cells [307], U2OS cells and MEF cells [308]. They found that KEAP1 suppresses NRF2 and activates P62, which coordinates the NRF2 regulated antioxidant defence system and the P62 mediated autophagy system. Thus, P62 activation and autophagy dysregulation all activate NRF2. The second mechanism is PI induced NRF2 activation [304], as NRF2 is mainly degraded through the proteasome system. Once the PI inhibit the proteasome, more NRF2 are accumulated in the cells and enter the nuclei to initiate NRF2 regulated gene activation. Therefore, I investigated whether either of these two mechanisms regulating NRF2 were relevant in MM.

First, I wanted to confirm whether PI induces accumulation of NRF2. This is important because the proteasome degradation system is the main way for the NRF2 degradation and PI form the backbone of current MM therapy. I found that PI inhibit the proteasome system and thus resulted in the accumulation of NRF2 in benign and malignant cells. This mechanism is confirmed in chapter 3 and 4, which detected the increased NRF2 protein in PI treated MM and BMSC. This finding led to further investigations of the NRF2 protective role on MM cells drug resistance and NRF2 role in BMSC protective role on MM cells as shown in 6.1.2-3.

Second, I confirmed that the NRF2-P62-autophagy axis mediates NRF2 upregulation in MM. In chapter 4, I reported that the primary MM cells demonstrate higher LC3II to LC3I turnover, which indicates primary MM cells have higher autophagy flux. While the KEAP1 is recruited for the activation of P62 to form autophagosomes, the NRF2 degradation pathway is disturbed and resulted with accumulated NRF2 in MM cells. The upregulated NRF2 further promote autophagy, which forms a positive loop for the cells to clear away unwanted cellular material.

Taken together there are at least three different mechanisms that contribute to the upregulation of NRF2 activation in MM cells and result in constitutive high NRF2

expression in MM cells. Moreover, my data show that the NRF2 upregulation plays a key role for MM cell survival. In chapter 3, I reported for the first time that primary MM cells exhibit high level NRF2 activation and that PI treatment further elevates the NRF2 activation. Finally, compared to the control group, KD-NRF2 in MM cells induces cell death and sensitise MM cells to PI treatment. These data confirm that MM cells upregulate NRF2 for survival and provide a biologic rationale for targeting NRF2 in patients with MM.

### **6.1.2 NRF2 promotes the survival of MM cells through upregulating antioxidant defence systems and autophagy**

NRF2 activates many pathways to promote the survival of MM cells. For the antioxidant system activation, other researcher have shown that MM cells are high in ROS stress and PI further increase the ROS level, which can be eliminated by NRF2 activated antioxidant systems [133]. One important NRF2 regulated cellular antioxidant is GSH, which is important for the ER to correct the misfolded protein [309] and important for the cells to prevent ROS stress induced apoptosis [310]. Moreover, GSH reduces PI induced cytotoxicity in MM cells [264]. In my project I revealed that ROS induced NRF2 promotes the survival of MM cells through NRF2 regulated GSH synthesis, which blocks ER stress associated apoptosis in MM cells. This finding links the previous findings together to decode a full pathway of how MM cells become resistant to PI.

NRF2 regulated autophagy has previously been reported to be essential for the survival of malignant plasma cells [174]. Furthermore, it was reported that combining an autophagy inhibitor with PI treatment sensitises MM cells to death. Moreover, a genetic study revealed that autophagy promotes MM oncogenesis [81]. In chapter 5, I detected high autophagy levels in primary MM cells, which is consistent with the above reports.

MM cells have high levels of autophagy and high levels of NRF2 are needed to activate the transcription of P62, which is needed for the formation of the autophagosome. A previous report has shown that the NRF2-P62- autophagy axis plays an important role in MM cell chemotherapy resistance [304]. My finding further

points out that the primary MM cells have much higher autophagy levels than MM cell lines, which may explain why primary MM cells hardly survive without the support of BMSC once aspirated out of their BM microenvironment. My findings taken together with previous work on the MM autophagosome confirm that NRF2 regulated autophagy increases play a key role in the survival of malignant MM cells through the upregulation of the antioxidant defence system and autophagy. Inhibiting autophagy in BMSC block its supportive role on MM cells, which highlights that autophagy in BMSC is essential to provide a pro-tumoral microenvironment for MM.

### **6.1.3 BMSC upregulate NRF2 when in co-culture with MM cells**

In chapter 4, I reported for the first time that MM cells induce NRF2 activation in BMSC. As KEAP1 senses the ROS level in the cells, this suggests that the NRF2 upregulation in BMSC may be induced by ROS. I detected increased ROS levels in the BMSC of patients with MM and confirmed that this is induced by the MM cells both *in vitro* and *in vivo*. These data confirm that MM cells induce BMSC NRF2 upregulation and it is driven by ROS. This is a new finding and demonstrates the importance of the crosstalk between malignant plasma cells and the non-malignant stromal cells in the microenvironment that support them. Furthermore, it extends the findings of Rushworth and Brittany who have previously shown that ROS induced NRF2 is pro-tumoral in the malignant plasma cell [133, 311]. My finding shows that NRF2 upregulation in BMSC is also important for the MM proliferation and it is induced by the MM stimulated ROS stress. These findings highlight the NRF2 role in the interaction of MM and BMSC leading to a pro-tumoral microenvironment for the MM.

### **6.1.4 BMSC are less sensitive to PI induced apoptosis compared to MM cells**

My data shown in chapter 4 reveal that higher dosage of PI is needed to induce the accumulation of NRF2 protein in the BMSC than MM cells and that BMSC are more resistance to PI induced apoptosis. The proteasome system functions in cellular stress to degrade unwanted and misfolded protein in MM cells. Therefore, the MM cells and BMSC have different sensitivity to PI treatment which is in favour of the patient and allows a much wider PI dosage range and generates less damage to the microenvironment than the tumour. In chapter 5 I confirmed that NRF2 regulated

autophagy in BMSC protects MM cells. Therefore, taken together as NRF2 upregulation in MM cells and BMSC both favour the MM cells and NRF2 inhibition in MM cells and BMSC both comprise MM cells, my data led me to hypothesise that inhibiting NRF2 in patients with MM will be antitumoral through both a direct effect on the cancer cells and indirect effects through modulation of the tumour microenvironment.

## **6.2 The role of the ER on survival of MM cells**

### **6.2.1 MM cells endure ER stress**

Functionally ER controls protein translocation, folding and modification. The correctly modified protein is then transported to the Golgi and vesicles for secretion or display on the surface of the cell. As plasma cells produce and secrete immunoglobulin the ER plays a key role in non-malignant and malignant plasma cell normal function.

Accordingly, MM cells are a widely used in vitro model for ER stress research, due to its high-level basal ER stress that is induced by excessive production of paraprotein. Then, the paraprotein is transported to the ER lumen for protein folding, which induces the ER stress response: UPR. UPR functions to slow down the protein translation and increases the protein folding process to restore ER homeostasis. Therefore, the mechanisms by which MM cells sustain such high levels of ER stress are expected to provide novel insights in the development of future treatments of MM.

### **6.2.2 PI induces ER stress**

ER stress has been reported as responsible for the progression and drug resistance of MM [258, 312]. Thus, targeting ER stress to induce apoptosis of MM cells is an MM treatment strategy.

PI are a first line drug for treatment of MM and have a number of reported mechanisms of action. One such mechanism is the targeting of ER function in MM cells. The proteasome degradation system coordinates the unfolded protein response to speed up

the degradation of unwanted or misfolded proteins. When the MM cells are treated with PI, the ER stress is increased and the unfolded protein response is unable to release the ER stress, which leads MM cells towards an ER stress associated apoptosis. In chapter 3, I confirmed that the PI induces ER stress in MM cells. But as MM patients still relapse to the PI treatment, which lead to a question of how MM cells escape the ER stress induced cell death. My research shows that the NRF2 regulated GSH production play a key role for the cells to release ER stress and then escape cell death.

### **6.2.3 ER stress responses**

A number of different pathways of ER stress response have been reported [313, 314], for example:

- 1) IRE1 $\alpha$ : IRE1 $\alpha$  upregulates the unfolded protein response mediated by activation of transcriptional factor XBP-1. IRE1 $\alpha$  also activates JNK and p38 MAPK mediated by TRAF2 and ASK1. Activated JNK translocate to the mitochondrial membrane and regulates mitochondria function and activates p38 MAPK which activates CHOP, which then contributes to the induction of ER stress induced cell death.
- 2) ATF6: During ER stress, ATF6 relocates to the Golgi to mediate ER expansion and protein modification.
- 3) PERK: PERK activates eIF2 $\alpha$  and induces ATF4, which is an inducer of CHOP.

These three pathways highlight the central role of CHOP in the mediation of ER stress associated apoptosis. For this reason, I investigated the function of CHOP in MM.

### **6.2.4 NRF2 regulate ER stress associated apoptosis**

CHOP plays a central role for ER stress induced apoptosis and other reports have confirmed that in MM cells the NRF2 regulated ER stress associated apoptosis is mediated by CHOP and ATF4 [315, 316]. In chapter 3, I further confirmed that the high NRF2 expression controls CHOP mediated ER stress induced apoptosis in PI treated MM cells. I also extended our understating of the role of the ER stress response in MM drug resistance, which is mediated by NRF2 regulated GSH production. These finding decode a full mechanism of the NRF2 role in MM cells drug resistance.

## **6.4 Autophagy role on survival of MM cells**

### **6.4.1 MM cells upregulate autophagy for survival**

Under normal conditions, autophagy plays a key role in maintaining cellular homeostasis. Under stress conditions, cells upregulate autophagy to remove damaged organelles and other components, which provides recycled materials to meet the energy and nutrient demands of the cell [317]. As MM cells need to degrade dysfunctional sub-cellular organelles and misfolded paraprotein to prevent the initiation of apoptosis, autophagy upregulation is therefore essential for MM cell survival [318]. In chapter 5, I confirmed this concept, and, in my work, I extended the study of autophagy to cells within the tumour microenvironment, which is autophagy upregulation in the BMSC is also important for its supportive effect on MM cells.

Targeting autophagy to sensitise MM cells to chemotherapy is attracting attention, as MM is might dependent on autophagy to degrade paraprotein. Besides that, I have found that PI treatment upregulates P62 mediated autophagy in MM cells for survival. Thus, a strategy of inhibit both autophagy and the ubiquitin-proteasome degradation system would likely be highly effective in the treatment of MM.

### **6.4.2 BMSC upregulate autophagy to protect MM cells**

My research further focused on the function of autophagy in the BMSC, which is essential for the BMSC protection effect on MM cells. As shown in chapter 5, ATG5-KD BMSC are unable to form autophagosome and autophagy impaired BMSC is less protective to MM cells. I further revealed that MM cells and PI treatment both induce NRF2 activation in BMSC and NRF2 regulate autophagy, which is mediated by P62. This data suggest NRF2 regulation plays a key role for the BMSC protective effect on MM cells. I confirmed the hypothesis using a lentivirus mediated shRNA targeted NRF2 silencing method. My data show that NRF2-KD BMSC have decreased P62 protein level and impaired autophagy and results in less protection to MM cells. These data highlight that NRF2 activated autophagy in the BMSC is pro-tumoral in MM.

### **6.4.3 Targeting NRF2 inhibition to overcome the drawback of autophagy inhibition treatment of MM**

Though autophagy is an important cellular way to unload cell stress, cells have other ways to clear away unwanted proteins, for example the proteasome degradation system. Thus, the autophagy inhibitor would be optimally used in combination with other drugs, for example PI to treat MM [319]. So, autophagy inhibition alone may not be effective to induce MM cell death.

Autophagy inhibition and PI combination therapy also have drawbacks. A phase 1 clinical trial have tested the combination of Bz and autophagy inhibitor treatment on MM patients. It reports that the MM patients' responses were not robust. They hypothesised that ER stress and the unfolded protein responses as the possible mechanisms for MM cell survival [319]. So, autophagy inhibition and PI combination therapy may also be insufficient to treat MM cells.

Furthermore, as shown in chapter 3, I confirmed that PI treatment induces NRF2 upregulation. As described in chapter 1, NRF2 activation initiates more P62 production. It is also reported that PI increases P62 phosphorylation and promote autophagy which contribute to MM cells drug resistance. As a result, a new strategy is needed to improve the outcome of PI and autophagy inhibitor combination in the treatment of MM. Targeting NRF2 to overcome the failure of autophagy inhibitor in MM cells has been reported [306]. In chapter 4, I further confirmed that knock down of NRF2 in BMSC impaired its autophagy and block the BMSC protection effect on MM cells. So NRF2 inhibition may provide a new therapy strategy for treatment of MM.

## **6.5 Concluding remarks and future investigations**

Although the newly developed drugs for the treatment of MM have significantly increased the patients' remission time, currently MM is still incurable. Thus, understanding the cellular mechanisms of MM cell chemotherapy resistance is needed to improve therapy.

In my thesis, I highlight the role of NRF2 regulation in MM cell survival. I report that NRF2 reduces ER stress associated apoptosis in response to PI treatment of MM cells through regulating CHOP and GSH. This is a new finding, which highlights the role of NRF2 regulated ER stress on MM cells drug resistance. I also show that NRF2 regulates BMSC autophagy which functions to digest the outsourced autophagy burden from MM cells, and that this is mediated by P62. This is a new finding that extended our understandings of the protective role of NRF2 in the cell to cell interaction. It shows that BMSC protective effect on MM cells is mediated by MM cells that outsource its autophagy.

My research also highlights the role of the microenvironment in the protection of MM cells. In the BM, different types of cells build up an MM niche, which promotes MM progression and protects MM cells from chemotherapy induced cell death. In my research, I extended our understanding that autophagy in BMSC supports MM cells proliferation, which is induced by the ROS transferred from MM cells.

Further investigation should focus on establishing the details of the complex network of MM cell and BM microenvironment interaction and to decode the mechanisms of BM microenvironment protective role on MM cells. For example: 1) to design NRF2 specific inhibitors for the possible application in the disturb the cell to cell interaction; 2) to investigate other cell types, such as macrophage cells, T cells et al. in the BM microenvironment that interact with MM cells and affect its sensitivity to the chemotherapy; 3) to investigate how to sensitise MM cells stem cells to chemotherapy; 4) to investigate mechanisms of how MM cells explore BM microenvironment to avoid mitochondria induced cell death.

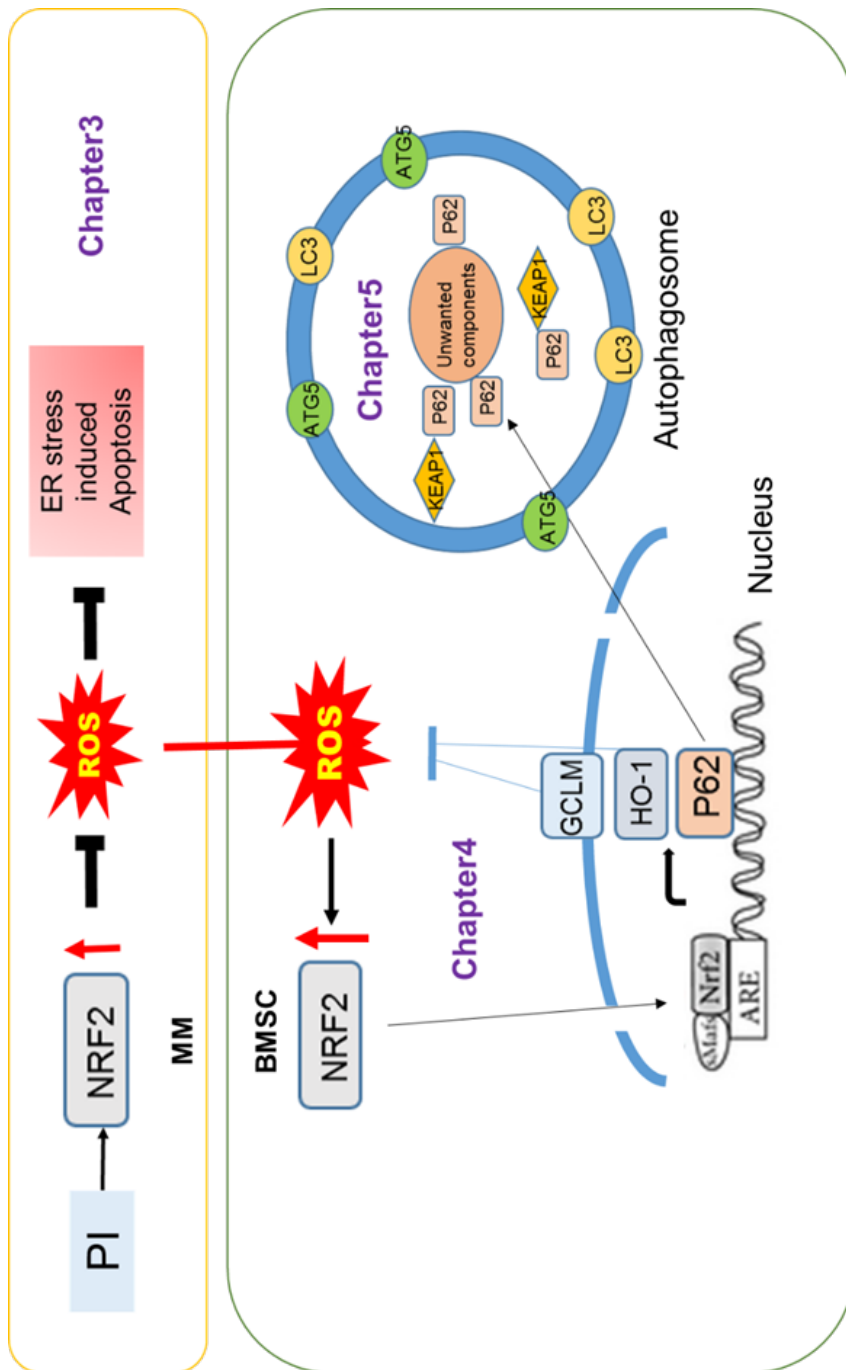


**Figure 6.39 Schematic representation of NRF2 regulation protect MM cells**

*In the PI treated MM cells (Chapter 3), NRF2 is upregulated to decrease PI induced ROS and ER stress associated MM apoptosis. MM cells also induces ROS stress and NRF2 upregulation in BMSC, which upregulates autophagy in the BMSC. Upregulated autophagy supports the proliferation of MM cells (chapter 5).*

## BIBLIOGRAPHY

1. Cancer, T.A.P.P.G.o.B., *All-Party Parliamentary Group Report on Blood Cancer*. 2016.
2. uk, c.r., *Myeloma statistics*. 2015, cancer research uk.
3. Kumar, S.K., et al., *Improved survival in multiple myeloma and the impact of novel therapies*. *Blood*, 2008. **111**(5): p. 2516-20.
4. Rajkumar, S.V. and S. Kumar, *Multiple Myeloma: Diagnosis and Treatment*. *Mayo Clin Proc*, 2016. **91**(1): p. 101-19.
5. Rajkumar, S.V., *Multiple myeloma*. *Curr Probl Cancer*, 2009. **33**(1): p. 7-64.
6. Burger, J.A., et al., *The microenvironment in mature B-cell malignancies: a target for new treatment strategies*. *Blood*, 2009. **114**(16): p. 3367-75.
7. Matsui, W., et al., *Characterization of clonogenic multiple myeloma cells*. *Blood*, 2004. **103**(6): p. 2332-6.
8. Bergsagel, P.L., et al., *In multiple myeloma, clonotypic B lymphocytes are detectable among CD19+ peripheral blood cells expressing CD38, CD56, and monotypic Ig light chain*. *Blood*, 1995. **85**(2): p. 436-47.
9. Nutt, S.L., et al., *The generation of antibody-secreting plasma cells*. *Nat Rev Immunol*, 2015. **15**(3): p. 160-71.
10. Cooper, E.H., *Production of lymphocytes and plasma cells in the rat following immunization with human serum albumin*. *Immunology*, 1961. **4**: p. 219-31.
11. Schooley, J.C., *Autoradiographic observations of plasma cell formation*. *J Immunol*, 1961. **86**: p. 331-7.
12. Nossal, G.J. and O. Makela, *Autoradiographic studies on the immune response. I. The kinetics of plasma cell proliferation*. *J Exp Med*, 1962. **115**: p. 209-30.
13. Okudaira, H. and K. Ishizaka, *Reaginic antibody formation in the mouse. XI. Participation of long-lived antibody-forming cells in persistent antibody formation*. *Cell Immunol*, 1981. **58**(1): p. 188-201.
14. Ho, F., et al., *Distinct short-lived and long-lived antibody-producing cell populations*. *Eur J Immunol*, 1986. **16**(10): p. 1297-301.
15. Manz, R.A., A. Thiel, and A. Radbruch, *Lifetime of plasma cells in the bone marrow*. *Nature*, 1997. **388**(6638): p. 133-4.
16. Miller, J.J., 3rd, *An Autoradiographic Study of Plasma Cell and Lymphocyte Survival in Rat Popliteal Lymph Nodes*. *J Immunol*, 1964. **92**: p. 673-81.
17. Hammarlund, E., et al., *Plasma cell survival in the absence of B cell memory*. *Nat Commun*, 2017. **8**(1): p. 1781.
18. Lin, Y., K. Wong, and K. Calame, *Repression of c-myc transcription by Blimp-1, an inducer of terminal B cell differentiation*. *Science*, 1997. **276**(5312): p. 596-9.
19. Lin, K.I., et al., *Blimp-1-dependent repression of Pax-5 is required for differentiation of B cells to immunoglobulin M-secreting plasma cells*. *Mol Cell Biol*, 2002. **22**(13): p. 4771-80.
20. Piskurich, J.F., et al., *BLIMP-1 mediates extinction of major histocompatibility class II transactivator expression in plasma cells*. *Nat Immunol*, 2000. **1**(6): p. 526-32.
21. Shaffer, A.L., et al., *Blimp-1 orchestrates plasma cell differentiation by extinguishing the mature B cell gene expression program*. *Immunity*, 2002. **17**(1): p. 51-62.
22. Revilla, I.D.R., et al., *The B-cell identity factor Pax5 regulates distinct transcriptional programmes in early and late B lymphopoiesis*. *EMBO J*, 2012. **31**(14): p. 3130-46.
23. Kallies, A., et al., *Plasma cell ontogeny defined by quantitative changes in blimp-1 expression*. *J Exp Med*, 2004. **200**(8): p. 967-77.
24. Benhamron, S., et al., *mTOR activation promotes plasma cell differentiation and bypasses XBP-1 for immunoglobulin secretion*. *Mol Cell Biol*, 2015. **35**(1): p. 153-66.

25. Teller, J., et al., *Blimp-1 controls plasma cell function through the regulation of immunoglobulin secretion and the unfolded protein response*. *Nat Immunol*, 2016. **17**(3): p. 323-30.
26. Bettigole, S.E. and L.H. Glimcher, *Endoplasmic reticulum stress in immunity*. *Annu Rev Immunol*, 2015. **33**: p. 107-38.
27. Pengo, N. and S. Cenci, *The role of autophagy in plasma cell ontogenesis*. *Autophagy*, 2013. **9**(6): p. 942-4.
28. Rajkumar, S.V., et al., *International Myeloma Working Group updated criteria for the diagnosis of multiple myeloma*. *Lancet Oncol*, 2014. **15**(12): p. e538-48.
29. Frank, C., et al., *Search for familial clustering of multiple myeloma with any cancer*. *Leukemia*, 2016. **30**(3): p. 627-32.
30. Greenberg, A.J., S.V. Rajkumar, and C.M. Vachon, *Familial monoclonal gammopathy of undetermined significance and multiple myeloma: epidemiology, risk factors, and biological characteristics*. *Blood*, 2012. **119**(23): p. 5359-66.
31. Grosbois, B., et al., *Multiple myeloma in two brothers. An immunochemical and immunogenetic familial study*. *Cancer*, 1986. **58**(11): p. 2417-21.
32. Lynch, H.T., et al., *Familial myeloma*. *N Engl J Med*, 2008. **359**(2): p. 152-7.
33. Redfield, R.R. and A. Naji, *Progression of monoclonal gammopathy of undetermined significance to multiple myeloma in a solid organ transplant*. *Transplantation*, 2011. **92**(12): p. e65-6; author reply e66.
34. Gupta, A., et al., *Plasma cell myeloma variant of post-transplant lymphoproliferative disorder in a solid organ transplant recipient: a case report*. *Nephrol Dial Transplant*, 2004. **19**(12): p. 3186-9.
35. Sun, X., et al., *Post-transplant plasma cell myeloma and polymorphic lymphoproliferative disorder with monoclonal serum protein occurring in solid organ transplant recipients*. *Mod Pathol*, 2004. **17**(4): p. 389-94.
36. Yee, T.T., et al., *Multiple myeloma and human immunodeficiency virus-1 (HIV-1) infection*. *Am J Hematol*, 2001. **66**(2): p. 123-5.
37. Shokunbi, W.A., et al., *Multiple myeloma co-existing with HIV-1 infection in a 65-year-old Nigerian man*. *AIDS*, 1991. **5**(1): p. 115-6.
38. McShane, C.M., et al., *Prior autoimmune disease and risk of monoclonal gammopathy of undetermined significance and multiple myeloma: a systematic review*. *Cancer Epidemiol Biomarkers Prev*, 2014. **23**(2): p. 332-42.
39. Morado, M., et al., *[Association of multiple myeloma and autoimmune hemolytic anemia]*. *Sangre (Barc)*, 1998. **43**(5): p. 467-8.
40. Benjlali, L. and L. Essaadouni, *[A multiple myeloma associated with autoimmune hemolytic anemia]*. *Presse Med*, 2013. **42**(11): p. 1533-5.
41. Brown, L.M., et al., *Risk of multiple myeloma and monoclonal gammopathy of undetermined significance among white and black male United States veterans with prior autoimmune, infectious, inflammatory, and allergic disorders*. *Blood*, 2008. **111**(7): p. 3388-94.
42. Crispin, P.J. and P.L. Cheah, *Autoimmune haemolytic anaemia and neuropathy with IgA osteosclerotic myeloma: a case report*. *Pathology*, 2017. **49**(6): p. 646-647.
43. Cuzick, J. and B.L. De Stavola, *Autoimmune disorders and multiple myeloma*. *Int J Epidemiol*, 1989. **18**(1): p. 283.
44. Gesundheit, B., et al., *Complete remission of multiple myeloma after autoimmune hemolytic anemia: possible association with interferon-alpha*. *Am J Hematol*, 2007. **82**(6): p. 489-92.
45. Costello, R., T. O'Callaghan, and G. Sebahoun, *Gaucher disease and multiple myeloma*. *Leuk Lymphoma*, 2006. **47**(7): p. 1365-8.

46. Hofmann, J.N., et al., *Body mass index and physical activity at different ages and risk of multiple myeloma in the NIH-AARP diet and health study*. Am J Epidemiol, 2013. **177**(8): p. 776-86.
47. Hosgood, H.D., 3rd, et al., *Diet and risk of multiple myeloma in Connecticut women*. Cancer Causes Control, 2007. **18**(10): p. 1065-76.
48. Lwin, S.T., et al., *Diet-induced obesity promotes a myeloma-like condition in vivo*. Leukemia, 2015. **29**(2): p. 507-10.
49. Brown, L.M., et al., *Diet and nutrition as risk factors for multiple myeloma among blacks and whites in the United States*. Cancer Causes Control, 2001. **12**(2): p. 117-25.
50. Juranic, Z., et al., *Could the use of appropriate diet help in the prevention of multiple myeloma?* J BUON, 2009. **14**(2): p. 321-2.
51. Vlainjac, H.D., et al., *Case-control study of multiple myeloma with special reference to diet as risk factor*. Neoplasma, 2003. **50**(1): p. 79-83.
52. Boffetta, P., et al., *Exposure to ultraviolet radiation and risk of malignant lymphoma and multiple myeloma--a multicentre European case-control study*. Int J Epidemiol, 2008. **37**(5): p. 1080-94.
53. Ishimaru, T. and S.C. Finch, *More on radiation exposure and multipel myeloma*. N Engl J Med, 1979. **301**(8): p. 439-40.
54. Teitelbaum, D.T. and N. Brautbar, *Benzene and multiple myeloma: appraisal of the scientific evidence*. Blood, 2000. **95**(9): p. 2995-7.
55. Bergsagel, D.E., et al., *Benzene and multiple myeloma: appraisal of the scientific evidence*. Blood, 1999. **94**(4): p. 1174-82.
56. Goldstein, B.D. and S.L. Shalat, *The casual relation between benzene exposure and multiple myeloma*. Blood, 2000. **95**(4): p. 1512-4.
57. Chretien, M.L., et al., *Understanding the role of hyperdiploidy in myeloma prognosis: which trisomies really matter?* Blood, 2015. **126**(25): p. 2713-9.
58. Chiecchio, L., et al., *Deletion of chromosome 13 detected by conventional cytogenetics is a critical prognostic factor in myeloma*. Leukemia, 2006. **20**(9): p. 1610-7.
59. Shaughnessy, J., et al., *High incidence of chromosome 13 deletion in multiple myeloma detected by multiprobe interphase FISH*. Blood, 2000. **96**(4): p. 1505-11.
60. Liebisch, P., et al., *Duplication of chromosome arms 9q and 11q: evidence for a novel, 14q32 translocation-independent pathogenetic pathway in multiple myeloma*. Genes Chromosomes Cancer, 2005. **42**(1): p. 78-81.
61. Sun, W.L., et al., *[Detection of deletion of the long arm of chromosome 13 and translocation of immunoglobulin heavy chain gene by interphase fluorescence in situ hybridization in patients with multiple myeloma]*. Zhongguo Yi Xue Ke Xue Yuan Xue Bao, 2008. **30**(4): p. 485-90.
62. Jelinek, D.F., *Mechanisms of myeloma cell growth control*. Hematol Oncol Clin North Am, 1999. **13**(6): p. 1145-57.
63. Morgan, G.J., B.A. Walker, and F.E. Davies, *The genetic architecture of multiple myeloma*. Nat Rev Cancer, 2012. **12**(5): p. 335-48.
64. Neri, A., et al., *p53 gene mutations in multiple myeloma are associated with advanced forms of malignancy*. Blood, 1993. **81**(1): p. 128-35.
65. Portier, M., et al., *p53 and RAS gene mutations in multiple myeloma*. Oncogene, 1992. **7**(12): p. 2539-43.
66. Martinez-Garcia, E., et al., *The MMSET histone methyl transferase switches global histone methylation and alters gene expression in t(4;14) multiple myeloma cells*. Blood, 2011. **117**(1): p. 211-20.

67. Mitsiades, C.S., et al., *Transcriptional signature of histone deacetylase inhibition in multiple myeloma: biological and clinical implications*. Proc Natl Acad Sci U S A, 2004. **101**(2): p. 540-5.
68. Dilworth, D., et al., *Germline CDKN2A mutation implicated in predisposition to multiple myeloma*. Blood, 2000. **95**(5): p. 1869-71.
69. Wei, X., et al., *Germline mutations in lysine specific demethylase 1 (LSD1/KDM1A) confer susceptibility to multiple myeloma*. Cancer Res, 2018.
70. Kataoka, T., et al., *The nucleotide sequences of rearranged and germline immunoglobulin VH genes of a mouse myeloma MC101 and evolution of VH genes in mouse*. J Biol Chem, 1982. **257**(1): p. 277-85.
71. Zwick, C., et al., *Over one-third of African-American MGUS and multiple myeloma patients are carriers of hyperphosphorylated paratarg-7, an autosomal dominantly inherited risk factor for MGUS/MM*. Int J Cancer, 2014. **135**(4): p. 934-8.
72. Grass, S., et al., *Risk of Japanese carriers of hyperphosphorylated paratarg-7, the first autosomal-dominantly inherited risk factor for hematological neoplasms, to develop monoclonal gammopathy of undetermined significance and multiple myeloma*. Cancer Sci, 2011. **102**(3): p. 565-8.
73. Adamia, S., et al., *Inherited and acquired variations in the hyaluronan synthase 1 (HAS1) gene may contribute to disease progression in multiple myeloma and Waldenstrom macroglobulinemia*. Blood, 2008. **112**(13): p. 5111-21.
74. Morgan, G.J., et al., *Inherited genetic susceptibility to multiple myeloma*. Leukemia, 2014. **28**(3): p. 518-24.
75. Lohr, J.G., et al., *Widespread genetic heterogeneity in multiple myeloma: implications for targeted therapy*. Cancer Cell, 2014. **25**(1): p. 91-101.
76. Usmani, S.Z., et al., *Defining and treating high-risk multiple myeloma*. Leukemia, 2015. **29**(11): p. 2119-25.
77. Sonneveld, P., et al., *Treatment of multiple myeloma with high-risk cytogenetics: a consensus of the International Myeloma Working Group*. Blood, 2016. **127**(24): p. 2955-62.
78. Hebraud, B., et al., *Role of additional chromosomal changes in the prognostic value of t(4;14) and del(17p) in multiple myeloma: the IFM experience*. Blood, 2015. **125**(13): p. 2095-100.
79. Avet-Loiseau, H., et al., *Prognostic significance of copy-number alterations in multiple myeloma*. J Clin Oncol, 2009. **27**(27): p. 4585-90.
80. Shah, V., et al., *Prediction of outcome in newly diagnosed myeloma: a meta-analysis of the molecular profiles of 1905 trial patients*. Leukemia, 2018. **32**(1): p. 102-110.
81. Went, M., et al., *Identification of multiple risk loci and regulatory mechanisms influencing susceptibility to multiple myeloma*. Nat Commun, 2018. **9**(1): p. 3707.
82. Li, N., et al., *Multiple myeloma risk variant at 7p15.3 creates an IRF4-binding site and interferes with CDCA7L expression*. Nat Commun, 2016. **7**: p. 13656.
83. Ramakrishnan, V. and S. Kumar, *PI3K/AKT/mTOR pathway in multiple myeloma: from basic biology to clinical promise*. Leuk Lymphoma, 2018: p. 1-11.
84. Moreau, P., *How I treat myeloma with new agents*. Blood, 2017. **130**(13): p. 1507-1513.
85. Adams, J., *The proteasome: structure, function, and role in the cell*. Cancer Treat Rev, 2003. **29 Suppl 1**: p. 3-9.
86. Obeng, E.A., et al., *Proteasome inhibitors induce a terminal unfolded protein response in multiple myeloma cells*. Blood, 2006. **107**(12): p. 4907-16.
87. Manasanch, E.E. and R.Z. Orlowski, *Proteasome inhibitors in cancer therapy*. Nat Rev Clin Oncol, 2017. **14**(7): p. 417-433.

88. Heinemeyer, W., et al., *The active sites of the eukaryotic 20 S proteasome and their involvement in subunit precursor processing*. J Biol Chem, 1997. **272**(40): p. 25200-9.
89. Moreau, P., et al., *Proteasome inhibitors in multiple myeloma: 10 years later*. Blood, 2012. **120**(5): p. 947-59.
90. Dick, L.R. and P.E. Fleming, *Building on bortezomib: second-generation proteasome inhibitors as anti-cancer therapy*. Drug Discov Today, 2010. **15**(5-6): p. 243-9.
91. Chen, J.F., et al., *Bortezomib, Thalidomide, and Dexamethasone (VTD) Induction Results in Better Overall Survival than Adriamycin, Thalidomide, and Dexamethasone (ATD) Induction in Previously Untreated Myeloma Patients Eligible for Transplants*. Acta Haematol, 2017. **137**(4): p. 207-208.
92. Chng, W.J., et al., *Carfilzomib-dexamethasone vs bortezomib-dexamethasone in relapsed or refractory multiple myeloma by cytogenetic risk in the phase 3 study ENDEAVOR*. Leukemia, 2017. **31**(6): p. 1368-1374.
93. de Oliveira, M.B., et al., *Anti-myeloma effects of ruxolitinib combined with bortezomib and lenalidomide: A rationale for JAK/STAT pathway inhibition in myeloma patients*. Cancer Lett, 2017. **403**: p. 206-215.
94. Dimopoulos, M.A., et al., *Carfilzomib or bortezomib in relapsed or refractory multiple myeloma (ENDEAVOR): an interim overall survival analysis of an open-label, randomised, phase 3 trial*. Lancet Oncol, 2017. **18**(10): p. 1327-1337.
95. Chakraborty, R., et al., *Outcomes of maintenance therapy with lenalidomide or bortezomib in multiple myeloma in the setting of early autologous stem cell transplantation*. Leukemia, 2018. **32**(3): p. 712-718.
96. Hu, J., et al., *Synergistic induction of apoptosis in multiple myeloma cells by bortezomib and hypoxia-activated prodrug TH-302, in vivo and in vitro*. Mol Cancer Ther, 2013. **12**(9): p. 1763-73.
97. Hideshima, T., et al., *Bortezomib induces canonical nuclear factor-kappaB activation in multiple myeloma cells*. Blood, 2009. **114**(5): p. 1046-52.
98. Noborio-Hatano, K., et al., *Bortezomib overcomes cell-adhesion-mediated drug resistance through downregulation of VLA-4 expression in multiple myeloma*. Oncogene, 2009. **28**(2): p. 231-42.
99. Hideshima, T., et al., *Molecular mechanisms mediating antimyeloma activity of proteasome inhibitor PS-341*. Blood, 2003. **101**(4): p. 1530-4.
100. Ookura, M., et al., *YM155 exerts potent cytotoxic activity against quiescent (G0/G1) multiple myeloma and bortezomib resistant cells via inhibition of survivin and Mcl-1*. Oncotarget, 2017. **8**(67): p. 111535-111550.
101. Attal, M., et al., *Lenalidomide, Bortezomib, and Dexamethasone with Transplantation for Myeloma*. N Engl J Med, 2017. **376**(14): p. 1311-1320.
102. Chauhan, D., et al., *Combination of proteasome inhibitors bortezomib and NPI-0052 trigger in vivo synergistic cytotoxicity in multiple myeloma*. Blood, 2008. **111**(3): p. 1654-64.
103. Wallington-Beddoe, C.T., et al., *Sphingosine kinase 2 inhibition synergises with bortezomib to target myeloma by enhancing endoplasmic reticulum stress*. Oncotarget, 2017. **8**(27): p. 43602-43616.
104. Yin, L., et al., *Targeting MUC1-C is synergistic with bortezomib in downregulating TIGAR and inducing ROS-mediated myeloma cell death*. Blood, 2014. **123**(19): p. 2997-3006.
105. Parlati, F., et al., *Carfilzomib can induce tumor cell death through selective inhibition of the chymotrypsin-like activity of the proteasome*. Blood, 2009. **114**(16): p. 3439-47.

106. Kuhn, D.J., et al., *Potent activity of carfilzomib, a novel, irreversible inhibitor of the ubiquitin-proteasome pathway, against preclinical models of multiple myeloma*. *Blood*, 2007. **110**(9): p. 3281-90.
107. Kumar, S.K., et al., *Randomized phase 2 trial of ixazomib and dexamethasone in relapsed multiple myeloma not refractory to bortezomib*. *Blood*, 2016. **128**(20): p. 2415-2422.
108. Teicher, B.A. and J.E. Tomaszewski, *Proteasome inhibitors*. *Biochem Pharmacol*, 2015. **96**(1): p. 1-9.
109. Moreau, P., et al., *Subcutaneous versus intravenous administration of bortezomib in patients with relapsed multiple myeloma: a randomised, phase 3, non-inferiority study*. *Lancet Oncol*, 2011. **12**(5): p. 431-40.
110. Hirschev, M.D., et al., *Dysregulated metabolism contributes to oncogenesis*. *Semin Cancer Biol*, 2015. **35 Suppl**: p. S129-S150.
111. Bajpai, R., et al., *Targeting glutamine metabolism in multiple myeloma enhances BIM binding to BCL-2 eliciting synthetic lethality to venetoclax*. *Oncogene*, 2016. **35**(30): p. 3955-64.
112. El Arfani, C., et al., *Metabolic Features of Multiple Myeloma*. *Int J Mol Sci*, 2018. **19**(4).
113. Bolzoni, M., et al., *Dependence on glutamine uptake and glutamine addiction characterize myeloma cells: a new attractive target*. *Blood*, 2016. **128**(5): p. 667-79.
114. Nakano, A., et al., *Up-regulation of hexokinase II in myeloma cells: targeting myeloma cells with 3-bromopyruvate*. *J Bioenerg Biomembr*, 2012. **44**(1): p. 31-8.
115. Wang, J., et al., *Cancer-derived immunoglobulin G promotes tumor cell growth and proliferation through inducing production of reactive oxygen species*. *Cell Death Dis*, 2013. **4**: p. e945.
116. Topf, U., et al., *Quantitative proteomics identifies redox switches for global translation modulation by mitochondrially produced reactive oxygen species*. *Nat Commun*, 2018. **9**(1): p. 324.
117. Liu, B. and S.B. Qian, *Translational reprogramming in cellular stress response*. *Wiley Interdiscip Rev RNA*, 2014. **5**(3): p. 301-15.
118. Trachootham, D., et al., *Redox regulation of cell survival*. *Antioxid Redox Signal*, 2008. **10**(8): p. 1343-74.
119. Kalyanaraman, B., et al., *Corrigendum to 'A review of the basics of mitochondrial bioenergetics, metabolism, and related signaling pathways in cancer cells: Therapeutic targeting of tumor mitochondria with lipophilic cationic compounds' [REDOX 14C (2017) 316-327]*. *Redox Biol*, 2018.
120. Saneesh Babu, P.S., et al., *Bis(3,5-diiodo-2,4,6-trihydroxyphenyl)squaraine photodynamic therapy disrupts redox homeostasis and induce mitochondria-mediated apoptosis in human breast cancer cells*. *Sci Rep*, 2017. **7**: p. 42126.
121. Schrader, M. and H.D. Fahimi, *Peroxisomes and oxidative stress*. *Biochim Biophys Acta*, 2006. **1763**(12): p. 1755-66.
122. Phaniendra, A., D.B. Jestadi, and L. Periyasamy, *Free radicals: properties, sources, targets, and their implication in various diseases*. *Indian J Clin Biochem*, 2015. **30**(1): p. 11-26.
123. Cao, S.S. and R.J. Kaufman, *Endoplasmic reticulum stress and oxidative stress in cell fate decision and human disease*. *Antioxid Redox Signal*, 2014. **21**(3): p. 396-413.
124. Droge, W., *Free radicals in the physiological control of cell function*. *Physiol Rev*, 2002. **82**(1): p. 47-95.
125. Del Maestro, R.F., *An approach to free radicals in medicine and biology*. *Acta Physiol Scand Suppl*, 1980. **492**: p. 153-68.

126. Pohjoismaki, J.L., et al., *Oxidative stress during mitochondrial biogenesis compromises mtDNA integrity in growing hearts and induces a global DNA repair response*. Nucleic Acids Res, 2012. **40**(14): p. 6595-607.
127. Hofer, T., et al., *Hydrogen peroxide causes greater oxidation in cellular RNA than in DNA*. Biol Chem, 2005. **386**(4): p. 333-7.
128. Dean, R.T., et al., *Biochemistry and pathology of radical-mediated protein oxidation*. Biochem J, 1997. **324 ( Pt 1)**: p. 1-18.
129. Butterfield, D.A., et al., *Structural and functional changes in proteins induced by free radical-mediated oxidative stress and protective action of the antioxidants N-tert-butyl-alpha-phenylnitron and vitamin E*. Ann N Y Acad Sci, 1998. **854**: p. 448-62.
130. Waris, G. and H. Ahsan, *Reactive oxygen species: role in the development of cancer and various chronic conditions*. J Carcinog, 2006. **5**: p. 14.
131. Wang, P.Y., et al., *Increased oxidative metabolism in the Li-Fraumeni syndrome*. N Engl J Med, 2013. **368**(11): p. 1027-32.
132. Higinbotham, K.G., et al., *GGT to GTT transversions in codon 12 of the K-ras oncogene in rat renal sarcomas induced with nickel subsulfide or nickel subsulfide/iron are consistent with oxidative damage to DNA*. Cancer Res, 1992. **52**(17): p. 4747-51.
133. Lipchick, B.C., E.E. Fink, and M.A. Nikiforov, *Oxidative stress and proteasome inhibitors in multiple myeloma*. Pharmacol Res, 2016. **105**: p. 210-5.
134. Fink, E.E., et al., *Mitochondrial thioredoxin reductase regulates major cytotoxicity pathways of proteasome inhibitors in multiple myeloma cells*. Leukemia, 2016. **30**(1): p. 104-11.
135. Amanso, A.M., V. Debbas, and F.R. Laurindo, *Proteasome inhibition represses unfolded protein response and Nox4, sensitizing vascular cells to endoplasmic reticulum stress-induced death*. PLoS One, 2011. **6**(1): p. e14591.
136. Maharjan, S., et al., *Mitochondrial impairment triggers cytosolic oxidative stress and cell death following proteasome inhibition*. Sci Rep, 2014. **4**: p. 5896.
137. Goel, A., D.R. Spitz, and G.J. Weiner, *Manipulation of cellular redox parameters for improving therapeutic responses in B-cell lymphoma and multiple myeloma*. J Cell Biochem, 2012. **113**(2): p. 419-25.
138. Ma, Q., *Role of nrf2 in oxidative stress and toxicity*. Annu Rev Pharmacol Toxicol, 2013. **53**: p. 401-26.
139. Satoh, T., et al., *Activation of the Keap1/Nrf2 pathway for neuroprotection by electrophilic [correction of electrophilic] phase II inducers*. Proc Natl Acad Sci U S A, 2006. **103**(3): p. 768-73.
140. Magesh, S., Y. Chen, and L. Hu, *Small molecule modulators of Keap1-Nrf2-ARE pathway as potential preventive and therapeutic agents*. Med Res Rev, 2012. **32**(4): p. 687-726.
141. Itoh, K., et al., *Keap1 represses nuclear activation of antioxidant responsive elements by Nrf2 through binding to the amino-terminal Neh2 domain*. Genes Dev, 1999. **13**(1): p. 76-86.
142. Lu, Q., et al., *Acetylation of cAMP-responsive element-binding protein (CREB) by CREB-binding protein enhances CREB-dependent transcription*. J Biol Chem, 2003. **278**(18): p. 15727-34.
143. Kwak, M.K., et al., *Enhanced expression of the transcription factor Nrf2 by cancer chemopreventive agents: role of antioxidant response element-like sequences in the nrf2 promoter*. Mol Cell Biol, 2002. **22**(9): p. 2883-92.
144. Shelton, P. and A.K. Jaiswal, *The transcription factor NF-E2-related factor 2 (Nrf2): a protooncogene?* FASEB J, 2013. **27**(2): p. 414-23.

145. Dinkova-Kostova, A.T. and A.Y. Abramov, *The emerging role of Nrf2 in mitochondrial function*. Free Radic Biol Med, 2015. **88**(Pt B): p. 179-188.
146. Salem, K., et al., *Copper-zinc superoxide dismutase-mediated redox regulation of bortezomib resistance in multiple myeloma*. Redox Biol, 2015. **4**: p. 23-33.
147. Yu, W., et al., *PGC-1alpha is responsible for survival of multiple myeloma cells under hyperglycemia and chemotherapy*. Oncol Rep, 2015. **33**(4): p. 2086-92.
148. Demasi, A.P., et al., *Expression of peroxiredoxins I and IV in multiple myeloma: association with immunoglobulin accumulation*. Virchows Arch, 2013. **463**(1): p. 47-55.
149. Kumar, G.S. and U.N. Das, *Free radical-dependent suppression of growth of mouse myeloma cells by alpha-linolenic and eicosapentaenoic acids in vitro*. Cancer Lett, 1995. **92**(1): p. 27-38.
150. Sebastian, S., et al., *Multiple myeloma cells' capacity to decompose H2O2 determines lenalidomide sensitivity*. Blood, 2017. **129**(8): p. 991-1007.
151. Tagde, A., et al., *MUC1-C drives MYC in multiple myeloma*. Blood, 2016. **127**(21): p. 2587-97.
152. McBrayer, S.K., et al., *Integrative gene expression profiling reveals G6PD-mediated resistance to RNA-directed nucleoside analogues in B-cell neoplasms*. PLoS One, 2012. **7**(7): p. e41455.
153. Boivin, P., et al., *Acquired erythroenzymopathies in blood disorders: study of 200 cases*. Br J Haematol, 1975. **31**(4): p. 531-43.
154. Li Volti, G., et al., *The Heme Oxygenase System in Hematological Malignancies*. Antioxid Redox Signal, 2017. **27**(6): p. 363-377.
155. Milan, E., et al., *A plastic SQSTM1/p62-dependent autophagic reserve maintains proteostasis and determines proteasome inhibitor susceptibility in multiple myeloma cells*. Autophagy, 2015. **11**(7): p. 1161-78.
156. Ursini, F., et al., *Diversity of glutathione peroxidases*. Methods Enzymol, 1995. **252**: p. 38-53.
157. Sen, C.K., *Glutathione homeostasis in response to exercise training and nutritional supplements*. Mol Cell Biochem, 1999. **196**(1-2): p. 31-42.
158. Sen, C.K., *Antioxidant and redox regulation of cellular signaling: introduction*. Med Sci Sports Exerc, 2001. **33**(3): p. 368-70.
159. Townsend, D.M. and K.D. Tew, *The role of glutathione-S-transferase in anti-cancer drug resistance*. Oncogene, 2003. **22**(47): p. 7369-75.
160. Loboda, A., et al., *Heme oxygenase-1 and the vascular bed: from molecular mechanisms to therapeutic opportunities*. Antioxid Redox Signal, 2008. **10**(10): p. 1767-812.
161. Birgisdottir, A.B., T. Lamark, and T. Johansen, *The LIR motif - crucial for selective autophagy*. J Cell Sci, 2013. **126**(Pt 15): p. 3237-47.
162. Moscat, J. and M.T. Diaz-Meco, *p62: a versatile multitasker takes on cancer*. Trends Biochem Sci, 2012. **37**(6): p. 230-6.
163. Komatsu, M., et al., *The selective autophagy substrate p62 activates the stress responsive transcription factor Nrf2 through inactivation of Keap1*. Nat Cell Biol, 2010. **12**(3): p. 213-23.
164. Lau, A., et al., *A noncanonical mechanism of Nrf2 activation by autophagy deficiency: direct interaction between Keap1 and p62*. Mol Cell Biol, 2010. **30**(13): p. 3275-85.
165. Chan, J.Y., et al., *Targeted disruption of the ubiquitous CNC-bZIP transcription factor, Nrf-1, results in anemia and embryonic lethality in mice*. EMBO J, 1998. **17**(6): p. 1779-87.

166. Chan, K., et al., *NRF2, a member of the NFE2 family of transcription factors, is not essential for murine erythropoiesis, growth, and development*. Proc Natl Acad Sci U S A, 1996. **93**(24): p. 13943-8.
167. Zhang, Y. and Y. Xiang, *Molecular and cellular basis for the unique functioning of Nrf1, an indispensable transcription factor for maintaining cell homeostasis and organ integrity*. Biochem J, 2016. **473**(8): p. 961-1000.
168. Steffen, J., et al., *Proteasomal degradation is transcriptionally controlled by TCF11 via an ERAD-dependent feedback loop*. Mol Cell, 2010. **40**(1): p. 147-58.
169. Sha, Z. and A.L. Goldberg, *Proteasome-mediated processing of Nrf1 is essential for coordinate induction of all proteasome subunits and p97*. Curr Biol, 2014. **24**(14): p. 1573-1583.
170. Sankaranarayanan, K. and A.K. Jaiswal, *Nrf3 negatively regulates antioxidant-response element-mediated expression and antioxidant induction of NAD(P)H:quinone oxidoreductase1 gene*. J Biol Chem, 2004. **279**(49): p. 50810-7.
171. Derjuga, A., et al., *Complexity of CNC transcription factors as revealed by gene targeting of the Nrf3 locus*. Mol Cell Biol, 2004. **24**(8): p. 3286-94.
172. Choi, A.M., S.W. Ryter, and B. Levine, *Autophagy in human health and disease*. N Engl J Med, 2013. **368**(19): p. 1845-6.
173. Komatsu, M., et al., *Homeostatic levels of p62 control cytoplasmic inclusion body formation in autophagy-deficient mice*. Cell, 2007. **131**(6): p. 1149-63.
174. Milan, E., M. Fabbri, and S. Cenci, *Autophagy in Plasma Cell Ontogeny and Malignancy*. J Clin Immunol, 2016. **36 Suppl 1**: p. 18-24.
175. Hoang, B., et al., *Effect of autophagy on multiple myeloma cell viability*. Mol Cancer Ther, 2009. **8**(7): p. 1974-84.
176. Lamy, L., et al., *Control of autophagic cell death by caspase-10 in multiple myeloma*. Cancer Cell, 2013. **23**(4): p. 435-49.
177. Kroemer, G. and B. Levine, *Autophagic cell death: the story of a misnomer*. Nat Rev Mol Cell Biol, 2008. **9**(12): p. 1004-10.
178. Carroll, R.G. and S.J. Martin, *Autophagy in multiple myeloma: what makes you stronger can also kill you*. Cancer Cell, 2013. **23**(4): p. 425-6.
179. White, E., *Deconvoluting the context-dependent role for autophagy in cancer*. Nat Rev Cancer, 2012. **12**(6): p. 401-10.
180. Bottone, M.G., et al., *Morphological Features of Organelles during Apoptosis: An Overview*. Cells, 2013. **2**(2): p. 294-305.
181. Galluzzi, L., J.M. Bravo-San Pedro, and G. Kroemer, *Organelle-specific initiation of cell death*. Nat Cell Biol, 2014. **16**(8): p. 728-36.
182. Ferri, K.F. and G. Kroemer, *Organelle-specific initiation of cell death pathways*. Nat Cell Biol, 2001. **3**(11): p. E255-63.
183. Nunez, R., et al., *Apoptotic volume decrease as a geometric determinant for cell dismantling into apoptotic bodies*. Cell Death Differ, 2010. **17**(11): p. 1665-71.
184. Soldani, C., et al., *Apoptosis in tumour cells photosensitized with Rose Bengal acetate is induced by multiple organelle photodamage*. Histochem Cell Biol, 2007. **128**(5): p. 485-95.
185. Fraschini, A., et al., *Changes in extranucleolar transcription during actinomycin D-induced apoptosis*. Histol Histopathol, 2005. **20**(1): p. 107-17.
186. Jiang, Z., et al., *The role of the Golgi apparatus in oxidative stress: is this organelle less significant than mitochondria?* Free Radic Biol Med, 2011. **50**(8): p. 907-17.
187. Bottone, M.G., et al., *Intracellular distribution of Tankyrases as detected by multicolor immunofluorescence techniques*. Eur J Histochem, 2012. **56**(1): p. e4.
188. Kurz, T., et al., *Lysosomes in iron metabolism, ageing and apoptosis*. Histochem Cell Biol, 2008. **129**(4): p. 389-406.

189. Cesen, M.H., et al., *Lysosomal pathways to cell death and their therapeutic applications*. Exp Cell Res, 2012. **318**(11): p. 1245-51.
190. Johansson, A.C., et al., *Regulation of apoptosis-associated lysosomal membrane permeabilization*. Apoptosis, 2010. **15**(5): p. 527-40.
191. Repnik, U. and B. Turk, *Lysosomal-mitochondrial cross-talk during cell death*. Mitochondrion, 2010. **10**(6): p. 662-9.
192. Green, D.R. and G. Kroemer, *The pathophysiology of mitochondrial cell death*. Science, 2004. **305**(5684): p. 626-9.
193. Kroemer, G., et al., *The biochemistry of programmed cell death*. FASEB J, 1995. **9**(13): p. 1277-87.
194. Giansanti, V., et al., *Study of the effects of a new pyrazolecarboxamide: changes in mitochondria and induction of apoptosis*. Int J Biochem Cell Biol, 2009. **41**(10): p. 1890-8.
195. Giansanti, V., et al., *Characterization of stress response in human retinal epithelial cells*. J Cell Mol Med, 2013. **17**(1): p. 103-15.
196. Ghibelli, L. and A. Grzanka, *Organelle cross-talk in apoptotic and survival pathways*. Int J Cell Biol, 2012. **2012**: p. 968586.
197. Lebedzinska, M., et al., *Interactions between the endoplasmic reticulum, mitochondria, plasma membrane and other subcellular organelles*. Int J Biochem Cell Biol, 2009. **41**(10): p. 1805-16.
198. Bravo-Sagua, R., et al., *Cell death and survival through the endoplasmic reticulum-mitochondrial axis*. Curr Mol Med, 2013. **13**(2): p. 317-29.
199. Ubah, O.C. and H.M. Wallace, *Cancer therapy: Targeting mitochondria and other sub-cellular organelles*. Curr Pharm Des, 2014. **20**(2): p. 201-22.
200. Brandizzi, F. and C. Barlowe, *Organization of the ER-Golgi interface for membrane traffic control*. Nat Rev Mol Cell Biol, 2013. **14**(6): p. 382-92.
201. Cheung, W.C. and B. Van Ness, *The bone marrow stromal microenvironment influences myeloma therapeutic response in vitro*. Leukemia, 2001. **15**(2): p. 264-71.
202. Podar, K., D. Chauhan, and K.C. Anderson, *Bone marrow microenvironment and the identification of new targets for myeloma therapy*. Leukemia, 2009. **23**(1): p. 10-24.
203. Hideshima, T., et al., *Understanding multiple myeloma pathogenesis in the bone marrow to identify new therapeutic targets*. Nat Rev Cancer, 2007. **7**(8): p. 585-98.
204. Basak, G.W., et al., *Multiple myeloma bone marrow niche*. Curr Pharm Biotechnol, 2009. **10**(3): p. 345-6.
205. Reagan, M.R. and C.J. Rosen, *Navigating the bone marrow niche: translational insights and cancer-driven dysfunction*. Nat Rev Rheumatol, 2016. **12**(3): p. 154-68.
206. Noll, J.E., et al., *Tug of war in the haematopoietic stem cell niche: do myeloma plasma cells compete for the HSC niche?* Blood Cancer J, 2012. **2**: p. e91.
207. Nakashima, T., M. Hayashi, and H. Takayanagi, *New insights into osteoclastogenic signaling mechanisms*. Trends Endocrinol Metab, 2012. **23**(11): p. 582-90.
208. Silbermann, R. and G.D. Roodman, *Myeloma bone disease: Pathophysiology and management*. J Bone Oncol, 2013. **2**(2): p. 59-69.
209. Biswas, S.K., *Metabolic Reprogramming of Immune Cells in Cancer Progression*. Immunity, 2015. **43**(3): p. 435-49.
210. Collier, H.A., *Is cancer a metabolic disease?* Am J Pathol, 2014. **184**(1): p. 4-17.
211. Seyfried, T.N., et al., *Cancer as a metabolic disease: implications for novel therapeutics*. Carcinogenesis, 2014. **35**(3): p. 515-27.
212. Warburg, O., *On the origin of cancer cells*. Science, 1956. **123**(3191): p. 309-14.
213. Racker, E., *Bioenergetics and the problem of tumor growth*. Am Sci, 1972. **60**(1): p. 56-63.

214. Fulda, S., L. Galluzzi, and G. Kroemer, *Targeting mitochondria for cancer therapy*. Nat Rev Drug Discov, 2010. **9**(6): p. 447-64.
215. Shapovalov, Y., et al., *Mitochondrial dysfunction in cancer cells due to aberrant mitochondrial replication*. J Biol Chem, 2011. **286**(25): p. 22331-8.
216. Mistry, P.K., et al., *Gaucher disease and malignancy: a model for cancer pathogenesis in an inborn error of metabolism*. Crit Rev Oncog, 2013. **18**(3): p. 235-46.
217. Nair, S., et al., *Type II NKT-TFH cells against Gaucher lipids regulate B-cell immunity and inflammation*. Blood, 2015. **125**(8): p. 1256-71.
218. Fairfield, H., et al., *Multiple myeloma in the marrow: pathogenesis and treatments*. Ann N Y Acad Sci, 2016. **1364**: p. 32-51.
219. Ludwig, C., et al., *Alterations in bone marrow metabolism are an early and consistent feature during the development of MGUS and multiple myeloma*. Blood Cancer J, 2015. **5**: p. e359.
220. Pavlova, N.N. and C.B. Thompson, *The Emerging Hallmarks of Cancer Metabolism*. Cell Metab, 2016. **23**(1): p. 27-47.
221. Caplain-Dandine, F., M.F. Kahn, and S. de Seze, *[Blood uric acid in myeloma]*. Rev Rhum Mal Osteoartic, 1977. **44**(1): p. 1-4.
222. Maiuolo, J., et al., *Regulation of uric acid metabolism and excretion*. Int J Cardiol, 2016. **213**: p. 8-14.
223. Yiu, A., et al., *Circulating uric acid levels and subsequent development of cancer in 493,281 individuals: findings from the AMORIS Study*. Oncotarget, 2017. **8**(26): p. 42332-42342.
224. Asosingh, K., et al., *Role of the hypoxic bone marrow microenvironment in 5T2MM murine myeloma tumor progression*. Haematologica, 2005. **90**(6): p. 810-7.
225. Morrison, S.J. and D.T. Scadden, *The bone marrow niche for haematopoietic stem cells*. Nature, 2014. **505**(7483): p. 327-34.
226. Mendez-Ferrer, S., et al., *Mesenchymal and haematopoietic stem cells form a unique bone marrow niche*. Nature, 2010. **466**(7308): p. 829-34.
227. Franqui-Machin, R., et al., *Cancer stem cells are the cause of drug resistance in multiple myeloma: fact or fiction?* Oncotarget, 2015. **6**(38): p. 40496-506.
228. McBrayer, S.K., et al., *Multiple myeloma exhibits novel dependence on GLUT4, GLUT8, and GLUT11: implications for glucose transporter-directed therapy*. Blood, 2012. **119**(20): p. 4686-97.
229. Bredella, M.A., et al., *Value of FDG PET in the assessment of patients with multiple myeloma*. AJR Am J Roentgenol, 2005. **184**(4): p. 1199-204.
230. Zamagni, E., et al., *Prognostic relevance of 18-F FDG PET/CT in newly diagnosed multiple myeloma patients treated with up-front autologous transplantation*. Blood, 2011. **118**(23): p. 5989-95.
231. Mundy, G.R., *Mechanisms of osteolytic bone destruction*. Bone, 1991. **12 Suppl 1**: p. S1-6.
232. Raaijmakers, M.H., et al., *Bone progenitor dysfunction induces myelodysplasia and secondary leukaemia*. Nature, 2010. **464**(7290): p. 852-7.
233. Bianco, P., P.G. Robey, and P.J. Simmons, *Mesenchymal stem cells: revisiting history, concepts, and assays*. Cell Stem Cell, 2008. **2**(4): p. 313-9.
234. Roccaro, A.M., et al., *SDF-1 inhibition targets the bone marrow niche for cancer therapy*. Cell Rep, 2014. **9**(1): p. 118-128.
235. Swami, A., et al., *Engineered nanomedicine for myeloma and bone microenvironment targeting*. Proc Natl Acad Sci U S A, 2014. **111**(28): p. 10287-92.
236. Bam, R., et al., *Primary myeloma interaction and growth in coculture with healthy donor hematopoietic bone marrow*. BMC Cancer, 2015. **15**: p. 864.

237. Kumar, S., et al., *Expression of VEGF and its receptors by myeloma cells*. *Leukemia*, 2003. **17**(10): p. 2025-31.
238. Goubran, H.A., et al., *Regulation of tumor growth and metastasis: the role of tumor microenvironment*. *Cancer Growth Metastasis*, 2014. **7**: p. 9-18.
239. Lentzsch, S., L.A. Ehrlich, and G.D. Roodman, *Pathophysiology of multiple myeloma bone disease*. *Hematol Oncol Clin North Am*, 2007. **21**(6): p. 1035-49, viii.
240. Ping, Y.F., X. Zhang, and X.W. Bian, *Cancer stem cells and their vascular niche: Do they benefit from each other?* *Cancer Lett*, 2016. **380**(2): p. 561-7.
241. Semenza, G.L., *Cancer-stromal cell interactions mediated by hypoxia-inducible factors promote angiogenesis, lymphangiogenesis, and metastasis*. *Oncogene*, 2013. **32**(35): p. 4057-63.
242. Martinez, L.M., et al., *Changes in the peripheral blood and bone marrow from untreated advanced breast cancer patients that are associated with the establishment of bone metastases*. *Clin Exp Metastasis*, 2014. **31**(2): p. 213-32.
243. Benito-Martin, A., et al., *The new deal: a potential role for secreted vesicles in innate immunity and tumor progression*. *Front Immunol*, 2015. **6**: p. 66.
244. Sceneay, J., M.J. Smyth, and A. Moller, *The pre-metastatic niche: finding common ground*. *Cancer Metastasis Rev*, 2013. **32**(3-4): p. 449-64.
245. Giuliani, N., et al., *Myeloma cells induce imbalance in the osteoprotegerin/osteoprotegerin ligand system in the human bone marrow environment*. *Blood*, 2001. **98**(13): p. 3527-33.
246. Andersen, T.L., et al., *Osteoclast nuclei of myeloma patients show chromosome translocations specific for the myeloma cell clone: a new type of cancer-host partnership?* *J Pathol*, 2007. **211**(1): p. 10-7.
247. Ehrlich, L.A., et al., *IL-3 is a potential inhibitor of osteoblast differentiation in multiple myeloma*. *Blood*, 2005. **106**(4): p. 1407-14.
248. Maier, H.J., et al., *Visualizing the autophagy pathway in avian cells and its application to studying infectious bronchitis virus*. *Autophagy*, 2013. **9**(4): p. 496-509.
249. Chapman, M.A., et al., *Initial genome sequencing and analysis of multiple myeloma*. *Nature*, 2011. **471**(7339): p. 467-72.
250. Bolli, N., et al., *Heterogeneity of genomic evolution and mutational profiles in multiple myeloma*. *Nat Commun*, 2014. **5**: p. 2997.
251. Egan, J.B., et al., *Whole-genome sequencing of multiple myeloma from diagnosis to plasma cell leukemia reveals genomic initiating events, evolution, and clonal tides*. *Blood*, 2012. **120**(5): p. 1060-6.
252. Lohr, J.G., et al., *Widespread genetic heterogeneity in multiple myeloma: implications for targeted therapy*. *Cancer Cell*, 2014. **25**(1): p. 91-101.
253. Murray, M.Y., M.J. Auger, and K.M. Bowles, *Overcoming bortezomib resistance in multiple myeloma*. *Biochem Soc Trans*, 2014. **42**(4): p. 804-8.
254. Hawley, T.S., et al., *Identification of an ABCB1 (P-glycoprotein)-positive carfilzomib-resistant myeloma subpopulation by the pluripotent stem cell fluorescent dye CDy1*. *American Journal of Hematology*, 2013. **88**(4): p. 265-272.
255. Ri, M., et al., *Bortezomib-resistant myeloma cell lines: a role for mutated PSMB5 in preventing the accumulation of unfolded proteins and fatal ER stress*. *Leukemia*, 2010. **24**(8): p. 1506-12.
256. Kumar, S.K., et al., *Continued improvement in survival in multiple myeloma: changes in early mortality and outcomes in older patients*. *Leukemia*, 2014. **28**(5): p. 1122-8.

257. Vincenz, L., et al., *Endoplasmic reticulum stress and the unfolded protein response: targeting the Achilles heel of multiple myeloma*. *Mol Cancer Ther*, 2013. **12**(6): p. 831-43.
258. Nikesitch, N., et al., *Endoplasmic reticulum stress in the development of multiple myeloma and drug resistance*. *Clin Transl Immunology*, 2018. **7**(1): p. e1007.
259. Ri, M., *Endoplasmic-reticulum stress pathway-associated mechanisms of action of proteasome inhibitors in multiple myeloma*. *Int J Hematol*, 2016. **104**(3): p. 273-80.
260. Zong, Z.H., et al., *Implication of Nrf2 and ATF4 in differential induction of CHOP by proteasome inhibition in thyroid cancer cells*. *Biochim Biophys Acta*, 2012. **1823**(8): p. 1395-404.
261. Cullinan, S.B. and J.A. Diehl, *PERK-dependent Activation of Nrf2 Contributes to Redox Homeostasis and Cell Survival following Endoplasmic Reticulum Stress*. *Journal of Biological Chemistry*, 2004. **279**(19): p. 20108-20117.
262. Rushworth, S.A., K.M. Bowles, and D.J. MacEwan, *High basal nuclear levels of Nrf2 in acute myeloid leukemia reduces sensitivity to proteasome inhibitors*. *Cancer Res*, 2011. **71**(5): p. 1999-2009.
263. Nerini-Molteni, S., et al., *Redox homeostasis modulates the sensitivity of myeloma cells to bortezomib*. *Br J Haematol*, 2008. **141**(4): p. 494-503.
264. Starheim, K.K., et al., *Intracellular glutathione determines bortezomib cytotoxicity in multiple myeloma cells*. *Blood Cancer J*, 2016. **6**(7): p. e446.
265. Rushworth, S.A., et al., *The high Nrf2 expression in human acute myeloid leukemia is driven by NF-kappaB and underlies its chemo-resistance*. *Blood*, 2012. **120**(26): p. 5188-98.
266. Lister, A., et al., *Nrf2 is overexpressed in pancreatic cancer: implications for cell proliferation and therapy*. *Mol Cancer*, 2011. **10**: p. 37.
267. Inami, Y., et al., *Persistent activation of Nrf2 through p62 in hepatocellular carcinoma cells*. *The Journal of Cell Biology*, 2011. **193**(2): p. 275-284.
268. Erickson, A.M., et al., *Identification of a variant antioxidant response element in the promoter of the human glutamate-cysteine ligase modifier subunit gene. Revision of the ARE consensus sequence*. *J Biol Chem*, 2002. **277**(34): p. 30730-7.
269. Loboda, A., et al., *Role of Nrf2/HO-1 system in development, oxidative stress response and diseases: an evolutionarily conserved mechanism*. *Cell Mol Life Sci*, 2016. **73**(17): p. 3221-47.
270. Lu, S.C., *Glutathione synthesis*. *Biochim Biophys Acta*, 2013. **1830**(5): p. 3143-53.
271. Liu, H.Y., et al., *Repurposing of the CDK inhibitor PHA-767491 as a NRF2 inhibitor drug candidate for cancer therapy via redox modulation*. *Invest New Drugs*, 2018. **36**(4): p. 590-600.
272. White-Gilbertson, S., Y. Hua, and B. Liu, *The role of endoplasmic reticulum stress in maintaining and targeting multiple myeloma: a double-edged sword of adaptation and apoptosis*. *Front Genet*, 2013. **4**: p. 109.
273. Eudy, B.J., C.A. Rowe, and S.S. Percival, *Glutathione pre-treatment prevents CHOP protein expression in 3T3-L1 adipocytes during palmitate induced ER stress*. *The FASEB Journal*, 2016. **30**(1 Supplement): p. lb309.
274. Abdi, J., G. Chen, and H. Chang, *Drug resistance in multiple myeloma: latest findings and new concepts on molecular mechanisms*. *Oncotarget*, 2013. **4**(12): p. 2186-207.
275. Gorrini, C., I.S. Harris, and T.W. Mak, *Modulation of oxidative stress as an anticancer strategy*. *Nat Rev Drug Discov*, 2013. **12**(12): p. 931-947.
276. Bianchi, G. and K.C. Anderson, *Understanding biology to tackle the disease: Multiple myeloma from bench to bedside, and back*. *CA Cancer J Clin*, 2014. **64**(6): p. 422-44.

277. Caligaris-Cappio, F., et al., *Role of bone marrow stromal cells in the growth of human multiple myeloma*. *Blood*, 1991. **77**(12): p. 2688-93.
278. Chauhan, D., et al., *Multiple myeloma cell adhesion-induced interleukin-6 expression in bone marrow stromal cells involves activation of NF-kappa B*. *Blood*, 1996. **87**(3): p. 1104-12.
279. Corso, A., et al., *Zoledronic acid down-regulates adhesion molecules of bone marrow stromal cells in multiple myeloma: a possible mechanism for its antitumor effect*. *Cancer*, 2005. **104**(1): p. 118-25.
280. Azab, A.K., et al., *RhoA and Rac1 GTPases play major and differential roles in stromal cell-derived factor-1-induced cell adhesion and chemotaxis in multiple myeloma*. *Blood*, 2009. **114**(3): p. 619-29.
281. Wang, L.H., et al., *Inhibition of adhesive interaction between multiple myeloma and bone marrow stromal cells by PPARgamma cross talk with NF-kappaB and C/EBP*. *Blood*, 2007. **110**(13): p. 4373-84.
282. Xu, G., et al., *Expression of XBP1s in bone marrow stromal cells is critical for myeloma cell growth and osteoclast formation*. *Blood*, 2012. **119**(18): p. 4205-14.
283. Fowler, J.A., et al., *Bone marrow stromal cells create a permissive microenvironment for myeloma development: a new stromal role for Wnt inhibitor Dkk1*. *Cancer Res*, 2012. **72**(9): p. 2183-9.
284. Wang, J., et al., *The bone marrow microenvironment enhances multiple myeloma progression by exosome-mediated activation of myeloid-derived suppressor cells*. *Oncotarget*, 2015. **6**(41): p. 43992-4004.
285. Michigami, T., et al., *Cell-cell contact between marrow stromal cells and myeloma cells via VCAM-1 and alpha(4)beta(1)-integrin enhances production of osteoclast-stimulating activity*. *Blood*, 2000. **96**(5): p. 1953-60.
286. Shain, K.H., et al., *Beta1 integrin adhesion enhances IL-6-mediated STAT3 signaling in myeloma cells: implications for microenvironment influence on tumor survival and proliferation*. *Cancer Res*, 2009. **69**(3): p. 1009-15.
287. Meads, M.B., et al., *Targeting PYK2 mediates microenvironment-specific cell death in multiple myeloma*. *Oncogene*, 2016. **35**(21): p. 2723-34.
288. Prabhala, R.H., et al., *Targeting IL-17A in multiple myeloma: a potential novel therapeutic approach in myeloma*. *Leukemia*, 2016. **30**(2): p. 379-89.
289. Teramachi, J., et al., *Blocking the ZZ domain of sequestosome1/p62 suppresses myeloma growth and osteoclast formation in vitro and induces dramatic bone formation in myeloma-bearing bones in vivo*. *Leukemia*, 2016. **30**(2): p. 390-8.
290. Marlein, C.R., et al., *NADPH oxidase-2 derived superoxide drives mitochondrial transfer from bone marrow stromal cells to leukemic blasts*. *Blood*, 2017. **130**(14): p. 1649-1660.
291. Kim, J.H., et al., *Nrf2 is required for normal postnatal bone acquisition in mice*. *Bone Res*, 2014. **2**: p. 14033.
292. Yang, W., et al., *Treatment with bone marrow mesenchymal stem cells combined with plumbagin alleviates spinal cord injury by affecting oxidative stress, inflammation, apoptotic and the activation of the Nrf2 pathway*. *Int J Mol Med*, 2016. **37**(4): p. 1075-82.
293. Mohammadzadeh, M., et al., *Nrf-2 overexpression in mesenchymal stem cells reduces oxidative stress-induced apoptosis and cytotoxicity*. *Cell Stress Chaperones*, 2012. **17**(5): p. 553-65.
294. Dan Dunn, J., et al., *Reactive oxygen species and mitochondria: A nexus of cellular homeostasis*. *Redox Biol*, 2015. **6**: p. 472-85.

295. Kucia, M., et al., *Trafficking of normal stem cells and metastasis of cancer stem cells involve similar mechanisms: pivotal role of the SDF-1-CXCR4 axis*. *Stem Cells*, 2005. **23**(7): p. 879-94.
296. Bouyssou, J.M., I.M. Ghobrial, and A.M. Roccaro, *Targeting SDF-1 in multiple myeloma tumor microenvironment*. *Cancer Lett*, 2016. **380**(1): p. 315-8.
297. Mirandola, L., et al., *Anti-Notch treatment prevents multiple myeloma cells localization to the bone marrow via the chemokine system CXCR4/SDF-1*. *Leukemia*, 2013. **27**(7): p. 1558-66.
298. Waldschmidt, J.M., et al., *CXCL12 and CXCR7 are relevant targets to reverse cell adhesion-mediated drug resistance in multiple myeloma*. *Br J Haematol*, 2017. **179**(1): p. 36-49.
299. Michallet, A.S., et al., *Compromising the unfolded protein response induces autophagy-mediated cell death in multiple myeloma cells*. *PLoS One*, 2011. **6**(10): p. e25820.
300. Phinney, D.G., et al., *Mesenchymal stem cells use extracellular vesicles to outsource mitophagy and shuttle microRNAs*. *Nat Commun*, 2015. **6**: p. 8472.
301. Jiang, T., et al., *p62 links autophagy and Nrf2 signaling*. *Free Radic Biol Med*, 2015. **88**(Pt B): p. 199-204.
302. Harder, B., et al., *Molecular mechanisms of Nrf2 regulation and how these influence chemical modulation for disease intervention*. *Biochem Soc Trans*, 2015. **43**(4): p. 680-6.
303. Menegon, S., A. Columbano, and S. Giordano, *The Dual Roles of NRF2 in Cancer*. *Trends Mol Med*, 2016. **22**(7): p. 578-593.
304. Li, B., et al., *The Nuclear Factor (Erythroid-derived 2)-like 2 and Proteasome Maturation Protein Axis Mediate Bortezomib Resistance in Multiple Myeloma*. *J Biol Chem*, 2015. **290**(50): p. 29854-68.
305. Barrera, L.N., et al., *Bortezomib induces heme oxygenase-1 expression in multiple myeloma*. *Cell Cycle*, 2012. **11**(12): p. 2248-52.
306. Riz, I., et al., *Noncanonical SQSTM1/p62-Nrf2 pathway activation mediates proteasome inhibitor resistance in multiple myeloma cells via redox, metabolic and translational reprogramming*. *Oncotarget*, 2016. **7**(41): p. 66360-66385.
307. Jain, A., et al., *p62/SQSTM1 is a target gene for transcription factor NRF2 and creates a positive feedback loop by inducing antioxidant response element-driven gene transcription*. *J Biol Chem*, 2010. **285**(29): p. 22576-91.
308. Fan, W., et al., *Keap1 facilitates p62-mediated ubiquitin aggregate clearance via autophagy*. *Autophagy*, 2010. **6**(5): p. 614-21.
309. Dixon, B.M., et al., *Assessment of endoplasmic reticulum glutathione redox status is confounded by extensive ex vivo oxidation*. *Antioxid Redox Signal*, 2008. **10**(5): p. 963-72.
310. Armstrong, J.S., et al., *Role of glutathione depletion and reactive oxygen species generation in apoptotic signaling in a human B lymphoma cell line*. *Cell Death Differ*, 2002. **9**(3): p. 252-63.
311. Rushworth, S.A. and D.J. Macewan, *The role of nrf2 and cytoprotection in regulating chemotherapy resistance of human leukemia cells*. *Cancers (Basel)*, 2011. **3**(2): p. 1605-21.
312. Wallington-Beddoe, C.T. and S.M. Pitson, *Enhancing ER stress in myeloma*. *Aging (Albany NY)*, 2017. **9**(7): p. 1645-1646.
313. Sano, R. and J.C. Reed, *ER stress-induced cell death mechanisms*. *Biochim Biophys Acta*, 2013. **1833**(12): p. 3460-3470.
314. Sovolyova, N., et al., *Stressed to death - mechanisms of ER stress-induced cell death*. *Biol Chem*, 2014. **395**(1): p. 1-13.

315. Zong, Z.H., et al., *Involvement of Nrf2 in proteasome inhibition-mediated induction of ORP150 in thyroid cancer cells*. *Oncotarget*, 2016. **7**(3): p. 3416-26.
316. Cullinan, S.B., et al., *Nrf2 is a direct PERK substrate and effector of PERK-dependent cell survival*. *Mol Cell Biol*, 2003. **23**(20): p. 7198-209.
317. Kroemer, G., G. Marino, and B. Levine, *Autophagy and the integrated stress response*. *Mol Cell*, 2010. **40**(2): p. 280-93.
318. Trajkovska, M., *A multiple myeloma survival factor*. *Nature Cell Biology*, 2013. **15**: p. 449.
319. Vogl, D.T., et al., *Combined autophagy and proteasome inhibition: a phase 1 trial of hydroxychloroquine and bortezomib in patients with relapsed/refractory myeloma*. *Autophagy*, 2014. **10**(8): p. 1380-90.

**Copies of publication arising from this thesis**

Attached is the following publication:

**Sun Y**, Abdul Aziz A, Bowles K, Rushworth S, High NRF2 expression controls endoplasmic reticulum stress induced apoptosis in multiple myeloma, **Cancer letter**, 2018 Jan, 1;412:37-45.



## Original Article

# High NRF2 expression controls endoplasmic reticulum stress induced apoptosis in multiple myeloma



Yu Sun <sup>a</sup>, Amina Abdul Aziz <sup>a</sup>, Kristian Bowles <sup>a, b</sup>, Stuart Rushworth <sup>a, \*</sup>

<sup>a</sup> Norwich Medical School, The University of East Anglia, Norwich Research Park, NR4 7TJ, United Kingdom

<sup>b</sup> Department of Haematology, Norfolk and Norwich University Hospitals NHS Trust, Colney Lane, Norwich, NR4 7UY, United Kingdom

## ARTICLE INFO

## Article history:

Received 8 August 2017

Received in revised form

29 September 2017

Accepted 6 October 2017

## Keywords:

NRF2 or nuclear factor erythroid 2 [NF-E2]-

related factor 2

Multiple myeloma

Oxidative stress

Endoplasmic reticulum

## ABSTRACT

Multiple myeloma (MM) is an incurable disease characterized by clonal plasma cell proliferation. The stress response transcription factor Nuclear factor erythroid 2 [NF-E2]-related factor 2 (NRF2) is known to be activated in MM in response to proteasome inhibitors (PI). Here, we hypothesize that the transcription factor NRF2 whose physiological role is to protect cells from reactive oxygen species via the regulation of drug metabolism and antioxidant gene plays an important role in MM cells survival and proliferation. We report for the first time that NRF2 is constitutively activated in circa 50% of MM primary samples and all MM cell lines. Moreover, genetic inhibition of constitutively expressed NRF2 reduced MM cell viability. We confirm that PI induced further expression of NRF2 in MM cell lines and primary MM. Furthermore, genetic inhibition of NRF2 of PI treated MM cells increased ER-stress through the regulation of CCAAT-enhancer-binding protein homologous protein (CHOP). Finally, inhibition of NRF2 in combination with PI treatment significantly increased apoptosis in MM cells. Here we identify NRF2 as a key regulator of MM survival in treatment naive and PI treated cells.

© 2017 Elsevier B.V. All rights reserved.

## Introduction

Multiple myeloma (MM) is an incurable disease characterized by clonal plasma cell proliferation [1–3]. Genetic studies demonstrate that MM is a highly complex and heterogeneous disease that undergoes clonal evolution towards a multi-drug resistant disease over time [4–7]. Thus, treatment relapse from the development of drug resistance clones is inevitable and presently MM remains incurable [8]. Therefore, better patient outcomes are expected to come from an improved understanding of the mechanisms of drug resistance which results in the development of novel treatment strategies that ‘re-sensitise’ MM cells to chemotherapy.

MM cells are dependent on the unfolded protein response to alleviate the endoplasmic reticulum (ER) stress caused by the excessive amounts of paraprotein being produced [9]. The proteasome inhibitors bortezomib and carfilzomib increase the accumulation of proteins, which elevate ER-stress and increase intracellular oxidative stress. This, in part accounts for proteasome inhibitor induced apoptosis in MM cells [10]. The transcription factor

(nuclear factor erythroid 2 [NF-E2]-related factor 2 (NRF2)) is a key mediator of oxidative stress through the direct regulation of over 200 genes, as well as through mechanisms of post transcriptional modification [11–13]. These genes are involved in various cellular processes including the regulation of glutathione (GSH) synthesis, detoxification and the regulation of inflammatory processes [14–17]. The transcription factor NRF2 has been shown to contribute to the malignant phenotypes of several cancers through effects on proliferation and drug sensitivity [18]. Moreover, in MM we identified the pro-tumoural function of heme oxygenase-1 (HO-1), an NRF2 regulated gene, through chemotherapy resistance [19].

NRF2 is regulated by Kelch-like ECH-associated protein 1 (KEAP1), which facilitates the ubiquitination and subsequent degradation of NRF2 by the proteasome [18]. Therefore, because proteasome inhibitors prevent the degradation of NRF2 by KEAP1, an increased transcriptional activity is induced in most cell types including malignant plasma cells [15,20]. Recently, NRF2 has also been shown to be involved in regulating ER-stress through the negative regulation of CCAAT-enhancer-binding protein homologous protein (CHOP) [21]. CHOP is induced by the transcription factor, Activating Transcription Factor 4 (ATF4), as part of the ER-stress response which then mediates apoptosis. Studies have shown that high NRF2 levels inhibit the expression of CHOP and

\* Corresponding author. Department of Molecular Haematology, Norwich Medical School, University of East Anglia, Norwich, NR4 7TJ, United Kingdom.

E-mail address: [s.rushworth@uea.ac.uk](mailto:s.rushworth@uea.ac.uk) (S. Rushworth).

therefore prevent ER-stress induced apoptosis [22]. Others have shown that modulating redox homeostasis in MM could increase sensitivity of MM to bortezomib [20]. Finally, a recent study has shown that elevated glutathione levels can block bortezomib induced stress responses [23]. Therefore, since NRF2 activation positively regulates glutathione levels and negatively regulates CHOP we wanted to determine in MM if NRF2 is highly expressed and if silencing the expression of NRF2 reduced cell viability. In addition, we aimed to determine the relationship between NRF2 activation, increased glutathione levels and CHOP deregulation in response to proteasome inhibitors.

## Materials and methods

### Materials

Anti- $\beta$ -actin (R&D Systems, Abingdon, UK #MAB1536), anti-NRF2 (Abcam, Cambridge, UK #62352), anti-GAPDH (Cell Signaling Technology, Cambridge, MA, USA #D16H11), anti-Sam68 (Santa Cruz Biotechnology, Santa Cruz, USA), anti-CHOP (Cell Signaling Technology #1649). All other reagents were obtained from Sigma-Aldrich (St Louis, MO, USA), unless indicated.

### Cell lines and primary cell isolation

DNA-fingerprinting authenticated MM derived cell lines were obtained from the European Collection of Cell Cultures. MM cell lines were maintained in medium RPMI 1640 supplemented with 10% (v/v) foetal bovine serum, 1% penicillin-streptomycin. Primary MM cells were obtained from MM patients' heparinized BM aspirates with informed consent in accordance with the Declaration of Helsinki and under approval from the United Kingdom National Research Ethics Service (07/H0310/146).

Histopaque 1077 density-gradient centrifugation method was used to isolate primary cells from MM patients' heparinized BM aspirates. The cells were then cultured in DMEM supplemented with 20% (v/v) foetal bovine serum and 1% penicillin-streptomycin. Primary MM cells were purified from other haematopoietic cells using magnetic-activated positive selection cell sorting with CD138+ MicroBeads (Miltenyi Biotec, Auburn, CA). All cells were incubated at 37 °C with 5% CO<sub>2</sub> and 95% relative humidity.

### Viability and apoptosis assay

Cell viability was determined by measuring levels of intracellular ATP using Cell Titer-GLO (Promega, Southampton, UK) according to manufacturers instructions. Plates were measured on FLUOstar optima Microplate Reader (BMG LABTECH, Germany). CyFlow Cube 6 flow cytometer (Sysmex, Milton Keynes, UK) was used to detect cell apoptosis. Cells were counter stained with Annexin-V and Propidium iodide (PI), then analysed by flow cytometry.

### Quantitative RT-PCR

ReliaPrep RNA cell miniprep Kit (Promega) was used to extract total RNA, according to the manufacturer's instructions. Reverse transcription (RT) was performed using the qPCR BIO cDNA synthesis kit (PCR Biosystems, London, UK). Relative quantitative real-time PCR using qPCR BIO SyGreen Mix (PCR Biosystems) was performed on cDNA generated from the reverse transcription of purified RNA. After pre-amplification (95 °C for 2 min), the PCRs were amplified for 45 cycles (95 °C for 15 s and 60 °C for 10 s and 72 °C for 10 s) on a 384-well LightCycler 480 (Roche, Burgess Hill, UK). Each mRNA expression was normalised against glyceraldehyde 3-phosphate dehydrogenase (GAPDH). Sequences of real-time PCR primers (Sigma) used in this study are listed in Table 1.

**Table 1**  
Oligonucleotide sequences for real-time PCR Sequences (5' to 3').

GAPDH	F GCACCACCAACTGCTTAGC R GGCATGGACTGTGGTCATA
NRF2	F CGTTTGTAGATGACAATGAG R AGAAGTTTCAGGTGACTGAG
HO-1	F ATGACACCAAGGACCAGAGC R GGGCAGAATCTTGCACTTGG
GCLM	F TGCAGTTGACATGGCCTGTT R TCACAGAATCCAGCTGTGCAA
ATF4	F CCTAGGTCTCTTAGATGATTACC R CAAGTCGAACTCCTCAAATC
CHOP	F CTTCCAGACTGATCCAAC R GATTCTTCTCTTCATTCCAG

### Protein extraction/SDS-PAGE analysis

Radioimmunoprecipitation assay buffer (50 mM Tris, pH 8.0, 150 mM NaCl, 1% NP-40, 0.1% SDS, 0.5% sodium deoxycholate, phosphatase inhibitor cocktail tablet and protease inhibitor cocktail tablet from Roche) was used to extract whole cell lysates. NE-PER nuclear and cytoplasmic extraction reagents (Thermo scientific) were used to extract nuclear lysates. Sodium dodecyl sulfate-polyacrylamide gel electrophoresis (SDS-PAGE) was used to separate proteins, then proteins were transferred to polyvinylidene difluoride membrane and Western blot analysis performed with the indicated antisera according to the manufacturer's guidelines. All images are representative of a minimum of three independent experiments. Detection was performed by electrochemical luminescence (ECL Chemdoc-It2 Imager (UVP).

### Lentiviral knockdown

Plasmid containing MISSION<sup>®</sup> shRNA NRF2 (NRF2-KD) were purchased from Sigma-Aldrich and transduced into 293 T cells. MISSION pLKO.1-puro Control Vector, was used as the lentivirus control (Con-KD). Control and target lentivirus stocks were produced as previously described [24].

### Promoter assay

The HO-1 promoter construct (pHO-1Luc4.0 and pHO-1mut ARE) was a kind gift from X. Chen, Baylor institute of Medicine, Houston. For the reporter assays a total of 0.5  $\mu$ g of reporter plasmids and pRL-CMV control constructs were co-transfected into U226. Transfected cells were incubated for 48 h before the indicated treatments. For reporter assay, cells were treated with Dual-Luciferase Reporter Assay System (Promega).

### ER-stress detection

ER-Tracker<sup>™</sup> Red (BODIPY<sup>®</sup> TR Glibenclamide, Thermo Scientific) was purchased from Invitrogen. The live cellular ER-stress levels were determined according to the manufacturer's guidelines by flow cytometry.

### GSH assay

GSH-Glo<sup>™</sup> Assay was purchased from Promega. The cellular GSH levels were determined according to the manufacturer's guidelines by flow cytometry.

### Statistical analysis

The Student's T test was used to compare results in control to treated groups. Results with  $p < 0.05$  were considered statistically significant (\*). We also use the Two-way ANOVA with Sidak's post-test. Results with  $p < 0.05$  were considered statistically significant (\*). Results represent the mean  $\pm$  SD of 4 independent experiments. For Western blotting, data are representative images of 3 independent experiments. We generated statistics with Graphpad Prism 5 software (Graphpad, San Diego, CA, USA).

## Results

### Increased NRF2 activity in MM is pro-tumoral

NRF2 has been shown to be constitutively activated in various cancers [25–27]. Therefore, we first evaluated the basal expression of NRF2 in MM cell lines and primary cells. NRF2 is highly expressed in all MM cell lines and 4/8 primary MM tested (Fig. 1A). The functional consequence of high NRF2 was examined using NRF2 targeted shRNA in MM1s (low NRF2 expression) and U226 (high NRF2). Fig. 1B shows that MM1s and U226 infected with lentivirus targeted to NRF2 have reduced NRF2 RNA expression. Fig. 1C shows that targeted NRF2-KD inhibits HO-1 and GCLM mRNA expression. Furthermore targeted NRF2-KD significantly reduces the viability of U226 and MM1s (Fig. 1D). Finally, the NRF2 inhibitor brusostat inhibits cell viability of both MM#9 and MM1s (Fig. 1E). These results suggest that NRF2 is critical to the survival of a subset of MM.

### Proteasome inhibition induces NRF2 activity in MM

Bortezomib and carfilzomib are proteasome inhibitors widely used in the treatment of MM. We therefore evaluated the nuclear NRF2 expression in proteasome inhibitor treated MM cell lines. Bortezomib and carfilzomib induced NRF2 protein in nuclear extracts (Fig. 2A) in all MM cell lines. Fig. 2B shows that NRF2

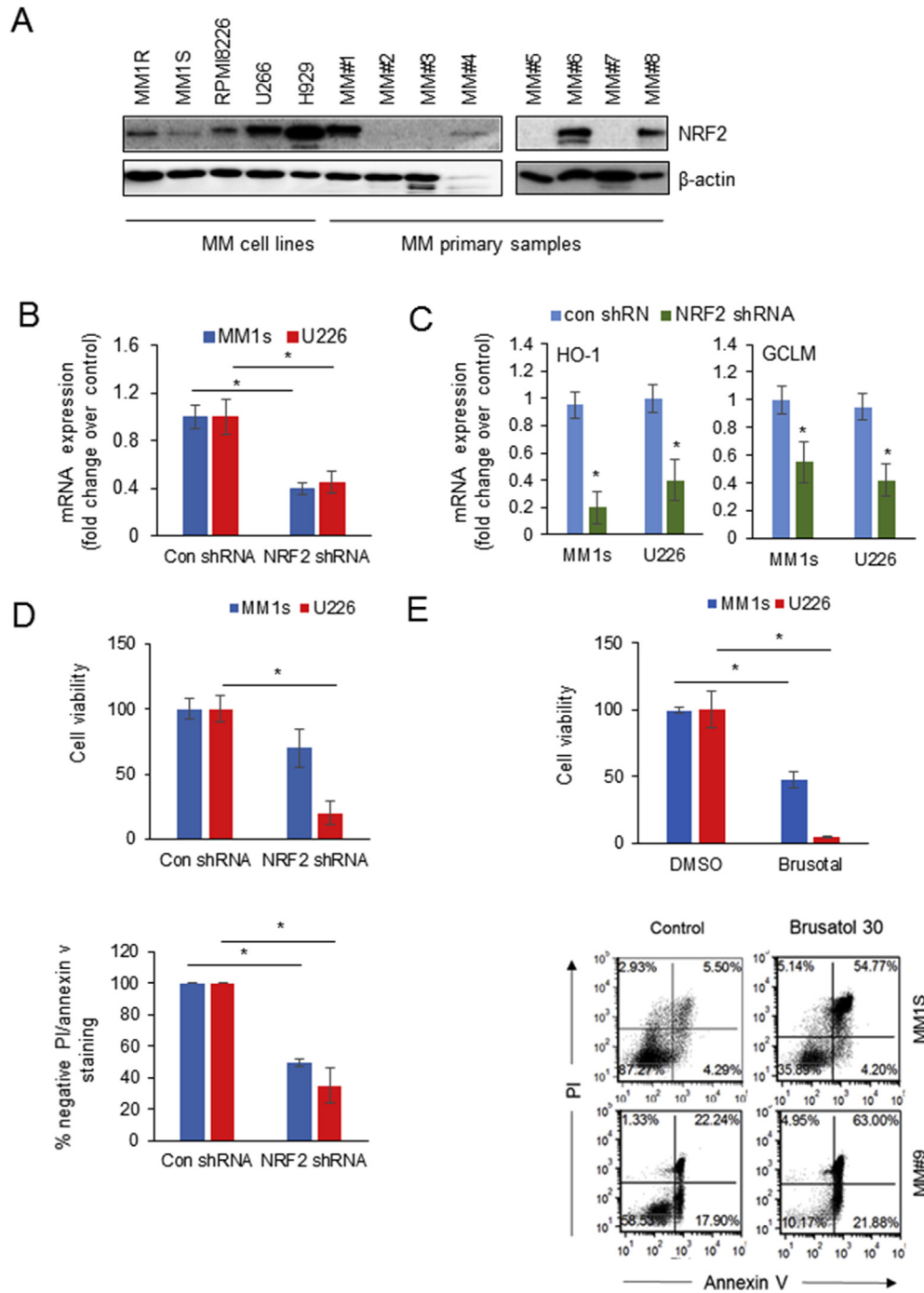


**Fig. 1. NRF2 expression in MM cell lines and primary MM cells.** (A) Whole cell protein was extracted from MM cell lines and primary MM cells and Western blotting was performed for NRF2 protein expression. Blots were re-probed for β-actin to show loading across samples. (B-C) Lentiviral mediated shRNA knockdown (KD) of NRF2 in MM1S and U266 cells. (B) RNA was extracted and analysed using qRT-PCR for NRF2 expression. Gene expression was normalised to GAPDH. (C) HO-1 and GCLM expression was analysed and normalised to GAPDH. (D) Cell viability was analysed using flow cytometer with PI/Annexin V staining and Cell-TiterGlo. (E). MM1s cells and MM#9 cells were treated with 30 nM brusatol for 24 h and then analysed for cell viability using flow cytometer with PI/Annexin V staining and Cell-TiterGlo.

accumulates and is present in the nucleus of primary MM cells treated with bortezomib and carfilzomib. Moreover, bortezomib and carfilzomib induced NRF2 regulated genes in U226 and MM1s cells and primary MM (Fig. 2C and D).

Next we wanted to determine if NRF2 was active when MM cells are treated with bortezomib and carfilzomib. To do this we used the HO-1 promoter assay in which a wild type HO-1 promoter or a mutant HO-1 promoter (NRF2 antioxidant response element

mutated; Fig. 3A) were transfected into the MM cell line MM1s. Cells were then treated with bortezomib and carfilzomib and promoter activity was examined. Fig. 3B shows that mutant HO-1 promoter had a significant reduction in activity compared to wildtype. Finally, we used NRF2-KD in MM1s and U266 cells and treated with bortezomib or carfilzomib. Fig. 3C shows that bortezomib and carfilzomib induced NRF2 up-regulated is inhibited by NRF2-KD. Fig. 3D shows that bortezomib induced NRF2 regulated

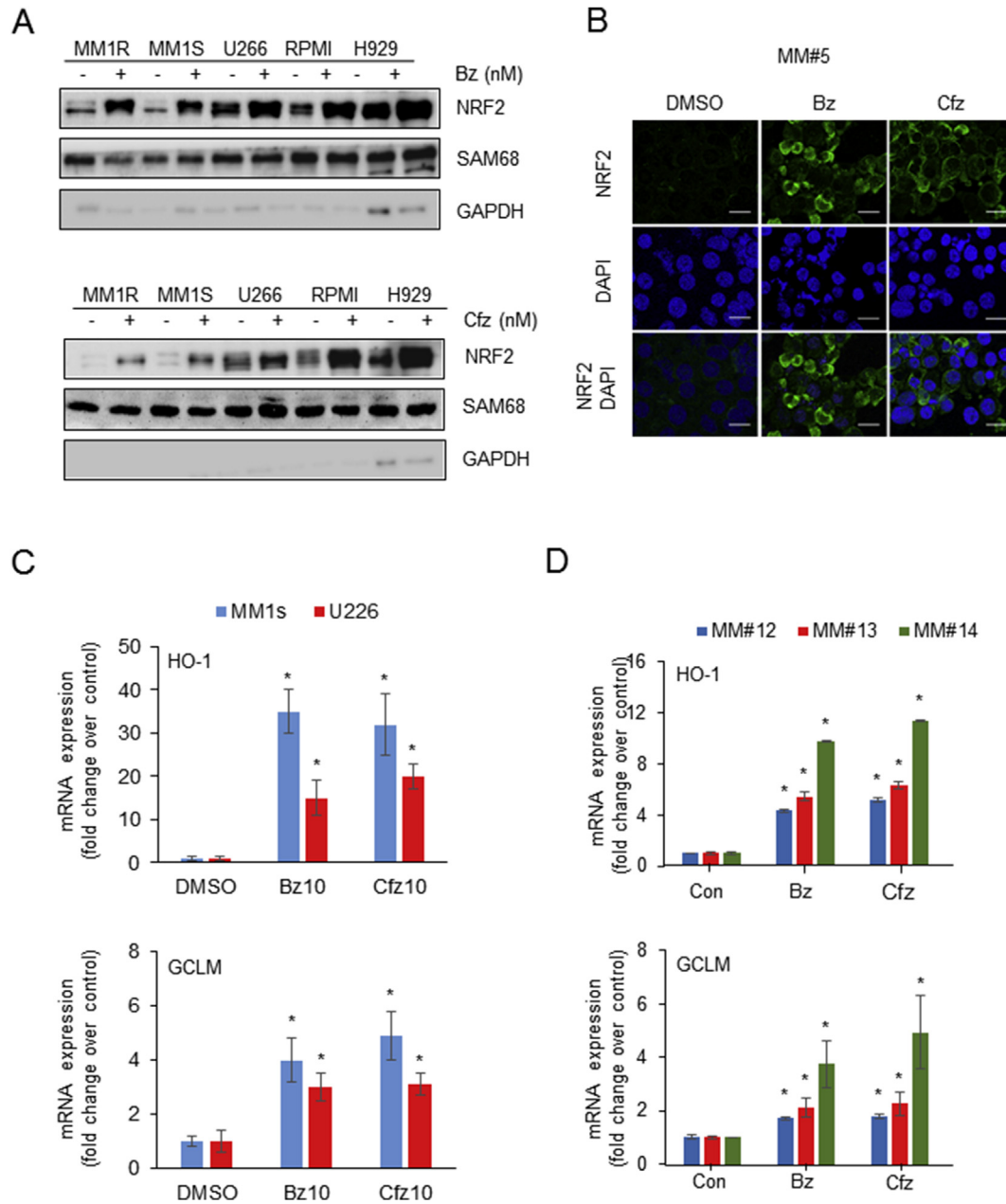


**Fig. 2. NRF2 is activated by proteasome inhibitors.** (A) MM cell lines were treated with bortezomib (Bz, 10 nM) and carfilzomib (Cfz, 10 nM) for 4 h. Nuclear protein was extracted and Western blotting was performed for NRF2 protein expression. Blots were reprobed for SAM68 and GAPDH to show loading across samples. (B) Primary MM was treated with Bz, 10 nM and Cfz, 10 nM for 4 h. Cells were fixed and stained with NRF2 and DAPI and then analysed using fluorescence microscopy. Scale bar = 10  $\mu$ m. (C and D), MM cell lines and primary MM cells were treated with Bz and Cfz for 4 h at 10 nM. RNA was extracted and analysed using qRT-PCR for HO-1 and GCLM expression. Gene expression was normalised to GAPDH.

genes were also inhibited by NRF2-KD in U266 cells. Together these data confirm that NRF2 induced transcription is activated by bortezomib and carfilzomib in MM.

#### *NRF2 inhibition induces ER-stress associated apoptosis through up-regulation of CHOP*

MM cells have high levels of ER-stress as a consequence of the large amount of immunoglobulin they produce [9,28,29]. Moreover, the addition of a proteasome inhibitor increases this stress response thus inducing apoptosis [30]. We therefore wanted to explore if NRF2 regulates ER-stress associated apoptosis in response to proteasome inhibition. Initially we identified that in

U266 and MM1s cells NRF2-KD induced CHOP expression, but not ATF4 expression (Fig. 4A). Next we wanted to determine if ER-stress was increased in response to NRF2-KD. Fig. 4B shows that using the ER tracker assay, NRF2-KD cells have a higher ER-stress compared to control-KD cells. Moreover, the addition of bortezomib or carfilzomib to the NRF2-KD cells further increased ER-stress (Fig. 4C).

Next we examined if CHOP and ATF4 were increased in response to bortezomib or carfilzomib. Fig. 4D shows that CHOP is increased in MM1s cells in response to proteasome inhibition. To determine if the ER-stress was an effect of increased CHOP expression we analysed CHOP mRNA expression in NRF2-KD cells when treated with bortezomib or carfilzomib. Fig. 5A shows that NRF2-KD cells have a significant increase in CHOP expression when treated with

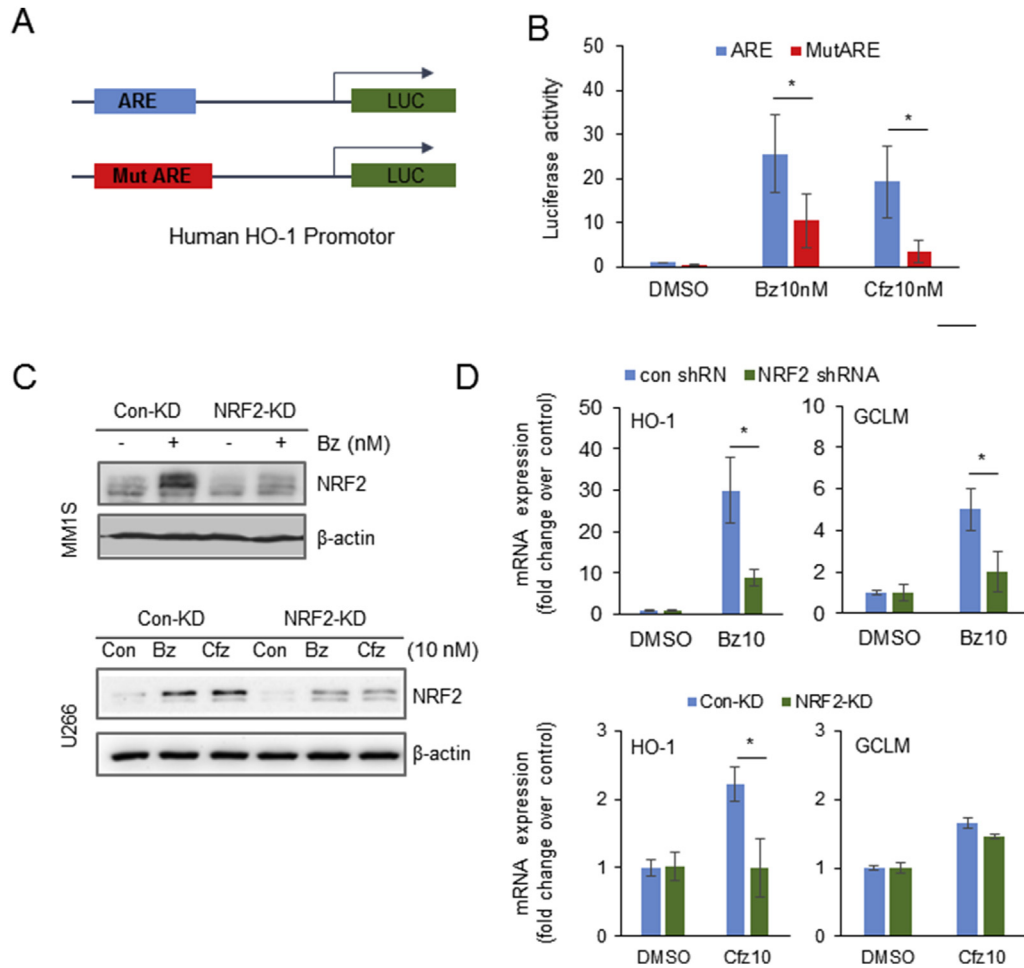


**Fig. 3. Bortezomib and carfilzomib induce NRF2 activity.** (A) Schematic of the human HO-1 promoter construct (pHO-1Luc4.0) or human HO-1 promoter with ARE mutation construct (pHO-1mutARE). (B) U266 cells were transfected with pHO-1Luc4.0 or pHO-1mutARE for 48 h and then treated with Bz (10 nM) or Cfz (10 nM) for 24 h. HO-1 promoter activation was measured by luciferase activity. (C and D) Lentiviral mediated shRNA knockdown (KD) of NRF2 in MM1S cells. (C) Cells were then treated with Bz (10 nM) or Cfz (10 nM) for 4 h and whole cell protein was extracted and Western blotting was performed for NRF2 protein expression. Blots were reprobbed for  $\beta$ -actin to show equal loading across samples (D) RNA was extracted and analysed for HO1 and GCLM. Gene expression was normalised to GAPDH.

bortezomib or carfilzomib as compared control-KD cells. Finally we confirmed the increase in CHOP using Western blotting in NRF2-KD cells treated with bortezomib and carfilzomib (Fig. 5B and C).

#### *NRF2 regulates ER-stress associated apoptosis in MM cells through its regulation of GSH synthesis*

CHOP mRNA expression has been shown to be controlled by direct NRF2 binding of the CHOP promoter or via an indirect NRF2 response [21]. The indirect response is mediated through glutathione (GSH) whose synthesis is tightly controlled by NRF2 [31]. To determine if GSH plays a role in regulating CHOP in MM we first analysed the GSH levels in MM cell lines treated with bortezomib. Fig. 6A shows that bortezomib increases GSH levels in MM cells. Next we wanted to determine if this was regulated by NRF2. Fig. 6B shows that GSH levels were not significantly increased in NRF2-KD MM cells compared to Con-KD cells. Next we wanted to examine if the precursor to GSH, N Acetyl Cysteine (NAC) could inhibit bortezomib induced CHOP mRNA expression and ER-stress. Fig. 6C and D shows that NAC inhibits bortezomib induced CHOP and ER-stress responses. Next we wanted to detect if the glutathione (GSH) synthesis inhibitor, buthionine sulfoximine (BSO) increased bortezomib induced CHOP mRNA expression and ER-stress responses. Fig. 6E and F shows that BSO increases bortezomib induced CHOP

and ER-stress responses. Finally, we show that bortezomib induced cell death in both MM1s and U226 is enhanced when NRF2 expression is inhibited (Fig. 6E and F). Taken together, these results confirm that NRF2 regulates bortezomib induced CHOP mediated apoptosis in MM at least in part through the generation of GSH (see Fig. 7).

#### **Discussion**

Here we report that NRF2 supports survival and chemotherapy resistance in MM. We find that NRF2 is constitutively expressed in approximately 50% of primary MM samples tested and all MM cell lines. Subsequently, genetic or drug induced inhibition of NRF2 reduces survival of MM. We find that inhibiting NRF2 induces upregulation of the ER-stress response protein CHOP. Moreover, treatment with PI further increased expression and activity of NRF2, which inhibits CHOP and increases glutathione. Silencing NRF2 prevents PI induced glutathione, which regulates CHOP expression. Consequently, genetic inhibition of NRF2 increases MM sensitivity to PI.

Proteasome inhibitors are highly effective in MM, however patients will inevitably relapse following treatment through the emergence of drug resistant clones [4–7,32]. Here we report that proteasome inhibitor induced NRF2 activation supports the

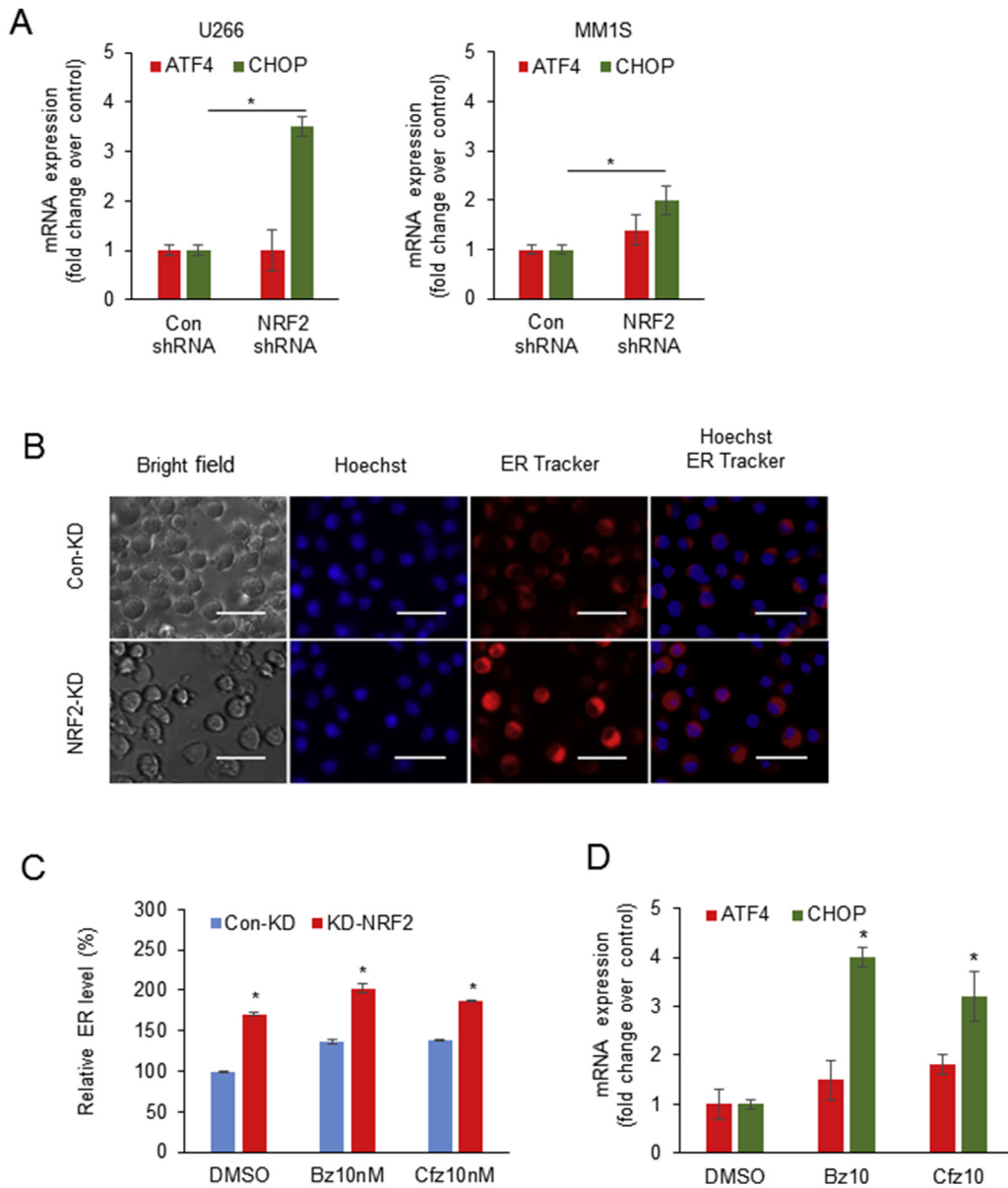


**Fig. 4. ER-stress is regulated by NRF2 in MM.** (A) Lentiviral mediated shRNA knockdown (KD) of NRF2 in MM1s and U266 cells. RNA was extracted and analysed for ATF4 and CHOP. Gene expression was normalised to GAPDH. (B) Control-KD and NRF2-KD MM1S cells were incubated with the Hoechst 33342 and the ER Tracker and visualized by fluorescence microscopy. Scale bar = 20  $\mu$ m. (C) Control-KD and NRF2-KD MM1S cells were incubated with the ER Tracker and analysed by flow cytometry. Results expressed as median fluorescence intensity. (D) MM1S cells were treated with bortezomib and carfilzomib for 4 h and RNA was extracted and analysed for ATF4 and CHOP. Gene expression was normalised to GAPDH.

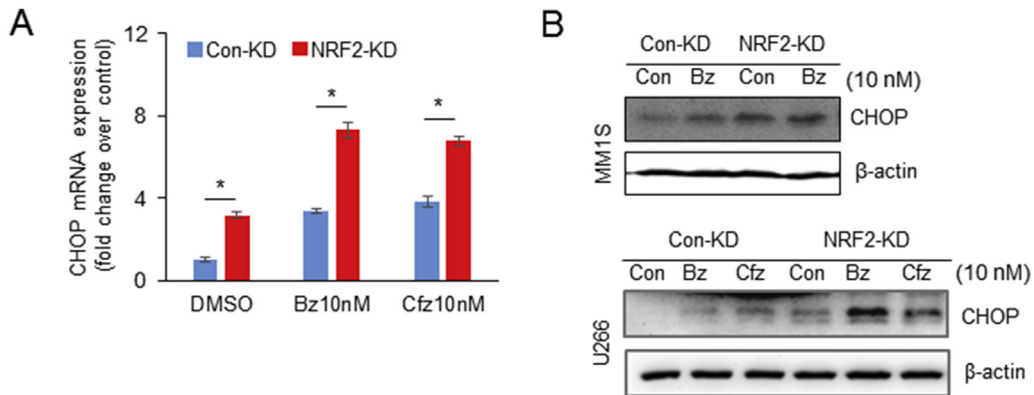


**Fig. 5. NRF2 regulate Chop expression in MM.** Lentiviral mediated shRNA knockdown (KD) of NRF2 in MM1S and U266 cells. Cells were treated with bortezomib and carfilzomib for 4 h. (A) MM1S cells RNA was extracted and analysed for ATF4 and CHOP. (B) Protein was extracted and Western blotting was performed for CHOP protein expression. Blots from Fig. 3C were reprobbed for CHOP protein expression.

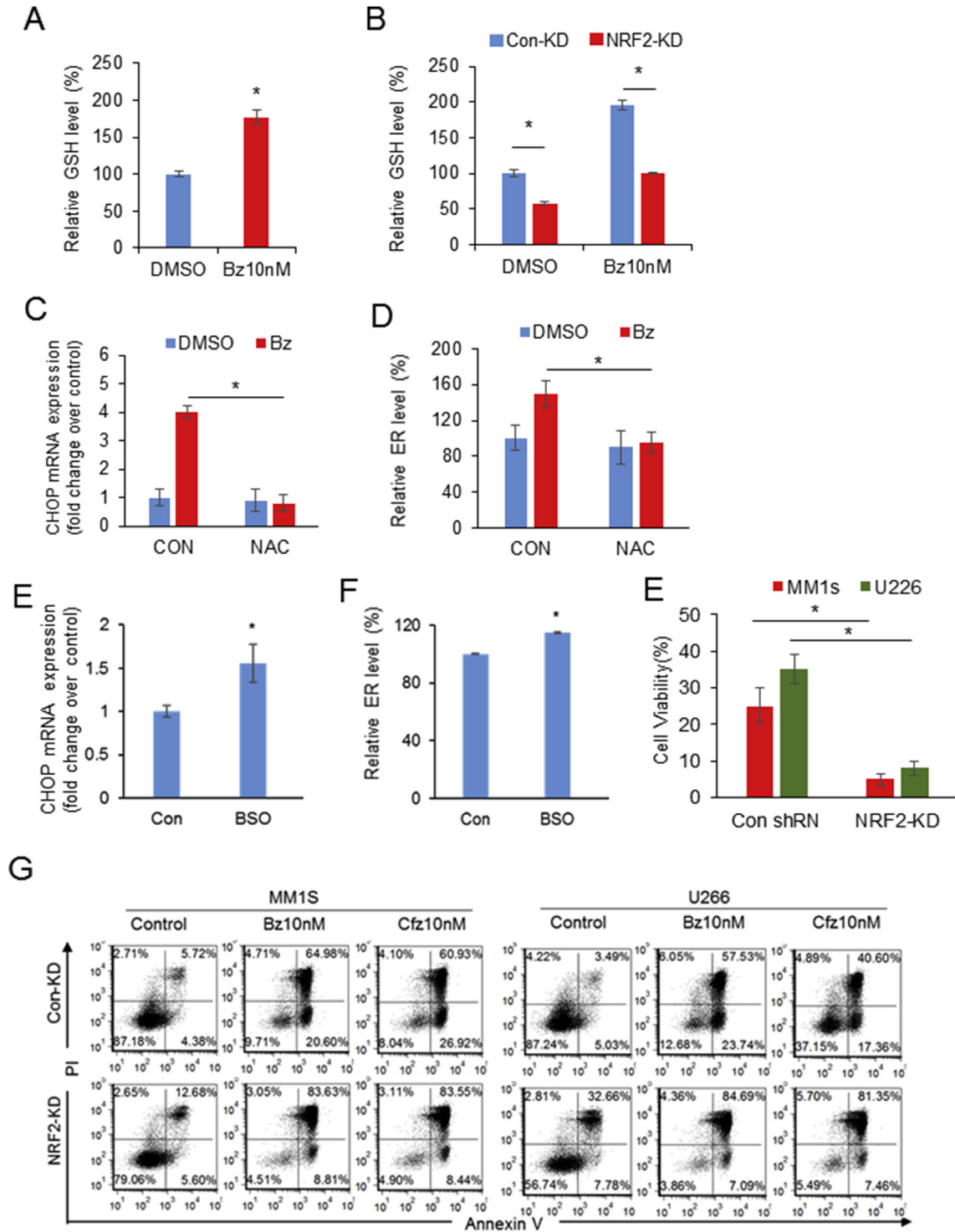


**Fig. 6. NRF2 regulates ER-stress associated apoptosis in MM cells through its regulation of GSH synthesis.** (A) MM1s cells were treated with Bz (10 nM) for 4 h. GSH assay was performed to detect GSH level. (B) Con-KD and NRF2-KD MM1s cells were treated with Bz (10 nM) for 4 h. GSH assay was performed to detect GSH level. (C) MM1s was treated with Bz (10 nM) in combination with NAC (100 μM) (C) or buthionine sulphoximine (BSO) 5 μM (E) for 4 h and then RNA was extracted and analysed using qRT-PCR for CHOP expression. Gene expression was normalised to GAPDH. MM1S treated with Bz (10 nM) in combination with NAC (100 μM) (D) or BSO 5 μM (F) for 4 h. Cells were incubated with the ER Tracker and analysed by flow cytometry. Results expressed as relative median fluorescence intensity. (G) Con-kd or NRF2-KD MM1s cells were incubated with Bz or Cfz for 36 h then cell viability was analysed using flow cytometer with PI/Annexin V staining.

survival of MM. We find that inhibiting NRF2 induces upregulation of the ER-stress response protein CHOP, which increases PI induced associated apoptosis. Subsequently, we demonstrate that NRF2 regulates CHOP and ER-stress associated apoptosis via the

regulation of GSH. Finally, we show that pharmacological inhibition of NRF2 induces MM apoptosis via the induction of CHOP.

The mechanisms of MM cellular resistance to PI include inherent or acquired mutation and inducible pro-survival signaling

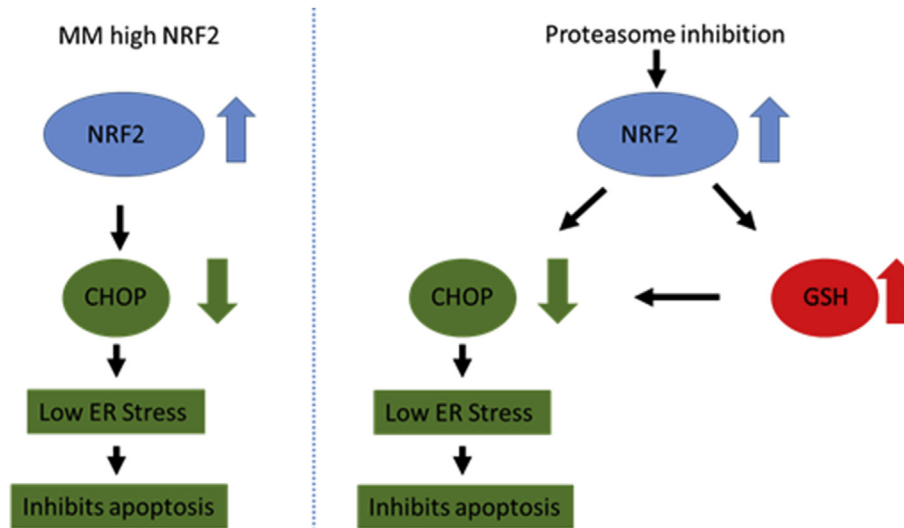


Fig. 7. Schematic representation of NRF2 activity in MM.

[8]. *In vitro* studies show that BMSC protect MM cells from carfilzomib and bortezomib induced apoptosis [33], which is a consequence of MM cell migration and adhesion to the BMSC [34]. In the present study we present data which suggest proteasome induced NRF2 activation protects the MM cells from carfilzomib and bortezomib induced apoptosis. The mechanism for this NRF2 acquired protection is the control of CHOP expression. This is because CHOP induction is associated with induced apoptosis. Thus the inhibition of this protein protects the MM cells from undergoing proteasome induced cell death.

Bortezomib has been shown to induce ER-stress response through the up-regulation of the unfolded protein response (UPR) [35]. The results of which show that bortezomib at doses less than 10 nM can induce transcriptional up-regulation of ATF4, an important effector of the UPR via its induction of CHOP induced apoptosis. In our experiments we show that bortezomib and carfilzomib at doses of 10 nM cannot induce ATF4 mRNA up-regulation. We observed, that NRF2-KD had no effect on ATF4 expression both alone or in combination with carfilzomib and bortezomib. Moreover, others have identified two distinct mechanism through which NRF2 regulates CHOP induction [21,31]. The first is through direct binding of the CHOP promoter which prevents ATF4 from binding and inducing expression of CHOP [21]. The second is via a GSH regulated mechanism [31]. In this study the authors suggest that exogenous GSH could prevent palmitate induced CHOP and associated ER-stress in adipocyte cultures. Moreover, others have shown that regulating redox homeostasis MM can enhance the sensitivity of MM to bortezomib through an NRF2 dependent mechanism [20]. Here we add to these important studies and show proteasome induced NRF2 activation regulates CHOP in MM in a GSH driven mechanism.

We found that GSH is elevated in MM when treated with carfilzomib and bortezomib and this elevation was inhibited when we knockdown NRF2 expression. Moreover, others have shown that GSH synthesis is regulated by the NRF2 signaling pathway [36]. This is through the regulation of multiple genes involved in regulating the synthesis and recycling of GSH. Our observations are consistent with the work of others who have previously reported the importance of GSH in regulating the survival of MM in response to proteasome inhibition and we extend that observation to place CHOP downstream of GSH.

In summary, although NRF2 in the non-malignant cell is a regulator of endogenous ROS, in the context of MM and

chemotherapy, NRF2 enhances the resistance of malignant cells via the up-regulation of the GSH. Here we report that PI induce the activation of the NRF2 pathway, which negatively regulates ER-stress via inhibition of CHOP expression. Specifically, NRF2 modulates the synthesis of GSH resulting in the suppression of CHOP induced apoptosis. Accordingly, we hypothesize that identification of a clinically relevant inhibitor of NRF2 will open up potential strategies in the treatment of MM.

#### Authorship contributions

SAR, KMB and YS designed the research. YS and AAA performed the research. KMB provided essential reagents. SAR and YS performed essential analysis. YS, SAR and KMB wrote the paper. All authors reviewed the manuscript.

#### Acknowledgements

The authors wish to thank the Norwich Medical School and The Ministry of Higher Education and Scientific Research of the State of Libya for funding. Additionally, we are grateful to Professor Richard Ball, Dr Mark Wilkinson and Mr Iain Sheriffs, Norwich Tissue Bank and Biorepository (UK) for help with sample collection and storage.

#### Conflict of interest

The authors declare no conflict of interest.

#### Appendix A. Supplementary data

Supplementary data related to this article can be found at <https://doi.org/10.1016/j.canlet.2017.10.005>.

#### References

- [1] T.S. Hawley, I. Riz, W. Yang, Y. Wakabayashi, L. DePalma, Y.-T. Chang, et al., Identification of an ABCB1 (P-glycoprotein)-positive carfilzomib-resistant myeloma subpopulation by the pluripotent stem cell fluorescent dye CDy1, *Am. J. Hematol.* 88 (4) (2013) 265–272.
- [2] M. Ri, S. Iida, T. Nakashima, H. Miyazaki, F. Mori, A. Ito, et al., Bortezomib-resistant myeloma cell lines: a role for mutated PSMB5 in preventing the accumulation of unfolded proteins and fatal ER stress, *Leukemia* 24 (8) (2010) 1506–1512.

- [3] S.K. Kumar, A. Dispenzieri, M.Q. Lacy, M.A. Gertz, F.K. Buadi, S. Pandey, et al., Continued improvement in survival in multiple myeloma: changes in early mortality and outcomes in older patients, *Leukemia* 28 (5) (2014) 1122–1128.
- [4] M.A. Chapman, M.S. Lawrence, J.J. Keats, K. Cibulskis, C. Sougnez, A.C. Schinzel, et al., Initial genome sequencing and analysis of multiple myeloma, *Nature* 471 (7339) (2011) 467–472.
- [5] N. Bolli, H. Avet-Loiseau, D.C. Wedge, P. Van Loo, L.B. Alexandrov, I. Martincorena, et al., Heterogeneity of genomic evolution and mutational profiles in multiple myeloma, *Nat. Commun.* 5 (2014) 2997.
- [6] J.B. Egan, C.X. Shi, W. Tembe, A. Christoforides, A. Kurdoglu, S. Sinari, et al., Whole-genome sequencing of multiple myeloma from diagnosis to plasma cell leukemia reveals genomic initiating events, evolution, and clonal tides, *Blood* 120 (5) (2012) 1060–1066.
- [7] J.G. Lohr, P. Stojanov, S.L. Carter, P. Cruz-Gordillo, M.S. Lawrence, D. Auclair, et al., Widespread genetic heterogeneity in multiple myeloma: implications for targeted therapy, *Cancer Cell* 25 (1) (2014) 91–101.
- [8] M.Y. Murray, M.J. Auger, K.M. Bowles, Overcoming bortezomib resistance in multiple myeloma, *Biochem. Soc. Trans.* 42 (4) (2014) 804–808.
- [9] M. Ri, Endoplasmic-reticulum stress pathway-associated mechanisms of action of proteasome inhibitors in multiple myeloma, *Int. J. Hematol.* 104 (3) (2016) 273–280.
- [10] E.E. Fink, S. Mannava, A. Bagati, A. Bianchi-Smiraglia, J.R. Nair, K. Moparthy, et al., Mitochondrial thioredoxin reductase regulates major cytotoxicity pathways of proteasome inhibitors in multiple myeloma cells, *Leukemia* 30 (1) (2016) 104–111.
- [11] A. Abdul-Aziz, D.J. MacEwan, K.M. Bowles, S.A. Rushworth, Oxidative stress responses and NRF2 in human leukaemia, *Oxid. Med. Cell Longev.* 2015 (2015), 454659.
- [12] N.M. Shah, L. Zaitseva, K.M. Bowles, D.J. MacEwan, S.A. Rushworth, NRF2-driven miR-125B1 and miR-29B1 transcriptional regulation controls a novel anti-apoptotic miRNA regulatory network for AML survival, *Cell Death Differ.* 22 (4) (2015) 654–664.
- [13] N.M. Shah, S.A. Rushworth, M.Y. Murray, K.M. Bowles, D.J. MacEwan, Understanding the role of NRF2-regulated miRNAs in human malignancies, *Oncotarget* 4 (8) (2013) 1130–1142.
- [14] S.A. Rushworth, S. Shah, D.J. MacEwan, TNF mediates the sustained activation of Nrf2 in human monocytes, *J. Immunol.* 187 (2) (2011) 702–707.
- [15] S.A. Rushworth, K.M. Bowles, D.J. MacEwan, High basal nuclear levels of Nrf2 in acute myeloid leukemia reduces sensitivity to proteasome inhibitors, *Cancer Res.* 71 (5) (2011) 1999–2009.
- [16] S.A. Rushworth, D.J. MacEwan, The role of Nrf2 and cytoprotection in regulating chemotherapy resistance of human leukemia cells, *Cancers (Basel)* 3 (2) (2011) 1605–1621.
- [17] S.A. Rushworth, D.J. MacEwan, M.A. O'Connell, Lipopolysaccharide-induced expression of NAD(P)H:quinone oxidoreductase 1 and heme oxygenase-1 protects against excessive inflammatory responses in human monocytes, *J. Immunol.* 181 (10) (2008) 6730–6737.
- [18] K. Itoh, N. Wakabayashi, Y. Katoh, T. Ishii, K. Igarashi, J.D. Engel, et al., Keap1 represses nuclear activation of antioxidant responsive elements by Nrf2 through binding to the amino-terminal Neh2 domain, *Genes Dev.* 13 (1) (1999) 76–86.
- [19] L.N. Barrera, S.A. Rushworth, K.M. Bowles, D.J. MacEwan, Bortezomib induces heme oxygenase-1 expression in multiple myeloma, *Cell Cycle* 11 (12) (2012) 2248–2252.
- [20] S. Nerini-Molteni, M. Ferrarini, S. Cozza, F. Caligaris-Cappio, R. Sitia, Redox homeostasis modulates the sensitivity of myeloma cells to bortezomib, *Br. J. Haematol.* 141 (4) (2008) 494–503.
- [21] Z.H. Zong, Z.X. Du, N. Li, C. Li, Q. Zhang, B.Q. Liu, et al., Implication of Nrf2 and ATF4 in differential induction of CHOP by proteasome inhibition in thyroid cancer cells, *Biochim. Biophys. Acta* 1823 (8) (2012) 1395–1404.
- [22] S.B. Cullinan, J.A. Diehl, PERK-dependent activation of Nrf2 contributes to redox homeostasis and cell survival following endoplasmic reticulum stress, *J. Biol. Chem.* 279 (19) (2004) 20108–20117.
- [23] K.K. Starheim, T. Holien, K. Misund, I. Johansson, K.A. Baranowska, A.M. Sponaas, et al., Intracellular glutathione determines bortezomib cytotoxicity in multiple myeloma cells, *Blood Cancer J.* 6 (7) (2016), e446.
- [24] A.M. Abdul-Aziz, M.S. Shafat, T.K. Mehta, F. Di Palma, M.J. Lawes, S.A. Rushworth, et al., MIF-induced stromal PKC $\beta$ /IL8 is essential in human acute myeloid leukemia, *Cancer Res.* 77 (2) (2017) 303–311.
- [25] S.A. Rushworth, L. Zaitseva, M.Y. Murray, N.M. Shah, K.M. Bowles, D.J. MacEwan, The high Nrf2 expression in human acute myeloid leukemia is driven by NF-kappaB and underlies its chemo-resistance, *Blood* 120 (26) (2012) 5188–5198.
- [26] A. Lister, T. Nedjadi, N.R. Kitteringham, F. Campbell, E. Costello, B. Lloyd, et al., Nrf2 is overexpressed in pancreatic cancer: implications for cell proliferation and therapy, *Mol. Cancer* 10 (2011) 37.
- [27] Y. Inami, S. Waguri, A. Sakamoto, T. Kouno, K. Nakada, O. Hino, et al., Persistent activation of Nrf2 through p62 in hepatocellular carcinoma cells, *J. Cell Biol.* 193 (2) (2011) 275–284.
- [28] L. Vincenz, R. Jager, M. O'Dwyer, A. Samali, Endoplasmic reticulum stress and the unfolded protein response: targeting the Achilles heel of multiple myeloma, *Mol. Cancer Ther.* 12 (6) (2013) 831–843.
- [29] S. White-Gilbertson, Y. Hua, B. Liu, The role of endoplasmic reticulum stress in maintaining and targeting multiple myeloma: a double-edged sword of adaptation and apoptosis, *Front. Genet.* 4 (2013) 109.
- [30] E.A. Obeng, L.M. Carlson, D.M. Gutman, W.J. Harrington Jr., K.P. Lee, L.H. Boise, Proteasome inhibitors induce a terminal unfolded protein response in multiple myeloma cells, *Blood* 107 (12) (2006) 4907–4916.
- [31] B.J. Eudy, C.A. Rowe, S.S. Percival, Glutathione pre-treatment prevents CHOP protein expression in 3T3-L1 adipocytes during palmitate induced ER stress, *FASEB J.* 30 (1 Suppl) (2016) lb309.
- [32] J. Abdi, G. Chen, H. Chang, Drug resistance in multiple myeloma: latest findings and new concepts on molecular mechanisms, *Oncotarget* 4 (12) (2013) 2186–2207.
- [33] S. Markovina, N.S. Callander, S.L. O'Connor, G. Xu, Y. Shi, C.P. Leith, et al., Bone marrow stromal cells from multiple myeloma patients uniquely induce bortezomib resistant NF-kappaB activity in myeloma cells, *Mol. Cancer* 9 (2010) 176.
- [34] S. Manier, A. Sacco, X. Leleu, I.M. Ghobrial, A.M. Roccaro, Bone marrow microenvironment in multiple myeloma progression, *J. Biomed. Biotechnol.* 2012 (2012), 157496.
- [35] J. Hu, N. Dang, E. Menu, E. De Bryune, D. Xu, B. Van Camp, et al., Activation of ATF4 mediates unwanted Mcl-1 accumulation by proteasome inhibition, *Blood* 119 (3) (2012) 826–837.
- [36] G. Gorrini, I.S. Harris, T.W. Mak, Modulation of oxidative stress as an anti-cancer strategy, *Nat. Rev. Drug Discov.* 12 (12) (2013) 931–947.